Pharmacometric modelling to inform and improve TB and HIV treatment: Focus on drug-drug interactions and neglected populations

by

Kamunkhwala Gausi

Thesis Presented for the Degree of

DOCTOR OF PHILOSOPHY

in the Division of Clinical Pharmacology

Department of Medicine

UNIVERSITY OF CAPE TOWN

Primary supervisor: A/Professor Paolo Denti

November 2021

Contributions to the field

This thesis includes some of the following contributions to the field of pharmacometrics and clinical pharmacology:

Full length original articles

1. Gausi, K., Wiesner, L., Norman, J., Wallis, C. L., Onyango-Makumbi, C., Chipato, T., Haas, D. W., Browning, R., Chakhtoura, N., Montepiedra, G., Aaron, L., McCarthy, K., Bradford, S., Vhembo, T., Stranix-Chibanda, L., Masheto, G. R., Violari, A., Mmbaga, B. T., Aurpibul, L., … Denti, P. (2020). Pharmacokinetics and Drug-Drug Interactions of Isoniazid and Efavirenz in Pregnant Women Living With HIV in High TB Incidence Settings: Importance of Genotyping. Clinical Pharmacology & Therapeutics, cpt.2044. https://doi.org/10.1002/cpt.2044

2. Court, R., Gausi, K., Mkhize, B., Wiesner, L., Waitt, C., McIlleron, H., Maartens, G., Denti, P., & Loveday, M. (2021). Bedaquiline exposure in pregnancy and breastfeeding in women with rifampicin-resistant tuberculosis. Authorea Preprints. https://doi.org/10.22541/AU.163726220.09199594/V1

3. Gausi, K., Ignatius, E. H., Sun, X., Kim, S., Moran, L., Wiesner, L., von Groote-Bidlingmaier, F., Hafner, R., Donahue, K., Vanker, N., Rosenkranz, S. L., Swindells, S., Diacon, A. H., Nuermberger, E. L., Dooley, K. E., & Denti, P. (2021). A Semi-Mechanistic Model of the Bactericidal Activity of High-Dose Isoniazid Against Multi-Drug-Resistant Tuberculosis: Results from a Randomised Clinical Trial. American Journal of Respiratory and Critical Care Medicine. https://doi.org/10.1164/rccm.202103-0534OC

4. Gausi, K., Chirehwa, M., Ignatius, E. H., Court, R., Sun, X., Moran, L., Hafner, R., Wiesner, L., Rosenkranz, S. L., De Jager, V., De Vries, N., Harding, J., Gumbo, T., Swindells, S., Diacon, A. H., Dooley, K. E., McIlleron, H., & Denti, P. Pharmacokinetics of high-dose isoniazid for treatment of multidrug resistant tuberculosis. (Accepted in the Journal of Antimicrobial Chemotherapy (JAC)).

Scientific conference presentations

1. Poster: Gausi, K., Wiesner, L., Norman, J., Wallis, C. L., Onyango-Makumbi, C., Chipato, T., Haas, D. W., Browning, R., Chakhtoura, N., Montepiedra, G., Aaron, L., McCarthy, K., Bradford, S., Vhembo, T., Stranix-Chibanda, L., Masheto, G. R., Violari, A., Mmbaga, B. T., Aurpibul, L., … Denti, P. Pharmacokinetics of isoniazid preventative therapy among HIV-infected pregnant women in high tuberculosis incidence settings. Presented at: 28th annual meeting Population Approach Group Europe (PAGE), Stockholm, Sweden, 2019. Abstract 8989

2. Poster: Gausi, K., Wiesner, L., Norman, J., Wallis, C. L., Onyango-Makumbi, C., Chipato, T., Haas, D. W., Browning, R., Chakhtoura, N., Montepiedra, G., Aaron, L., McCarthy, K., Bradford, S., Vhembo, T., Stranix-Chibanda, L., Masheto, G. R., Violari, A., Mmbaga, B. T., Aurpibul, L., … Denti, P. pregnancy associated with decreased serum isoniazid levels in women living with HIV. Presented at: Conference on retrovirus and opportunistic infection (CROI), Seattle, Washington, 2019. Abstract 759

3. Poster: Gausi, K., Wiesner, L., Norman, J., Wallis, C. L., Onyango-Makumbi, C., Chipato, T., Haas, D. W., Browning, R., Chakhtoura, N., Montepiedra, G., Aaron, L., McCarthy, K., Bradford, S., Vhembo, T., Stranix-Chibanda, L., Masheto, G. R., Violari, A., Mmbaga, B. T., Aurpibul, L., … Denti, P. Impact of isoniazid and pregnancy on efavirenz pharmacokinetics in women living with HIV. Presented at: 10th International AIDS converence (IAS), Mexico City, Mexico. Abstract 2775.

4. Oral presentation: Gausi, K., Ignatius, E. H., Sun, X., Kim, S., Moran, L., Wiesner, L., von Groote-Bidlingmaier, F., Hafner, R., Donahue, K., Vanker, N., Rosenkranz, S. L., Swindells, S., Diacon, A. H., Nuermberger, E. L., Dooley, K. E., & Denti, P. PK-PD of isoniazid given at different doses among patients with MDR-TB with INH resistant mediated by inhA mutations; Modelling results from ACTG A5312. Presented at:Internation workshop on clinical pharmacology of tuberculosis drugs, London, United Kingdom, 2019. Abstract 11.

5. Oral presentation: Gausi, K., Ignatius, E. H., Sun, X., Kim, S., Moran, L., Wiesner, L., von Groote-Bidlingmaier, F., Hafner, R., Donahue, K., Vanker, N., Rosenkranz, S. L., Swindells, S., Diacon, A. H., Nuermberger, E. L., Dooley, K. E., & Denti, P. (2021). A semi-mechanistic model of the bactericidal activity of high-dose isoniazid against multidrug-resistant tuberculosis. Presented at: 31st European Congress of clinical microbiology and infectious diseases (ECCMID), online, 2021. Abstract 981

6. Poster: Gausi, K., Chirehwa, M., Ignatius,E H., Court, R., Sun, X., Moran, L., Hafner, R., Wiesner, L., Rosenkranz, S. L., Gumbo, T., Swindells, S., Diacon, A., Dooley, K. E., McIlleron, H., Denti, P. Pharmacokinetics of high dose isoniazid among individuals with multidrug-resistant tuberculosis. Presented at: 29th annual meeting Population Approach Group Europe (PAGE), Online, 2021. Abstract 9821

Declaration of work

I, Kamunkhwala Gausi, hereby declare that the work on which this dissertation/thesis is based is my original work (except where acknowledgements indicate otherwise) and that neither the whole work nor any part of it has been, is being, or is to be submitted for another degree in this or any other university. Chapters three, four, five and six of the thesis have been published in an international journal and contents remain unchanged from the printed versions excepted where formatting was required to maintain consistency in the thesis. All co-authors gave their written consent to include the publications as part of a PhD.

I empower the university to reproduce for the purpose of research either the whole or any portion of the contents in any manner whatsoever

SIGNATURE DATE: 30 November 2021

"I confirm that I have been granted permission by the University of Cape Town's Doctoral Degrees Board to include the following publication(s) in my PhD thesis, and where co-authorships are involved, my co-authors have agreed that I may include the publication(s):"

1. Gausi, K., Wiesner, L., Norman, J., Wallis, C. L., Onyango-Makumbi, C., Chipato, T., Haas, D. W., Browning, R., Chakhtoura, N., Montepiedra, G., Aaron, L., McCarthy, K., Bradford, S., Vhembo, T., Stranix-Chibanda, L., Masheto, G. R., Violari, A., Mmbaga, B. T., Aurpibul, L., … Denti, P. (2020). Pharmacokinetics and Drug-Drug Interactions of Isoniazid and Efavirenz in Pregnant Women Living With HIV in High TB Incidence Settings: Importance of Genotyping. *Clinical Pharmacology & Therapeutics*, cpt.2044. https://doi.org/10.1002/cpt.2044

2. Court, R., Gausi, K., Mkhize, B., Wiesner, L., Waitt, C., McIlleron, H., Maartens, G., Denti, P., & Loveday, M. (2021). Bedaquiline exposure in pregnancy and breastfeeding in women with rifampicin-resistant tuberculosis. *Authorea Preprints*. https://doi.org/10.22541/AU.163726220.09199594/V1 accepted by *BJCP.*

3. Gausi, K., Chirehwa, M., Ignatius,E H., Court, R., Sun, X., Moran, L., Hafner, R., Wiesner, L., Rosenkranz, S. L., De Jager, V., De Vries, N., Harding, J., Gumbo, T., Swindells, S., Diacon, A., Dooley, K. E., McIlleron, H., Denti, P. Pharmacokinetics of standard vs high-dose isoniazid for treatment of multidrug-resistant tuberculosis. *Accepted in the JAC*.

4. Gausi, K., Ignatius, E. H., Sun, X., Kim, S., Moran, L., Wiesner, L., von Groote-Bidlingmaier, F., Hafner, R., Donahue, K., Vanker, N., Rosenkranz, S. L., Swindells, S., Diacon, A. H., Nuermberger, E. L., Dooley, K. E., & Denti, P. (2021). A Semi-Mechanistic Model of the Bactericidal Activity of High-Dose Isoniazid Against Multi-Drug-Resistant Tuberculosis: Results from a Randomised Clinical Trial. *American Journal of Respiratory and Critical Care Medicine*. https://doi.org/10.1164/rccm.202103-0534OC

SIGNATURE: DATE: 10 December 2021

STUDENT NAME: Kamunkhwala Gausi STUDENT NUMBER: GSXKAM002

Acknowledgements

I would like to offer my special thanks to the following whom/which contributed to the successful completion of the research

Supervision

A/Prof. Paolo Denti, I am grateful for the opportunity to be part of the pharmacometrics group, for the continuous support, patience, motivation and immense knowledge. His guidance helped me in all the time of research and writing of this thesis. I could not have imagined having a better supervisor and mentor for my PhD study.

Funding

My sincere thanks go to my PhD funders, the **Virtual consortium** whose aim is to investigate the challenges of TB treatment for individuals on second-line ART whilst promoting African leadership and capacity building.

Others

I would like to thank **Prof Gary Maartens**, and **Prof Helen McIlleron** for providing scientific input and support for my research. In addition, I appreciate the scientific input on pharmacokinetic sample processing and assay analysis received from Dr Lubbe Wiesner and Jennifer Norman of the analytical laboratory.

I appreciate all my **colleagues** in the pharmacometrics modelling group for all the discussion, advice, and for answering the numerous questions I had in the course of my PhD with unfailing patience. Their feedback improved this thesis content significantly. The research would not have been smooth without the conducive environment in the division of clinical pharmacology

Research collaboration and support

I am grateful for the opportunity provided by **Neva Coello, Sebastian Weber, Sebastien Lorenzo** and the **Next Generation Scientist Program** (NGS) team. The experience will forever be remembered!

I am thankful for the support from **Dr Kelly E Dooley, Amita Gupta** and **Dr Elisa Ignatius**, our colleagues and collaborators at John Hopkin University, for their insightful input and for sharing their knowledge on the pharmacology of TB and HIV.

The modelling work was performed using facilities provided by the University of Cape Town's ICTS High-Performance Computing team: http://hpc.uct.ac.za

Special thanks to the study participants and study teams of the IMPAACT P1078, ACTG A5312 and PODRtb study for dedicating their time to the project's success. I would like to express my gratitude to all co-authors in the publications presented in this thesis for their feedback on my research outputs.

Personal

I thank God for my family, especially my sisters (Fyness, Joan and Caroline), for inspiring, supporting, encouraging and motivating me throughout this journey. I am also grateful for the advice and guidance from Mr Katumbi and Singini.

Abstract

Pharmacometric modelling to inform and improve TB and HIV treatment: Focus on drug-drug interactions and neglected populations

The global scale-up of tuberculosis treatment administered with antiretroviral therapy (ART) is the primary contributor to the 11 million averted deaths among individuals living with HIV observed between 2000 and 2019 in adults and children. Unfortunately, not all patients in need could fully benefit from these recent improvements in treatment because neglected populations are often excluded from clinical trials, including pregnant and breastfeeding women, children, adolescents, those with co-morbidities requiring additional drug treatments, and those with drug-resistant strains. This leaves many unanswered questions surrounding the management of TB, HIV, and TB/HIV in these vulnerable subpopulations. In this thesis, we utilise population pharmacokinetics and pharmacodynamic modelling to improve TB and HIV treatment in neglected populations using data from patients with TB or/and HIV. We analyse the pharmacogenomics, pharmacokinetics, and drug-drug interaction of efavirenz, isoniazid, and bedaquiline in pregnant women and characterise the pharmacokinetics and pharmacodynamics of high dose isoniazid in adults with multidrug-resistant tuberculosis.

We found that isoniazid and efavirenz exposures were reduced during pregnancy, but the main determinants of drug concentration were N-acetyltransferase 2 and *CYP2B6* genotypes, which resulted in a 5-fold difference for both drugs between rapid and slow metabolisers. Bedaquiline exposures were lower during both postpartum and antepartum compared to historical data in non-pregnant patients.

For high dose isoniazid, we observed markedly lower isoniazid exposures in participants on combination MDR-TB treatment compared to monotherapy and identified saturable kinetics at doses >10 mg/kg. We suggest that dosing isoniazid based on N-acetyltransferase 2 acetylator status might help patients attain effective exposures against inhA-mutated isolates.

Table of Contents

List of tables

List of figures

List of Acronyms and abbreviations

Abbreviations and acronyms	Definition
AIC	Akaike Information Criterion
ALT	Alanine Aminotransferase
ART	Antiretroviral Therapy
AST	Aspartate transaminase
AUC_{0-24}	24-hour area under the concentration-time curve
BLQ	Below the Limit of Quantification
BOV	Between-Occasion Variability
BSV	Between subject variability
CI	Confidence interval
CL	Clearance
CL_H	Hepatic clearance
CL_{int}	Intrinsic clearance
$CL_{int,max}$	Maximum intrinsic clearance
Cmax	Maximum plasma concentration
Cmin	Minimum plasma concentration
DR-TB	Drug-resistant tuberculosis
EH	Hepatic extraction
F	Oral bioavailability
FDC	Fixed-dose combination
FFM	Fat-free mass
FOCE-I	First-order conditional estimation with eta-epsilon interaction
F_{prehep}	Prehepactic oral bioavailability
fU	Unbound fraction
GOF	Goodness of fit plots
HAART	Highly Active Antiretroviral Therapy
HIV	Human immunodeficiency virus
ka	Absorption rate constant
km	Michaelis-menten constant
k	Rate of elimination
LLOQ	Lower limit of quantification
M.tb	*Mycobacterium tuberculosis*
MDR	Multi-drug resistant
MTT	Mean transit time
NAT2	N-acetyltransferase 2
NCA	Noncompartmental Analysis
NN	Number of absorption transit compartments
OFV	Objective function value
PD	Pharmacodynamics
PK	Pharmacokinetics
PK-PD	Pharmacokinetics-pharmacodynamics
P-pg	P-glycoprotein
PsN	Perl-speaks-NONMEM
Q	Intercompartmental clearance
QH	Hepatic plasma flow
SIR	Sampling Importance Resampling
TB	Tuberculosis
Tmax	Time to maximum plasma concentration

V	Volume of distribution
Vc	Volume of distribution of the central compartment
VH	Volume of distribution of the liver
Vp	Volume of distribution of the peripheral compartment
VPC	Visual Predictive Check
WHO	World Health Organization

Chapter 1: Introduction and literature review

1.1 Global disease burden of HIV and tuberculosis

One of the world's most serious health and development challenges is the Human Immunodeficiency Virus (HIV), which causes acquired immunodeficiency syndrome (AIDS), accounting for more than 2.3 million death per year (WHO, 2021b). In 2020 approximately 38 million people were living with HIV globally, of whom 2.78 million were children (<19 years old) (UNAIDS, 2021).

Sub-Saharan Africa is the global epicentre of HIV transmission, accounting for 57% of all new infections in 2019 (UNAIDS, 2020a) and home to two thirds (67%) of people living with HIV (PLWHIV) (UNAIDS, 2021). Within Sub-Sahara, South Africa has one of the highest HIV incidences; it has an overall HIV prevalence rate of approximately 13.7%, with 8.2 million people living with HIV and 19.5% of the adult population (aged 15–49 years) HIV positive (Statistics South Africa, 2021).

Although the global 2020 incidence of HIV declined by 31% and 53% in adults and children, respectively compared with 2010, there were still 1.5 million new cases reported in 2020 (UNAIDS, 2021). The global scale-up of antiretroviral therapy (ART) is one of the primary contributors to the decline of new infections and AIDS-related deaths. The increase in access to ARTs has averted an estimated 12.1 million AIDS-related death and has contributed to a 47% reduction in AIDS-related deaths since 2010 (UNAIDS, 2021). In addition, women have a 12% greater decline in deaths from AIDS-related illnesses due to increased treatment coverage compared to men (73% of women are on treatment compared to 61% of men living with HIV) and better adherence to treatment (UNAIDS, 2020).

Tuberculosis has remained the main cause of death amongst people living with HIV and accounts for approximately one-third of AIDS-related deaths(UNAIDS, 2020b). Additionally, tuberculosis is one of the leading causes of death from a single infectious agent, ranking above HIV/AIDS (WHO, 2021a). In South Africa, TB is the leading cause of death, accounting for 58,000 deaths in 2019, of which 36,000 were HIV positive (Monedero-Recuero et al., 2021). The risk of developing tuberculosis is 21 times higher in people living with HIV, and in 2018 approximately 251 000 people living with HIV died from tuberculosis (UNAIDS, 2020a). For this reason, intensified efforts have been focused on addressing the challenges caused by the double burden of disease. Some of these are intensive tuberculosis case-finding and treatment, preventive therapy, tuberculosis infection control, and early ART initiation within tuberculosis treatment (Pathmanathan et al., 2017). The administration of tuberculosis treatment with ART prevented an estimated 11 million deaths between 2000 to 2019 (WHO, 2020) in individuals living with HIV. Approximately 85% of individuals infected with tuberculosis can be treated successfully with a 6-month drug regimen, and the treatment also curtails onward transmission of infection (WHO, 2020a).

1.2 Tuberculosis and HIV in neglected populations

Although there have been many improvements in treatments for HIV and tuberculosis, not all patients have benefited from it. Neglected populations (Grimsrud et al., 2015) such as pregnant and breastfeeding women, children, adolescents, those with co-morbidities, or those with infections driven by drug-resistant strains, are commonly excluded from clinical trials. This leaves many unanswered questions surrounding the clinical management of tuberculosis, HIV, and tuberculosis/HIV in these vulnerable subpopulations. This thesis

focuses on the neglected population of individuals with co-morbidities, drug-resistance tuberculosis, pregnant women, and their infants.

Both tuberculosis and HIV infections cause high morbidity and mortality in pregnant and postpartum women and their infants. Pregnant women are at higher risk of tuberculosis infections because pregnancy suppresses the T-helper 1 proinflammatory response, which increases susceptibility to infections and reactivation of tuberculosis (Singh & Perfect, 2007). The risk persists to early postpartum, as seen in a study by Zenner *et al*. in 2012, who showed that developing tuberculosis is twice as likely during early postpartum compared to nonpregnant women. In addition, both HIV and pregnancy may mask the symptoms of tuberculosis and cause atypical symptoms (Mathad & Gupta, 2012), complicating the diagnosis and treatment of the infection. The situation is further complicated by the physiological changes due to pregnancy that may change the pharmacokinetics of a drug (Westin et al., 2018). Pregnant or lactating mothers with tuberculosis and their infants have an increased risk of preeclampsia, vaginal bleeding, low birth weight, maternal and infant death (Mathad et al., 2014).

Tuberculosis can be transmitted from mother to child, either vertically from the mother to the foetus, at delivery through aspiration/ingestion of infected amniotic fluid or genital secretion, or more commonly horizontally postpartum through droplets from the mother that are inhaled by her child (Kodadhala et al., 2016). Therefore, infants born to mothers with tuberculosis are at a high risk of infection. The risk is further increased, as Infants have a higher likelihood of tuberculosis disease progression during the first year due to their immature immunity (Bekker, 2016). If infants born to mothers with tuberculosis are left untreated and do not receive appropriate prophylaxis, 50% of them will develop the disease (Bekker, 2016). High neonatal mortality (up to 60%) and morbidity emphasise the importance

of tuberculosis preventative therapy, early diagnosis, and treatment of infants suffering from tuberculosis (Martin & Black, 2012).

1.2.1 Pregnancy-induced physiological changes.

Pregnancy has been associated with physiological changes that affect the pharmacokinetics of drugs. Some of the changes include plasma albumin levels, bodyweight and composition, plasma volume, blood flow, and induction or inhibition of drug metabolising enzymes (Pinheiro & Stika, 2020).

According to literature, antepartum albumin levels tend to decrease as pregnancy progresses, attributing towards augmented plasma volume and urinary albumin excretion (Feghali & Mattison, 2011; Maher et al., 1993). The reduction in protein concentrations in plasma leads to higher free drug concentration, especially for highly protein-bound drugs, consequently impacting the clearance of the drug. Pregnancy induces an increase in weight and body fat, leading to lipophilic drugs distributing more widely (lowering plasma concentration) and lingering longer in the body (Pinheiro & Stika, 2020). In addition, pregnancy has been reported to increase plasma volume by approximately 42%, reaching over 3.5 L at 38 weeks of gestation (Feghali et al., 2015), increasing the distribution and dilution of hydrophilic drugs during pregnancy, lowering plasma concentration. Cardiac output rises to around 7 L/min at 16 weeks gestation, then plateaus off, remaining high for the remainder of the prenatal period; this cascades to increased hepatic and renal blood flow, potentially increasing drug clearance (Qasqas et al., 2004). The activity of enzymes and transporters can be altered by pregnancy (Pinheiro & Stika, 2020), which may increase or decrease the clearance, therefore causing drug exposure to either go up or down. All these changes caused by pregnancy prevail after giving birth and can take a couple of weeks to revert to normal (de Kock et al., 2017).

1.3 Tuberculosis disease

Tuberculosis is an airborne disease that is caused by the bacterium *Mycobacterium tuberculosis* (*M.tb*). There exist seven other related mycobacterial species that can cause a disease similar to tuberculosis, together these mycobacterial species, including *M.tb* are known as *M.tb* complex. Tuberculosis is transmitted through the aspiration of infectious nuclei droplets containing viable bacilli formed when a patient with active pulmonary tuberculosis coughs. These droplets can remain suspended in the air for several hours. Once inhaled, the droplets are engulfed by alveolar macrophages, but *M.tb* can evade death by inhibiting the phagosome-lysosome fusion (Sturgill-Koszycki et al., 1994). The macrophages and immune cells become localised at the infection site creating an ordered cellular architecture called granuloma, which evolves to necrotic lesions characterised by hypoxia and nutrient deprivation (Barry et al., 2009). This kills the majority of *M.tb,* but some survive extracellularly in the solid caseous material (Dannenberg, 2009). Therefore, in order to be effective, antituberculosis drugs must be transported from the circulatory system to the non-vascularised pulmonary lesion, then diffuse into caseum and necrotic foci, permeate the *M.tb* cell envelope, and then reach the target at sufficient concentrations and for the required length of time (Dartois, 2014).

An infected individual might harbour *M.tb* and not show any symptoms (latent infection) or develop progressive tuberculosis disease. One-third of the world population is estimated to have latent tuberculosis and might be at risk to develop tuberculosis disease once immunocompromised (Dye et al., 1999). The typical site of tuberculosis infection is the lungs (pulmonary tuberculosis), but any other organs, such as the brain, larynx, lymph node, spine, or kidney, can also be infected.

In vitro M.tb can achieve a doubling time of up to 16 hours in the optimal conditions, whilst the growth rates in the human host vary depending on the site and stage of infection (Beste et al., 2009). Two distinct acute phases characterise tuberculosis; the actively growing bacteria phase and the persistent phase, where *M.tb* is either slow-growing or non-growing (Stewart et al., 2003). The ability of *M.tb* to remain in the persistent phase (a state intractable to immune clearance) for decades is key to *M.tb's* success and a major barrier to tuberculosis control since most antituberculosis drugs are inactive against non-dividing cells (Beste et al., 2009). The host environmental conditions like pH, nutrient deprivation, low oxygen, and exposure to reactive nitrogen and oxygen species influence the bacilli metabolic state, all of which may contribute to antibiotic tolerance (Bonnett et al., 2018).

1.4 Tuberculosis treatment

Streptomycin, the first effective antituberculosis agent, was discovered in 1944 (Schatz et al., 1944). At almost the same time, para-aminosalicylic acid (PAS) was also developed and used to treat tuberculosis (Lehmann, 1946). The two were administered alone, which led to the development of resistance, resulting in abolishing monotherapy and establishing the first combination therapy (HINSHAW, 1946; Murray et al., 2015). Since then, combinational chemotherapy has been used to prevent the development of drug-resistance tuberculosis.

The current world health organisation (WHO) recommended regimen comprises a 2-month of four first-line antituberculosis agents (i.e., isoniazid, rifampicin, ethambutol, and pyrazinamide) followed by 4-month of isoniazid and rifampicin. Nevertheless, antituberculosis drug resistance continues to emerge, despite the establishment of antituberculosis combination therapy. The drug resistance is partly due to patient non-

adherence, impacted by the lengthy treatment, complexity of the regimen, and adverse drug effects (Torfs et al., 2019).

1.4.1 Tuberculosis drug resistance

M.tb drug resistance has been reported to primarily emerge due to mutation in genes encoding either drug-activation enzymes, or drug targets in response to the selection pressure of antibiotics (Culyba et al., 2015; von Wintersdorff et al., 2016). The mutation occurs randomly, but continuous drug exposure during lengthy treatment regimens cause the mutated strain to have an evolutionary advantage, helping it to take hold. Subtherapeutic drug exposure can result in “windows” of temporary monotherapy, thus creating an ideal environment for the development of resistance. Hence drug concentration is the primary determinant of mutation (Singh et al., 2020). The mutations due to subtherapeutic concentration generally appear at the cost of fitness and often result in decreased growth, survival, and virulence of the bacteria (Nguyen, 2016).

One cause of subtherapeutic drug exposure is noncompliance to drug regimens, which is common in TB treatment due to the lengthy treatment regimen with multiple drugs (Zhang et al., 2012). However, subtherapeutic drug exposures are also due to natural interindividual variability in PK characteristics or poorly designed dosing schedules whereby some patients may be systematically underdosed. An example is low weight patients, which achieve lower drug concentrations if dosed based on a constant mg/kg dosing strategy (Denti et al., 2022).

Other sources of *M.tb* drug resistance are an intrinsic mechanism like drug efflux pumps, which eject the drug molecules entering the bacterial cells (Nasiruddin et al., 2017), impermeability of cell envelope presenting as a barrier for antibiotics (Nguyen, 2016), and

evolution of enzymes to modify or degrade different antibiotics (Smith et al., 2012). Lastly, when exposed to drugs or hypoxic environment, *M.tb* tends to change its metabolism and counter drug effect, achieving what is called phenotypic drug tolerance. This gives rise to subpopulations of M.tb composed of cells with epigenetic drug tolerance known as persisters. With the increase in the emergence of drug-resistant strains and the lack of new antituberculosis drugs, there is a need to optimise the use of old drugs, improve our knowledge on the mode of action of antituberculosis drugs and mechanism of drug resistance to facilitate better strategies for the treatment of drug-resistant tuberculosis (Mouton et al., 2011; Singh et al., 2020).

1.4.2 Multi-drug resistant TB

Multi-drug resistant tuberculosis (MDR-TB) is a type of drug-resistant tuberculosis that occurs when *M.tb* does not respond to at least isoniazid and rifampicin, the two most important antituberculosis drugs(WHO, 2020b). An individual can acquire MDR-TB either by infection with a drug-resistant strain (primary resistance) or by developing resistance while on treatment (acquired resistance) as a result of subtherapeutic drug concentration or non-adherence to medication regimen (Wood & Iseman, 1993). MDR-TB is a global health threat and challenging to treat because access to drug susceptibility testing is poor, especially in low-income settings where tuberculosis is most prevalent. The MDR-TB treatment regimen is longer, and most second-line drug (SLD) treatments are unsuccessful, toxic, or both. In 2019, 3.3% of the new tuberculosis cases and 17.7% of previously treated cases globally had MDR-TB, and the MDR-TB treatment success rate was estimated to be relatively 28% lower than drug-sensitive (DS) (WHO, 2020). South Africa is part of the top 10 countries representing 70% of the global drug-resistant TB burden (Monedero-Recuero et al., 2021) and accounts for

approximately 10% of global rifampicin-resistant and MDR-TB (Motsoaledi & Matsotso, 2019).

The WHO currently recommends a shorter-course multidrug-resistant tuberculosis regimen, which incorporates high-dose isoniazid, ethionamide, ethambutol, bedaquiline, moxifloxacin, pyrazinamide, and clofazimine and has a treatment duration of 9-12 months (Mirzayev et al., 2021). A rare type of MDR-TB is extensively drug-resistant tuberculosis, defined as *M.tb* resistant to rifampicin and isoniazid, plus any fluoroquinolone and at least one additional Group A drug (i.e., , bedaquiline and linezolid) (WHO, 2020b).

1.4.3 Drug-drug interaction between ART and tuberculosis drugs

Whenever more than one drug is administered, which is always the case in TB treatment or patients co-infected with HIV and tuberculosis, drug-drug interactions (DDI) are possible. A DDI is the phenomenon observed when a response to a combination of drugs is different from the response to each agent when individually administered (Kannan et al., 2016). DDI is one source of medication errors that is widely under-recognised with a significant risk of harm to patients and costly for the healthcare systems (Khoo et al., 2014). DDIs can be classified into pharmacodynamics or pharmacokinetics DDI. Pharmacodynamics DDI occurs when drugs have an additive effect, increasing the overall effect, or opposing effect, decreasing or even cancelling the drug effect (Snyder, Polasek, & Doogue, 2012). In contrast, pharmacokinetics DDI occurs when the systemic concentration of one drug is changed by another drug, altering the amount or/and length of time that the drug is present at the site of action (Snyder et al., 2012). Pharmacokinetic DDIs are likely to increase or decrease the exposure of the drugs, leading to worse efficacy or toxicity, respectively. DDIs account for 16 - 20% of all adverse events in any hospital setting and 19% of drug-related adverse effects (Kannan et al., 2016).

Many well-known DDIs or potential DDIs scenarios arise when tuberculosis and HIV are treated at the same time. ARVs are among the drugs with a high risk for DDIs because of their ability to inhibit or induce liver enzymes such as *cytochrome P450 isoenzymes (CYPs)*, which metabolise a broad array of other drugs (Khoo et al., 2014). The risk of a drug being a victim of DDI depends on the drugs substrate. Below is a list of some potential DDIs that occurs within tuberculosis regimen or when co-administered with ARV. One of the extensively used and important treatments of tuberculosis rifampicin has a broad drug-drug interaction effect that might cause serious adverse events. Rifampicin induces the activities of several *CYPs* (e.g., *CYP2A6, CYP2B6, CYP2C3, CYP2C9, CYP3C19*, and *CYP3A4*), *uridine diphosphate glucuronosyltransferase (UGT)* and *Glutathione S-transferases (GSTs*), which are responsible for metabolising some ART and tuberculosis-treatment (Pelkonen et al., 2008). Efavirenz, a drug frequently prescribed initially for HIV therapy, induces *CYP3A4* and CYP2B6 while inhibiting *CYP2C19* and *CYP2C8* (Tsibris & Hirsch, 2015). Isoniazid is one of the safest and cost-effective medications for tuberculosis prophylaxis and is reported to inhibit *CYP2C19, CYP3A, CYP2E1, CYP1A2, CYP2D6* (Desta, Soukhova, & Flockhart, 2001), and *CYP2A6* (Luetkemeyer et al., 2015). The risk of DDIs differs with certain patient groups and clinical scenarios; this is why it is important to study the DDI or take them into account to optimise treatments.

1.4.4 Pharmacology of Isoniazid

Isoniazid is the most widely used antituberculosis drug. The drug was first synthesised in 1912 from ethyl isonicotinate and hydrazine, but its antituberculosis activity was only recognised in 1952 (BERNSTEIN et al., 1952). It was introduced into clinical use in 1954, resulting in a substantial drop in morbidity and mortality related to tuberculosis, becoming the cornerstone in most effective regimens against active or latent tuberculosis (Metushi et al., 2016).

Isoniazid has bacteriostatic and bactericidal activity against slow-growing and rapidly-growing *M.tb*, respectively. Also, it is recognised to be effective against intracellular bacilli in macrophages and extracellular *M.tb* (Mitchison & Selkon, 1956). It has excellent bactericidal activity against DS-TB; at the standard (5 mg/kg), reducing bacterial burden by 90 to 95% within the first two days of treatment (Donald & Diacon, 2008). In addition, isoniazid is widely approved, orally available, better-tolerated than many second-line antituberculosis agents, low-cost, and relatively free of drug-drug interactions (Dooley et al., 2020).

1.4.4.1 Absorption

Isoniazid is water-soluble and well absorbed, with a bioavailability of approximately 90%. The isoniazid absorption occurs mainly in the intestine (up to 60%) and is less absorbed in the stomach due to higher pH levels (Mariappan & Singh, 2003). Isoniazid absorption is reported to have a short and very variable delay of roughly 20 minutes before reaching the systemic circulation (Wilkins et al., 2011). Following oral administration of a standard dose of either 5 mg/kg or 300 mg/day, a peak plasma concentration of 5 mg/L is achieved in 1 to 2 hours (Peloquin et al., 1997). In addition, isoniazid absorption (especially bioavailability) is reduced by concomitant food intake but unaffected by antacids. The effect of food on isoniazid absorption may be due to delay in gastric emptying or most likely due to the unabsorbable condensation which are formed when isoniazid reacts with various carbohydrates (Rao et al., 1971).

1.4.4.2 Distribution

Isoniazid is widely distributed in the body fluids (including cerebrospinal fluid and breast milk) and tissues, with an apparent volume of distribution of approximately 0.6 L/kg with the largest accumulation in the liver (Klein et al., 2016b). The drug penetrated caseous tissues,

and macrophages, hence its activity against intracellular *M.tb* (Kjellsson et al., 2012). Sturkenboom et al. reported low levels of isoniazid protein binding of approximately 6.54%.

1.4.4.3 Excretion

Isoniazid is predominantly metabolised (50 – 90%) by *N-acetyltransferase 2 (NAT2)* to N-acetylisoniazid (AcINH). The secondary pathways are amidase formulating hydrazine and isonicotinic acid and *CYP2E1* formulating metabolic intermediates. In humans, *NAT2* expression is highest in the liver and gut (specifically small intestine and colon) and is coded by a polymorphic gene (Husain et al., 2007). The distribution of acetylator status is trimodal, and individuals can be grouped into rapid, intermediate, and slow *NAT2* acetylator, and the isoniazid exposure of the different phenotypes differs considerably (Sabbagh et al., 2009). The difference in *NAT2* genotype is reported to account for 88% of the variability in isoniazid clearance (Klein et al., 2016b). Both the unchanged isoniazid and its metabolites are excreted via the kidney.

1.4.4.4 *NAT2* genotyping and acetylator status

NAT2 polymorphism was first discovered in 1960 when individual variability in isoniazid-induced neurotoxicity was attributed to genetic variability in *NAT2* activity (Price Evans et al., 1960). *NAT2* is encoded by 870-bp gene, and over 65 *NAT2* variants possessing one or more SNPs have been identified within this coding region (Muma & Shi, 1968). Seven most frequent SNPs in the *NAT2* gene (rs1801279 (191G>A), rs1041983 (282C>T), rs1801280 (341T>C), rs1799929 (481C>T), rs1799930 (590G>A), rs1208 (803A>G) and rs1799931 (857G>A)) have been reported to highly correlate with isoniazid acetylator status (Mrozikiewicz et al., 1996; Parkin et al., 1997; Wang et al., 2012). These have been identified as the gold standard for classifying *NAT2* acetylator status into rapid, intermediate, and slow

acetylator. The use of two SNPs (341, and 590) has an accuracy of 85.2%, three SNPs (341, 590, and 847) have an accuracy of 97.6%, while there was not much difference in accuracy when 5, 6, or 7 SNPs were used (Verma et al., 2021). A tag-SNP rs1495741 has also been reported to be strongly related to *NAT2* activity (García-Closas et al., 2011). Using the rs1495741 SNP alone has an accuracy of 77.7% (Hein & Doll, 2012).

1.4.4.5 Drug interaction

Isoniazid has a biphasic effect on the inhibition-induction of *CYP2E1*, which may result in increased toxic metabolites in fast acetylators (Dargan et al., 2011). Furthermore, *CYP2A6*, an ancillary metabolic pathway of efavirenz, is inhibited by isoniazid (Luetkemeyer et al., 2015), increasing the potential for interaction between the two drugs. Apart from this, isoniazid inhibits *CYP2C19*, *CYP3A*, *CYP1A2*, and *CYP2D6* (Desta et al., 2001). Chirehwa et al. 2018, reported a DDI between efavirenz and isoniazid, which results in reduced isoniazid exposures specifically for rapid *NAT2* acetylator , similar results were observed by Bhatt et al. 2014. Isoniazid may inhibit monoamine oxidase and cause hypertensive crisis in individuals who consume substances rich in monoamines (e.g., cheese and red wine) (Toutoungi et al., 1985). Wright et al. (1982) reported an increase in anticoagulant activity of warfarin due to isoniazid co-administration. Lastly, an increase in the half-life of isoniazid has been reported by drugs that increase microsomal enzyme activity in the liver, such as PAS, procainamide, and chlorpromazine and reduced by ethanol and other drugs that decrease microsomal enzyme activity in the liver (Holdiness, 1984).

1.4.4.6 Mechanism of action

Isoniazid is highly active against *M.tb* with a 0.05 – 0.20 mg/L concentration that inhibits the bacilli (Ad Hoc Committee, 1995). Isoniazid is a pro-drug that enters the mycobacterial cell by passive diffusion. The drug is activated by *M.tb* catalase-peroxidase enzyme (KatG) (Timmins & Deretic, 2006). The KatG-derived activated isoniazid has multiple cellular targets, the primary target is the enoyl acyl carrier protein reductase (inhA) enzyme, involved in the elongation of fatty acids in mycolic acid synthesis, unique and important in mycobacterial cell wall lipids (Banerjee et al., 1994). The activated isoniazid reacts with reduced nicotinamide adenine dinucleotide (NADH) to form isoniazid-NAD adduct and then attacks inhA (Rozwarski, 1998). The secondary target is Nicotinamide adenine dinucleotide phosphate (NADPH)-dependent dihydrofolate reductase, an enzyme involved in nucleic acid synthesis. This enzyme is reported by Argyrou et al. (2006) to be inhibited by isoniazid-NADP adducts. In addition, 16 other proteins involved in the metabolic activity of *M.tb* have been identified to bind to INH-NAD, reducing their activity (Argyrou, Jin, et al., 2006).

1.4.4.7 Mechanism of resistance

Isoniazid resistance is the most frequent antituberculosis drugs resistance, occurring at a frequency of 1 in 10^6 bacilli *in vitro*. Depending on the mutation, the resistant strain minimum inhibitory concentrations (MIC) vary from 0.2 to ≥ 100 mg/L (Dutta & Karakousis, 2017; Winder, 1982). Mutation in KatG is the major mechanism of isoniazid resistance, with approximately 50% - 80% of isoniazid resistance strains containing the KatG gene mutation (Zhang & Young, 1994). The mutation result in a range of moderate to high-level isoniazid resistance with MIC ranging from 2 to >10, and the partial deletion of the KatG gene is associated with MICs of >25.6 (Lempens et al., 2018). In addition to KatG mutation, isoniazid

resistance arises due to mutations in the promoter region of inhA operon, resulting in overexpression of inhA, or mutation at the inhA target site, lowering inhA affinity to isoniazid (Banerjee et al., 1994). InhA mutation tends to result in low-level resistance (MIC of 0.2 – 1 mg/L) and confer resistance to ethionamide and prothionamide (Vilchèze & Jacobs, 2014; Zhang & Young, 1994). Apart from the two most prevalent isoniazid resistance mechanisms, other sources of resistance are potential redox alteration, drug excretion by efflux pumps, and mycothiol biosynthesis alteration have been reported by Vilchèze & Jacobs., 2014.

1.4.4.8 Adverse events

Isoniazid adverse reactions include hepatoxicity, rash, peripheral neuropathy, mild central nervous system, and gastrointestinal effects. The risk of isoniazid-induced hepatoxicity is reported to be higher in rapid acetylators due to the increase in acetylhydrazine formation; however, contrasting results of higher risk in slow acetylators have also been reported (Bose et al., 2011; Huang, 2003; Wang et al., 2012). The risk of isoniazid hepatoxicity is age-related and increases markedly over 35 years (Black, 1974). Isoniazid-induced neurotoxicity is due to the effect of the drug on the vitamin B6 group metabolism. Isoniazid metabolite hydrazones inhibit the conversion of pyridoxine to pyridoxal phosphate, which also inactivates the latter, hence causing vitamin B6 deficiency (Miller, 1980). Common isoniazid-induced gastrointestinal side effects include nausea, vomiting and diarrhoea; however, these are very uncommon (Robson & Sullivan, 1963).

1.4.5 Pharmacology of bedaquiline

Bedaquiline is a diarylquinoline antibiotic is recently approved for the treatment of MDR-TB. Bedaquiline is highly active against *M.tb* and displays *in vitro* activity against DS and drug-

resistance strains at a MIC range of 0.002 – 0.013 mg/l (Sarathy et al., 2019). The drug has bactericidal activity against non-replicating *M.tb* at a therapeutically attenable concentration (Vocat et al., 2015). Studies have shown that the inclusion of bedaquiline in the DS regimen improve sputum conversion and reduce chemotherapy duration and relapse (Pym et al., 2016; Vocat et al., 2015). The bedaquiline mechanism of action is through the inhibition of adenosine triphosphate (ATP) synthesis, a crucial process to *M.tb* growth and survival (Sarathy et al., 2019). Pre-existing bedaquiline resistance mediated by spontaneous gene mutation is present in approximately 1 in 10^7 – 10^8 *M.tb* organisms (Andries et al., 2005).

Orally administered bedaquiline reaches its maximum plasma concentration at approximately 5 hours (Jannsen Products, 2015). The bioavailability of the drug is increased by around two-folds when given with a meal (van Heeswijk et al., 2014). Bedaquiline protein-binding is 99.9%, it is widely distributed throughout the body, and accumulates in tissues. Bedaquiline is metabolised primarily by *CYP3A4* into an active N-desmethyl metabolite referred to as M2. *CYP2C8* and *CYP2C19* are minor metabolic pathways (Li et al., 2019). M2 is 99.7% protein-bound, circulates at ten-fold lower concentrations than bedaquiline, and has 3-6 times less activity against *M.tb* than bedaquiline (van Heeswijk et al., 2014). Bedaquiline has a long terminal half-life of approximately 5.5 months, reflecting the slow release of the drug from the tissues into the systemic circulation (Jannsen Products, 2015). The clearance of bedaquiline is reported to be 52% faster in black individuals compared to other races (McLeay et al., 2014). Since bedaquiline is a substrate of *CYP3A4*, drugs that induce or inhibit the enzyme can affect bedaquiline exposures. Examples of such drugs are rifamycins, non-nucleoside reverse transcriptase inhibitors, protease inhibitors, and azole antifungals.

Bedaquiline adverse events include cardiac toxicity, hepatoxicity and can cause nausea, arthralgia and headache (Diacon, Donald, et al., 2012). Bedaquiline was found to increase the potential of QT prolongation via its M2 metabolite (Li et al., 2019). Prolonged QTc increases the risk of fatal arrhythmia torsade de pointes (TdP) and sudden cardiac death (Al-Khatib et al., 2018). Elevated liver transaminases are anticipated to occur in approximately 15-20% of patients administered bedaquiline (Pym et al., 2016).

1.4.6 Tuberculosis treatment efficacy measures

Predictors of long-term outcomes are essential in research assessing treatment response to quantify the efficacy of a drug, especially for long treatment regimens, as lengthy follow-up might be expensive and logistically challenging. Therefore, biomarkers and correlate endpoints predicting long-term outcomes are necessary. Early bactericidal activity (EBA) studies utilise the mycobacteria quantifying method to assess the drop in bacteria load over a period of 2 - 14 days, thus evaluating the EBA of a single drug or combination. These studies are relatively quick, their results are reproducible and provide information on the drug's efficacy in relation to dosage and pharmacokinetics (Rockwood et al., 2016).

The two most common methods of quantifying mycobacteria in EBA studies are measuring colony-forming units (CFU) and time to culture positivity (TTP). The two are most effective at quantifying actively-growing *M.tb*, which are considerably lower in number later in treatment, hence has limited ability to extrapolate EBA to later treatment period, but there are currently limited biomarkers capable of quantifying the slow- or non-growing *M.tb*. Routinely CFU is quantified by plating the sputum sample on a solid media, then incubating the culture in appropriate conditions for a specified period of time. The colonies formed on

the plate are manually counted to determine CFU, assuming that each colony has arisen from a single bacterium (MacLean et al., 2019). CFU is widely considered the gold standard for determining bacteria load but is labour intensive, error-prone, has a long turn-around-time, requires extensive bio-safety level 3, and mostly counts actively growing *M.tb*. An alternative way of quantifying *M.tb* is through the culture in liquid media and determination of TTP, which can be determined by a liquid culture system called Mycobacteria Growth Indicator Tube (MGIT). MGIT consist of small tubes with a solution containing oxygen in which *M.tb* is inoculated to grow. At the bottom of the tube is a special substance that starts to glow when the oxygen in the tube is reduced. *M.tb* metabolic activity depletes oxygen, hence the fluorescent light is used to detect whether or not the oxygen is used up, indicating the presence of *M.tb* (Hillemann et al., 2006). Studies have shown that TTP negatively correlates with CFU and that liquid media are more sensitive than solid media for mycobacteria sputum culture (Bowness et al., 2015; Diacon, Maritz, et al., 2012). The major shortfall of TTP is that it mostly quantifies bacterial load of growing *M.tb*, while non-replicating persisters, with little to nonmetabolic activity, have little contribution to oxygen depletion in MGIT (Sloan et al., 2015).

1.5 HIV treatment

HIV treatment strategies were introduced in 1987, five years after the discovery of the virus. Earlier regimen consisting of one or two drugs frequently led to treatment failure. In 1995 highly active antiretroviral therapy (HAART) composed of three or more agents were introduced and dramatically improved treatment outcomes (Piacenti, 2006). ART aims to maintain an individual's optimal health and eliminate HIV transmission by rapid and durable viral suppression in all persons with HIV (Saag et al., 2020). Hence viral load and CD4 count

are the most vital surrogate markers of treatment efficacy (Piacenti, 2006). Antiretroviral agents are classified based on their mechanism of action, with each class targeting a unique step in the replication cycle of HIV. The four most common classes include nucleoside reverse transcriptase inhibitors (NRTIs), non-nucleoside reverse transcriptase inhibitors (NNRTIs), protease inhibitors (PIs), and integrase strand transfer inhibitors (INSTIs). The key principle of HAART is the combination of drugs with different mechanisms of action, which prevent the virus from developing single-agent resistance. The standard of care regimen for most treatment-naïve patients includes two nucleoside reverse transcriptase inhibitors plus one non-nucleoside reverse transcriptase inhibitor or integrase strand transfer inhibitor (Saag et al., 2020).

1.5.1 Pharmacology of efavirenz

Efavirenz is a potent, widely used antiretroviral agent, a member of the nonnucleoside reverse transcriptase inhibitors, which was the preferred and now the alternative agent for the initial treatment of HIV infection in WHO guidelines (WHO, 2021a). The efavirenz mechanism of action prevents the formation of viral double-stranded DNA from the single-stranded viral RNA genome (Bristol-Myers Squibb, 2015). The suggested therapeutic range for efavirenz is 1 to 4 mg/L; however, concentrations below or above this range do not strictly result in treatment failure or toxicity, respectively (Desta et al., 2019).

Efavirenz has a long half-life of 52-76 hours after a single dose and 40-55 hours at steady-state since the drug induces its own metabolism (Bristol-Myers Squibb, 2015). Efavirenz is highly protein-bound (99.5 – 99.75), primarily to albumin (Boffito et al., 2003). The bioavailability of efavirenz increases with food intake, and a dose of 600 mg taken with food resulted in an increase of area under the concentration curve (AUC) by 28% (Bristol-Myers

Squibb, 2015). Efavirenz presents first-order kinetics at doses between 200 to 600 mg and saturable absorption with doses higher than 1200 mg (Barrett et al., 2002).

Efavirenz main metabolic pathway is *CYP2B6*, and *CYP2A6* is the minor pathway accounting for around 23% of overall EFV metabolism *in vitro* (Desta et al., 2007). *CYP2B6* is highly polymorphic, which represents a major source of interindividual variability in efavirenz exposures. These polymorphisms have been linked to the heterogeneity of treatment response and toxicity observed in patients receiving efavirenz (Rotger et al., 2006). *CYP2B6* genotype can be classified into four phenotypes: normal, intermediate, slow, and ultra-slow metabolisers with a difference in efavirenz clearance of approximately four folds between slow and normal metabolisers (Desta et al., 2019; Dooley, et al., 2015). Three nonsynonymous variants of *CYP2B6 are* reported to be associated with efavirenz exposure. These are rs3745274 (516 G→T) (Haas et al., 2009), rs28399499 (983 T→C) (Wang et al., 2006) and rs4803419 (15582 C→T) (Holzinger et al., 2012). The effect of the rs4803419 polymorphism is modest compared to the first two (rs3745274 and rs28399499 (Holzinger et al., 2012).
Drug-drug interactions resulting from *CYP2B6* inhibition increase efavirenz exposure, and once the activity of *CYP2B6* has been diminished, the influence of *CYP2A6* becomes more apparent (Iulio et al., 2009). Efavirenz can affect the metabolism of a large number of drugs since it induces *CYP3A4* and uridine diphosphate glucuronosyltransferase (UGT) and inhibits *CYP2C9* and *CYP2C19* (Fellay et al., 2005). The most common adverse event reported for efavirenz are early central nervous system symptoms, rash, hepatoxicity and hyperlipidaemia (Pérez-Molina, 2002).

1.6 Study justification

Preventing new *M.tb* infections and progression of latent tuberculosis is critical to reducing the burden of tuberculosis disease and deaths. To address this global need, WHO and the United Nations (UN) unanimously came up with the objective to end the tuberculosis epidemic by 2030 and endorsed WHO's END tuberculosis Strategy at the World Health Assembly in May 2014 (Singh et al., 2020). This strategy has led to an increase in tuberculosis treatment research and the development of new drugs and regimens. To achieve this goal, there is a need to prioritise research addressing the knowledge gap in identifying optimal tuberculosis regimens for treatment and prevention in neglected populations, especially pregnant women, and individuals with drug-resistant tuberculosis.

One study addressing the gap of knowledge for pregnant women was International Maternal Paediatric Adolescent AIDS Clinical Trials Network (IMPAACT) P1078, which investigated the safety and efficacy of administering isoniazid preventative treatment (IPT) to pregnant women living with HIV (Gupta, et al., 2019). In 2017 the WHO recommended that all HIV-infected persons residing in low- and middle-income regions where tuberculosis is endemic receive at least 6 months of isoniazid preventative therapy, including pregnant women. However, data on the safety and efficacy of administering IPT to pregnant women living with HIV (a population with a high risk of adverse events) while undergoing antiretroviral therapy (ART) were not available, and so was information on the optimal timing of IPT in pregnancy. This information is vital considering that pregnancy induces several *CYPs* while Isoniazid inhibits a few *CYPs*. In addition, the timing of the IPT is crucial since Ouyang et al. (2009) estimated an increased liver toxicity risk due to IPT in HIV-positive pregnant women compared to nonpregnant. Furthermore, not much is known about the pharmacokinetics of

isoniazid in pregnancy, and little information is available on efavirenz pharmacokinetics in pregnancy

Breastfeeding is recommended for neonates and infants since breastmilk provides optimal nutrition. Nevertheless, there is a risk of transmission in women with tuberculosis and the possibility of neonatal drug exposure via breast milk. Breastfeeding has been recognised to be safe in mothers who are no longer infectious and have drug-susceptible tuberculosis (Kodadhala et al., 2016). However, there is uncertainty in women with drug-resistant tuberculosis since second-line therapy may be less efficacious, and there are no published data describing the extent to which second-line drugs are excreted in breast milk and could subsequently expose breastfed infants (Loveday et al., 2020). Bedaquiline is of particular interest since the drug has a very long half-life, hence any toxic exposure in breast milk would be long-lived. Additionally, there is little information on the pharmacokinetics of bedaquiline in pregnant women.

There is accumulating evidence that high isoniazid doses are effective against tuberculosis with low to moderate levels of isoniazid resistance (Böttger, 2011; Lempens et al., 2018; Rieder & Van Deun, 2017). This in part, led to WHO recommending a shorter-course MDR-TB regimen that incorporates high dose isoniazid. However, the pharmacokinetics of high dose isoniazid within the MDR-TB regimen has not been well described. The larger number of drugs co-administered within the MDR-TB regimen compared to the DS regimen increase the potential of DDIs within the MDR-TB regimen.

The emerging threat of drug-resistance *M.tb* strain has made it essential to optimise and customise old and new drugs for individual patients or subgroups. This is to ensure that adequate concentrations of the active drug reach the target site and for the required time in all individuals. The AIDS Clinical Trials Group (ACTG) A5312, INHindsight study investigated

the optimal dose of isoniazid for patients with isoniazid-resistant tuberculosis mediated by inhA mutations.

1.7 Objective

This thesis aims to utilise population pharmacokinetics and pharmacodynamic modelling to improve tuberculosis and HIV treatment in neglected populations using data from patients with tuberculosis and/or HIV.

- Specific objectives in pregnant women:
    - Characterize the effect of pregnancy on isoniazid, efavirenz and bedaquiline.
    - Analyse the influence of genetic polymorphisms in the metabolism of efavirenz and isoniazid and their DDI.
    - Characterise the exposure of the bedaquiline in breastmilk.
- Specific objectives in adults with MDR-TB
    - Characterise the pharmacokinetics and pharmacodynamics of standard and high doses of isoniazid (5 – 15 mg/kg).
    - Analyse the DDIs between isoniazid and concomitant drugs within the MDR-TB regimen.

Chapter 2: Methodology

2.1 Study designs and data description

2.1.1 IMPAACT P1078 study

P1078 (NCT01494038) was a Phase IV, multicentre, randomized, double-blind, placebo-controlled non-inferiority study to determine safety, risks, and benefits of immediate versus deferred isoniazid preventative therapy in HIV-infected pregnant women and their infants (Gupta, et al., 2019). The study enrolled 956 pregnant women (≥ 18 years old) between 14 and 34 weeks (34 weeks, 6 days) of gestation, with high risk for tuberculosis infection and disease (i.e., reside in high tuberculosis prevalence area, defined as having 60 tuberculosis cases per 100,000 population in the WHO tuberculosis annual report or documented local burden). The study sites were located in 8 countries: Haiti, Thailand, India, Uganda, Zimbabwe, Botswana, South Africa, and Tanzania.

The women were required to be on WHO standard of care HIV treatment, weigh more than 35 kg at screening, with an absolute neutrophil count of ≥ 750 cells/mm^3, haemoglobin ≥ 7.5g/dL, platelet count ≥ 50,00/mm^3, aspartate transaminase (AST), alanine transaminase (ALT) and total bilirubin ≤ 1.25 times the upper limit of normal. Women with positive tuberculosis symptoms reported to be exposed to isoniazid in the past year prior to the study, evidence of acute hepatitis, peripheral neuropathy, or heavy alcohol use were excluded from the study. Adherence to isoniazid (or placebo) was monitored by self-report, and pill count was defined as the percentage of expected doses/pills taken during the entire treatment period, while ART adherence was self-reported.

At enrolment, participants were randomized 1:1 to either Arm A (immediate isoniazid treatment) or Arm B (deferred isoniazid treatment). Participants were stratified by gestational age in each arm as follows:

Stratum A: ≥ 14 to < 24 weeks gestational age at study entry

Stratum B: ≥ 24 to ≤ 34 weeks (34 weeks, 6 days) gestational age at enrolment.

Participants in arm A (immediate isoniazid treatment) received 300 mg of isoniazid once daily, initiated at enrolment and continued for 28 weeks. After 28 weeks, participants were switched to placebo until 40 weeks postpartum. Participants in arm B were given placebo from enrolment to 12 weeks postpartum, then switched to 300 mg isoniazid daily dose from 12 to 40 weeks postpartum. Isoniazid or a matching placebo was administered without food (1 hour before or 2 hours after a meal). All participants received open-label pyridoxine (vitamin B6) and prenatal multivitamins from enrolment to 40 weeks postpartum. The study duration was from enrolment through to 48 weeks post-delivery. Intensive pharmacokinetic sampling was performed on a subset of participants, with PK samples drawn at pre-dose, 1, 2, 4, 6, 8, and 12 hours post-dose. A single sparse PK samples (at ≥ 2 hours post-dose) were captured in the rest of the participants, who were not part of the intensive PK study. Both sparse and intensive samples were captured during the antepartum (between 28 – 40 weeks gestation) and postpartum visit (week 16 postpartum (± 4 weeks)).

The blood samples were centrifuged at 800 G for 10 minutes, and plasma was aliquoted into cryovial and immediately frozen at -70°C. The samples were later transported to the division of Clinical Pharmacology, University of Cape Town, where they were later thawed, and drug plasma concentrations were determined by liquid chromatography-tandem mass spectrometry.

The captured PK samples were used to quantify the concentration of both isoniazid and efavirenz. Isoniazid calibrations range from 0.105 to 25.0 mg/L, the inter-day accuracy and precision ranged from 92.2% to 104.5%, and 6.5% to 10.8%, respectively (Chirehwa et al., 2018b). Efavirenz calibration range from 0.0195 to 20.0 mg/L, the inter-day accuracy and precision ranged from 95.2% to 100.2%, and 3.2% to 11.3%, respectively(Dooley at al., 2015). The study schema is presented in **Figure 2.1**.

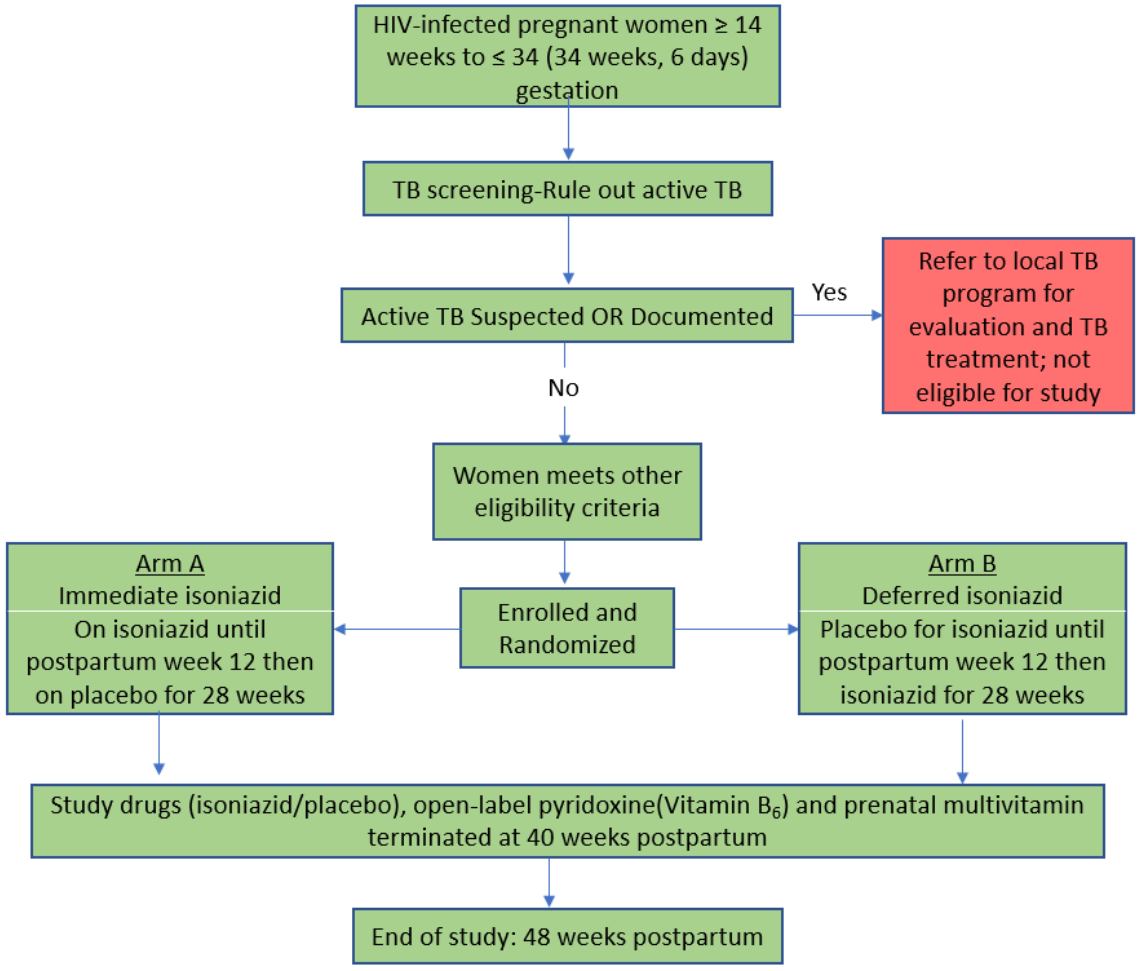

Figure 2.1: Schematic representation of the IMPAACT P1078 study

2.1.2 ACTG A5312 INHindsight study

The INHindsight study (NCT01936831) was a two-step, phase IIa, open-label, randomized clinical trial examining the bactericidal activity of isoniazid (INH) at different doses for

treatment of isolates with *inhA* mutations or *katG* mutations and DS-*M.tb* at the standard dose (Dooley et al., 2020). The study was conducted at a single site and laboratory (Task Applied Science, Cape Town, South Africa).

The study enrolled adults (age ≥ 18 ≤ 65 years) with sputum smear-positive pulmonary tuberculosis with a strain shown to have *inhA* promoter or gene mutations but not *katG* mutations (*inhA* group) or neither *inhA* nor *katG* mutations (control group). Participants were required to weigh between 40 and90 kg, have an absolute neutrophil count of >750 cells/mm^3, haemoglobin of >7.4 g/dL, platelet count of >50,000/mm^3, AST and ALT of <3 times the upper limit of normal (ULN), total bilirubin of <2.5 x ULN. Individuals with HIV were required to have a CD4 count >50 cells/mm^3 to participate. The exclusion criteria included nervous system tuberculosis patients receiving second-line tuberculosis drugs for more than 7 days, and grade 2 or higher peripheral neuropathy.

The enrolled participants all received vitamin B6 ≥25 mg daily for 7 days. Those with DS-TB received isoniazid 5 mg/kg daily for 7 days. While those with *inhA* mutated *M.tb* were randomised 1:1:1 to receive 5, 10, or 15 mg/kg daily for 7 days. **Figure 2.2** displays the schematic of the INHindsight study design. Sputum samples were collected overnight over 16 hours at pre-entry (day -1), pre-treatment (day 0), and then daily during isoniazid monotherapy administration (day 1-7). Minimal inhibitor concentration (MIC) was determined using 1% agar proportion method. Pharmacokinetic samples were captured on day 6 after isoniazid initiation; the samples were drawn at pre-dose, 0.5, 1, 2, 4, 6, 8, 12, and 24 hours post-dosing. The processing of the samples was similar to that of IMPAACT P1078 study presented in **section 2.1.1**.

Blood samples for routine safety testing were captured at entry, day 7 and day 21. The participants were transitioned to local tuberculosis program after completion of study treatment. The sputum and pharmacokinetic sampling schedule are shown in **Figure 2.3**.

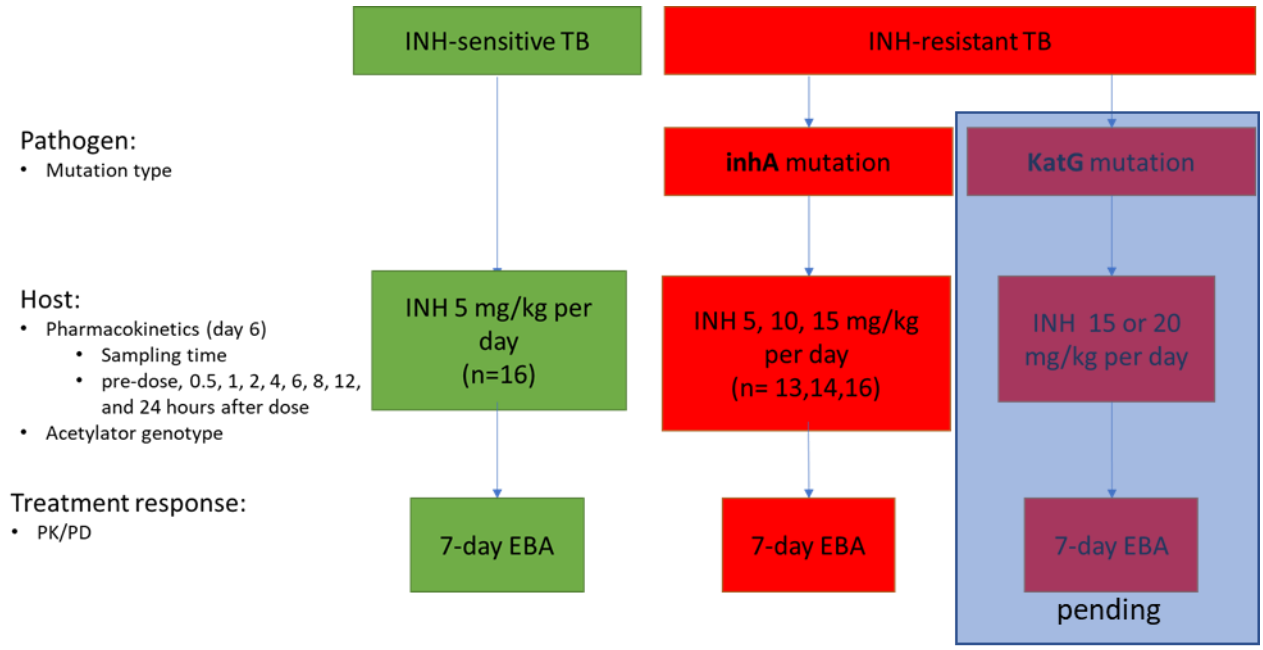

Figure 2.2: schematic of the INHindsight study design. The KatG arm data is not yet available.

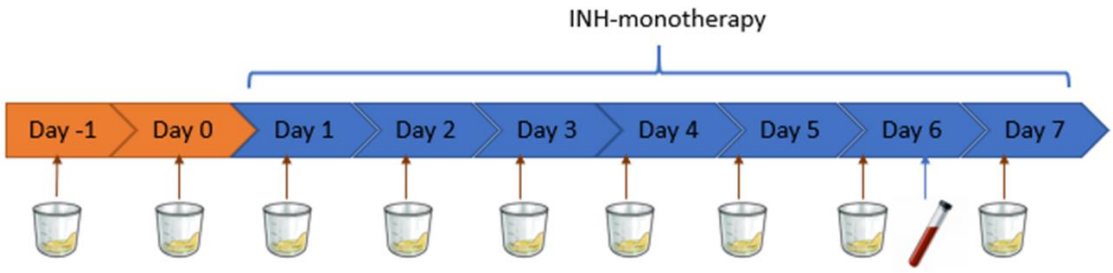

Figure 2.3: schedule for sputum and pharmacokinetic sampling in the INHindsight study.

2.1.3 PODRtb study

Pharmacometric Optimization of Second Line Drugs for MDR Tuberculosis Treatment (PODrtb, ClinicalTrials.gov Identifier: NCT02727582) was an observational cohort study in patients with pulmonary MDR-TB, using pharmacometric models to define the PK-efficacy

and -toxicity relationship of MDR-TB treatment (Court et al., 2019). The study was conducted at the Brooklyn Chest and DP Marais tuberculosis hospitals in Cape Town, South Africa. The target population were adults (>18 years of age) diagnosed with pulmonary MDR-TB or rifampicin-monoresistant tuberculosis, eligible for the standard MDR-TB treatment regimen. At the time of the study (between 2016 and 2017), the standard MDR treatment regimen comprised pyrazinamide, moxifloxacin, kanamycin, cycloserine (dosed as terizidone), ethionamide and/or isoniazid. Critically ill or medically unstable patients (e.g., organ failure – on a ventilator, receiving dialysis, fulminant hepatitis) were excluded from the study.

Blood samples were collected following observed drug dose, approximately 4 (2-6) weeks after the start of treatment, to characterise the steady-state population PK of the MDR-TB drugs over a 24-hour dosing interval. In addition, a subset of the study participants was enrolled in a comparative substudy in which the MDR-TB drugs were administered as crushed tablets. These participants had 2 PK visits: the first in which they received the drugs as whole tablet formulations (as the rest of the cohort) and the second, 1-2 weeks later, where the drugs were administered as crushed tablets. Further details of the study procedure are provided in **section 5.3.2**. In this thesis, we focus on the pharmacokinetics of isoniazid. Participants with rifampicin-mono-resistant tuberculosis were treated with standard doses of isoniazid (5 mg/kg), while those with low-level isoniazid resistance were given high doses of isoniazid (10–15 mg/kg). Dosing was performed under fasting conditions. Blood sampling was scheduled at pre-dose and 2, 4, 6, 8, and 10 h post-dose on both pharmacokinetic sampling occasions. The processing of the samples was the same as the ACTG A5312 study presented in **section 2.1.2**.

2.1.4 Bedaquiline in pregnant women study

This thesis analysed data from an observational study assessing treatment, pregnancy and infant outcomes in women exposed to second-line tuberculosis treatment while pregnant (Loveday et al., 2020). The study also characterised plasma concentrations of the second-line tuberculosis drugs in these women and their infants. The study site was King Dinuzulu Hospital (KDH) in Durban, KwaZulu-Natal, an area with a high burden of tuberculosis and HIV and the third-highest incidence of DR-TB in South Africa (Loveday et al., 2020). The study aimed to review the management of pregnant women on second-line tuberculosis drugs to help inform their future management. The inclusion criteria included women ≥18 years of age with DR-TB who were pregnant at the time of diagnosis or fell pregnant during the lengthy treatment.

A subset of the study participants was enrolled in a PK substudy aimed at enhancing the understanding of the second-line tuberculosis drug exposure in pregnant women, breastmilk and infants. Two pharmacokinetic sampling visits were scheduled, the first prior to delivery in the third trimester and the second at 6 weeks post-delivery, to compare pregnant versus postpartum drug levels. During the postpartum visit, the infant and breast milk samples were collected.

In this thesis, we focus on the pharmacokinetics of bedaquiline in the study population. Bedaquiline was administered at a loading dose of 400 mg once daily for two weeks before switching to a maintenance dose of 200 mg three times a week (Monday, Wednesday, and Friday), as per guidelines. The pharmacokinetics samples were captured during the maintenance dosing of bedaquiline. The samples were drawn immediately prior to dosing and at 2, 4, and 6 hours post-dose if the pharmacokinetic visit corresponded to the dosing day. If the PK visit was on a day the women were scheduled to take the bedaquiline the next day,

then four PK samples were captured 2 hours apart, and the time of the last dose was recorded. If available, breastmilk samples were taken from breastfeeding mothers at the same time as the blood draws. The times of breastfeeding was recorded. For each infant a single PK sample was drawn on the day of the postpartum visit to assess infant drug exposure. The blood samples were centrifuged at 800 G for 10 minutes, and plasma was aliquoted into cryovial and immediately frozen at were stored at -80°C and transported to the University of Cape Town, Division of Clinical Pharmacology laboratory, where plasma and breastmilk bedaquiline and M2 assays were performed using liquid chromatography with tandem mass spectrometry. Further details of the methodology used to quantify bedaquiline and M2 concentration are provided in **section 4.3.2.**

2.2 Pharmacometrics

Pharmacometrics is the science of developing and applying statistical and mathematical models to characterise, understand, and predict a drug's pharmacokinetics, pharmacodynamics, biomarker and clinical outcomes (Ette & Williams, 2013). Essentially pharmacometrics describes the pharmacokinetics-pharmacodynamics behaviour of drugs by applying quantitative models representing the biology, pharmacology, physiology, and disease progress in relation to the effects and adverse drug reactions in patients (Jeffrey S Barrett et al., 2008)

Pharmacokinetics describes the dynamic movements and the time course of drug concentration in different body spaces such as plasma, blood, urine and tissues (Gabrielsson & Weiner, 2016). Simply put, pharmacokinetics describes what the body does to the drug, i.e., a drug's absorption, distribution, metabolism, and excretion processes.

Pharmacodynamics describes the relationship between drug concentration at the site of action and the resulting effect, including the time course and intensity of therapeutic and adverse effects (Southwood et al., 2018). Together pharmacokinetics and pharmacodynamics characterise the relationship between dose and response. The US Food and Drug Administration (FDA, 1999) recommends the use of a branch of pharmacometrics called population pharmacokinetic modelling to identify differences in safety and efficacy of drugs among population subgroups.

2.2.1 Population pharmacokinetics

Population pharmacokinetics is the study of variability in drug concentrations among individuals after the administration of clinically relevant dosage regimens (Aarons, 1991). Certain individual characteristics, such as demographical, pathophysiological, and therapeutical (e.g., bodyweight, metabolic function, presence of other therapy), can alter the dose-concentration-response relationships. Population pharmacokinetics seeks to identify factors that are associated with a significant shift in drug exposure to suggest an appropriate dose modification.

2.2.2 Nonlinear mixed-effects modelling

Data collected for pharmacokinetics analysis frequently involves longitudinal data like drug concentrations of the same participants captured at various times points after single or multiple doses. In longitudinal studies, observations captured from the same individual over time are not independent of each other, therefore it is required to apply special statistical techniques that take into account the fact that the observations are correlated (Twisk, 2013).

Mixed-effects modelling accounts for the correlation of observation via the inclusion of random effects.

Population pharmacokinetics applies nonlinear mixed-effects modelling to jointly analyse the individual data contributed by all sampled patients. The population model consists of a structural model, i.e. a function describing the typical time course of the response variable (i.e. drug concentration), and a stochastic model, i.e. individual parameters are treated as random variables across the patient population(Mould & Upton, 2012). The model is able to separate and estimate different sources of variability in parameter estimates, namely between-subject variability (BSV), between-occasion variability (BOV), and residual unexplained variability (RUV).

The nonlinear mixed-effects model can be mathematically described as follows:

$$y_{ij} = f(x_{ij}, \theta_i) + \varepsilon_{ij}$$

where y_{ij} is the continuous dependent variable of the j^{th} patient at the i^{th} sample. f is the function describing the individual prediction based on the individual parameter θ_i (parameters like clearance and volume). x_{ij} *is* the independent variable describing dose, time and covariates, and ε_{ij} is the residual errors assuming normal distribution with mean zero and variance δ^2.

$$\theta_i = \theta_p \cdot e^{\eta_i}$$

Where θ_p is the population parameter value and η_i is the random effect describing the random deviation between individual parameter value and the population parameter, it is assumed to be a gaussian distribution with mean zero and estimated variance of ω^2.

In population models, the variability is often grouped into two layers, the random effect is classified as level one (L1) parameters, and the random variability in residual error is classified

as level two (L2). The participant's ID is called the L1 data item since it is used to group observation according to the L1 random effect (i.e., parameter-level random effect). The L2 is the second layer of variability, at observation level, also called residual unexplained variability. When simultaneously modelling two types of response variables the model has a separate error term for each response variable. If these observations are obtained at the same time or even from the same sample (e.g. parent and metabolite) a correlation between the error terms might exist; meaning that whichever circumstance may have affected the observation of the one variable, may have affected in a similar or contrary fashion the other variable. (e.g., often circumstances influencing the concentration of the parent would also affect the metabolite). In such a case, characterisation of covariance between the ε variables should be explored. The NONMEM L2 data item is used to group observations according to level two random effects, grouping observations within individual records (i.e., observation-level random error) (Boeckmann et al., 2011).

Population pharmacokinetics modelling offers several advantages over classical analysis methods such as non-compartmental (NCA) analysis. Firstly, it does not suffer from the same strict requirement on data as NCA (i.e., rich sampling and adherence to sampling schedule) but allows for the analysis of sparse data without compromising the results. Therefore, increasing the feasibility of studies and reducing the burden of frequent blood sampling (Collart et al., 1992). Population pharmacokinetics allows analysis of data from unbalanced designs, and strict adherence to protocol sampling times in all patients is not required. Consequently, it is possible to analyse integrated data from different studies. Hence population pharmacokinetics is suitable for situations in which a traditional study design with intensive sampling and large numbers of patients in each cohort is not possible. This includes

studies in elderly patients, pregnant women, or paediatric, who do not lend themselves to the usual forms of pharmacokinetic analysis (FDA, 1999).

Secondly, population pharmacokinetics offers a semi-mechanistic platform enabling the model to identify relationships between parameters and physiological processes. Finally, population pharmacokinetic models are more reliable for prediction and extrapolation, which are challenging in NCA because there is no guarantee that predictions based on NCA results are physiologically plausible (Vo et al., 2017). On the contrary, prediction and extrapolation are easily achievable in population pharmacokinetics using simulations of validated models. Simulations can be used to facilitate treatment optimisation or assess drug response in other sub-populations or improve study design, and it is an effective tool in reducing the sample size required for analysis (Gobburu & Marroum, 2001).

2.2.3 Pharmacodynamics

Pharmacodynamics describes the mechanism of drug action and define the relationship between drug exposure and response (Upton & Mould, 2014). Numerous methods to characterize exposure-response relationships are available, the type of data will guide the decision on which method to use. The most common tuberculosis pharmacodynamic endpoint is clearance of M.tb from sputum (sputum negativity) or time to sputum negativity when getting repeated sputa, which have moderate sensitivity (Linguissi et al., 2014). A more robust endpoint for tuberculosis is the extent of bacterial killing, which is frequently quantified by the change in CFU or TTP after a specified treatment period (bacterial time-kill curves) (Chen et al., 2017) discussed in **section 1.4.6** in chapter 1. PK/PD indices are also commonly used to evaluate antibiotics' exposure-response relationship and guide dose

selection (Chen et al., 2017). However, PK/PD indices have several shortfalls as they ignore the time-courses of the PK, PD and bacterial dynamics (Nielsen & Friberg, 2013).

An empirical model can describe the time-kill curves (decline in CFU) with constant exponential decline rates (mono- or bi-exponential). Alternatively, bacterial load (CFU) can be described by a simple mechanism-based model involving a single or several bacterial compartments assuming a first-order rate constant for bacterial multiplication (k_{growth}) and a first-order rate for the death of the bacteria (k_{death}). The equation explaining the observed exponential growth of the bacteria seen in the time-kill curve without the addition of drug can be written as follows:

$$\frac{dB}{dt} = k_{growth} \times B - k_{death} \times B$$

Where *B* is the bacteria burden (e.g., quantified as CFU). Often there is insufficient information in the data to separately define the multiplication and death rate constants, hence the net result of the growth rate and the death rate is estimated ($k_{net} = k_{growth} - k_{death}$) (Nielsen & Friberg, 2013).

The growth of the *M.tb* in MGIT until TTP is achieved can be described by an exponential or logistic growth model. The logistic growth model is applied when the bacterial count has the capability to reach the system carrying capacity (N_{max}).

$$N_{MGIT}(T) = N_0 \cdot e^{k_{growth} \cdot T} \text{ (Exponential growth model)}$$

$$N_{MGIT}(T) = \frac{N_{max}}{1 + \left(\frac{N_{max} - N_0}{N_0}\right) e^{-k_{growth} \cdot T}} \text{ (Logistic growth model)}$$

where N_{MGIT} is the number of bacteria in the MGIT culture, *T* is the time elapsed since inoculation at which the bacteria in the MGIT reaches the detection threshold (TTP achieved). N_0 is the number of bacteria inoculated in the MGIT, and N_{max} is the carrying capacity of the

MGIT culture. To jointly model the CFU and TTP, it is assumed that the relative amount of CFU corresponds to the MGIT inoculum (N_0) since CFU quantify the bacterial load in the patient at the time of sputum collection. A delay in the growth of the bacteria in the MGIT has been observed in some experiments. This can be due to the fact that during inoculation, the bacteria might not be in their logarithmic growth phase. The possible causes are post-antibiotic effects of drugs administered to the patients during treatment and the harsh treatment of the bacteria with sodium hydroxide and other antibiotics during the decontamination process for the sputum (Chigutsa et al., 2013). As a result, the bacteria might require recovering before growing in the MGIT. This delay is captured using a lag time in the growth of the bacteria in MGIT.

To link the drug concentration to its bactericidal effect, there is a need for a mathematical function describing the PKPD relationship. The mathematical function frequently used to describe the PKPD relationship is a sigmoidal E_{max} model.

$$E = \frac{E_{max} \cdot C^{\gamma}}{EC_{50}^{\gamma} + C^{\gamma}}$$

Where E_{max} is the maximum effect that the drug can achieve and EC_{50} is the drug concentration that would result in half of the maximum effect. C is the concentration driving the response, and γ is the Hill or sigmoid factor that describes the steepness of the exposure-response relationship and, in most cases, is fixed to 1 (Nielsen & Friberg, 2013). This relationship is popular as it originates from the receptor theory. When sufficiently high concentrations cannot be achieved to identify E_{max}, simpler equations are used to describe the exposure-response relationship. The simpler equations include linear or power functions (Upton & Mould, 2014). The concentration (C) modulating the effect can be plasma concentration (direct response model), or there might be a delay in the onset of response

relative to plasma concentration. The delayed response can be described by an indirect model like the effect compartment model or the indirect effect/turnover model.

2.3 Software

Pharmacokinetic analyses in this thesis were performed in NONMEM 7.4/7.5, using the first-order conditional estimation with interaction (FOCE-I) followed by Sampling Important Resampling (SIR) and/or non-parametric bootstrap to determine the parameter precision (Boeckmann et al., 2011). Perl-speaks-NONMEM version 4.8.1, Pirana version 2.9.9, and R with the package xpose4 were used to facilitate model development, tracking and documentation, data manipulation, and generation of model diagnostics (Keizer et al., 2013).

2.4 Procedure for model development

Generally, the pharmacokinetics model development procedure begins with identifying the correct structural model. This implies testing several alternative models, from simple to more complex, starting with a one-compartment structural model with first-order absorption and elimination, then trying two- or three-compartments disposition, more complex absorption (lagged, transit compartments, or saturable) or elimination (nonlinear clearance or semi-mechanistic models). The random variability tested in the model included random effects at subject, occasion (each dose) and visit (each PK sampling visit) level and were assumed to follow a lognormal distribution. The residual unexplained variability was described either by additive, proportional or combined error models. The effect of body size on disposition parameters was described with allometric scaling using total body weight or fat-free mass as the size descriptor (Holford & Anderson, 2017).

Model development was guided by evaluating the drop in the objective function value (ΔOFV) of nested models, and Akaike information criteria (AIC) (Olofsen & Dahan, 2015) was used for non-nested models. OFV was assumed as χ^2-distributed, with a 3.84 drop in OFV being significant at $p<0.05$ for one additional parameter (i.e., 1 degree of freedom). Furthermore, an inspection of a set of diagnostic plots, including visual prediction checks (VPCs), physiological plausibility, and clinical relevance of the results, were considered in model development decisions.

To include covariates in the model, we first selected potential covariates based on prior knowledge, biological plausibility, therapeutic interest, information from experts and scientific interest. Secondly, we assessed the distribution and range of the covariates to evaluate the strength of the data in identifying an association, if one exists. Thirdly, we evaluated if there was a correlation between the covariates. If a correlation existed between two or more covariates, then we kept the most meaningful/plausible one and tested them separately. Then we searched for trends in the parameters versus covariates plots, keeping in mind that they might be affected by shrinkage. These plots aided in identifying the shape of the relationship for the continuous covariates, hence informing the equation (i.e., linear, power, Emax, exponential, two-spline) to be used when testing the covariate. Categorical covariates were evaluated using a different factor for each classification compared to the reference value (Mould & Upton, 2013). The inclusion of covariates was investigated using a supervised stepwise approach with forward inclusion ($p<0.05$) and backward elimination ($p<0.01$, $\Delta OFV=6.64$ for $df=1$).

Concentrations below the limit of quantification (BLQ) were handled in a manner similarly to the M6 method proposed by Beal et al. and with the additive error term for all imputed value inflated by half of the lower limit of quantification (LLOQ) to mitigate the effect of imputation

(Beal, 2001). When the terminal phase of a pharmacokinetic profile contained a series of LLOQ values, only the first was used for estimation in the model fit, while subsequent LLOQ values were ignored in the fit but retained for simulation-based diagnostics such as VPCs.

Chapter 3: Pharmacokinetics and drug-drug interactions of isoniazid and efavirenz in pregnant women living with HIV in high TB incidence settings: importance of genotyping.

3.1 Abstract

World Health Organization guidelines recommend that individuals living with HIV receive ≥6 months of isoniazid preventive therapy, including pregnant women. Yet, plasma isoniazid exposure during pregnancy, in the antiretroviral therapy era, has not been well described. We investigated pregnancy-induced and pharmacogenetic-associated pharmacokinetic changes and drug-drug-interactions between isoniazid and efavirenz in pregnant women. 847 women received isoniazid for 28 weeks, either during pregnancy or at 12 weeks postpartum, and 786 women received efavirenz. After adjusting for *NAT2* and *CYP2B6* genotype and weight, pregnancy increased isoniazid and efavirenz clearance by 26% and 15%, respectively. Isoniazid decreased efavirenz clearance by 7% in *CYP2B6* normal metabolizers and 13% in slow and intermediate metabolizers. Overall, both isoniazid and efavirenz exposures were reduced during pregnancy, but the main determinants of drug concentration were *NAT2* and *CYP2B6* genotypes, which resulted in a 5-fold difference for both drugs between rapid and slow metabolizers.

3.2 Introduction

HIV and tuberculosis (TB) are leading causes of morbidity and mortality among women of reproductive age, particularly among those living in low- and middle-income countries (LMIC) (Selwyn et al., 1989; WHO, 2017). Pregnant women living with HIV have an increased susceptibility to tuberculosis infection and progression from latent TB infection to active disease (Singh & Perfect, 2007). To reduce the risk of HIV-associated TB, the World Health Organization (WHO) recommends 6 months of isoniazid preventive treatment (IPT) along with antiretroviral therapy (World Health Organization, 2018). This recommendation was also made for pregnant women, based on limited data. Both antiretrovirals and anti-TB regimens often include drugs that inhibit or induce liver enzymes, including cytochrome-P450 (CYP) isoenzymes, causing potential drug-drug interactions (Khoo et al., 2014). The situation is further complicated in pregnancy, which is associated with physiological changes, altered body weight and composition, changes in plasma protein concentrations, and other processes that can affect drug pharmacokinetics (PK) (Dickmann & Isoherranen, 2013; Jeong, 2010; Pinheiro & Stika, 2020; Tsutsumi et al., 2001).

The metabolism of both efavirenz (a commonly used antiretroviral to treat HIV) and isoniazid are affected by genetic polymorphisms in specific drug-metabolizing genes, and plasma drug levels can be further influenced by pregnancy. Studies to date, while small in number of participants and limited in geographic diversity have shown, a predicted 2-fold increase in *CYP2B6* activity during pregnancy (Dickmann & Isoherranen, 2013). Dooley et al. (Dooley, et al., 2015) observed a 19% increase in plasma efavirenz clearance during pregnancy compared to the postpartum period, and Olagunju et al. (Olagunju et al., 2015) reported similar findings. Furthermore, an ancillary metabolic pathway of efavirenz, *CYP2A6*, is inhibited by isoniazid, thus potentially causing a drug-drug interaction (Luetkemeyer et al., 2015). There is currently

little data regarding the effect of pharmacogenomics and pregnancy on isoniazid PK and on the drug-drug interaction between isoniazid and efavirenz in pregnancy and postpartum.

As part of the recently completely IMPAACT study P1078 TB APPRISE trial which investigated the safety and efficacy of administering IPT to pregnant women living with HIV, and reported a significantly higher rate of adverse pregnancy outcomes in women who received IPT during pregnancy (Gupta, et al., 2019), we analysed the key pharmacogenetic polymorphisms of efavirenz and isoniazid metabolism, the changes in the drug concentrations and PK of these two drugs during pregnancy, and their drug-drug interactions.

3.3 Methods

3.3.1 Participants and study design

This analysis used PK data collected in IMPAACT study P1078. The study design is reported in the primary manuscript (Gupta, et al., 2019), summarised here and we report the PK procedure. IMPAACT study P1078 was a prospective, double-blind, placebo-controlled, randomized, noninferiority trial conducted in eight countries, and had a total of 13 sites. Local and collaborating institutional review boards approved the trial, and all women provided informed consent. Full details on ethics approval are provided in primary manuscript (Gupta, et al., 2019).

HIV-positive pregnant women ≥ 18 years old were recruited if gestational age was 14 to 34 weeks, on WHO-recommended HIV treatment for prevention of mother-to-child transmission, weighing more than 35 kg. At study entry, women were randomized either to Arm A (immediate 28 weeks of 300-mg isoniazid daily treatment, then placebo) or Arm B

(deferred isoniazid treatment, placebo until week 12 postpartum, then 28 weeks of 300-mg isoniazid). Adherence to isoniazid (or placebo) was monitored by self-report and pill count defined as the percentage of expected doses/pills taken during the entire treatment period, while ART adherence was self-reported.

3.3.2 Sample collection

Intensive samples were captured at pre-dose, 1, 2, 4, 6, 8, and 12 hours post-dosing, while sparse sampling occurred at least 2 hours post-dosing. Both sparse and intensive samples were captured on two visits: during pregnancy (between 28-40 weeks gestation) and week 16 postpartum (± 4 weeks). Blood samples were centrifuged at 800 G for 10 minutes, and plasma was aliquoted into cryovials and immediately frozen at -70°C to await further processing. Plasma concentrations were determined by liquid chromatography-tandem mass spectrometry. Isoniazid calibrations range from 0.105 to 25.0 mg/L, the inter-day accuracy and precision ranged from 92.2% to 104.5%, and 6.5% to 10.8%, respectively (Chirehwa et al., 2018b). Efavirenz calibration range from 0.0195 to 20.0 mg/L, the inter-day accuracy and precision ranged from 95.2% to 100.2%, and 3.2% to 11.3%, respectively (Dooley, et al., 2015).

Composite *CYP2B6* genotype was defined based on combinations of four polymorphisms as follows: normal (1: 15582CC-516GG-983TT or 2: 15582CT-516GG-983TT); intermediate (3: 15582TT-516GG-983TT; 4: 15582CC-516GT-983TT; 5: 15582CC-516GG-983CT; 6: 15582CT-516GT-983TT; or 7: 15582CT-516GG-983CT); and slow metabolizer genotype (8: 15582CC-516TT-983TT; 9: 15582CC-516GT-983CT; 10: 15582CC-516GG-983CC, each with or without 11: -48GT; and 12: -48GG) (Holzinger et al., 2012). Individuals with 983CC were considered

ultra-slow metabolizers (The term “normal” is used for consistency with standard nomenclature, not to suggest that others are abnormal.) For *NAT2*, genotypes were categorized based on combinations of rs1801279 (*NAT2**14), rs1801280 (*NAT2**5), rs1799930 (*NAT2**6), and rs1799931 (*NAT2**7), as slow, homozygous for the variant allele at any of the four loci (i.e., AA, CC, AA, AA, respectively), or heterozygous at 2 or more loci; intermediate, heterozygous at a single locus; or rapid, no variant allele at any locus (i.e., GG, TT, GG, GG, respectively) (Boukouvala sotiria et al., 2016; McDonagh et al., 2014). Genotyping was done in VANTAGE (Vanderbilt Technology for Advanced Genomics) using MassARRAY® iPLEX Gold (Agena Bioscience™, California, USA) and Taqman (ThermoFisher Scientific, Massachusetts, USA).

3.3.3 Data Analysis

Isoniazid and efavirenz concentrations were interpreted using population PK modelling using NONMEM version 7.4.3 (Boeckmann et al., 2011). Perl-speaks-NONMEM version 4.8.1, Pirana, and R with the package xpose4 were used to facilitate the model development process, data manipulation, and generation of model diagnostics (Keizer et al., 2013). To describe the PK of both isoniazid and efavirenz, one- and two-compartment models were tested with first-order absorption (with or without lag time or a chain of transit compartments), and first-order elimination. Since both drugs are mainly hepatically cleared, a well-stirred liver model (Gordi, Xie, Huong, et al., 2005), was tested to capture the effect of first-pass metabolism. The liver hepatic blood flow Q_h (Yang et al., 2007) was assumed to be 90 L/h in a typical individual and adjusted for the effect of body size using allometric scaling (Mehvar, 2018). The free fraction (f_u) of efavirenz and isoniazid in plasma were fixed to 0.5% (Alghamdi et al., 2018) and 95% (Sturkenboom et al., 2015), respectively. The pre-hepatic bioavailability of a typical individual was fixed to a reference value of 1.

The intensive data was used to develop the base model since these women were monitored closely, dosing was observed, and richer sampling schedule allowed for the identification of the structural model. This model was then used to explore the sparse data and identify implausible values, which were flagged as outliers and removed from model development analysis. An extreme value of conditional weighted residuals (CWRES) (Hooker et al., 2007), i.e., absolute value ≥ 4, was used as a criterion to identify outliers. Since CWRES values for data observations arising from the postulated model are assumed to be normally distributed, randomly obtaining an absolute value ≥ 4 has a probability of <0.00633%, only a chance of 1 out of 10,000. We assumed that pharmacokinetics of both drugs were at steady state at the time of PK visit unless participant had been on efavirenz for less than 16 days (Eckhardt & Gulick, 2017), or missed dose in the previous 3 days had been reported.

Random effects at occasion- (each dose), visit- (each PK sampling visit), and/or subject-level were included on the pharmacokinetic parameters if statistically significant using a lognormal distribution. Between-occasion-variability (BOV) was tested on absorption parameters, while between-visit-variability (BVV) and between-subject-variability (BSV) were tested on disposition parameters. A combination of proportional and additive error was used to model unexplained residual variability.

Model development was guided by evaluating the drops in objective function value (ΔOFV) of nested models. The OFV was assumed as χ^2-distributed, hence with a 3.84 drop in OFV being significant at $p<0.05$ for one additional parameter (i.e., 1 degree of freedom). Besides statistical significance, a set of diagnostic plots, including visual prediction checks (VPCs) and physiological plausibility of the results were considered in model development decisions.

Since enzyme metabolic status has been widely reported to critically affect pharmacokinetics of both drugs, *NAT2* genotype effect on isoniazid clearance and *CYP2B6* and *CYP2A6* genotype

on efavirenz clearance were tested early in model development process (Luetkemeyer et al., 2015; Parkin et al., 1997). Allometric scaling was applied on all clearance and volume of distribution parameters (Anderson & Holford, 2008) to account for body size effect. Other covariate effects on the PK parameters, including pregnancy and drug-drug interaction, were investigated using a stepwise approach with forward inclusion ($p<0.05$) and backward elimination ($p<0.01$).

Concentrations below limit of quantification (BLQ) were handled similarly to M6 method by Beal (Beal, 2001), to mitigate the effect of the M6 method imputation the additive error for the imputed values was inflated by LLOQ/2. Only subset of participants were included in the genotype study, those with missing genotypic information where assigned a phenotype using mixture model (Keizer et al., 2012). Participants with missing weight and height were assigned the typical values depending on whether pregnant or postpartum. The original protocol focused on IPT, hence did not include capturing ART PK information (i.e., efavirenz dosing time) for sparse sampling. This was later amended, resulting in 32% of the women having a missing efavirenz dosing time in at least one PK visit during the early phase of the trial. Women with missing dose times during one visit were assumed to take medication at the same time throughout the trial consistently; therefore, dosing time of the recorded visit was imputed on the missing visit. For women with missing dosing time at both visits, a median dosing time (i.e., 20:30) from the data was imputed.

3.4 Results

3.4.1 Study profile

PK samples were available from 847 women on 300-mg isoniazid (748 of whom were treated with efavirenz (600mg dose), 80 with nevirapine, 17 with lopinavir, and 2 with atazanavir based ART). Of the 847 on isoniazid, 32 underwent intensive sampling (at pre-dose, 1, 2, 4, 6, 8, and 12 hours post-dosing), providing 300 observations, while 815 underwent sparse sampling (at least 2 hours post-dosing), providing 1015 observations, of which 88 were identified as implausible outliers (outliers were identified per the description in **Methods**) and were removed from the model building process. 210 women had isoniazid profiles available during both pregnancy and postpartum, since they had started isoniazid at a late gestational age such that their 28 weeks of isoniazid had not elapsed prior to their postpartum PK visit.

The number of participants on efavirenz in the different arms (isoniazid or placebo treatment) varied because of ART switching over the course of the study, but the majority were on efavirenz. Of 786 women on efavirenz, 21 underwent intensive sampling, providing 266 observations, and 765 underwent sparse sampling, providing 1363 observations, of which 15 were identified as implausible outliers (outliers were identified per the description in **Methods**) then removed from the model building process. Baseline characteristics of all women are summarised in **Table 3.1.**

Table 3.1: Demographic, clinical, and laboratory characteristics of women on isoniazid and efavirenz during pregnancy and at postpartum.

Characteristics (median and range, or n and %)	**Participants in isoniazid PK analysis**		**Participants in efavirenz PK analysis**	
	Pregnancy (n=420)	**Postpartum (n=637)**	**Pregnancy (n=712)**	**Postpartum (n=670)**
Age (years)	29 (18 – 45)	29 (19 – 42)	29 (18-45)	29 (18-45)
Weight (kg)	68 (39 – 167)	62 (38 – 165)	67 (42 – 164)	61 (37 – 114)
Body mass index (kg/m^2)	27 (18 – 61)	24 (16 – 45)	27 (18 – 61)	25 (16 – 49)
Gestation/postnatal age (weeks) at PK sampling time	26 (14 – 34)	16 (7 – 23)	26 (14 – 34)	16 (7 – 23)
Baseline Viral load (copies/mL)	<40 (<40 – 237000)	<40 (<40 – 465000)	<40 (<40 – 237000)	<40 (<40 – 465000)
Drug regimen				
On isoniazid	420 (100%)	637 (100%)	352 (49%)	540 (80%)
On efavirenz	371 (88%)	563 (88%)	712 (100%)	670 (100%)
On nevirapine	11 (3%)	47 (8%)	-	-
On lopinavir/ritonavir	5 (1%)	5 (1%)	-	-
On atazanavir/ritonavir	2 (0%)	2 (0%)	-	-
Days on EFV at PK sampling time	125 (18 – 3800)	264 (1 – 4228)	125 (18 – 3800)	408 (1 – 4228)
Drug metabolizing genotype	***NAT2* acetylation status**		***CYP2B6* metabolizer status**	
Rapid	52 (12%)	70 (11%)	168 (24%)	146 (22%)
Intermediate	140 (33%)	202 (32%)	299 (42%)	264 (40%)
Slow	159 (39%)	199 (31%)	118 (16%)	102 (15%)
Ultra-slow	-	-	1 (0%)	2 (0%)
Missing	69 (16%)	166 (26%)	126 (18%)	156 (23%)
			***CYP2A6* metabolizer status**	
Normal			501 (70%)	439 (65%)
Intermediate			81 (11%)	71 (11%)
Slow			4 (1%)	4 (1%)
Missing			126 (18%)	156 (23%)

210 women had isoniazid profiles during both pregnancy and postpartum.

596 women had efavirenz profiles available during both pregnancy and postpartum.

3.4.2 Distribution of drug metabolizer genotypes

The distribution of drug metabolizer genotypes for *NAT2*, *CYP2B6*, and *CYP2A6* (classified into three phenotypes as described in the **Methods**), stratified by country, is illustrated in **Figure 3.1**. Rapid isoniazid acetylator *NAT2* genotypes (had site range of 4% – 31%) were the least

prevalent group in all 8 countries, which varied considerably by sites. Intermediate metabolizer *CYP2B6* (had site range of 43% – 63%), were frequent in all countries genotypes as were *CYP2A6* normal metabolizer genotypes (had site range of 76% – 93%).

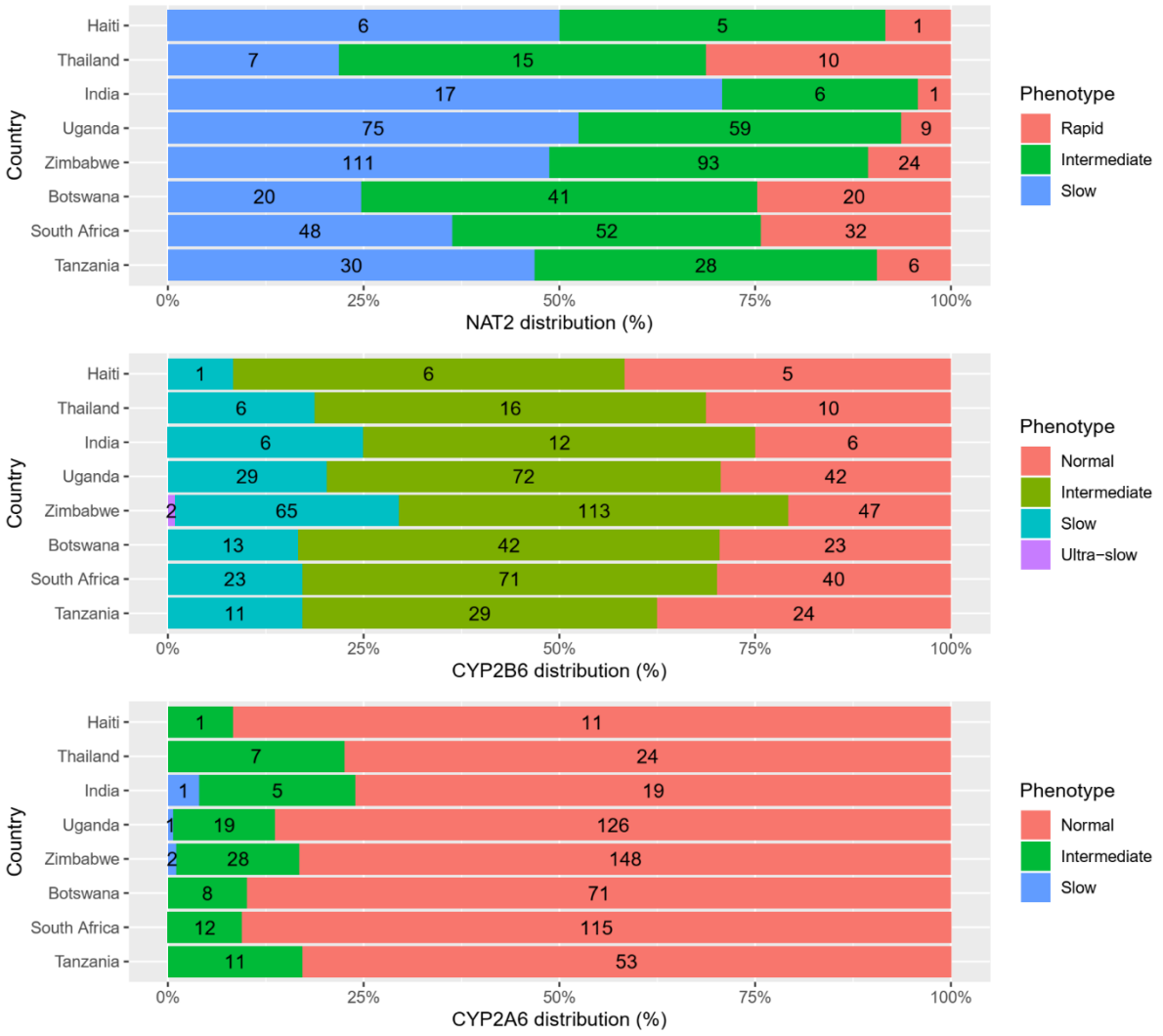

Figure 3.1: Distribution of the enzyme metabolizer genotypes for NAT2, CYP2B6, and CYP2A6 in the participants across the 8 countries involved in the study

3.4.3 Structural model

A two-compartment disposition model best described the PK of both isoniazid and efavirenz with first-order-absorption through a chain of transit-compartments (Savic et al., 2007). Drug elimination implemented with a well-stirred liver model (Gordi, Xie, Huong, et al., 2005), was able to describe both hepatic clearance and first-pass extraction (E_H) with the parameter of

hepatic intrinsic clearance (CL_{int}), as shown in **Figure 3.2**. Parameter estimates for isoniazid and efavirenz, and the precisions for each are presented in **Table 3.2** and **Table 3.3**, respectively.

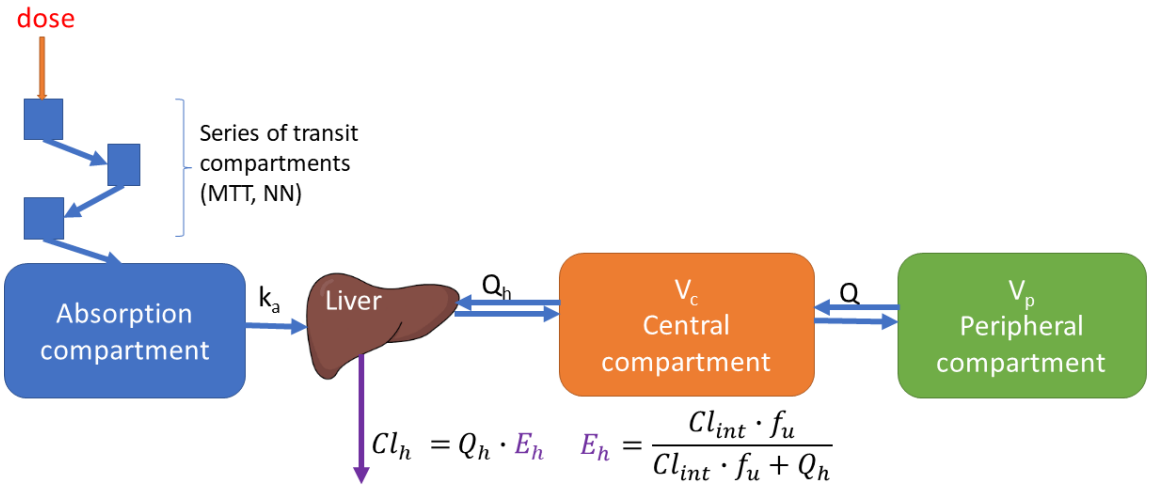

Figure 3.2: Schematic representation of the PK model of both efavirenz and isoniazid. The absorption is described with a series of transit-compartment to capture the delay in absorption, and a rate constant ka. The hepatic extraction (Eh) is responsible for both first-pass metabolism and the systemic elimination with first-order kinetics. Vc represents the volume of distribution in the central compartment. Drug transfer between the central and peripheral compartment is defined by intercompartmental clearance Q/F, were F represents the oral bioavailability.

3.4.4 Isoniazid Pharmacokinetics – Covariate effects

Allometric scaling was applied to all clearance, volume, and liver parameters to account for body size effect, improving the fit, and explaining part of between-subject variability (ΔOFV = −44). When fat-free mass replaced bodyweight for allometric scaling of clearance (but not volume) parameters, it improved the fit of the model (ΔOFV = −6.27). The population parameters of clearance were normalised to an individual with fat-free mass of 39 kg and for volume to a weight of 67 kg. *NAT2* genotype significantly affected clearance of isoniazid (ΔOFV = −273, χ^2 df=2 $p \ll 0.001$), as CL_{int} varied greatly between rapid, intermediate, and slow acetylators. After adjusting for body size and *NAT2* genotype, pregnancy was found to increase clearance by 26% (ΔOFV = −49.6, χ^2 df = 1 $p \ll 0.001$). There was no significant difference in clearance between participants on the four different ART (efavirenz, nevirapine-

, lopinavir/ritonavir-, and atazanavir/ritonavir-based) regimens (ΔOFV = −6.34, χ^2 df = 3 p =0.0964). Inclusion of pregnancy on any other parameter, including the central compartment volume of distribution did not improve model fit.

Table 3.2: Final PK parameter estimates for isoniazid

Parameter	Typical Value (95% CI[a])	Variability[b], %CV (95% CI[a])
CL_{int}[c] (L/h) *NAT2* Rapid	72.3 (61.5 – 86.7)	69.2 (64.2 – 74.2)*
CL_{int}[c] (L/h) *NAT2* Intermediate	38.5 (34.6 – 43.2)	
CL_{int}[c] (L/h) *NAT2* Slow	14.5 (13.1 – 16.0)	
V_c[d] (L)	37.6 (33.9 – 40.7)	
V_p[d] (L)	13.3 (10.5 – 16.9)	
Q/F[c] (L/h)	3.32 (2.53 – 4.54)	
k_a (1/h)	2.69 (1.91 – 3.51)	145 (116 - 172)[#]
MTT (h)	0.342 (0.209 – 0.459)	116 (98.7 - 150)[#]
NN	48.4 (22.2 – 83.8)	
Q_H[c] (L/h)	90 FIXED	
fu (%)	95 FIXED	
Prehepatic relative bioavailability	1 FIXED	12.3 (8.20 – 15.7)[#]
Proportional error (%)	13.2 (11.3 – 15.3)	
Additive error (mg/L)	0.0378 (0.0335 -0.0449)	
Pregnancy effect on CL (%)	**+26.2 (19.8 – 33.2)**	

Abbreviations: CL_{int} clearance intrinsic; V_c apparent central volume of distribution for INH; V_P apparent peripheral volume of distribution for INH; Q/F apparent intercompartmental clearance for INH; k_a first-order rate constant of INH absorption; MTT absorption mean transit time; NN Number of absorption transit compartment; Q_H blood liver flow (Yang et al., 2007); fu unbound fraction of isoniazid in plasma (Alghamdi et al., 2018).

[a] 95% confidence intervals (CIs) were obtained with the SIR procedure

[b] Variability was modelled with log-normal distribution and is presented as an approximate percentage CV.

[c] Clearance parameters are allometrically scaled based on fat-free mass (typical value reported for 39 kg which was the median fat-free mass weight of the study population). $CL = \theta_1 \times \left(\frac{FFM}{39}\right)^{0.75} \times e^{BSVCL}$

[d] Volume pf distribution parameters are scaled based on weight (typical value reported for 67 kg which was the median weight of the study population). $V = \theta_2 \times \left(\frac{WT}{67}\right)^{1}$

** Between subject variability (BSV).*

[#] Between occasion variability BOV.

Figure 3.3 displays the model-predicted individual exposures of isoniazid stratified by both *NAT2* genotype and pregnancy status. The $AUC_{0\text{-}24}$ of isoniazid boxplot shows that isoniazid exposure differs between the three genotypes, and decreased exposures were observed during antepartum compared to postpartum in all three genotypes. Combining all genotypes, the overall median (interquartile range) of isoniazid $AUC_{0\text{-}24}$ antepartum was 8.05 (4.43-16.7)

mg·h/L, compared to 11.1 (6.26 – 23.9) mg·h/L postpartum. Maximum concentrations (C_{max}) during pregnancy and postpartum were 2.89 (1.97 – 4.13) mg/L and 3.69 (2.64 – 5.13) mg/L, respectively. The postpartum $AUC_{0\text{-}24}$ was 1.4-fold greater compared to antepartum, while slow acetylator $AUC_{0\text{-}24}$ was 5-fold greater compared to rapid acetylators. An isoniazid $AUC_{0\text{-}24}$ of 10.52 mg·h/L has been associated with 90% of early bactericidal activity in patients with active tuberculosis (Donald et al., 2007).

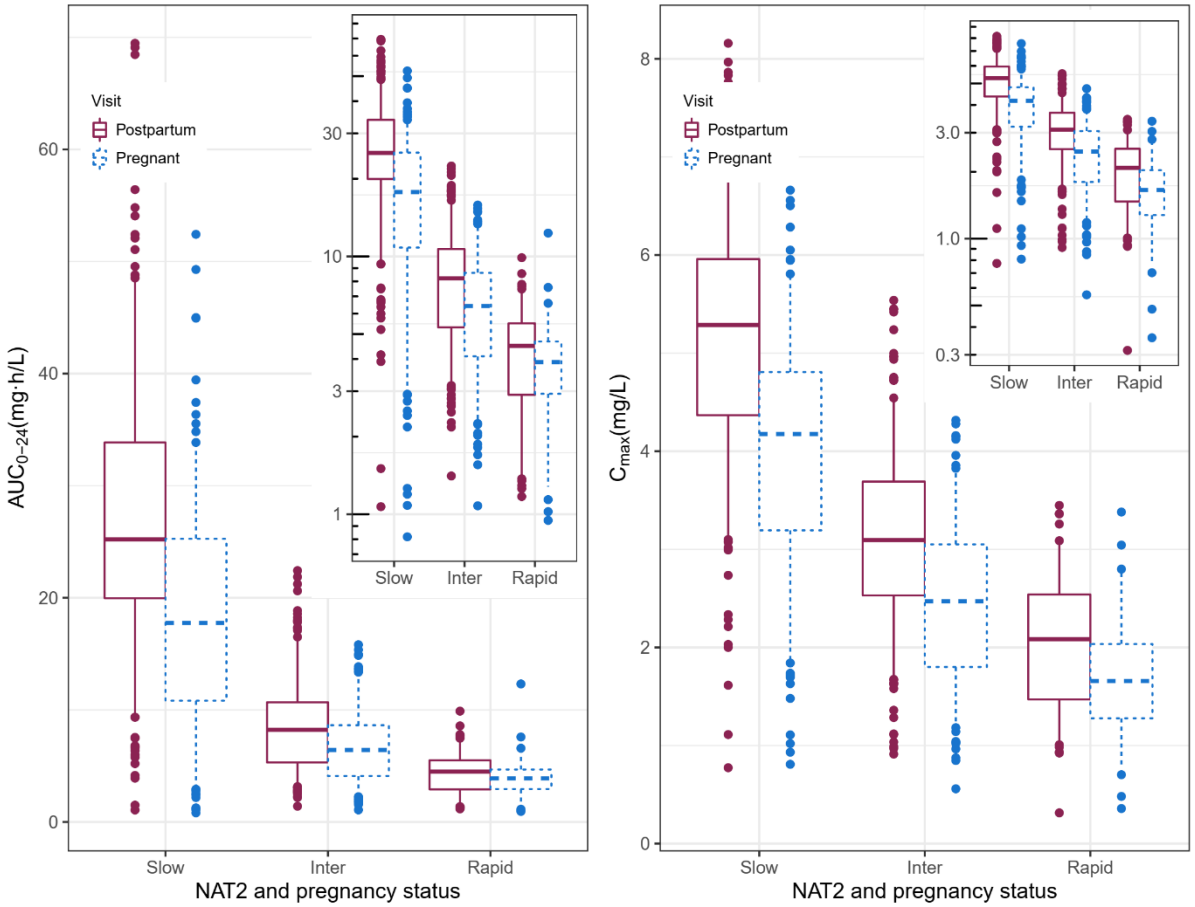

Figure 3.3: Isoniazid exposures stratified by NAT2 genotype and pregnancy. The box plot (with box representing median and inter-quartile range and whiskers the 5th-95th interval)) summarises isoniazid C_{max} on the right and $AUC_{0\text{-}24}$ on the left for the three genotypes (slow, intermediate, and rapid acetylator) for both the antepartum (red solid line) and postpartum (blue dashed lines) visit. $AUC_{0\text{-}24}$ was calculated by integrating between the 0 and 24hr after dosing time points. The inset panel shows the same values on the log-scale.

3.4.5 Efavirenz pharmacokinetics - Covariate effects

Efavirenz had a structural model similar to isoniazid, except the first-order absorption rate constant (k_a) was unstable when sparse and intensive data were pooled together; so, the value observed in the intensive PK data analysis was used as a fixed constant. Allometric scaling with bodyweight on all clearance and volume parameters improved the model fit and explained part of the between-subject variability (ΔOFV = −28.6). Using fat-free mass instead of total bodyweight for clearance (but not volume) parameters further improved the model (ΔOFV = −12.5). *CYP2B6* genotype significantly affected the clearance of efavirenz (ΔOFV = −399, χ^2 df = 2 p $\ll 0.001$). After adjusting for body size and *CYP2B6* genotype, pregnancy was found to increase the clearance of efavirenz by 16% (ΔOFV = −75.5, χ^2 df = 1 p $\ll$0.001). Clearance in women co-administrated isoniazid and efavirenz was 7% lower in normal metabolizers and 13% lower in slow and intermediate metabolizers (ΔOFV = −39.2, χ^2 df = 2 p $\ll$0.001) regardless of pregnancy status. Effect of *CYP2A6* phenotype on the clearance and bioavailability of efavirenz was investigated among *CYP2B6* slow metabolizers, in whom *CYP2A6* may be more important for efavirenz clearance, but no significant effect was observed.

Table 3.3: Final parameter estimates for efavirenz

Parameter	Typical Value (95% CI[a])	Variability, %CV (95% CI)
CL_{intri}[c] (L/h) *CYP2B6* normal	2690 (2300 – 3030)	53.8 (48.9 – 59.2)*
CL_{intri}[c] (L/h) *CYP2B6* intermediate	1940 (1790 – 2100)	
CL_{intri}[c] (L/h) *CYP2B6* slow	545 (487 – 624)	
V_c[d] (L)	135 (109 – 165)	
V_p[d] (L)	512 (487 – 623)	
Q/F[c] (L/h)	26.9 (19.8 – 36.5)	
k_a (1/h)	1.75 FIXED	180 (114.9- 227)[#]
MTT (h)	1.78 (1.20 – 2.39)	131 (103- 166)[#]
NN	48.4 (11.3 – 64.7)	
Q_H[c] (L/h)	90 FIXED	
fu (%)	0.5 FIXED	
Prehepatic relative Bioavailability	1 FIXED	23.2 (20.7 – 26.1)[#]
Proportional Error (%)	6.91 (4.72 – 9.45)	
Additive Error (mg/L)	0.353 (0.303 – 0.408)	
Pregnancy Effect on CL (%)	**+15.9 (9.75 – 21.9)**	
INH effect on CL/F (L/h) in *CYP2B6* Normal metabolizers (%)	**-6.87 (-12.1 – -1.13)**	
INH effect on CL/F (L/h) in *CYP2B6* Inter and slow metabolizers (%)	**-13.4 (-17.3 – -9.06)**	

Abbreviations: CL_{int} clearance intrinsic; V_c apparent central volume of distribution for INH; V_P apparent peripheral volume of distribution for INH; Q/F apparent intercompartmental clearance for INH; k_a first-order rate constant of INH absorption; MTT absorption mean transit time; NN Number of absorption transit compartment; Q_H blood liver flow; fu unbound fraction of efavirenz in plasma.

[a] 95% confidence intervals (CIs) were obtained with the SIR procedure

[b] Variability was modelled with log-normal distribution and is presented as an approximate percentage CV.

[c] Clearance parameters are allometrically scaled based on fat-free mass (typical value reported for 39 kg which was the median fat-free mass weight of the study population). $CL = \theta_1 \times \left(\frac{FFM}{39}\right)^{0.75} \times e^{BSVCL}$

[d] Volume pf distribution parameters are scaled based on weight (typical value reported for 67 kg which was the median weight of the study population). $V = \theta_2 \times \left(\frac{WT}{67}\right)^{1}$

** Between subject variability (BSV).*

[#] Between occasion variability (BOV).

The model-predicted individual exposures are shown in **Figure 3.4**, where panels A and B stratify by CYP2B6 genotype and pregnancy status, while panel C and D stratify by CYP2B6 genotype and isoniazid co-administration. **Figure 3.4** shows that efavirenz varied between the three genotypes, and panel A and B shows a decrease in exposures during pregnancy. The overall exposure of efavirenz was higher postpartum compared to pregnancy with median (interquartile range) postpartum $AUC_{0\text{-}24}$ of 70.6 (47.9 – 118) mg·h/L, compared to 55.8 (38.6 - 92.7) mg·h/L antepartum. Concentrations at 12 hours post-dosing (C_{12}) antepartum and postpartum were 2.18 (1.48– 3.68) mg/L and 2.69 (1.87 – 4.71) mg/L, respectively. Among

normal CYP2B6 metabolizers 13 (9%) women had postpartum efavirenz C_{12} of <1 mg/L compared to 25 (15%) women antepartum.

We observed a drug-drug interaction consisting of increased exposure of efavirenz in participants on concomitant isoniazid displayed in panel C and D of **Figure 3.4**. The difference in exposure in the slow and intermediate metabolizers was more apparent than in the normal metabolizers resulting in high concentration in slow CYP2B6 metabolizers. For example, choosing a threshold of 15 mg/L (similar to the upper quartile of C_{12} in CYP2B6 slow metabolizers co-administered isoniazid in **Figure 3.4** panel D), among *CYP2B6* slow metabolizers in the absence of isoniazid, efavirenz C_{12} was >15 mg/L in 4 (9%) individuals, compared to 45 (35%) individuals with presence of isoniazid. As a point of reference, a therapeutic range for plasma efavirenz concentrations of 1–4 mg/L has been suggested (Marzolini et al., 2001), although concentrations somewhat <1 mg/L do not consistently predict treatment failure and concentrations >4 mg/L do not consistently predict toxicity. The overall median (interquartile range) of $AUC_{0\text{-}24}$ was 66.8 (45.2 – 114) mg·h/L when isoniazid was present and 55.4 (39.7 - 98.1) mg·h/L when absent, corresponding to a 1.2-fold increase in efavirenz $AUC_{0\text{-}24}$ due to the presence of isoniazid. All four panels in **Figure 3.4** show that, while pregnancy and isoniazid affected efavirenz exposure, these effects were modest compared to CYP2B6 genotype, which resulted in a 5-fold difference between slow to normal metabolizers.

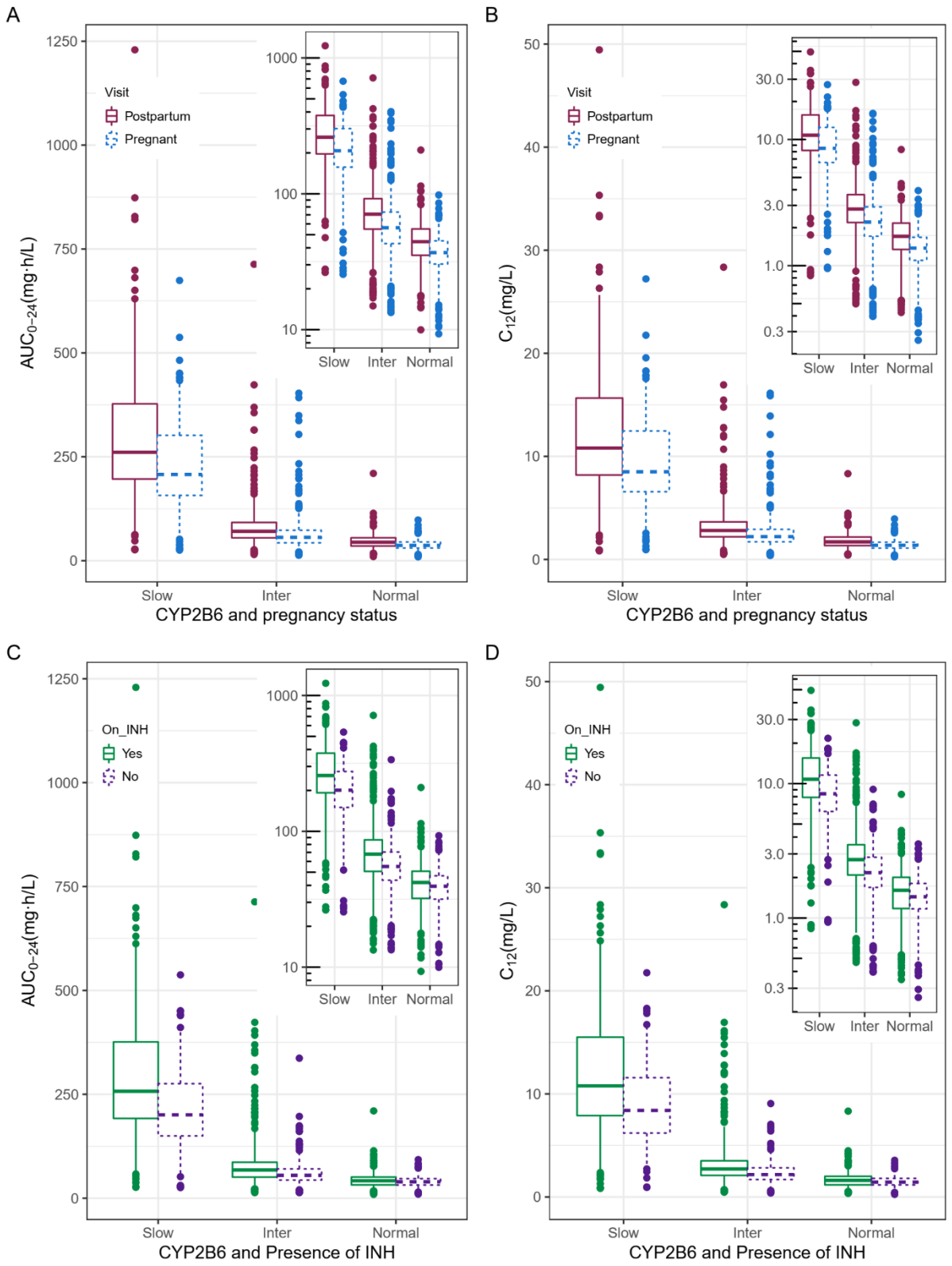

Figure 3.4: Efavirenz exposures stratified by CYP2B6 genotype, pregnancy and isoniazid co-administration Panel A and B displays box plot (with box representing median and inter-quartile range and whiskers the 5th-95th interval) summarizing AUC_{0-24} and C_{12} respectively for the three genotypes (slow, intermediate, and normal metabolizer) stratified by pregnancy (solid line) and postpartum (dashed lines) visit. While panel C and D stratify AUC_{0-24} and C_{12} respectively using INH co-administration

3.5 Discussion

We performed the largest study of its kind, assessing isoniazid and efavirenz PK, genetic polymorphisms, and drug-drug interactions in a geographic diverse population of pregnant and postpartum women living with HIV in high TB burden regions of the world. We show that pregnancy modestly increases the clearance of both isoniazid and efavirenz, therefore increasing the risk of low (and possibly sub-therapeutic) drug exposure during pregnancy. Notably, though we also show that drug metabolizer genotypes profoundly affect plasma exposure of these two drugs, to an extent far greater than of pregnancy. For this reason, the risk of lower plasma drug exposure during pregnancy is likely greatest only in women who are *CYP2B6* normal metabolizers or *NAT2* rapid acetylator, since they clear the drug faster compared to the other genotypes and are already exposed to lower concentrations. Additionally, we report that efavirenz exposure is increased by isoniazid co-administration, especially in *CYP2B6* intermediate and slow metabolizers. Lastly, high concentration observed in slow *CYP2B6* and *NAT2* genotype increases the risk of adverse effects.

The increase in clearance of isoniazid and efavirenz may be due to several physiological changes related to pregnancy, e.g., plasma albumin levels (Pinheiro & Stika, 2020), bodyweight and composition, plasma volume (Jeong, 2010), hepatic blood flow (Jeong, 2010), and induction or inhibition of drug metabolising enzymes. The pregnancy-induced increase in weight was accounted for in the model using allometric scaling, while no unbound concentration was captured, therefore we could not confirm or disprove the effect of pregnancy on the protein-binding of efavirenz. Antepartum increase in hepatic blood (Jeong, 2010), potentially increase the hepatic clearance of drugs with high hepatic extraction ratio, this may be more apparent in low binding drugs like isoniazid compared to efavirenz. The other reason for changes in drug clearance during pregnancy is induction or inhibition of drug-

metabolizing enzymes. Pregnancy increases the activity of *CYP2B6* (Dickmann & Isoherranen, 2013) and *CYP3A4* (Pinheiro & Stika, 2020) (major and minor route of efavirenz metabolism (Desta et al., 2019)). Tsutsumi et al. (Tsutsumi et al., 2001) observed a reduction in *NAT2* activity during pregnancy, but the reduction was clinically not significant. The reported clearance increase is modest compared to the large between-subject variability in drug exposure due to host genetics. However, these changes may be of relevance for rapid/normal metabolizers, who already experience lower exposure, as further increase in clearance might increase their risk for sub-therapeutic concentrations.

Similar to previous reports (Bertrand et al., 2014; Dooley, et al., 2015; Luetkemeyer et al., 2015), we observed a drug-drug interaction between isoniazid and efavirenz, as isoniazid decreases the clearance of efavirenz, particularly for intermediate and slow efavirenz metabolizers. This is thought to be due to isoniazid's inhibition of *CYP2A6* (Xia Wen et al., 2002). However, for individuals who are *CYP2B6* slow metabolizers, *CYP2A6* assumes increased importance in clearing efavirenz, so that *CYP2B6* slow metabolizers on isoniazid may have a higher risk of efavirenz toxicity. Our analysis did not detect any difference in isoniazid exposure between different ARTs (efavirenz-, nevirapine-, lopinavir/ritonavir-, and atazanavir/ritonavir-based), which contrasts with previous reports (Chirehwa et al., 2018a; Sekaggya-Wiltshire et al., 2018). However, it may be that our analysis was not powered to detect these differences since 88% of the participants were on efavirenz-based ART.

Previously reported isoniazid exposures varied widely between studies. This might be due to effects of large between-subject and -occasion variability, different proportions of *NAT2* acetylator genotypes, different drug formulations, drug-drug interactions, and instability of isoniazid in plasma (Poole & Meyer, 1960), which makes PK studies of isoniazid somewhat

challenging. This wide range is well summarised in a recent review by Daskapan et al. (Daskapan et al., 2019). Comparing our results with previous reports on non-pregnant populations (Daskapan et al., 2019; Seng et al., 2015; Zabost et al., 2013), we observed lower exposures of isoniazid for both pregnancy and postpartum visits, while the ratio in exposures between slow and rapid *NAT2* genotype was similar (clearance for rapid acetylators was observed to be 4-fold faster than those of slow acetylators). It is unclear if the relatively low concentrations we observed at both visits are due to efavirenz exposure, as most women were on efavirenz-based regimen. It is also possible that the effect of pregnancy on isoniazid clearance takes time to reverse fully, and women in the postpartum visit may also have clearance levels higher than the general (non-pregnant, adult) population. It has been previously discussed that using postpartum period as a control to study effects of pregnancy may be suboptimal because of factors that include lactation and delayed reversal of pregnancy-related physiological changes (de Kock et al., 2017). Efavirenz exposures in our study were in line with previous reports in non-pregnant individuals (Desta et al., 2019; L. Dickinson et al., 2015; Orrell et al., 2016). Similarly, the ratio between normal and slow *CYP2B6* metabolizers exposures was similar, with a C_{12} ratio of five.

In our study, we report genotype frequencies from a large cohort of patients with wide geographical representation. A frequency of *NAT2* slow acetylators above 50% worldwide has been reported (Sabbagh et al., 2011). Studies have shown greater than two-fold difference in the prevalence of *NAT2* slow acetylators in agriculturists (slow acetylators more prevalent) compared to pastoralists in central Asian population and sub-Saharan African populations (Patin et al., 2006). A pooled analysis by Sabbagh et al. (Sabbagh et al., 2011) shows the highest level of within-population diversity of *NAT2* genotype in Africans. In our study population, *NAT2* slow acetylators were most prevalent, followed by intermediate. Among

CYP genes in humans, *CYP2B6* is one of the most polymorphic gene (Zanger & Klein, 2013). A meta-analysis by Zhou et al. (Zhou et al., 2017) reported *CYP2B6* normal metabolizer status in 61%, 38%, 76%, 45%, and 58% in Europeans, Africans, East Asians, South Asians, and admixed Americans respectively. In comparison, 65%, 65%, 31%, 66%, and 72% distribution of *CYP2A6* normal functioning gene were reported in Europeans, Africans, East Asians, South Asians, and admixed Americans, respectively. In the present study, Intermediate followed by normal metabolizer *CYP2B6* genotypes were frequent in all countries, as were *CYP2A6* normal metabolizer genotypes.

Our study had some limitations, much of which we believe have been mitigated by use of a model-based approach analysis. Genotype data was not available in a subset of patients, 179 (21%) for isoniazid, and 173 (22%) for efavirenz, but this was addressed by imputation using a mixture model to assign individuals with missing information to a phenotype group. Blood draws during sparse sampling visits were scheduled for 2 hours after isoniazid dose. Because efavirenz is typically taken at night, this resulted in concentrations drawn 10-14 hours after efavirenz dose. Exact time of dose was not always reliably recorded for sparse sampling visits. For a portion of the study, timing of ART dosing was not recorded, so that information was imputed. While imputed data cannot be expected to be fully accurate, our approach was feasible to implement and expected to be robust since most women were taking efavirenz in the evening and were sampled the following morning, hence the slow terminal half-life (40 - 55 hours (Squibb, 2010)) and accumulation of efavirenz minimized the impact of imprecise dosing time information. The uncertainty around self-reported or imputed dosing times and sampling schedule chosen for the sparse data may be the reasons for high variability observed in the absorption parameters, but this had a minor effect in our analysis since the structural model was built using the intensive data which had rich and reliable information for the entire

PK profile. Similarly, the method we used for the identification and exclusion of implausible outlier values prevented these few samples from affecting the development of the PK models.

In conclusion, our study showed modest reductions in isoniazid and efavirenz exposure during pregnancy compared to postpartum. While the size of this effect is modest and unlikely to be of clinical significance for most patients, lower exposure may be important in normal *CYP2B6* and rapid *NAT2* acetylator, for whom the resulting concentrations may be sub-therapeutic, thus possibly leading to ineffective treatment and development of drug resistance. We also confirm the previously reported increased efavirenz exposure in individuals on concomitant isoniazid. This effect was overall modest but was most pronounced in *CYP2B6* intermediate and slow metabolizers, who already had higher efavirenz levels and may therefore, be at higher risk of efavirenz-related toxicities.

3.6 Supplementary material

Table s3.1: Participants Phenotype distribution of NAT2, CYP2B6, and CYP2A6 across the 8 countries.

***NAT2* Distribution**					
Country	Rapid	Intermediate	Slow		Total
Tanzania	6 (9%)	28(44%)	30(47%)	-	64
South Africa	32(24%)	52(40%)	48(36%)	-	134
Botswana	20(25%)	41(51%)	20(25%)	-	78
Zimbabwe	24(11%)	93(41%)	111(49%)	-	227
Uganda	9(6%)	59(41%)	75(52%)	-	143
India	1(4%)	6(25%)	17(71%)	-	24
Thailand	10(31%)	15(47%)	7(22%)	-	32
Haiti	1(8%)	5(42%)	6(50%)	-	12
Total	103(14%)	301(42%)	314(44%)	-	714
CYP2B6 Distribution					
	Normal	Intermediate	Slow	Ultra-slow	Total
Tanzania	24 (38%)	29(45%)	11(17%)	-	64
South Africa	40(30%)	71(53%)	23(17%)	-	134
Botswana	23(29%)	42(54%)	13(17%)	-	78
Zimbabwe	47(20%)	113(50%)	65(29%)	2(1%)	227
Uganda	42(29%)	72(50%)	29(20%)	-	143
India	6(25%)	12(50%)	6(25%)	-	24
Thailand	10(31%)	16(50%)	6(19%)	-	32
Haiti	5(42%)	6(50%)	1(8%)	-	12
Total	197(28%)	361(51%)	154(22%)	2(0%)	714
***CYP2A6* Distribution**					
	Normal	Intermediate	Slow		Total
Tanzania	53 (83%)	11(17%)	-	-	64
South Africa	115(91%)	12(10%)	-	-	127
Botswana	71(90%)	8(10%)	-	-	79
Zimbabwe	148(83%)	28(16%)	2(1%)	-	178
Uganda	126(86%)	19(13%)	1(1%)	-	146
India	19(76%)	5(20%)	1(4%)	-	24
Thailand	24(77%)	7(23%)	-	-	31
Haiti	11(92%)	1(8%)	-	-	12
Total	567(85%)	91(14%)	4(1%)	-	662

Table s3.2: Isoniazid clearance parameters stratified by NAT2 genotype

NAT2 Phenotype status	Intrinsic Clearance – CL_{int} (L/h)	Hepatic Clearance – CL_h (L/h)	Extraction Ratio - E_h (fraction)	Bioavailability after first pass – F_h (fraction)	Oral Clearance - CL/F (L/h)
Rapid	72.3	24.2	65%	35%	68.7
Intermediate	38.5	18.5	49%	51%	36.6
Slow	14.5	10.1	27%	73%	13.8

For a typical individual (67kg), liver hepatic plasma flow (Q_h) 37.4 L/h and scaled to each patient's size using individual FFM.

Table s3.3: Efavirenz clearance parameters stratified by CYP2B6 genotype

CYP2B6 Phenotype status	Intrinsic Clearance – Clint(L/h)	Hepatic Clearance – CLh (L/h)	Extraction Ratio - Eh (fraction)	Bioavailability after first pass – Fh (fraction)	Oral Clearance - CL/F (L/h)
Normal	2690	9.89	26%	74%	13.5
Intermediate	1940	7.70	21%	79%	9.70
Slow	545	2.54	7%	93%	2.73

For a typical individual (67kg), liver hepatic plasma flow (Q_h) 37.4 L/h and scaled to each patient's size using individual FFM.

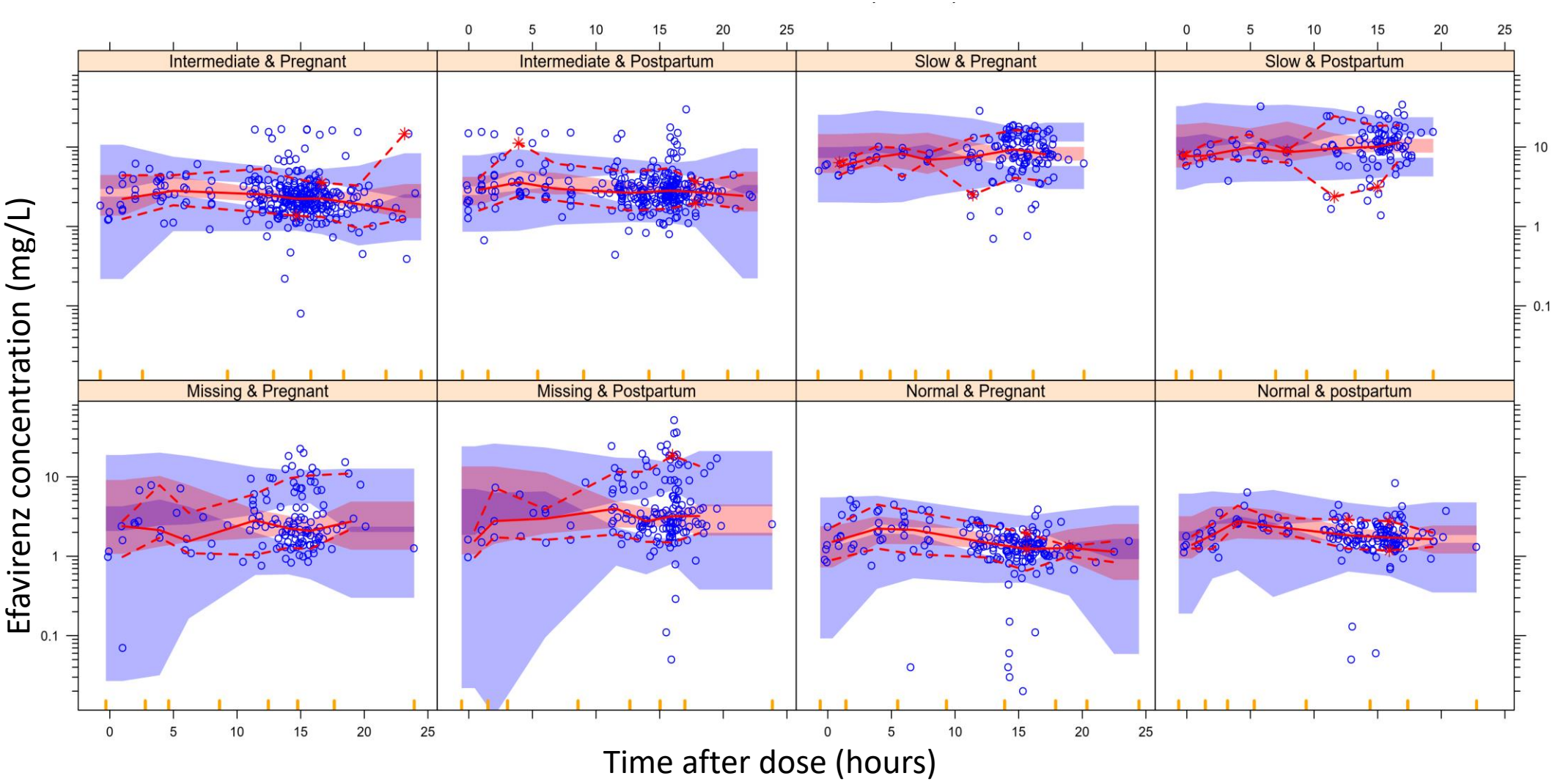

Figure s3. 1: Visual predictive check. Visual predictive check of the Efavirenz model, stratified by CYP2B6 genotype and pregnant status. The solid and dashed lines are the 5th, 50th, and 95th percentiles of the observations, while the shaded areas represent the 95% model-predicted confidence intervals for the same percentiles

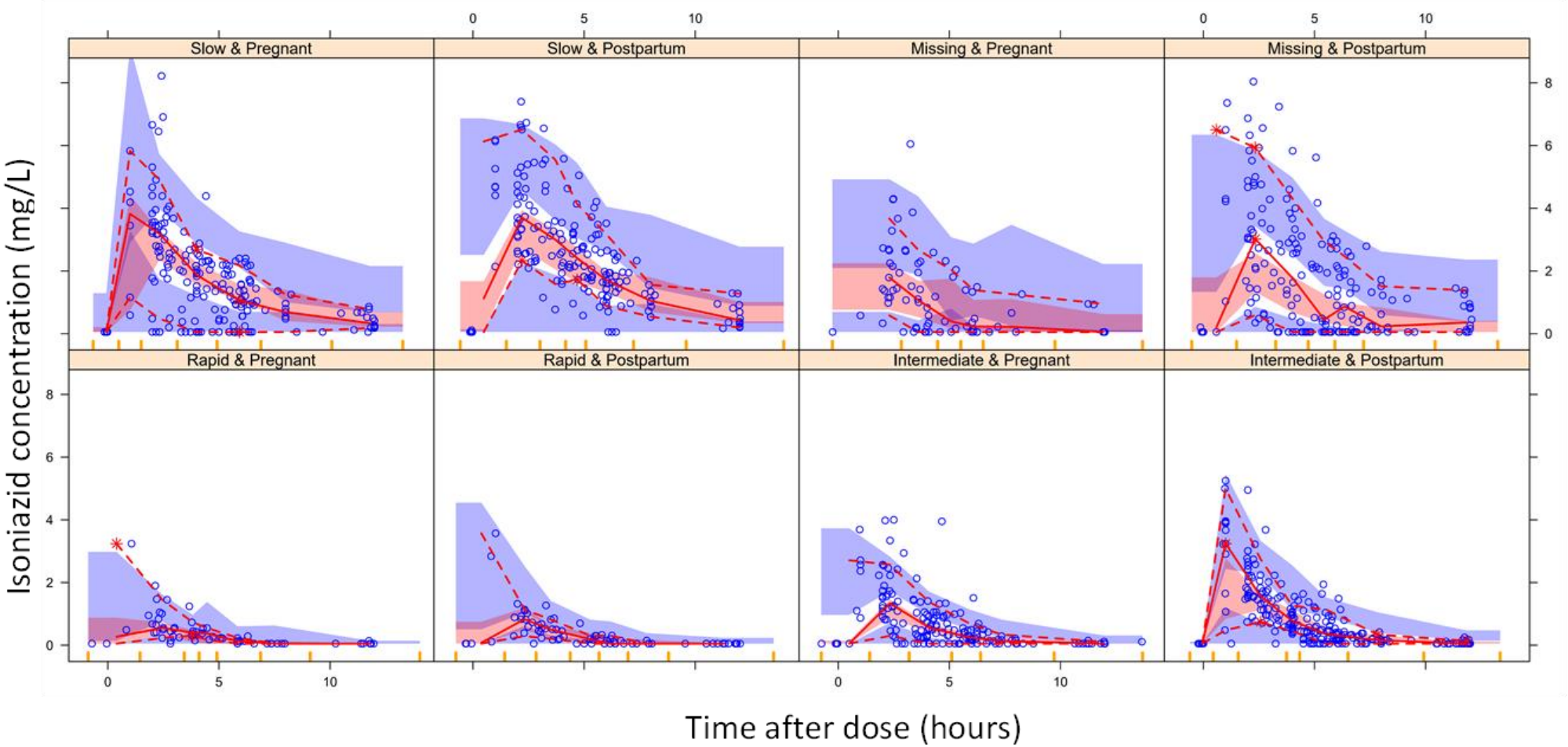

Figure s3.2: Visual predictive check. Visual predictive check of the isoniazid model, stratified by NAT2 genotype and pregnant status. The solid and dashed lines are the 5th, 50th, and 95th percentiles of the observations, while the shaded areas represent the 95% model-predicted confidence intervals for the same percentiles

Chapter 4: Bedaquiline exposure in pregnancy and breastfeeding in women with rifampicin-resistant tuberculosis

4.1 Abstract

Aim

We aimed to explore the effect of pregnancy on bedaquiline pharmacokinetics and describe bedaquiline exposure in the breast milk of mothers treated for rifampicin-resistant TB, where there is no human data available.

Methods

We performed a longitudinal pharmacokinetic study in pregnant women treated for rifampicin-resistant TB to explore the effect of pregnancy on bedaquiline exposure. Pharmacokinetic sampling was performed at four time-points over six hours in the third trimester, and again at approximately six weeks postpartum. We obtained serial breast milk samples from breastfeeding mothers, and a single plasma sample taken from breastfed and non-breastfed infants to assess bedaquiline exposure. We used liquid chromatography-tandem mass spectrometry to perform the breast milk and plasma bedaquiline assays, and population pharmacokinetic modelling to interpret the bedaquiline concentrations.

Results

We recruited 13 women, six of whom completed the ante- and postpartum PK sampling. All participants were HIV-positive on antiretroviral therapy. We observed lower ante- and postpartum bedaquiline exposures than reported in non-pregnant controls. Bedaquiline

concentrations in breast milk were higher than maternal plasma (milk to maternal plasma ratio: 14:1). A single random plasma bedaquiline and M2 concentration was available in four infants (median age: 6.5 weeks): concentrations in the one breastfed infant were similar to maternal plasma concentrations; concentrations in the three non-breastfed infants were detectable but lower than maternal plasma concentrations.

Conclusion

We report low exposure of bedaquiline in pregnant women treated for rifampicin-resistant TB. Bedaquiline significantly accumulates in breast milk; breastfed infants receive mg/kg doses of bedaquiline equivalent to maternal doses.

4.2 Introduction

Acquisition of data quantifying the exposure of second-line TB drugs in pregnant woman treated for rifampicin-resistant TB (RR-TB) is a priority. Until recently, pregnant, and breastfeeding women have typically been excluded from clinical trials of new drugs, including TB treatment (Gupta, Hughes, et al., 2019). The World Health Organization (WHO) currently recommends individualised treatment regimens with drugs with a preferred safety profile for pregnant women with RR-TB (WHO, 2020c), although there are limited human data guiding these recommendations.

Bedaquiline is a group A drug, recommended for inclusion in all RR-TB treatment regimens, and although used in pregnant women, safety data is lacking. The design of pharmacokinetic studies to explore the effect of pregnancy on long half-life drugs like bedaquiline is challenging, as cumulative drug concentrations could mask pregnancy-related effects on drug

exposure. Physiological changes in pregnancy result in decreased concentrations of many drugs, particularly in the third trimester (Pinheiro & Stika, 2020). Pharmacokinetics in pregnancy may be complex: one of the reasons for reduced drug concentrations in pregnancy is the reduction in plasma concentrations of the two key drug-binding proteins: albumin and α1-acid glycoprotein (Schalkwijk et al., 2017). Reduction in these binding protein concentrations reduces the total (bound and unbound) concentrations of drugs, but the unbound fraction typically increases, resulting in unbound drug concentrations that are similar to non-pregnant women. As only the unbound drug is pharmacologically active, recommendations to increase the dose of drugs in pregnancy to approximate total concentrations in non-pregnant women could therefore increase the risk of toxicity. However, pregnancy also increases several drug clearance mechanisms, which could reduce unbound drug concentrations. Although measurement of unbound bedaquiline concentrations is preferable to rationally optimize dosing in pregnancy (bedaquiline is >99% protein-bound) (van Heeswijk et al., 2014), an understanding of the effect of pregnancy on total bedaquiline concentrations would provide a much-needed foundation to understand the effect of pregnancy on the unbound fraction.

Data on the secretion of key drugs for RR-TB into breast milk are scarce. The studies describing RR-TB drug exposure in breast milk are small with little or no infant plasma pharmacokinetic data available - the study designs are also unclear or unstated. Linezolid (Lim et al., 2017), levofloxacin (Cahill et al., 2005) and cycloserine (Tran & Montakantikul, 1998) penetrate poorly into breast milk and exposure to breastfed infants is therefore likely to be low. Clofazimine, in contrast, demonstrates effective breast milk penetration with skin discoloration observed in the infants of breastfeeding mothers treated with clofazimine for leprosy (Loveday et al., 2020; Ozturk & Tatliparmak, 2017);. clofazimine exposure in breast

milk in the context of mothers treated for TB is unfortunately lacking. Animal studies have shown that bedaquiline is concentrated in rat milk with concentrations 6- to 12- fold higher than the concentration in maternal plasma (Jannsen Products, 2015), but there are currently no human data available. Information on clinically relevant infant exposure to RR-TB drugs through breastfeeding with mother-infant pairs has not been done and is an important knowledge gap.

An international consensus panel on the inclusion of pregnant and postpartum women in TB drug trials, convened by the NIH, identified the safety, tolerability and pharmacokinetics of novel agents and regimens for treatment of RR-TB as research priorities (Gupta et al., 2016). It is ethically imperative to study drug dosing and safety in populations where drugs are used, this has not been done satisfactorily for RR-TB (Gupta, Hughes, et al., 2019). We therefore conducted an observational study of bedaquiline exposure in pregnant and breastfeeding women with RR-TB.

4.3 Methods

4.3.1 Study design

We performed a longitudinal pharmacokinetic study in pregnant women ≥ 18 years of age treated for RR-TB, and their infants, at King Dinuzulu Hospital in Durban, Kwazulu-Natal (KDH) - nested within a cohort, which has been previously described. (Loveday et al., 2021) KDH is a specialist provincial RR-TB hospital where, until recently, all pregnant women with RR-TB were referred for care. With some individual regimen variability, all participants were treated with a minimum of five drugs including bedaquiline. Other drugs included: pyrazinamide, isoniazid, clofazimine, linezolid, moxifloxacin, and less commonly: ethambutol, terizidone,

levofloxacin, ethionamide and para-aminosalycylic acid. We performed pharmacokinetic sampling pre-dose, and at 2, 4, and 6 hours post-dose in the third trimester of pregnancy (≥28 weeks), and at the six week postpartum visit. Dosing on both sampling days was observed after a standard breakfast consisting of a cup of tea/coffee and a peanut-butter sandwich; the tablets were ingested with 250 mL of water. Considering bedaquiline is dosed three times a week (after the two-week loading dose), it was not always logistically possible to schedule pharmacokinetic sampling on a day when bedaquiline was administered. We therefore recorded the last date and time when bedaquiline was dosed to interpret the exposures with our modelling. The use of concurrent medications, including antiretroviral therapy, and the start date of all TB drugs, including bedaquiline, were recorded. If available, breast milk samples were taken from breastfeeding mothers by manual expression at the same timepoints that blood was drawn at the postpartum visit (i.e., pre-dose, 2, 4 and 6 hours post-dose); samples were frozen within 30 minutes of sampling at minus 80°C. To evaluate infant drug exposure, a single random plasma sample was taken from infants at the postpartum visit. If applicable, the time of the most recent breastfeed prior to the infant blood draw was recorded.

4.3.2 Bedaquiline assays

Plasma and breast milk samples were stored at minus 80°C and transported to the University of Cape Town, Division of Clinical Pharmacology laboratory where total plasma and breast milk bedaquiline and M2 assays were performed using liquid chromatography with tandem mass spectrometry. The plasma assay for total bedaquiline has previously been described (Brill et al., 2017). Bedaquiline and its M2 metabolite in breast milk were analysed with a validated assay developed at the Division of Clinical Pharmacology laboratory validated using

Food and Drug Administration and European Medicines Agency guidelines (European medicines agency, 2011; FDA & Center fr drug evaluation and research, 2018); the standards and quality checks were performed using blank donated breast milk.; the standards and quality checks were performed using blank donated breast milk. The extraction procedure consisted of protein precipitation and solid phase extraction, followed by gradient liquid chromatography on an Agilent Poroshell 120 SB-C18 (2.1 mm x 50 mm, 2.7 µm) analytical column with tandem mass spectrometry detection. An AB Sciex API 3000 mass spectrometer at unit resolution in the multiple reaction monitoring mode was used to monitor the transitions of the protonated precursor ions m/z 555.1, m/z 561.1, m/z 541.1, and m/z 545.1 to the product ions m/z 58.2, m/z 64.1, m/z 480.3, and m/z 480.4 for bedaquiline, TMC207-d6, M2, and M2-d3C13, respectively. Electro Spray Ionisation was used for ion production. The calibration curves fitted quadratic (weighted by 1/concentration) regressions based on peak area ratios over the ranges 0.0780 – 5.00 µg/mL for bedaquiline and 0.0312 – 2.00 µg/mL for M2. The combined accuracy (%Nom) and precision (%CV) statistics of the lower limit of quantification, low, medium, and high-quality controls of bedaquiline and M2 during intra- and inter validations were between 96.7% and 106.5%, and 3.4% and 7.5%, respectively.

4.3.3 Pharmacokinetic Modelling

Bedaquiline concentrations were interpreted using population pharmacokinetic modelling in NONMEM version 7.4.5 (Boeckmann et al., 2011). Perl-speaks-NONMEM version 5.2.6, Pirana version 3.0, and R with the package xpose4 were used to facilitate the model development process, data manipulation, and generation of model diagnostics (Keizer et al., 2013). As a starting point, we used a published population pharmacokinetic model of bedaquiline in non-pregnant adults with HIV and drug-resistant tuberculosis (Brill et al., 2017). Briefly, the

published model consists of three disposition compartments for bedaquiline and one disposition compartment for M2. There was a correlation between bedaquiline and M2 between-subject-variability on clearance, and residual variabilities. The effect of body weight on all disposition parameters was included using allometric scaling, and albumin also affects the drug disposition parameters. The co-administration of ritonavir-boosted lopinavir reduced bedaquiline and M2 clearance by 65% and 42%, respectively. Molar concentrations were used during model development to account for mass balance between bedaquiline and its metabolite M2. Participant albumin information were not captured in the current study, therefore we imputed a reported albumin concentration from a previously study in South Africa patients with RR-TB (Ngwalero et al., 2021).

When analysing the data, we first fit the original model as published, without re-estimating any of the population parameters, but using the study covariate, doses, and dosing regimen information. This is similar to using the current data as an "external" validation of the model, i.e., assessing how the previous model predicts the current data based solely on covariate information and assuming no effect of pregnancy (which was not part of the original model). Afterwards, we attempted to use the data to re-estimate parameter values, using the general principles of model development (Mould & Upton, 2013), including drops in NONMEM objective function value (OFV) for assessment of statistical significance and inspection of diagnostic plots. Throughout the modelling process, we assumed 100% treatment adherence unless the participant disclosed otherwise.

4.3.4 Calculation of the milk: plasma ratio (M:P)

The PK of bedaquiline and M2 in breast milk of the mothers with paired plasma and milk samples was characterised using an effect compartment (Upton & Mould, 2014). The effect

compartment model described an accumulation ratio (M:P), and a time delay in the equilibration between the breast milk and plasma concentrations (Egbelowo et al., 2021; Sheiner et al., 1979). Further information about the effect compartment is provided in the supplementary material.

4.3.5 Calculation of infant bedaquiline intake with breast milk

To estimate how much bedaquiline is ingested per day by a typical child breastfed by a mother receiving bedaquiline, we assumed an average infant milk ingestion of 0.15 L/kg/day (Wilson, 1983). The following equation was used to calculate the infant dose (Gilbert-Barness, 1995):

$$D_{infant} = C_m \cdot V_m$$

where *Vm* is the volume of milk ingested by breastfeeding, and C_m is the drug concentration in breast milk. This was calculated using the formula below:

$$C_m = M{:}P \cdot C_{pavg}$$

where C_{pavg} is the average maternal plasma concentration, which will vary depending on the date when participants were initiated on treatment with bedaquiline relative to the date of PK sampling. *M:P* is the breast milk-to-plasma ratio.

4.3.6 Ethics

Ethics approval for the study was granted by the South African Medical Research Council Ethics Committee (EC017-6/2016), and the University of Cape Town Human Research Ethics Committee (HREC: 666/2018). Informed consent was taken from all participants in a language of their choice (either English or isiXhosa).

4.4 Results

4.4.1 Study population and sampling

Bedaquiline pharmacokinetic samples were available from 13 women in the third trimester of pregnancy, at 30 (IQR: 25 - 37) weeks gestation, six of whom returned for postpartum sampling at 7 (IQR: 6.5 – 8) weeks after delivery. Seventy-one plasma samples of bedaquiline parent and metabolite concentration were available for analysis. Participant characteristics are shown in **Table 4.1**. All participants were living with HIV and treated with antiretroviral therapy (ART), most commonly on nevirapine-based ART (n=10, 83.3%): two women were treated with dolutegravir, and one woman received lopinavir/ritonavir. Serial breast milk samples at the same time-points that plasma was sampled, were available in two breastfeeding participants. A single random plasma bedaquiline concentration was available from four infants on the postpartum PK sampling day, of whom one was breastfed. The range of gestational age at time of delivery of the four infants who had PK sampling was 33-38 weeks. The serial post-dose bedaquiline and M2 concentrations at each sampling time point are shown in **Table 4.2**.

Table 4.1: Characteristics of pregnant women treated for rifampicin-resistant tuberculosis

Median (range)	Antepartum (n=13)	Postpartum (n=6)	Infants (n=4) – PK visit
Baseline characteristics			
Age (years)	30 (23 - 48)	30 (23 - 48)	6.5 (6 - 8) weeks
Height (cm)	160 (140 - 176)	162 (152 - 163)	53 (50 - 55)
HIV status (Pos/neg)	(13/0)	(6/0)	
TB type (RR[a]/MDR[b]/Pre-XDR[c]/XDR/missing)	(6/3/2/1/1)	(2/2/0/1/1)	
Previous TB (yes/no/missing)	(7/5/1)	(2/3/1)	
CD4 (cells/mm3)	311 (44-1008)	545 (253-1008)	
ART[d] (NVP[e]/LPV[f]/DTG[g])	10/1/2	**5**/0/1	
Characteristics on the Pharmacokinetic day			
Weight (Kg)	61 (55 - 104)	67(52 - 84)	4.1 (2.6 - 7.1)
Time since EFV[h] switch (Days)	31 (13 - 375)	175 (85 - 421)	
Gestational age/time after delivery (weeks)	30 (25 - 37)	7 (6.5 - 8)	
Inpatients/outpatients	12/1	0/6	
Race (black/white)	13/0	6/0	
Time since BDQ[i] initiation (days)	27 (13 - 96)	154 (81 - 201)	

RR[a]: rifampicin-resistant; MDR[b]: multidrug-resistant; XDR[c]: extremely drug-resistant; ART[d]: antiretroviral therapy; NVP[e]: nevirapine; LPV: lopinavir[f]; DTG: dolutegravir[g]; EFV[h]: efavirenz

*Table 4. 2: Median (range) bedaquiline and metabolite (M2) concentrations per time point**

Time point	Bedaquiline (n=13)				Metabolite, M2 (n=13)			
	Antepartum		Postpartum		Antepartum		Postpartum	
Time	No.	Concentration (mg/L)	No.	Concentration (mg/L)	No.	Concentration (mg/L)	No.	Concentration (mg/L)
Predose	6	0.419 (0.146 – 0.997)	2	0.186 (0.135– 0.237)	6	0.183 (0.0479 – 0.297	2	0.0584 (0.0440-0.0728)
2 hrs	6	0.621 (0.225 – 1.78)	2	0.237 (0.205 – 0.2678)	6	0.160 (0.0455 – 0.283)	2	0.0630 (0.0425 – 0.0834)
4 hrs	5	1.05 (0.393 – 1.95)	1	1.06	5	0.144 (0.0469 – 0.286)	1	0.0467
6 hrs	5	1.69 (0.296 – 2.93)	1	1.14	5	0.181 (0.0454 – 0.285)	1	0.0547
24 hrs	7	0.308 (0.265 – 0.505)	4	0.3085 (0.227 – 0.312)	7	0.168 (0.0799 – 0.281)	4	0.128 (0.106-0.166)
26 hrs	7	0.250 (0.226 – 0.461)	4	0.281 (0.242-0.293)	7	0.142 (0.0618 – 0.254)	4	0.107 (0.0989-0.128)
28 hrs	7	0.228 (0.188 – 0.419)	4	0.275 (0.263-0.296)	7	0.145 (0.0618 - 0.227)	4	0.112 (0.107-0.132)
30 hrs	7	0.205 (0.169-0.347)	3	0.284 (0.234-0.299)	7	0.133 (0.0585 – 0.224)	3	0.111 (0.0970-0.120)

*Time point: approximation of the time after dose; No.: Number of participants at each timepoint

4.4.2 Pharmacokinetic model

When we used the published model (Brill et al., 2017) to predict the expected exposures in these patients (thus using the original population parameter estimates and assuming no effect of pregnancy), the model overpredicted both bedaquiline and M2 concentrations on both antepartum and postpartum visits, as presented in the visual predictive check (VPC) in **Figure 4.1**. The VPC shows that the PK terminal elimination phase of the participant not on lopinavir/ritonavir were approximately 50% lower that the model prediction (for both the metabolite and parent) as illustrated by the deviation of the 50th percentiles of the observations (red line) from the median of the model predicted confidence interval (black line). If the pharmacokinetic parameters in this study were in line with the previous report, we would have expected to observe higher bedaquiline concentrations. Only the data from the participant co-administered lopinavir/ritonavir, who had higher bedaquiline concentrations due to a drug-drug interaction, was in line with the model prediction

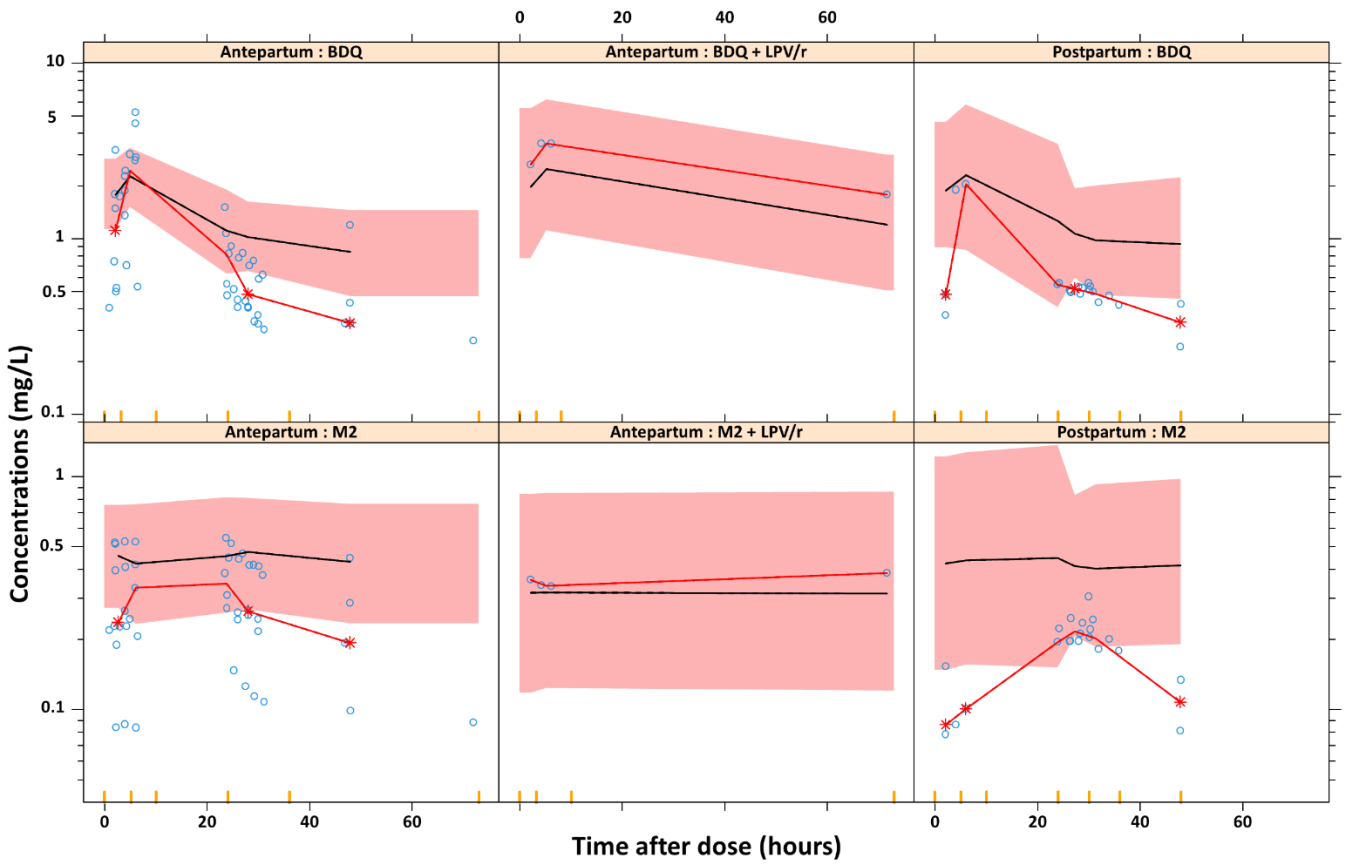

Figure 4.1: Visual predictive check (VPC) of the bedaquiline and M2, the top panels represent the parent, and the bottom panels represent the metabolite bedaquiline concentrations. The first column displays antepartum concentrations, while the last and middle columns show postpartum concentration and antepartum concentration in participants co-administered lopinavir/ritonavir, respectively. Due to the small sample size in each panel, we plotted the 50th percentiles of the observations (red line) - the shaded areas represent the 95% model-predicted confidence intervals, and the black line is the median of the model predicted confidence interval.

PK measures are shown in Table S4.2. We encountered several challenges when attempting to fit the original model to the current data by re-estimating the parameter values. The model structure is complex, with multiple disposition compartments, and the current data did not reliably support the re-estimation of all parameters - some of the parameter estimates obtained when attempting to re-fit were unstable and/or implausible. In other words, while the model could be adapted to fit the study data, this could be achieved in multiple different ways, e.g., assuming a larger clearance or lower bioavailability (both ante- and postpartum),

and a larger peripheral volume of distribution. We experienced further complications when trying to estimate a significant difference between the two pharmacokinetic sampling visits, i.e., possibly due to pregnancy status. All the scenarios were nearly equivalent in terms of goodness of fit, and there was no meaningful difference in terms of statistical significance, thus leaving the choice largely in the domain of speculation. Choosing a different scenario (on which parameter a difference is ascribed to) would imply a different interpretation of the results, and if the different options for the model were to be used to predict concentrations and suggest dose adjustments, they could come to very different conclusions. We also attempted to use a frequentist prior approach (Chan Kwong et al., 2020) to try and stabilise the parameter estimates, but the results became highly dependent on the assumptions on the prior precision of each parameter, thus not solving the problem. For this reason, we decided to simply use the model as originally published and acknowledge that the concentrations we observed are lower than expected, assuming that the pharmacokinetics are the same as non-pregnant patients.

4.4.3 Breast milk and infant exposures

A graphical overview of the infant and breast milk data is provided in **Figures 4.2 and 4.3**, together with the plasma concentrations in the respective mothers. The PK profiles for bedaquiline and M2 are shown: maternal plasma concentrations ante- and postpartum, breast milk and infant concentrations. The model estimated an M:P ratio of 13.6 (%relative standard error (RSE): 10.1) and, 4.84 (%RSE: 5.10) for bedaquiline and M2, respectively. The average bedaquiline concentration in the mothers' postpartum PK samples was 0.4 mg/L; using this value the infant bedaquiline dose would be 0.816 mg/kg/day. Similarly, the average maternal postpartum M2 concentration was 0.1, the infant M2 dose would therefore be 0.07

mg/kg/day. In comparison, a 70-kg individual administered the standard dose of 200 mg bedaquiline three times a week would result in approximately 1.22 mg/kg/day dose of bedaquiline.

Table S4.3 in the appendix displays the breast milk concentrations and their corresponding M:P ratio. Further details of the breast milk concentration model are presented in the supplementary text in the appendix. Bedaquiline and M2 concentrations in the infant who was breastfed were similar to maternal plasma concentrations, while for the three infants who were not breastfed, bedaquiline and M2 concentrations were detectable but lower than maternal plasma values (see **Figures 4.2 and 4.3**).

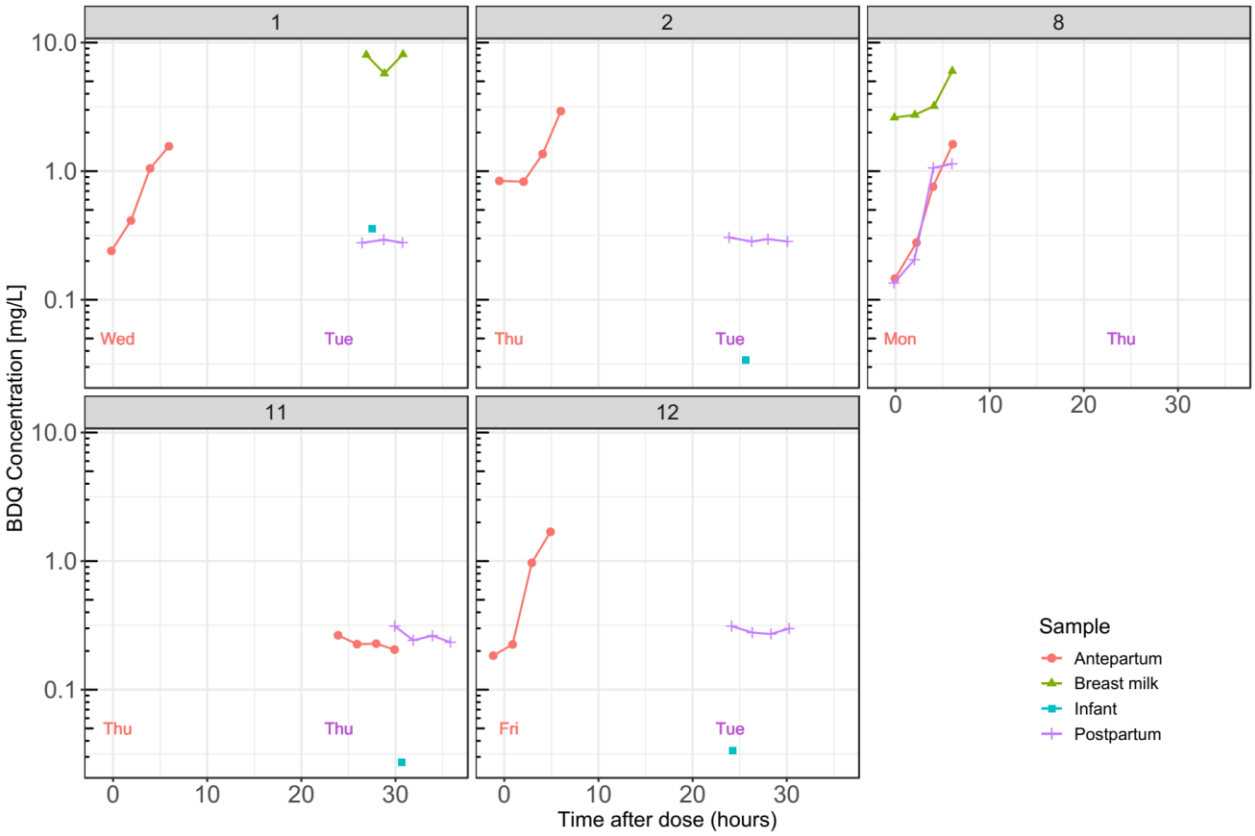

Figure 4.2: Pharmacokinetic profiles of bedaquiline concentrations stratified by participant ID. The red dots and purple crosses represent maternal plasma concentrations ante- and postpartum, respectively. The green triangles represent breast milk; the blue squares represent infant plasma concentrations.

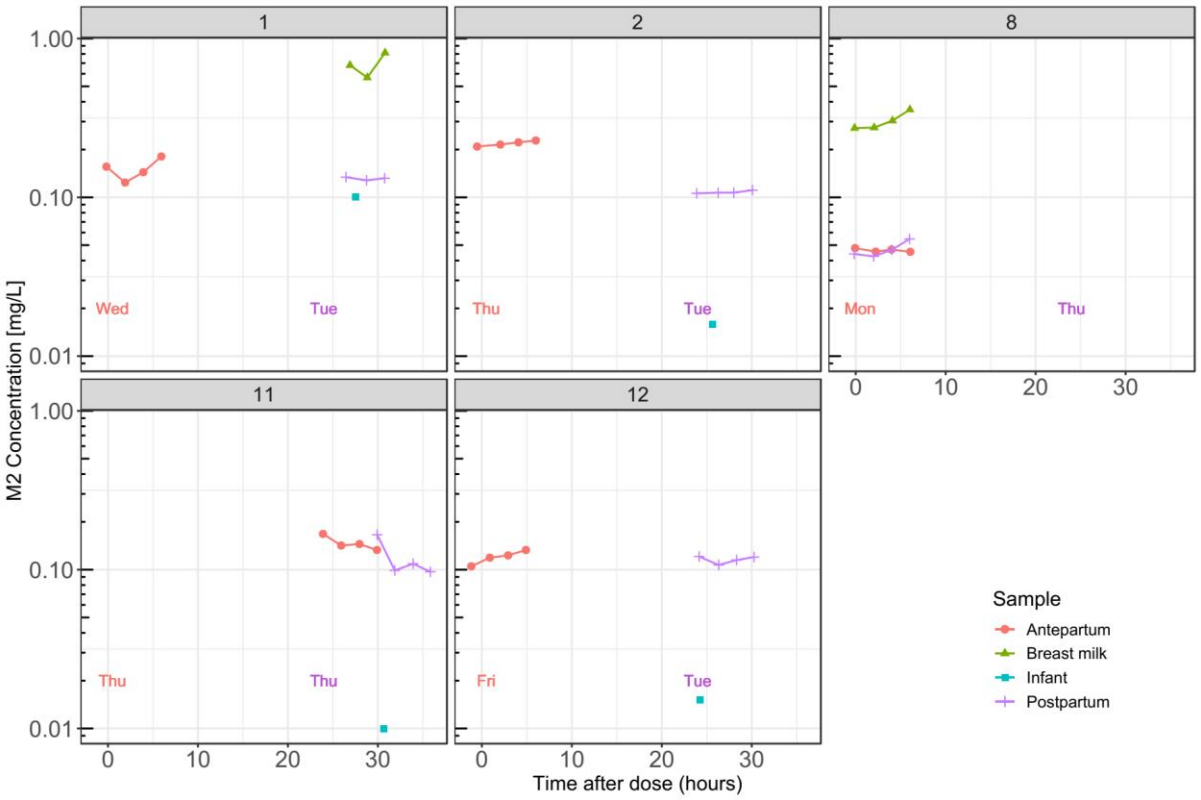

Figure 4.3: Pharmacokinetic profiles of M2 concentrations stratified by participant ID. The red dots and purple crosses represent maternal plasma concentrations ante- and postpartum, respectively. The green triangles represent breast milk; the blue squares represent infant plasma concentrations.

4.5 Discussion

To our knowledge, this report is the first description of the exposure of bedaquiline in pregnant women. We found bedaquiline and M2 exposure in pregnant women to be approximately 50% lower than expected in non-pregnant patients (Brill et al., 2017). Although we were underpowered, we found no significant difference between ante- and postpartum exposures.

There are several possible reasons for the low bedaquiline exposures we observed in the third trimester. First, increased metabolism of bedaquiline is a possible explanation - pregnancy is known to induce CYP3A4, which is the major route of bedaquiline metabolism (Svensson et al., 2013). The increase in CYP3A4 expression would lead to higher clearance and lower bioavailability of bedaquiline since it is present in both entero- and hepatocytes. Second, pregnancy reduces plasma albumin concentrations, to which bedaquiline is highly bound (

Feghali & Mattison, 2011). The unbound fraction of bedaquiline may therefore increase, subsequently increasing its clearance and tissue distribution. In such a scenario, the total (bound+unbound) concentrations of bedaquiline in plasma would decrease, but this effect could be counter balanced by the large unbound fraction, thus maintaining relatively unchanged unbound levels. However, exploration of unbound bedaquiline exposure is required before a recommendation for a dose adjustment can be made. Thirdly, changes in body size (and possibly composition) may have affected bedaquiline disposition, but it is unlikely that the increased weight in pregnancy affected the exposure of bedaquiline as we used allometric scaling to account for this in the model, and changes in body size alone are therefore unlikely to explain the decreased bedaquiline concentrations we observed.

Similarly, we observed lower-than-expected bedaquiline levels at the postpartum visit. While it is generally accepted that pharmacokinetic sampling approximately six weeks postpartum is a reasonable time-point to allow the physiologic changes related to pregnancy to subside (Eke et al., 2021), there are some limitations in using this timeline as a control when exploring the effect of pregnancy on drugs with a long half-life such as bedaquiline. Given that the terminal half-life of bedaquiline is more than five months, (van Heeswijk et al., 2014) any change in pharmacokinetic parameters may only become apparent on drug exposure after a considerable amount of time, possibly months. Thus, even if most of the pregnancy effects (if any) had reversed in the first weeks after delivery, there may not have been sufficient time for the exposure of bedaquiline to reach a new equilibrium before the scheduled postpartum pharmacokinetic visit. An alternative explanation is that adherence could have decreased in the postpartum period; a systematic review reported poor postpartum adherence in patients

on ART (Nachega et al., 2012). Sub-therapeutic bedaquiline exposures could affect clinical outcomes and increase the risk of selecting for drug resistance.

We observed concerningly high concentrations of bedaquiline in the breast milk samples we analysed, markedly higher than the maternal bedaquiline plasma concentrations, in keeping with the findings of an animal study (Jannsen Products, 2015). The breastfeeding infant had a plasma bedaquiline concentration similar to maternal plasma (Figure 2), which could have implications for infant safety. In a previous animal study, rat pups who were breastfed to mothers treated with bedaquiline were reported to have low body weight. (Jannsen Products, 2015) In contrast, therapeutic concentrations of bedaquiline in infants (possible with long half-life drugs, which accumulate slowly, such as bedaquiline) could potentially be protective in infants exposed to RR-TB, obviating the need for TB preventive therapy. The three infants who were not breastfed had sub-therapeutic bedaquiline concentrations, likely from transplacental exposure, which could select for drug resistance should the infants develop RR-TB. A pre-clinical study in rats treated with bedaquiline also demonstrated placental bedaquiline distribution.

The gestational age at birth of the neonates who had had PK sampling ranged from 33 to 38 weeks – see Table S1. The CYP3A system in the liver and intestinal wall of preterm neonates has lower activity compared with adults, but activity increases rapidly in the first months of life. (Brussee et al., 2018) Since bedaquiline is metabolised largely by CYP3A4, the immaturity of the infant CYP3A4 metabolic system may have contributed to the high infant bedaquiline concentrations we observed. Although the WHO recommends all three group A drugs including bedaquiline for the treatment of children with MDR-TB age >=3 years (European medicines agency, 2013), there is a lack of safety data of the use of bedaquiline in children <6 years. (WHO, 2019) The consequence of the therapeutic bedaquiline concentrations we

observed in the breastfeeding infant is unknown, but there are potential implications for infant safety (Jannsen Products, 2015).

The main factors determining the transfer of a drug into breast milk are its physicochemical characteristics (such as lipid solubility and degree of ionisation at different pH conditions) and its plasma pharmacokinetics (Chaves & Lamounier, 2004). Fat-soluble drugs like bedaquiline cross lipid-protein cell membranes easily, hence transferring readily into breast milk (Chaves & Lamounier, 2004). The ease with which drug molecules cross cellular membranes depends on the drug's degree of ionisation, which may vary in different pH conditions. Weak bases like bedaquiline (pKa = 8.9) (Feng et al., 2015) tend to be slightly less ionised in plasma compared to milk. This means that unionised plasma bedaquiline will transfer into breast milk, were it is more likely to be ionised, favouring milk accumulation of the drug (Howard & Lawrence, 1999). Transfer of drugs into breast milk may also be greater in drugs with a low affinity for maternal plasma proteins, but bedaquiline is highly protein-bound (>99.9%) (van Heeswijk et al., 2014). An additional factor is molecular weight, as drugs with low weight (<200 Da) reach breast milk more easily, but the molecular weight of bedaquiline is 555.504 Da (Svensson et al., 2015). Drugs, which have a long plasma half-life and therefore accumulate, such as bedaquiline, are prone to transfer into breast milk compared with molecules which are cleared rapidly. The high concentration of bedaquiline in breast milk suggests that the mammary glands could be a clearing site for bedaquiline. Excretion could be significant, since, on average, a baby consumes about 0.15 L/kg/day of breast milk (Wilson, 1983). Moreover, bedaquiline metabolism in breast tissue cannot be excluded, as there are contradictory reports on the expression of CYP3A4 in human breast tissue. (Hellmold et al., 1998; Huang et al., 1996; Iscan et al., 2001)

Our study has several limitations. First, we did not measure unbound bedaquiline concentrations or albumin levels, so we are unable to conclusively determine if the reasons for the low concentrations observed are related to protein binding. Second, there was a high rate of participant loss to follow up, which limited our sample size, as many participants were unable for logistical reasons, to complete the postpartum PK sampling day. Third, PK sampling was not always performed on a day when bedaquiline was scheduled to be administered (dosing is three times a week). Although this was accounted for in our modelling, considering we did not use an adherence measure, the date and time of the last bedaquiline dose was obtained via participant self-report, which could be unreliable.

We report low exposures of bedaquiline in this series of pregnant women treated for RR-TB. Future studies should analyse bound and unbound bedaquiline concentrations with an adherence measure to better understand the effect of pregnancy on bedaquiline exposure and assess whether a different dosing recommendation for bedaquiline in pregnancy is indicated. Bedaquiline appeared to significantly accumulate into human milk, which could be an exposure risk for breastfeeding babies, and should therefore be investigated further.

4.6 Supplemental Pharmacokinetic model of breast milk

The characterisation of bedaquiline and M2 concentration in breast milk was obtained by modelling the plasma and milk concentrations in the participants with paired plasma and breast milk samples. The plasma and milk bedaquiline and M2 raw concentrations are shown in **Table s4.1**.

Table s4.1. Maternal, human milk and infant bedaquiline and M2 concentrations in the women with corresponding breastmilk samples and the calculated M:P ratio (M:P= milk/maternal plasma) and absolute infant dose.

ID	TAD* (hours)	BDQ maternal plasma (mg/L)	M2 maternal plasma (mg/L)	BDQ milk (mg/L)	M2 Milk (mg/L)	BDQ M:P	M2 M:P
1	26.45	0.277	0.134	8.02	0.679	29.0	5.07
1	28.75	0.293	0.128	5.75	0.568	19.6	4.44
1	30.75	0.278	0.132	8.11	0.814	29.2	6.17
8	47.83	0.135	0.044	2.61	0.273	19.3	6.20
8	2	0.205	0.0425	2.74	0.275	13.4	6.47
8	4.01	1.06	0.0467	3.21	0.304	3.02	6.51
8	5.98	1.14	0.0547	6.01	0.357	5.27	6.523

*** TAD: Time after the last bedaquiline dose.**

The modelling procedure comprised two steps. As a first step, we used the previously published plasma PK model (Brill et al., 2017) to describe the individual plasma concentrations around the time when breastmilk samples were collected. As mentioned in the results section of the main manuscript, the Brill model overpredicted the overall concentration of both bedaquiline and M2 in our cohort of patients, as shown in the VPC in **Figure 4.1**. However, while at the population level the model was systematically over-predicting the concentrations, at an individual level, (thanks to the between-subject and -occasion random effects) the model was able to fit the plasma concentrations reasonably well in the participants with paired plasma and human milk concentration, as shown in **Figure s4.1**.

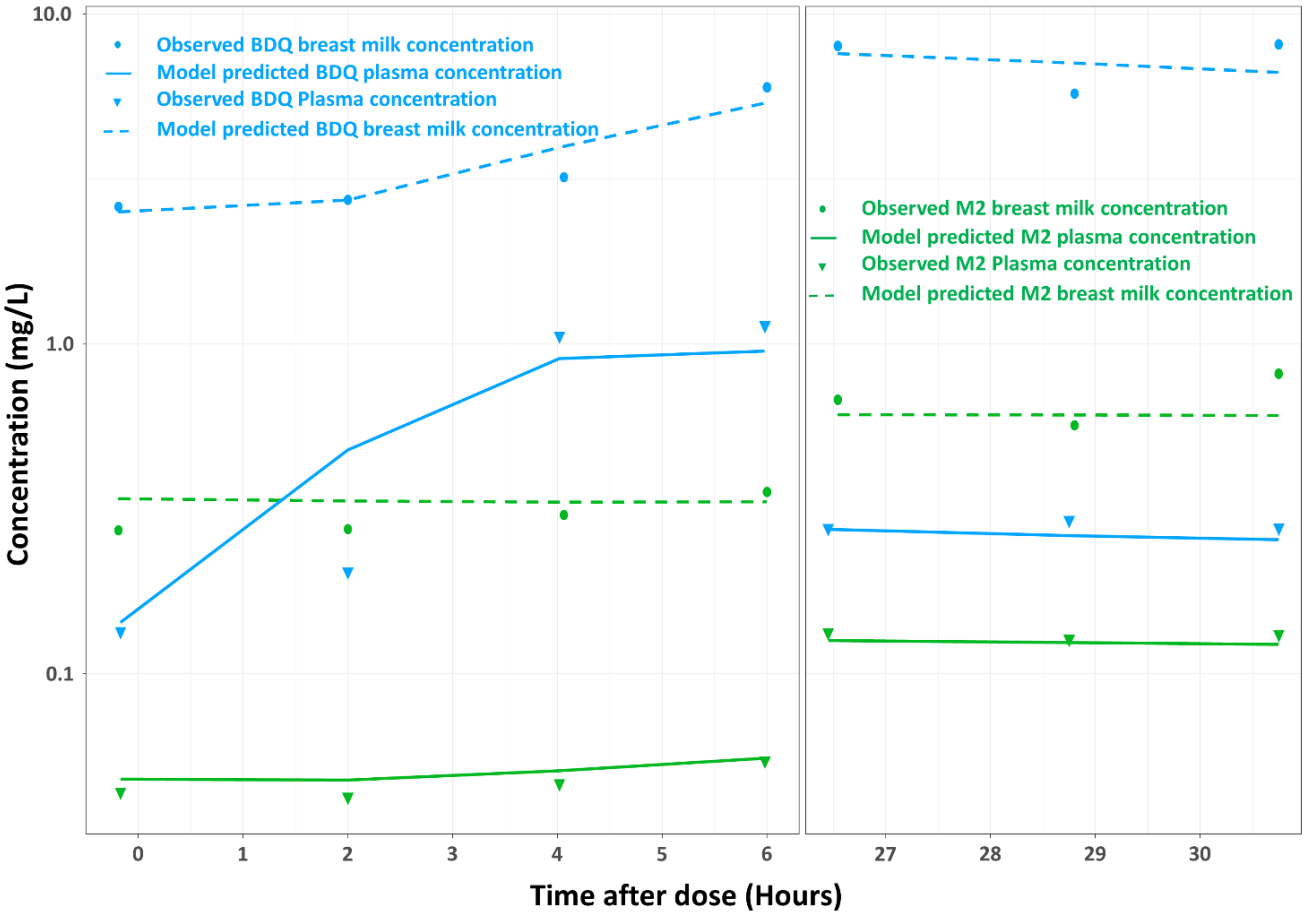

Figure s4. 1: Pharmacokinetics profile of bedaquiline and M2 of the two individuals contributing breast milk samples. Bedaquiline concentrations are plotted in blue and M2 in green. The solid line represents the model-predicted plasma concentration, while the dashed lines represent the breast milk concentrations. The circles represent the observed breast milk concentrations, while the triangles represent the observed plasma concentrations.

As a second step, we fixed the individual plasma PK parameters and used the model-predicted plasma concentration profile as an input (forcing function) for the model fitting the breast milk concentrations. This is called a sequential modelling approach, and Zhang et al. (L. Zhang et al., 2003) showed that it performs as well as the simultaneous modelling method, which was not feasible in our scenario, since the plasma PK model showed a systematic over-prediction at population level.

To characterise the link between plasma and milk concentrations, we used an effect compartment approach (Upton & Mould, 2014), as shown in the diagram in **Figure s4.2**

depicting the structural model. This paradigm describes the concentrations of bedaquiline (and M2) in human milk as dependent on plasma concentrations, but it assumes no significant transfer of drug between plasma and breastmilk (negligible mass transfer), so that the movement of drug into the breastmilk compartment does not affect the amount in the central compartment.

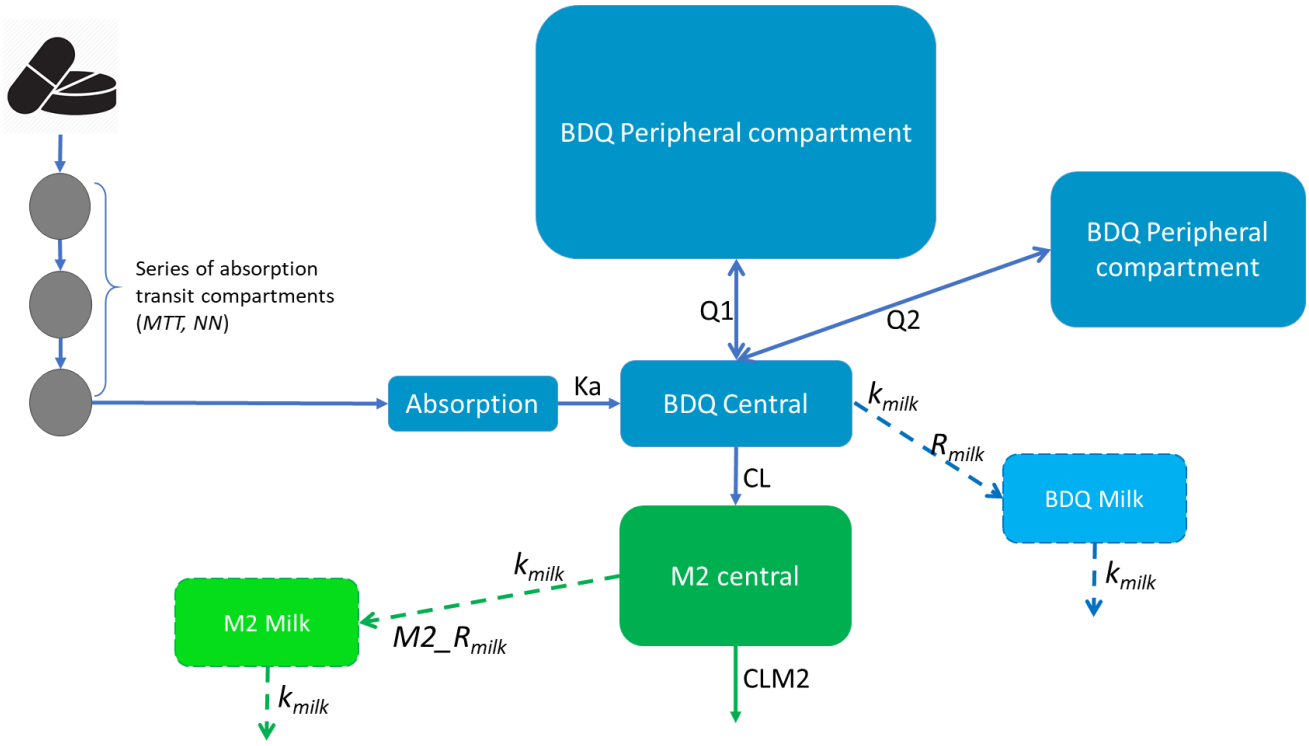

Figure s4. 2: Schematic representation of the PK model of bedaquiline and M2 in plasma and human milk. The plasma PK model is as reported by Brill et al., 2017***. The absorption is described with a series of transit-compartments (NN) and mean transit time (MTT) to capture the delay in absorption, and a rate constant ka. Drug transfer between the central and peripheral compartments is defined by intercompartmental clearance Q1 and Q2. Bedaquiline and M2 clearances are denoted by CL and CLM2, respectively. Kmilk is the plasma and human milk equilibration rate constant and Rmilk and M2_Rmilk are bedaquiline and M2 accumulation ratios, respectively***

The equation describing the concentration in breastmilk is:

$$\frac{dC_{milk}}{dt} = K_{milk} \cdot \left(R_{milk} \cdot C_{plasma} - C_{milk}\right)$$

where C_{milk} is the concentration in human milk, C_{plasma} is the plasma concentration, K_{milk} is the first-order plasma-to-breastmilk equilibration rate constant, and R_{milk} is the accumulation

ratio between plasma and breastmilk, previously referred to as pseudo-partition coefficient (Egbelowo et al., 2021; Sheiner et al., 1979). K_{milk} describes the "delay" in the transfer of drugs from plasma to milk. It can also be parameterised as a half-life ($T_{1/2milk} = In(2)/K_{milk}$) which can be interpreted as the time required to achieve 50% of the equilibrium target between human milk and plasma. R_{milk} is the ratio between the concentrations in human milk and plasma at equilibrium. Two separate effect compartments were fit, one for bedaquiline and the other M2.

The model parameters are presented in **Table s4.2.** The final model did not find any significant difference for K_{milk} of BDQ and M2, so a single parameter was estimated. The model supported between-subject variability (BSV) in bedaquiline R_{milk} (ΔOFV=5.05) and only proportional error for both bedaquiline and M2. The model-predicted profile and the individual PK profile of the plasma and milk concentration are depicted in **Figure s4.1**, showing satisfactory goodness of fit.

Table s4. 2: Final pharmacokinetic parameter estimates for bedaquiline and M2 in human milk.

Parameter	Typical Value (%RSE)	Between-Subject Variability [a], %CV
$T_{1/2milk}$ - half-life of delay in plasma to milk equilibration (h)	8.15 (36.5)	
R_{milk} - BDQ accumulation ratio (.)	13.6 (10.1)	10.9 (34.2)
M2_R_{milk} - M2 accumulation ratio (.)	4.84 (5.10)	
BDQ Proportional error (%)	16.0 (21.1)	
M2 Proportional error (%)	13.3 (27.5)	

[a] Variability was modelled with log-normal distribution and is presented as an approximate percentage CV.

The model estimated a bedaquiline milk to plasma accumulation ratio of 13.6 and M2 milk to plasma ratio of 4.84. A single K_{milk} with a half-life of 8.15 was estimated for both bedaquiline and M2. However, the large delay in the milk to plasma equilibration might be driven by a

single unexpectedly low plasma concentration in the first 6 hours, hence should be interpreted with caution.

Table s4. 3: Characteristics of 13 HIV-positive women treated for rifampicin-resistant tuberculosis

TB treatment regimen	ART regimen	Gestational age at birth, wks	Time on bedaquiline, days		Time from delivery to Postpartum PK, days	Breastfeeding status
			Antepartum PK	Postpartum PK		
LZD, BDQ, hdINH, LFX, CFZ, PZA, EMB	TDF, FTC, NVP	33	19	81	44	Yes
INH, PZA, EMB, BDQ, LVX, Moxy	TDF, FTC, NVP	38	84	201	46	No
INH, PZA, CFZ, LZD, BDQ, LVX	TDF, FTC, NVP	37	96	166	48	No
LZD, BDQ, hdINH, LFX, CFZ, PZA, EMB	TDF, FTC, NVP	37	57			No
INH, PZA, EMB, ETH, CFZ, LZD, BDQ,	TDF, FTC, NVP	40	13			No
PZA, TRZ, CFZ, LZD, BDQ, DLM	TDF, FTC, NVP	39	15			No
LZD, BDQ, hdINH, LFX, CFZ, PZA, EMB	3TC+RIT+LPV	38	31			No
LZD, BDQ, hdINH, LFX, CFZ, PZA, EMB	TDF, FTC, NVP	40	27	184	44	Yes
LZD, BDQ, hdINH, LFX, CFZ, PZA, EMB	TDF, FTC, NVP	39	17			No
LZD, BDQ, DLM, LFX, CFZ, PZA, EMB, TRZ, PAS	TDF, FTC, NVP	39	25			No
LZD, BDQ, DLM, LFX, CFZ, PZA, EMB, TRZ, PAS	TDF, FTC, NVP	38	31	143	44	No
LZD, BDQ, hdINH, LFX, CFZ, PZA, EMB	DTG, TDF, 3TC	34	35	81	46	No
LZD, BDQ, hdINH, LFX, CFZ, PZA, EMB	DTG, TDF, 3TC	36	18			No

LZD: linezolid; BDQ: bedaquiline; DLM: delamanid; hdINH: high-dose INH; INH: isoniazid; CFZ: clofazimine, PZA: pyrazinamide, EMB: ethambutol; ETH: ethionamide; DLM: delamanid; TRZ: terizidone; LFZ: levofloxacin; PAS: para-aminosalycylic acid; TDF: tenfovir; 3TC: lamivudine; FTC: emtricitabine; RIT: ritonavir; LPV: lopinavir; DTG: dolutegravir

Chapter 5: Pharmacokinetics of high-dose isoniazid for treatment of multidrug resistant tuberculosis.

5.1 Abstract

Background

The WHO-endorsed shorter-course regimen for MDR-TB includes high-dose isoniazid. The pharmacokinetics of high-dose isoniazid within MDR-TB regimens has not been well described.

Objective

To characterize isoniazid pharmacokinetics at 5-15 mg/kg as monotherapy or part of MDR-TB treatment regimen.

Methods

We used nonlinear mixed-effects modelling to evaluate the combined data from INHindsight, a 7-day early bactericidal activity study with isoniazid monotherapy, and PODRtb, an observational study of patients on MDR-TB treatment including terizidone, pyrazinamide, moxifloxacin, ethionamide, ethambutol and kanamycin, ethionamide or/and isoniazid.

Results

A total of 58 and 103 participants from INHindsight and PODRtb study, respectively, were included in the analysis. A two-compartment model with hepatic elimination best described the data. NAT2 genotype caused multi-modal clearance, and saturable first-pass was observed beyond 10 mg/kg dosing. Saturable isoniazid kinetics predicted an increased exposure of approximately 50% beyond linearity at 20mg/kg dose. Participants treated with

the MDR-TB regimen had a 65.6% lower AUC compared to participants on monotherapy. Ethionamide co-administration was associated with a 29% increase in isoniazid AUC.

Conclusion

Markedly lower isoniazid exposures were observed in participants on combination MDR-TB treatment compared to monotherapy exposures. Isoniazid displays saturable kinetics at doses >10 mg/kg. The safety implications of these phenomena remain unclear.

5.2 Introduction

Isoniazid is a key drug in first-line TB treatment regimens because of its potent early bactericidal activity (Jhun & Koh, 2020). Resistance to isoniazid or dual resistance to isoniazid and rifampicin, i.e. multidrug-resistant TB (MDR-TB) is common. Globally in 2019, approximately 13.1% of new cases and 17.4% of previously treated TB cases had isoniazid resistance, 21.4% of isoniazid-resistant cases are also resistant to rifampicin (WHO, 2020a). Isoniazid is a prodrug that is activated by the *Mycobacterium tuberculosis* catalase-peroxidase encoded by *katG* (Warren et al., 2009). The active form of isoniazid interrupts mycolic acid synthesis by binding tightly to the NADH-dependent enoyl acyl carrier protein reductase *InhA* (Banerjee et al., 1994). The primary sources of isoniazid resistance are *katG* and *inhA* mutations associated with high-level and low-to-intermediate-level phenotypic resistance, respectively (BLUM et al., 1990). Increased isoniazid doses have been reported to be effective against TB with low to moderate levels of isoniazid resistance (Böttger, 2011; Gausi et al., 2021; Lempens et al., 2018; Rieder & Van Deun, 2017).

MDR-TB is a global health threat and is challenging to treat because many second-line drugs are poorly efficacious, toxic or both. However, several clinical trials have shown favorable results when isoniazid was included as part of the treatment regimen, in doses 2- to 3-fold those used for drug-sensitive TB (Böttger, 2011; Gausi et al., 2021; Lempens et al., 2018; Rieder & Van Deun, 2017). Therefore, WHO has endorsed the shorter- course MDR-TB regimen, which includes high-dose isoniazid, ethionamide, ethambutol, bedaquiline, moxifloxacin, pyrazinamide, and clofazimine with a treatment duration of 9-12 months (Chesov et al., 2017).

Although the pharmacokinetics (PK) of isoniazid has been extensively studied in patients on standard doses for drug-sensitive TB, the PK of isoniazid at higher doses and in the context of regimens used to treat MDR-TB has not been well characterized. When drug clearance is dependent on an enzyme system with a fixed capacity, nonlinear PK may be observed when the drug concentration exceeds enzymatic capacity. One such drug is Isoniazid, which is predominately metabolized (50-90%) in the liver and intestine by N-acetyltransferase 2 (NAT2) (McDonagh et al., 2014). The higher number of drugs used in MDR-TB treatment regimens increases the potential for drug-drug interactions (DDIs). Therefore, we aim to characterize the PK of standard (5 mg/kg) to high-dose isoniazid (10-15 mg/kg) as monotherapy or part of the MDR-TB treatment regimen, thus exploring DDIs within the MDR-TB regimen.

5.3 Methods

5.3.1 Study design and participants.

We used data from two studies for our analysis: the INHindsight (Dooley et al., 2020), a phase IIa early bactericidal activity (EBA) trial, and PODRtb, a prospective observational study of hospitalized patients on standard treatment for MDR-TB, using pharmacometrics towards optimized use of second-line drugs for MDR-TB (Chirehwa et al., 2021). The studies were approved by the local Institutional Review Board or Ethics Committee at each site and participants in both studies provided written informed consent prior to enrolment.

The INHindsight study recruited adults (≥ 18 years) with sputum smear-positive pulmonary TB with an infecting strain of *Mycobacterium tuberculosis* with the *inhA*-mutation conferring isoniazid resistance, or no mutations as a comparative control. HIV negative patients and HIV

positive patients with a CD4 count of >50 cells/mm^3 were eligible to participate. The study was conducted at Task Applied Science in Cape Town, South Africa.

The PODRtb study recruited MDR-TB inpatients with rifampicin-monoresistance (RMR-TB) or MDR-TB aged ≥18 years at Brooklyn Chest and DP Marais TB hospitals in Cape Town, South Africa. Critically ill patients and those unable to provide informed consent were excluded. At the time of the study, the standard MDR-TB treatment regimen comprised pyrazinamide, moxifloxacin, kanamycin, cycloserine (dosed as terizidone), ethionamide and/or high-dose isoniazid. Ethambutol was added if there had been no prior ethambutol exposure or ethambutol exposure has been for <1 month prior to treatment initiation. The choice of ethionamide and/or isoniazid use was at the discretion of the treating clinician (Chirehwa et al., 2021). Further details on the study design are reported in earlier publications (Chirehwa et al., 2021; Dooley et al., 2020).

5.3.2 Study procedure

Study participants for the INHindsight study with isoniazid-resistant TB (*inhA* mutations) were randomized to receive isoniazid doses of 5, 10, or 15 mg/kg, respectively, while those with drug-sensitive isolates were administered 5 mg/kg. Isoniazid (Betabs-Isoniazid 100-mg formulation) was given as monotherapy for 7 days, and PK sampling was performed on day 6. Blood samples were drawn pre-dose and at 30 minutes, 1, 2, 4, 6, 8, 12, and 24 hours post-dose. *NAT2* genotypic information was categorized into rapid, intermediate, and slow acetylator as previously described (Gausi et al., 2020; Sabbagh et al., 2009).

PODRtb PK sampling sessions were scheduled ≥2 weeks after treatment initiation. A subset of participants were enrolled in a comparative PK substudy in which the drugs were

administered as crushed tablets 1-2 weeks after the first PK sampling occasion when drugs were administered as whole tablet formulations. Within the PK substudy, isoniazid tablets were crushed with a standard-size mortar and pestle, the contents were mixed with 200 ml of water. After ingestion, tablet remnants adhering to mortar, pestle or mixing cup wall were scraped off with a spatula, mixed with a small unmeasured amount of water, and swallowed by the participant (Court et al., 2019). In cases of low-level INH resistance, participants were given high isoniazid doses (10–15 mg/kg); while patients with RMR-TB were treated with standard isoniazid doses (5 mg/kg). Isoniazid formulation information was not captured. Blood sampling was scheduled at pre-dose , 2, 4, 6, 8, and 10 hours post-dose on both PK sampling occasions (Chirehwa et al., 2021).

Dosing was performed under fasting conditions in both studies and was strictly observed by the study physician or nurse. Blood samples were centrifuged at 800 G for 10 minutes, and plasma was aliquoted into cryovials and immediately frozen at -70°C. Isoniazid plasma concentrations were quantified using liquid chromatography-tandem mass spectrometry in the Division of Clinical Pharmacology, University of Cape Town, South Africa. Isoniazid calibration ranged from 0.105 to 25.0 mg/L, the inter-day accuracy and precision ranged from 92.2% to 104.5%, and 6.5% to 10.8%, respectively (Chirehwa et al., 2018b). The similarities in the two studies were ideal for pooling, especially since population PK models are capable of handling such data.(Svensson et al., 2012)

5.3.3 Pharmacokinetics analysis

Isoniazid concentrations were interpreted using population PK modelling in NONMEM version 7.4.3 (Boeckmann et al., 2011) and ancillary software (Keizer et al., 2013).

To describe isoniazid PK, one- and two-compartment models were tested with first-order absorption (with or without lag time or a chain of transit compartments) and first-order elimination. Since isoniazid is mostly hepatically cleared, we tested a hepatic elimination model to capture the effect of first-pass metabolism (with and without saturation of extraction ratio (E_h) characterized by Michaelis-Menten parameterization), as described by Chirehwa et al. (Chirehwa et al., 2016).

The structural model with saturable hepatic extraction had the oral administered isoniazid transferred from the absorption compartment into the liver, where it undergoes first-pass metabolism. The drug is then transferred into the disposition compartment, however from the central compartment, isoniazid is recirculated to the liver for further clearance. The saturable intrinsic hepatic clearance (CL_h) is determined by hepatic blood flow (Q_h) and E_h as follows:

$$CL_h = Q_h \cdot E_h$$

E_h is defined as:

$$E_h = \frac{CL_{int} \cdot f_u}{CL_{int} \cdot f_u + Q_h}$$

Where f_u is the unbound fraction, and CL_{int} is the intrinsic clearance. CL_{int} is defined by Michaelis-Menten parameterization as follows:

$$CL_{int} = \frac{V_{max}}{C_h + K_m}$$
$$CL_{int,max} = \frac{V_{max}}{K_m}$$

Where $Cl_{int,max}$ is the maximum CL_{int}, C_h is the liver concentration, and K_m is Michaelis constant, a parameter denoting the drug concentration that produces 50% of the maximal clearance of the system. The liver volume and Q_h (Yang et al., 2007) were assumed to be 1 L and 90 L/h,

respectively, in a typical individual (56.1 kg fat-free mass) and adjusted for effect of body size using allometric scaling (Holford & Anderson, 2017). f_u was fixed to 95% (Sturkenboom et al., 2015).

Random effects at occasion- (each dose), visit- (each PK sampling visit), and/or subject-level were included on the PK parameters if statistically significant using a log-normal distribution (Mould & Upton, 2013). A combination of proportional and additive error was used to model unexplained residual variability. Concentrations below the limit of quantification (BLQ) were handled similarly to the M6 method suggested by Beal et al. with additive error for all imputed values inflated by half of the lower limit of quantification (LLOQ) to mitigate the effect of imputation (Beal, 2001). When the terminal phase of a PK profile contained a series of LLOQ values, only the first was used for estimation, while subsequent LLOQ values were ignored when estimating but retained for simulation-based diagnostics such as visual prediction checks (VPCs).

We initially analyzed the INHindsight data separately before adding the PODRtb data. Model development was guided by evaluating drops in NONMEM objective function value (ΔOFV) of nested models. The OFV was assumed as $\chi 2$-distributed, $p<0.05$ was required for one additional parameter (i.e. ΔOFV=3.84, df=1). Aside from statistical significance, diagnostic plots, including visual prediction checks (VPCs), physiological plausibility, and clinical relevance of the results, were considered in model development decisions.

The effect of *NAT2* genotype on the clearance of isoniazid was tested early in the model developing process because *NAT2* has been reported to critically affect the PK of isoniazid (Cordes et al., 2016; Gausi et al., 2020). A mixture model was implemented to assign participants with missing genotype to the subpopulations (Keizer et al., 2012). the

proportions were fixed to those with available genotype information, which was in line with reports from similar populations (Gausi et al., 2020). Allometric scaling was applied on all clearance and volume of distribution parameters (Holford & Anderson, 2017) to account for the effect of body size. In addition, we tested other covariates on isoniazid's PK parameters, including the effect of tablet crushing, co-administered drugs, and study effect. The effect of concomitant TB drug was assessed one at a time as a dichotomous covariate (with or without the concomitant drug). The group with the higher number of participants was set as the reference and its PK parameter (especially clearance and bioavailability) were compared with the group with a smaller number of participants. These were investigated using a supervised stepwise approach with forward inclusion ($p<0.05$) and backward elimination ($p<0.01$, $\Delta OFV=6.64$ for $df=1$).

5.4 Results

5.4.1 Study Profile

Isoniazid PK samples were available for 161 participants (58 participants from the INHindsight study (one participant withdrew consent on day 5) and 103 in the PODRtb study, of whom 18 were enrolled in the crushed tablet substudy. The participants had a median weight of 51 kg, 106 (66%) were males and 86 (53%) were HIV negative *NAT2* information was not available in the PODRtb study, while in the INHinsight study, intermediate *NAT2* acetylator was predominant (54%). Participants baseline characteristics and a summary of the study information is presented in **Table 5.1.**

Table 5.1: Study information and baseline characteristics of participants from INHindsight and PODRtb study

Characteristics	**INHindsight**	**PODRTB**
No. of participants	**N=58**	**N=103**
Design and objective	a two-stage, two-step, phase IIa, open-label, randomized clinical trial evaluating EBA of high isoniazid dose.	Observation study evaluating effects of 2nd-line drug exposures on treatment response and toxicity in MDR-TB patients.
Isoniazid dose	5-15 mg/kg monotherapy.	5-15 mg/kg co-administered with MDR-TB treatment.
Population	Adults with pulmonary TB strain shown to have *inhA* mutation or no mutations (control group).	Adults on MDR-TB therapy, with rifampicin mono-resistant or MDR TB.
No of samples	517	724
PK sample after dose initiation (Days)	6	≥14
PK sampling times (hr)	pre-dose, 0.5, 1, 2, 4, 6, 8, 12, and 24	pre-dose, 2, 4, 6, 8, and 10 h
Median (range)		
Weight (kg)	51 (41-82)	48 (30-85)
Height (m)	1.68 (1.47 – 1.87)	1.66 (1.43–1.85)
Fat-free mass (kg)	44.6 (29.9 – 56.7)	40.9 (24.1-58.9)
BMI ($kg \cdot m^2$)	18.1 (14.6 – 30.9)	17.3 (11.5–32.0)
Age (years)	32 (18-58)	35 (19-69)
No. of participants with the following characteristics		

Sex (Male/Female)	**43**/15	**63**/40
Race (Black/Colored/White)	21/**36**/1	-
NAT2 phenotype (Rapid/ intermediate/slow/missing)	8/**32**/14/4	-
Mutation (none/*inhA*/ katG/*inhA*&katG/mono-RIF)	16/**42**/0/0/0	0/**62**/3/1/37
HIV status (Positive/Negative)	12**/46**	**64**/39
Administered crushed tablet (Yes/No)	0/58	18/85
Concomitant drug information		
Lopinavir/ritonavir (Yes/No)	1**/57**	11**/92**
Efavirenz (Yes/No)	5**/53**	36/**67**
Ethambutol (Yes/No)	0/**58**	**88**/15
Ethionamide (Yes/No)	0/**58**	56/47
Pyrazinamide (Yes/No)	0/**58**	**103**/0
Kanamycin (Yes/No)	0/**58**	**91**/12
Moxifloxacin (Yes/No)	0/**58**	**101**/2
Cycloserine (yes/No)	0/**58**	**102**/1
Pyridoxine (Yes/No)	**58**/0	**103**/0

5.4.2 Pharmacokinetic model

A two-compartment disposition model best described the PK of isoniazid with first-order absorption through a chain of transit-compartments (Savic et al., 2007). Drug elimination implemented with a well-stirred liver model (Chirehwa et al., 2016; Gordi, Xie, & Jusko, 2005) was able to describe hepatic clearance and first-pass hepatic extraction (E_H) with the parameter of intrinsic hepatic clearance (CL_{int}), The hepatic elimination model resulted in a ΔOFV=-15.1 compared to a normal first-order elimination Inclusion of saturation of Cl_{int}, and thus E_h, further improved the model fit (ΔOFV=-20, p≪0.001). The final model parameters were estimated relative to pre-hepatic bioavailability (bioavailability before first-pass (F_{preH})) whose typical value fixed to the reference of 1. A schematic diagram of the final model is shown in **Figure 4.1**. Parameter estimates and their precisions are presented in **Table 4.2.**

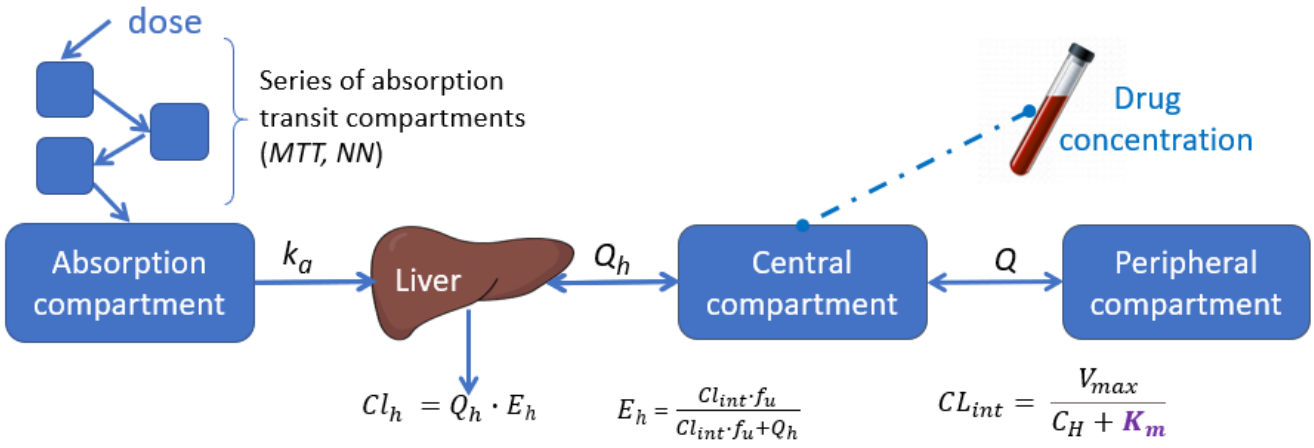

Figure 5.1: Schematic representation of the PK model of isoniazid. The absorption is described with a series of transit-compartments (NN) and mean transit time (MTT) to capture the delay in absorption, and a rate constant k_a. The hepatic extraction (Eh) is responsible for first-pass metabolism and the systemic elimination with first-order kinetics. Drug transfer between the central and peripheral compartment is defined by intercompartmental clearance Q/F, where F represents the oral bioavailability. Cl_{int} is the intrinsic clearance, C_h is the hepatic clearance and $Cl_{int,max}$ is the maximum Cl_{int}, f_u represent the fraction unbound, K_m is the drug concentration that produces 50% of the maximal elimination rate of the system, and Q_h is the hepatic blood flow.

Table 5.2:Final PK parameter estimates for isoniazid.

Parameter	Typical Value (95% CI[a])	Variability [b], %CV (95% CI[a])
$CL_{int.max}$[c] (L/h) *NAT2* Rapid	51.7 (38.8 – 56.0)	32.1 (20.5 – 43.1)*
$CL_{int.max}$[c c] (L/h) *NAT2* Intermediate	29.6 (21.8 – 35.0)	
$CL_{int.max}$[c] (L/h) *NAT2* Slow	12.5 (10.3 – 14.7)	
V_c [a] (L)	41.2 (37.1 – 43.8)	
V_p [a] (L)	9.97 (7.08 – 11.9)	
V_H [a] (L)	1 FIXED	
Q[c] (L/h)	2.26 (1.62 – 2.83)	
k_a (1/h)	5.50 (3.96 – 5.58)	155 (117 - 172)[#]
MTT (h)	0.154 (0.102– 0.200)	106 (93.3- 138)[#]
NN (.)	2.55 (1.67 – 3.02)	
Q_H[c] (L/h)	90 FIXED	
fu (%)	95 FIXED	
Prehepatic relative bioavailability [F_{preH}] - INHindsight (%)	100 FIXED	21.4 (14.3 – 23.4)[#]
Prehepatic relative bioavailability [F_{preH}] – PODRtb[f] (%)	34.5 (28.4 – 42.3)	63.3 (42.3 – 69.3)[#g]
Scaling parameter for between-occasion variability in F_{preH}– PODRtb (folds)	2.96 (2.56 – 4.52)	
Effect of dose on PODRtb F_{preH} - per unit increase from 10 mg/kg (%)	+2.82 (1.40 – 4.24)	
Proportional error (%)	12.3(10.8 – 14.0)	
Additive error (mg/L)	0.021[e] FIXED	
K_m(mg/L)	19.5 (14.2 – 34.5)	
Ethionamide effect on CL_{int} (%)	-29.5 (-40.1 – -14.6)	

Abbreviations: CL_{int} clearance intrinsic; V_c apparent central volume of distribution; V_P apparent peripheral volume of distribution; V_H apparent hepatic volume of distribution; Q apparent intercompartmental clearance for INH; k_a first-order rate constant of INH absorption; MTT absorption mean transit time; NN Number of absorption transit compartment; Q_H blood liver flow [19]; fu unbound fraction of isoniazid in plasma (Alghamdi et al., 2018); K_m drug concentration that produces 50% of the maximal elimination rate of the system.

Shrinkage of variability in the final model are below 30% for all estimates, and epsilon shrinkage is 15%

[a] 95% confidence intervals (CIs) were obtained with a 200-sample nonparametric bootstrap

[b] Variability was modelled with log-normal distribution and is presented as an approximate percentage CV.

[c] Clearance parameters are allometrically scaled based on fat-free mass (typical value reported for 44 kg, which was the median fat-free mass of the study population)

[d] Volume of distribution parameters are scaled based on weight (typical value reported for 51 kg, which was the median weight of the study population).

[e] Additive error was fixed to 20% of the LLOQ.

[f] The reference of the PODRTB estimated Prehepatic relative bioavailability – PODRtb (F_{preH}) was 10 mg/kg dose.

[g] Inflated between occasion variability due to the scaling parameter of the PODRtb study bioavailability.

** Between subject variability.*

[#] Between occasion variability

Allometric scaling was applied on all disposition parameters, including those for the hepatic model (Cl_{int}, $V_{h,}$ and Q_h) to account for effect of body size, improving model fit (ΔOFV=-17.6), and explaining part of between-subject variability (a drop of 12% in BSVCL). Replacing body weight with fat-free mass for clearance parameters (but not volume) further improved model fit (ΔOFV=-18.6). *NAT2* genotype significantly affected clearance of isoniazid (ΔOFV=-90, $p \ll 0.001$), as CL_{int} varied greatly between rapid (51.7 L/h), intermediate (29.6 L/h), and slow (12.5 L/h) acetylators. After adjusting for body size and *NAT2* genotype, the model detected a 29% decrease in isoniazid intrinsic clearance due to ethionamide co-administration (ΔOFV=−16.1, $p \ll 0.001$) irrespective of *NAT2* genotypes. There was no significant effect of crushed tablets on F_{preH} (p= 0.130); however, the model estimated faster absorption for crushed tablets (no delay before first-order absorption) and a transit compartment model with an estimated mean transit time of 9 minutes for the whole tablets (ΔOFV=−28, $p \ll 0.001$). There was no significant effect of efavirenz co-administration on clearance (p=0.265).

A significant difference was identified in F_{preH} of isoniazid between the two studies (ΔOFV=−144, $p \ll 0.001$); PODRtb study F_{preH} was 65.5% lower compared to the INHindsight study. The PODRtb study had between-occasion variability in F_{preH} of 3 folds greater than the INHindsight study (ΔOFV=−102, $p < 0.001$). **Figure 5.2** displays F_{preH} of the two studies stratified by the three-dose categories, F_{preH} for PODRtb is lower and more variable than the INHindsight. F_{preH} of a typical individual in the INHindsight study was fixed to 1, presented by the green dashed line in **Figure 5.2.** The F_{preH} of the PODRtb study was dose-dependent, with a 2.82% increase in F_{preH} with a unit increase in dose/kg displayed in **Figure 5.2** (ΔOFV=−19.8, $p \ll 0.001$). In contrast, there was no significant difference between the INHindsight F_{preH} across the different doses. **Figure 5.3** shows the comparison of the exposures observed in the

two studies with that of historical drug-sensitive TB data (Hong et al., 2020). For easy comparison with previous reports, the rapid and intermediate *NAT2* exposure in Figure 3 were merged. The boxplot illustrates that the INHindsight exposures are in line with historical data, while the PODRtb exposures are lower for all the *NAT2* genotypes. When trying to replace the study effect with any of the co-administered drugs, the model fit did not improve. In particular, the model could not meaningfully discriminate between study effect and the three co-administered drugs that nearly all PODRtb study participants were taking, namely pyrazinamide, moxifloxacin, and terizidone/cycloserine. The decrease in OFV when testing each of these drugs was similar to that of study effect, so we decided to simply include study effect in the final model.

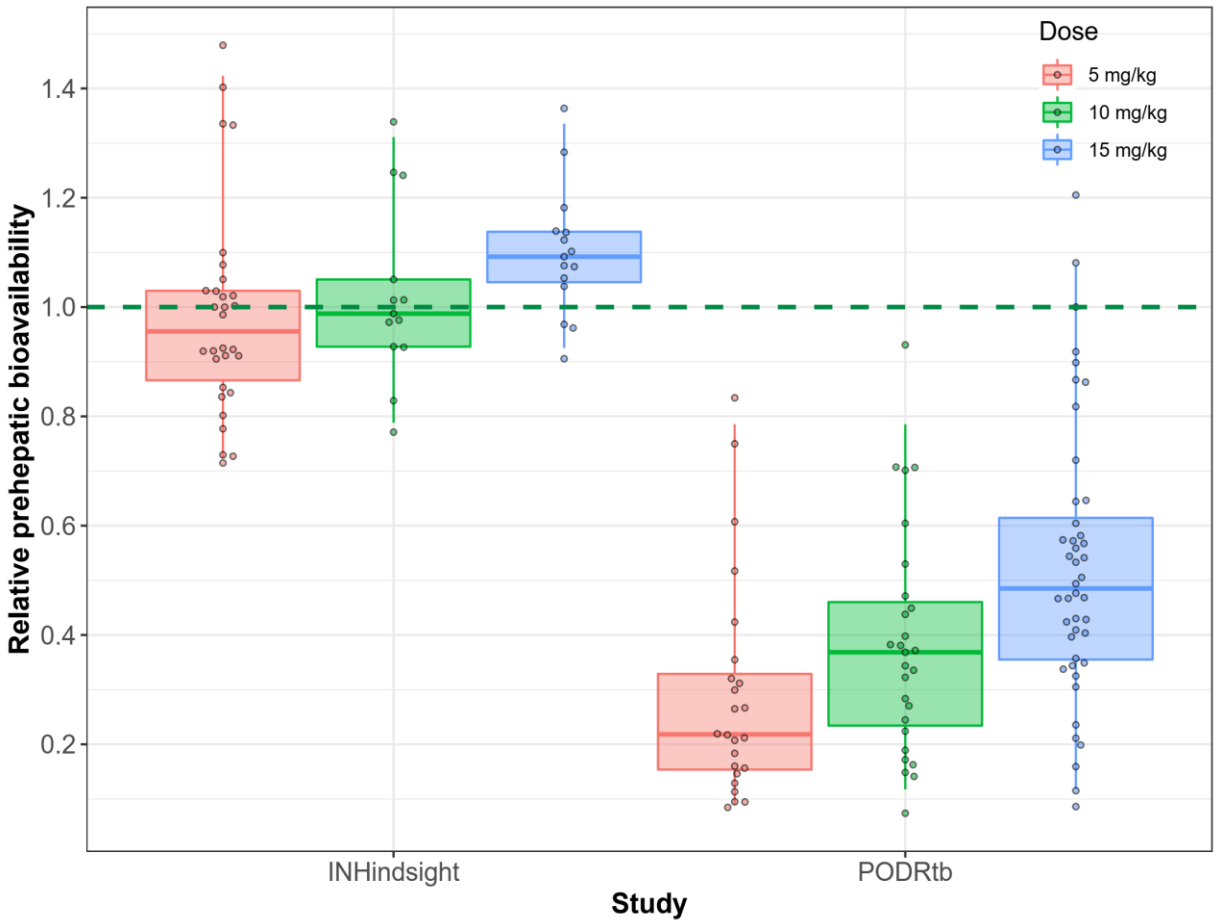

Figure 5.2: Boxplot of relative prehepatic bioavailability for the two studies (INHindsight and PODRtb) stratified by the three-dose categories. The green line is the reference relative prehepatic bioavailability, which was fixed to 1. All values for NAT2 for the PODRtb study were imputed using a mixture model.

Nonlinear PK of isoniazid was observed at higher doses, as the drug-metabolizing enzymes in the liver were exposed to a concentration higher than the predicted K_m (19.5 mg/L). Such isoniazid concentrations were only achieved in the liver during absorption before the first pass, while the central compartment concentration was below the predicted K_m. **Figure 5.4** shows the dose exposure relationship, illustrating how the nonlinear model (which the data supported) a more-than-proportional increases in exposure with higher doses (approximately a 50% increase in $AUC_{0\text{-}24}$ above linearity at a dose of 20 mg/kg). The marks on the x-axis of **Figure 5.4** represent the mg/kg dose that the patients in the two studies received. Model

evaluation through VPC (**Figure 5.5**) shows that the model generally described the data well.

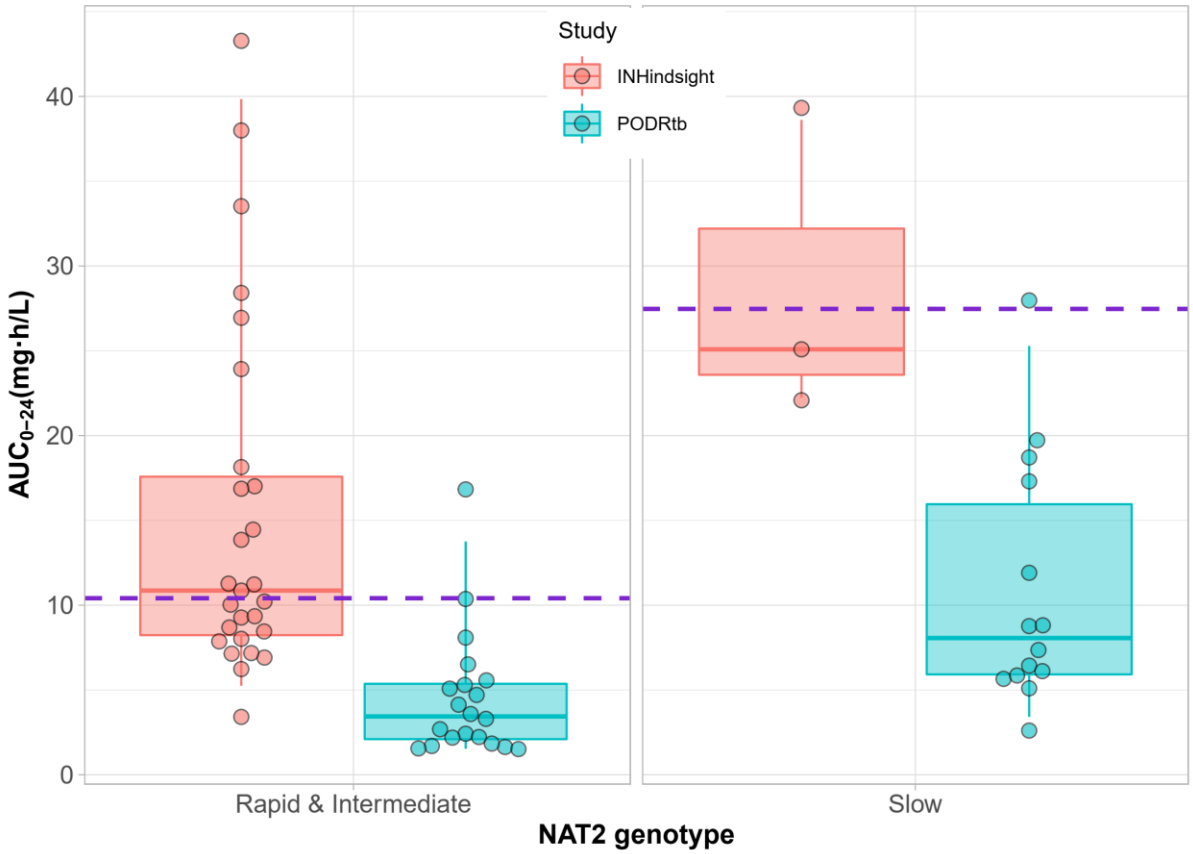

Figure 5. 3: A boxplot comparing the exposure of participants administered the standard dose (5mg/kg) in the two studies (INHindsight and PODRtb), stratified by NAT2 genotype. The purple line represents isoniazid AUC0-24 from historical data (Hong et al., 2020)***, 10.4 and 27.5 for the Rapid & Intermediate, and slow respectively. A weighted geometric mean for the Rapid and intermediate was calculated to determine the purple line in the Rapid & intermediate panel.***

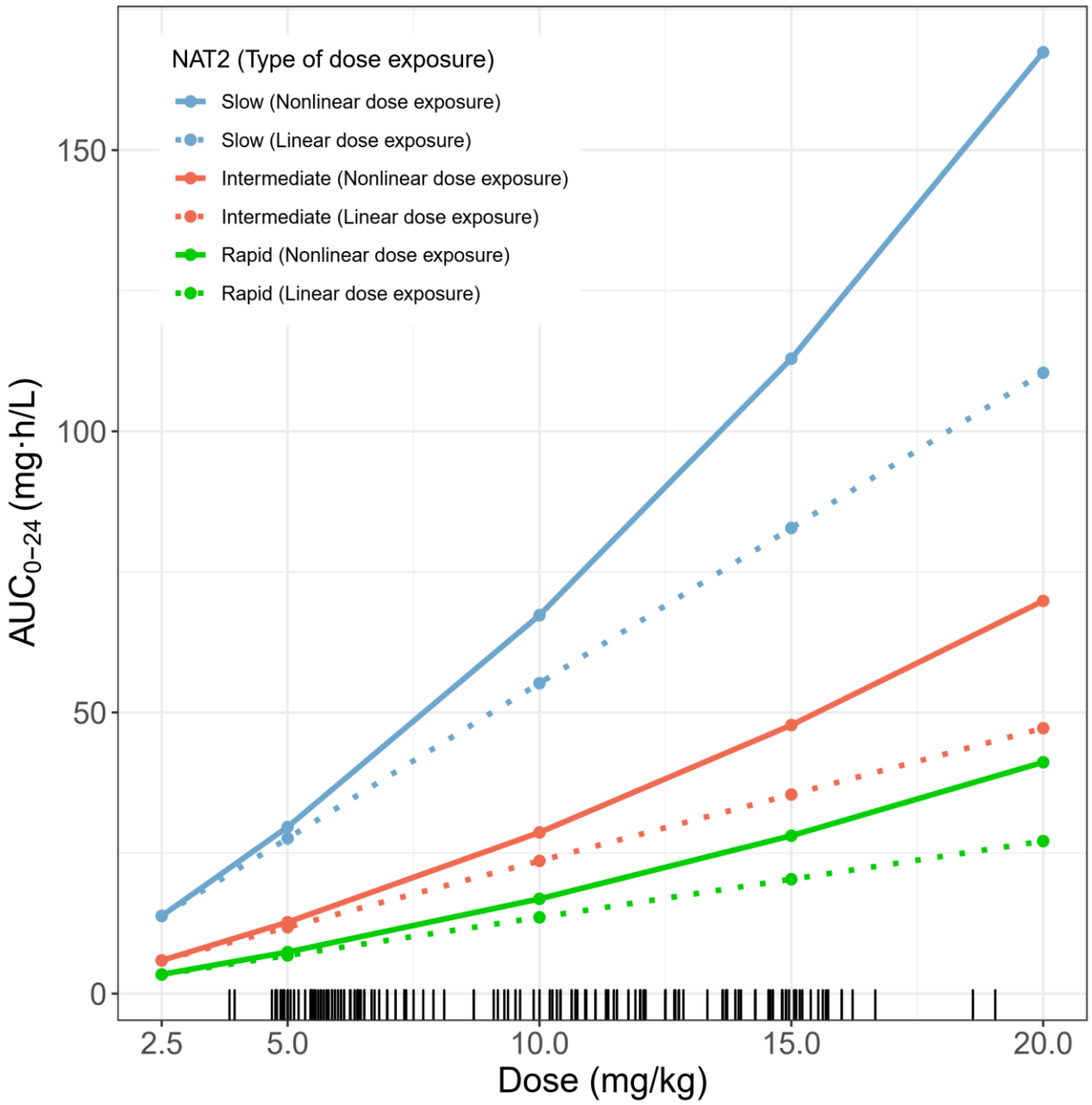

Figure 5.4: Lineplot comparing the isoniazid exposure for different doses, stratified by NAT2 genotype for a linear dose exposure and nonlinear dose exposure model. The three colours represent the different NAT2 genotype, the solid lines represent nonlinear dose exposure, and the dotted line represent linear dose exposure. The marks on the x-axis represent the mg/kg dose observed in the two studies.

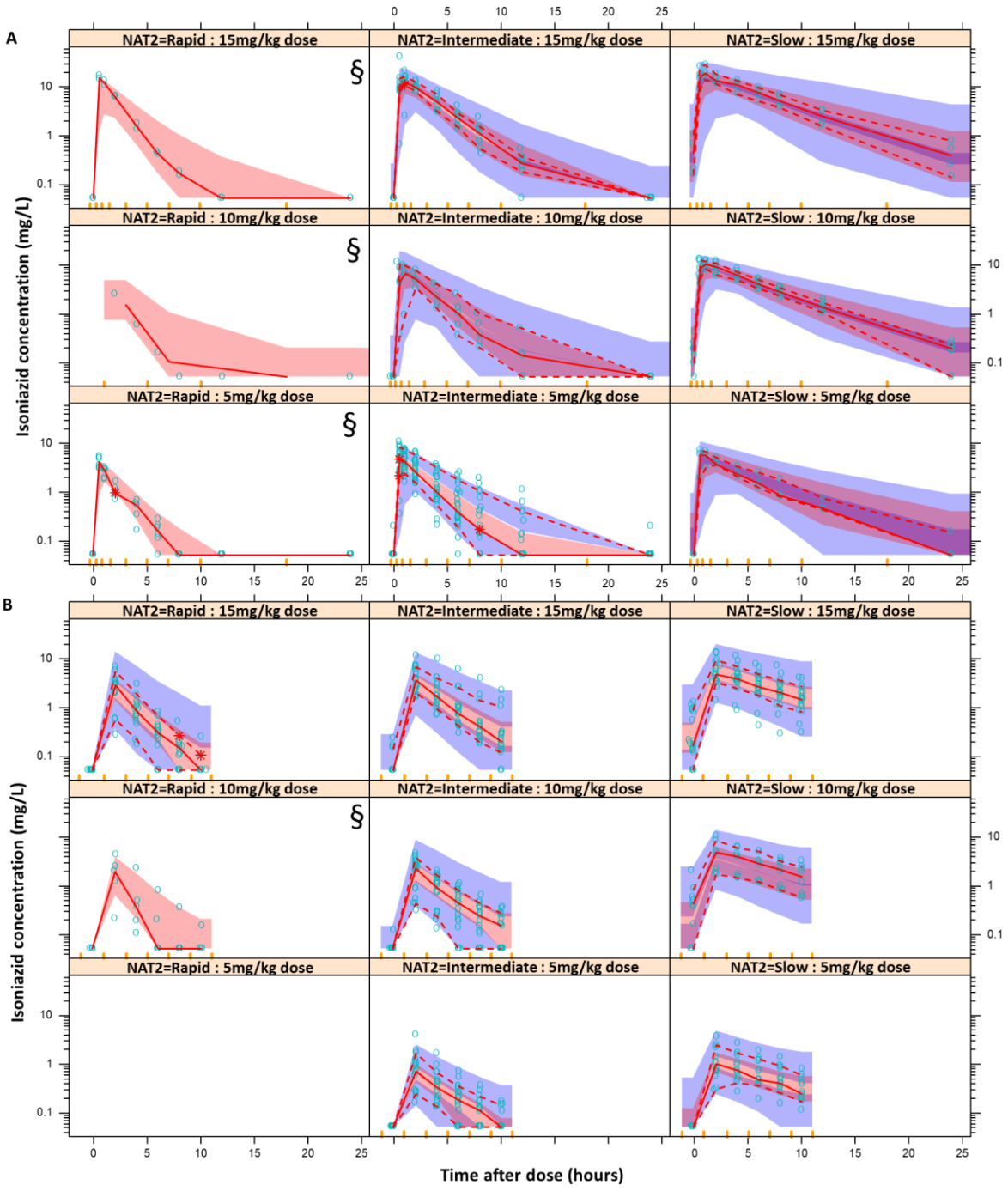

Figure 5.5: Visual predictive check (VPC) of the isoniazid model, stratified by dose and NAT2 genotype. Panel A is the VPC of the INHindsight, while panel B is for the PODRtb data. The solid and dashed lines are the 10th, 50th, and 90th percentiles of the observations, while the shaded areas represent the 95% model-predicted confidence intervals for the same percentiles. For the panels with few data, represented by §, we display only the 50th percentile.

5.5 Discussion

The WHO recommendation of high-dose isoniazid as part of the MDR-TB regimen makes understanding its PK in these patients a research priority. Our study addresses this research gap by describing the PK and DDI profile of high dose isoniazid with other drugs within the MDR-TB regimen. We had three main findings: first, we observed markedly lower isoniazid exposures in PODRtb participants receiving the same mg/kg doses, most likely due to a DDI with one of the drugs in the MDR-TB regimen affecting absorption of isoniazid. Second, the pharmacokinetics of isoniazid at high doses, particularly >10 mg/kg, is nonlinear. Third, isoniazid exposure is modestly increased with ethionamide co-administration, irrespective of *NAT2* genotype. These three finding may need to be considered when recommending isoniazid for the treatment of drug-resistant TB. The findings are further discussed below.

Compared to both INHindsight (on isoniazid monotherapy) and historical data (Hong et al., 2020), we unexpectedly observed low Isoniazid exposures in the participants from the PODRtb study who were dosed with other MDR-TB drugs. Additionally, a dose-dependent F_{preH} was observed in the PODRtb study, the estimated F_{preH} compared to INHindsight was 21%, 34% and 45% at 5, 10, 15 mg/kg dose, respectively**.** The low exposure and dose-dependent bioavailability may suggest a dose-dependent DDI in the gut. While the lower exposure could be a study effect, the assay methodology, the handling of samples, and the study participants and procedures were similar in the two studies. The key difference between the INHindsight and the PODRtb studies is that participants in the PODRtb study were treated with isoniazid co-administered with other second-line anti-TB drugs which may have affected the absorption of isoniazid. Since most PODRtb patients were on pyrazinamide,

moxifloxacin, and terizidone/cycloserine, the model was unable to distinguish whether the lower exposure was study-specific or due to a DDI with one of these agents in the study regimen. Apart from these three drugs the model was able to distinguish that the other co-administered drugs were not the perpetrator of the DDI in favor of study effect. Similar findings were reported by Winckler et al., 2021 who showed an 80% reduction in isoniazid exposure (median area under the concentration curve (AUC) of 13.1 mg·h/L) in children dosed with isoniazid at 20 mg/kg of as part of an MDR-TB treatment regimen including ethambutol, fluoroquinolones, pyrazinamide, and terizidone, compared to exposures (median AUC 78.1 mg·h/L) in children on an MDR-TB preventive regimen including isoniazid, ethambutol, and fluoroquinolones. The authors postulated that one of the companion MDR-TB drugs could have affected the absorption of isoniazid, specifically terizidone, a structural analogue of cycloserine. Terizidone/cycloserine is postulated to interfere with the absorption of both isoniazid and ethionamide (Global Alliance for TB Drug Development., 2008). A preclinical study observed that ethionamide exposure (AUC) was significantly reduced when co-administered with D-cycloserine but not when the two drugs were administered separately (Ranjan et al., 2019). The chemical structure of ethionamide is similar to that of isoniazid, therefore it is possible that an interaction between both isoniazid and ethionamide exists at the absorption level. If indeed there is an interaction in absorption, dosing isoniazid 12 hours after or before the other MDR-TB drugs might reduce its effect, however this strategy will need further study and might be logistically challenging for directly observed therapy.

Drugs whose absorption, distribution, and excretion involve enzymes or carrier-mediated systems are known to saturate at high concentrations (Ludden, 1991). Isoniazid is

predominately metabolized (50 – 90%) by *NAT2* (Klein et al., 2016b), expressed highest in the liver and gut (Husain et al., 2007). Saturation of this pathway or any other pathway responsible for clearing isoniazid would explain our observed nonlinear pharmacokinetics. A hepatic elimination model characterized the extraction ratio, and saturation was described using Michaelis-Menten kinetics. The model predicts saturation of isoniazid with K_m of 19.5 mg/L, and this concentration was only achieved in the liver before first-pass, during the absorption of isoniazid. The nonlinear pharmacokinetics of isoniazid were apparent with doses higher than 10 mg/kg (approximately a 37% and 50% increase in AUC_{0-24} above linearity at a dose of 15% and 20 mg/kg, respectively) as shown in **Figure 5.4.**

We report a 29% decrease in the clearance of isoniazid due to the co-administration of ethionamide. This effect was irrespective of the *NAT2* phenotype. Ethionamide is a structural analogue of isoniazid, and the two drugs are known to share other similarities like hepatotoxicity, therapeutic targets, and drug resistance (Lehloenya et al., 2015). A study by Chirehwa *et al., 2021* found a similar decrease in ethionamide clearance when co-administered with isoniazid. The underlying mechanism for this interaction is unknown, as the two drugs have distinct metabolic pathways (Klein et al., 2016a; Phillips & Shephard, 2017). However, it is possible that the two drugs inhibit each other's clearance pathways in a manner not yet described or compete for the same transporters.

Chirehwa *et al*. reported a 29% decrease in the AUC_{24} of isoniazid rapid *NAT2* acetylator when co-administered with efavirenz (Chirehwa et al., 2018a). Two other studies reported similar findings (Bhatt et al., 2014; Sekaggya Wiltshire et al., 2014). Our analysis did not detect any substantial change in the exposure of isoniazid when co-administered with efavirenz, possibly

due to the small number of rapid *NAT2* acetylators and participants on efavirenz-based ART regimens (25%) in these cohorts.

Administration of crushed medication is regularly practiced in some centers, particularly in children who may not tolerate whole tablet formulations. Crushing tablets may affect the absorption and bioavailability of the active drug ingredients (Royal pharmaceurical society, 2011). A non-compartmental analysis of the PODRtb PK data reported a significantly decreased isoniazid exposure when the drug was administered crushed, and mixed with water (Court et al., 2019). Our model estimated that isoniazid reached the systemic circulation faster when it was administered crushed compared to the whole tablet formulation. The bioavailability of crushed or whole isoniazid was comparable. Similar results of faster absorption were reported when comparing the pharmacokinetics of whole versus crushed cycloserine (Chirehwa et al., 2020).

Our study had several limitations, much of which we believe has been mitigated by using a model-based approach for data analysis. *NAT2* genotype data was not available for all participants, but this was addressed by imputation using a mixture model to assign the individual with missing information to a phenotype group. Most of the PODRtb patients were on pyrazinamide, moxifloxacin, and cycloserine, Therefore the model was unable to discriminate between the study effect and a potential DDI with these three most common drugs in the PODRtb study. However, the Winckler *et al*.,(Winckler et al., 2021) study did not observe any interaction between isoniazid and levofloxacin, hence interaction with fluoroquinolones is unexpected. Pyrazinamide is co-administered with isoniazid for drug-sensitive TB treatment, and to our knowledge, no interactions have been reported. Finally, different isoniazid formulations were used in the two studies and, while we expect the two

formulations to be bioequivalent, we cannot exclude the effect of the different formulations on the absorption or/and exposure.

In conclusion, our study showed nonlinear pharmacokinetics of isoniazid when dosed above 10 mg/kg. The saturation in isoniazid metabolising enzyme should be considered when recommending doses greater than 10 mg/kg, especially for slow NAT2 acetylators who may have higher isoniazid concentrations and consequently be at increased risk of toxicity. Additionally, we observed that patients with MDR-TB taking the multidrug treatment had unexpectedly very low isoniazid exposures compared to patients with MDR-TB taking isoniazid alone, an effect which may potentially be due to drug interactions with a companion drug. There is evidence that the interacting drug might be terizidone/cycloserine, however further investigations are required, especially since the effect is major. The perpetrator of the DDI is not ethionamide, which instead was observed to cause a modest increase in isoniazid exposure when co-administered. This is not likely to be of clinical relevance, except possibly in patients with slow NAT2 acetylator status. However, further studies are needed on the PK of high-dose isoniazid in patients receiving the WHO shorter regimen, which includes ethionamide but not cycloserine/terizidone.

Chapter 6: A semi-mechanistic model of the bactericidal activity of high-dose isoniazid against multi-drug-resistant tuberculosis

6.1 Abstract

Rationale: There is accumulating evidence that higher-than-standard doses of isoniazid are effective against low-to-intermediate-level isoniazid-resistant strains of *Mycobacterium tuberculosis*, but the optimal dose remains unknown.

Objective Characterizing the association between isoniazid pharmacokinetics (standard or high-dose) and early bactericidal activity against *M. tuberculosis* (drug-sensitive and inhA-mutated) and *N-acetyltransferase 2* status.

Methods: ACTG A5312/INHindsight is 7-day early bactericidal activity study with isoniazid at normal dose (5 mg/kg) for patients with drug-sensitive bacteria and 5, 10, and 15 mg/kg doses for patients with *inhA* mutants. Participants with pulmonary TB received daily isoniazid monotherapy and collected sputum daily. Colony-forming units (CFU) on solid culture and time-to-positivity (TTP) in liquid culture were jointly analysed using nonlinear mixed-effects modelling.

Measurements and Main Results: Fifty-nine adults were included in this analysis. Decline in sputum CFU was described by a one-compartment model, while an exponential bacterial growth model was used to interpret TTP data. The model found bacterial kill is modulated by isoniazid concentration using an effect compartment and a sigmoidal Emax relationship. The model predicted lower potency but similar maximum-kill of isoniazid against inhA-mutated isolates compared to drug-sensitive. Based on simulations from the PK/PD model, to achieve a drop in bacterial load comparable to 5mg/kg against drug-sensitive TB, 10- and

15-mg/kg doses are necessary against inhA-mutated isolates in slow and intermediate *N-acetyltransferase 2* acetylators, respectively. Fast acetylators underperformed even at 15 mg/kg.

Conclusions: Dosing of isoniazid based on *N-acetyltransferase 2* acetylator status may help patients attain effective exposures against inhA-mutated isolates.

6.2 Introduction

Antimicrobial resistance is a grave threat to global public health, responsible for approximately 700,000 deaths yearly (Review on Antimicrobial Resistance, 2014). Individuals with drug-resistant tuberculosis (TB) receive less active, poorly tolerated, or hard to access drugs. Detection of resistance is sporadic, given that diagnostic platforms and assay cut-offs are not well-established or available for many second-line drugs, but we have rapid tests to detect resistance to rifampicin and isoniazid. The primary mechanisms of isoniazid resistance are 1) prevention of activation of the pro-drug isoniazid due to katG mutation and 2) mutation of the promoter region of inhA, leading to overexpression of isoniazid target InhA (Karakousis et al., 2008). InhA mutation tends to result in low-to-intermediate-level phenotypic resistance (Lempens et al., 2018), while katG mutation results in high-level resistance that may or may not be overcome with safe isoniazid doses.

There is an urgent need to optimize existing agents until new ones are widely available to overcome the threat of drug resistance (Mouton et al., 2011). Improved treatment, including dose customization for individual patients or patient subgroups, can be driven by exposure-response relationships, a pharmacologic framework that provides an evidence-based method of dose selection. There is accumulating evidence that higher-than-standard doses of isoniazid are effective against low- to intermediate-level isoniazid-resistant strains, but the optimal “high-dose” is unknown, making isoniazid a prime candidate for exposure-response modelling to assess its use against drug-resistant strains. For many drugs, there is high inter-individual variability in drug-exposures, and this variability sources are unknown and unpredictable. For isoniazid, however, the main determinant of drug exposures is *N-acetyltransferase 2* (*NAT2*) status (exposure varies by 2-7 fold between slow and rapid

acetylators (Donald et al., 1997; Zabost et al., 2013)), and these genetic polymorphisms can be determine with available technology, albeit not at the point of care.

INHindsight trial was designed to assess effect of isoniazid dose escalation on its early bactericidal activity (EBA) against inhA-mutated isolates. We previously reported (Dooley et al., 2020) measurable EBA against inhA-mutated isolates at high-dose isoniazid (mean $EBA_{CFU0\text{-}7}$ of 0.17 and 0.22 log_{10}CFU/mL/day, at 10 and 15 mg/kg respectively in inhA group compared to 0.16 log_{10}CFU/mL/day in drug-sensitive). TB biomarkers (colony-forming-units (CFU) and time-to-positivity (TTP)) and isoniazid exposure are characterized by large inter- and intra-individual variability, and the measurement of the biomarkers is very noisy (Rockwood et al., 2016). To adjust for factors that modulate exposure-response-relationships and tease out signal from noise, model-based approach which can jointly characterize the relationship between isoniazid dose, its exposure, and TB biomarkers are needed. Such an approach becomes even more useful when identifying subgroups that may need dose adjustments (Ogasawara et al., 2018). Modelling can incorporate complex pharmacologic properties, such as delayed onset of action caused by isoniazid activation and is capable of simulating different clinical scenarios. This study employs such methods to characterize the association between isoniazid pharmacokinetics (at high or standard dose) and its early bactericidal activity against Mycobacterium-tuberculosis (drug-sensitive and inhA-mutated).

6.3 Methods

6.3.1 Study Design and Participants.

This analysis used isoniazid pharmacokinetics and EBA data collected in the INHindsight trial, a 7-day early bactericidal activity study conducted in South Africa. It was approved by the

local ethics committee and the South African Health Products Regulatory Authority. All participants gave written informed consent. Adults with sputum smear-positive pulmonary TB, treatment-naïve with an infecting strain shown to have inhA mutation or no mutations (control group) were eligible. Chest radiographs were performed to determine cavitary disease status. Further details of the study design were reported previously (Dooley et al., 2020).

6.3.2 Study procedures

In brief, participants infected with inhA-mutated *Mycobacterium tuberculosis (M.tb)* were randomized to receive isoniazid doses of 5, 10, or 15 mg/kg, respectively, while those with drug-sensitive isolates were administered 5 mg/kg. All participants received isoniazid monotherapy for 7 days; sputum samples were collected daily from two days before initiation of isoniazid until day 7 of treatment, and pharmacokinetic (PK) sampling occurred on day 6. Sputum samples were cultured on solid media to capture CFU and in liquid media to capture TTP. Isoniazid minimum inhibitory concentration (MIC) was estimated as previously described (Dooley et al., 2020). *NAT2* genotypic information and PK samples were captured and analysed as described in the **Supplemental Methods**. *NAT2* was assigned the following phenotype: fast, intermediate, or slow, utilizing the Sabbagh et.al suggestion (Sabbagh et al., 2009).

6.3.3 Pharmacokinetic/Pharmacodynamic Modelling

Isoniazid pharmacokinetics/pharmacodynamics was modelled using NONMEM version 7.4.3 and ancillary software (Keizer et al., 2013). Full details on model development are available in **Supplemental Methods**.

In brief, several structural PK models were tested to describe isoniazid plasma concentrations. Effect of *NAT2* genotype on clearance was tested, and allometric scaling was applied on all clearance and volume of distribution parameters (Anderson & Holford, 2008) to account for body size. *M.tb* bacterial load in patients was characterized using a compartmental model and a first-order kill rate. Both CFU and TTP were used jointly to quantify bacterial load: (i) CFU was directly obtained as an observation from the bacterial load compartment, while (ii) TTP was obtained by modelling the growth of *M.tb* in Mycobacterial Growth Indicator Tubes (MGIT) using the bacterial load in the patient (CFU on solid culture media) as the initial amount of bacteria transferred into the tube, which then grows and is detected after crossing a threshold. To link the PK and pharmacodynamics (PD), the effect of isoniazid exposure was tested on the kill rate using overall AUC (constant kill), instantaneous isoniazid concentration in plasma, or isoniazid effective concentration in a hypothetical effect compartment (R. Upton & Mould, 2014).

Model development was guided using graphical assessment of the goodness of fit plots, likelihood ratio tests (using supervised stepwise approach with forward inclusion ($p<0.05$), and backward elimination ($p<0.01$)), as described by Mould and Upton (Mould & Upton, 2013). Simulation-based diagnostics including visual predictive checks (VPC) were used for model validation. The PK model was developed first, then individual PK parameter estimates from the PK model were fixed in the PK/PD model. Monte Carlo simulations were performed with the final model to predict change in CFU from baseline for the drug-sensitive vs. inhA-mutated isolates under the three dose levels.

6.4 Results

6.4.1 Enrolment and Baseline Characteristics.

Among 59 adults included, 16 were controls with drug-sensitive *M.tb*; among the 43 participants with inhA-mutated *M.tb*, 13, 14, and 16 were randomized to the 5-, 10-, and 15-mg/kg arms. The participants had a median weight of 51 kg, 20% were HIV-positive, and 88% had cavitary disease (**Table 6.1**). PK samples were captured in 58 participants as one participant withdrew consent for family reasons on day 5, providing a total of 517 PK observations. Sputum bacillary load as measured by CFU and TTP was captured in all 59 participants, providing 449 and 524 observations for CFU and TTP, respectively. CFU missingness (15.4%) was due to contamination, while TTP missingness (1.3%) was due to leakage. Among the 55 participants who consented to genetic sample collection, intermediate *NAT2* acetylators were predominant (54%) and rapid the least prevalent (14%). MIC data were available for 27 participants and ranged from 0.2 to 1 mg/L in the drug-sensitive arm and 0.2 to 4 mg/L in the inhA-mutated arms, reason of missing MIC is provided in supplementary methods.

Table 6.1: Demographic, clinical, and laboratory characteristics of participants stratified by the 4 arms

Characteristics (median and range, n, or n (%))	**Drug-sensitive**	**inhA-mutated**			**Total**
Dosing (mg/kg)	**5 (N=16)**	**5 (N=13)**	**10 (N=14)**	**15 (N=16)**	**(N=59)**
Sex (M/F)	12/4	10/3	11/3	10/6	43/16
Race*					
Black	6 (38%)	6 (46%)	4 (29%)	5 (31%)	21 (36%)
Coloured/Mixed	9 (56%)	7 (54%)	10 (71%)	11 (69%)	37 (63%)
White	1 (6%)	0 (0%)	0 (0%)	0 (0%)	1 (2%)
Age (years)	30 (19-58)	31 (20-58)	32 (20-58)	34 (18-55)	32 (18-58)
BMI (kg/m^2)	18.0 (15.2-29.7)	18.1 (16.2-30.9)	17.7 (14.6-23.6)	18.5 (15.4-30.1)	18.1 (16.6-19.4)
HIV status (Negative/ Positive)	13/3	11/2	11/3	12/4	47/12
Cavities (Yes/No)	12/4	11/2	14/0	15/1	52/7
***NAT2* acetylation status**					
Rapid	4 (25%)	2 (15%)	0 (0%)	2 (13%)	8 (14%)
Intermediate	10 (63%)	8 (62%)	6 (43%)	8 (50%)	32 (54%)
Slow	2 (12%)	1 (8%)	7 (50%)	5 (31%)	15 (25%)
Missing	0 (0%)	2 (15%)	1 (7%)	1 (6%)	4 (7%)

*Percentage do not always add to 100% due to rounding.

6.4.2 Pharmacokinetics/pharmacodynamics model

The schematic of the final PK/PD model structure is displayed in **Figure 6.1**, and a VPC of the PD and PK model are shown in **Figure 6.2 and Figure E6.2 respectively,** indicating adequate model fit. The PK of isoniazid was best described by a two-compartment model with transit compartments absorption and first-order elimination using a well-stirred liver model. We included the effects of allometric scaling using fat-free mass on disposition parameters and *NAT2* genotype on clearance (see **Supplemental Results** for additional details and parameter values).

The decline of bacterial load in patients was best described using a one-compartment model with first-order killing of *M.tb* modulated by the isoniazid effect. The baseline bacterial load was lower in patients with drug-sensitive than those with drug-resistant TB; among patients with inhA-mutated isolates, a significant difference in baseline bacterial load was also found in participants administered 5mg/kg dose, therefore three baseline CFU parameters were estimated. The model for TTP used exponential growth in the MGIT since a logistic growth model did not substantially improve the fit and made the model unstable. A delay of about 6 hours in the onset of the growth was observed for sputum samples collected after initiation of isoniazid treatment compared to baseline ($p \ll 0.001$), and inhA-mutated isolates were found to grow with a doubling time 4 hours slower than drug-sensitive isolates ($p \ll 0.001$).

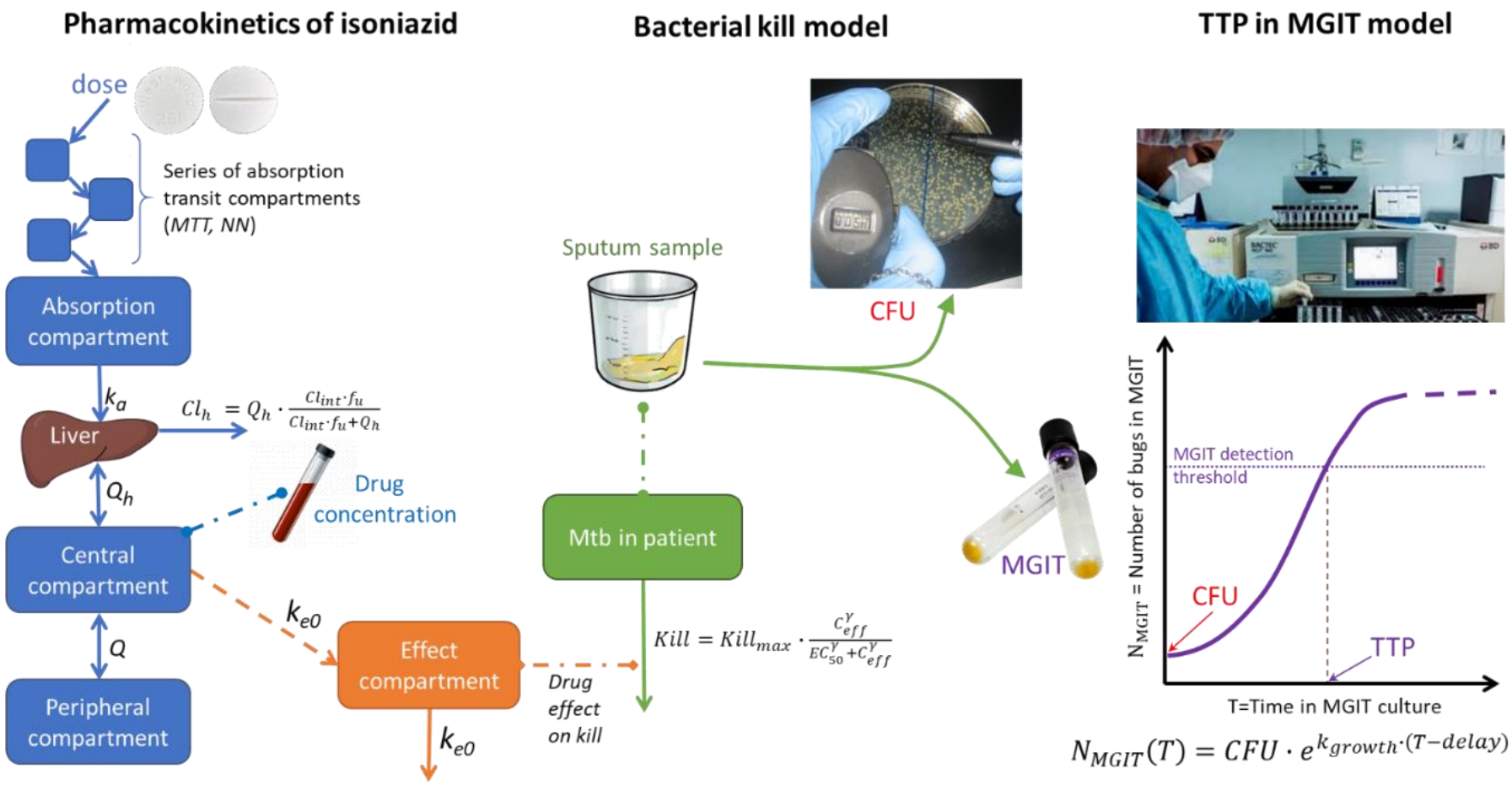

Figure 6.1: Schematic representation of the PK/PD model used to describe the pharmacokinetics of isoniazid, the drug-induced decline in bacteria load, and the growth of M.tb in MGIT.

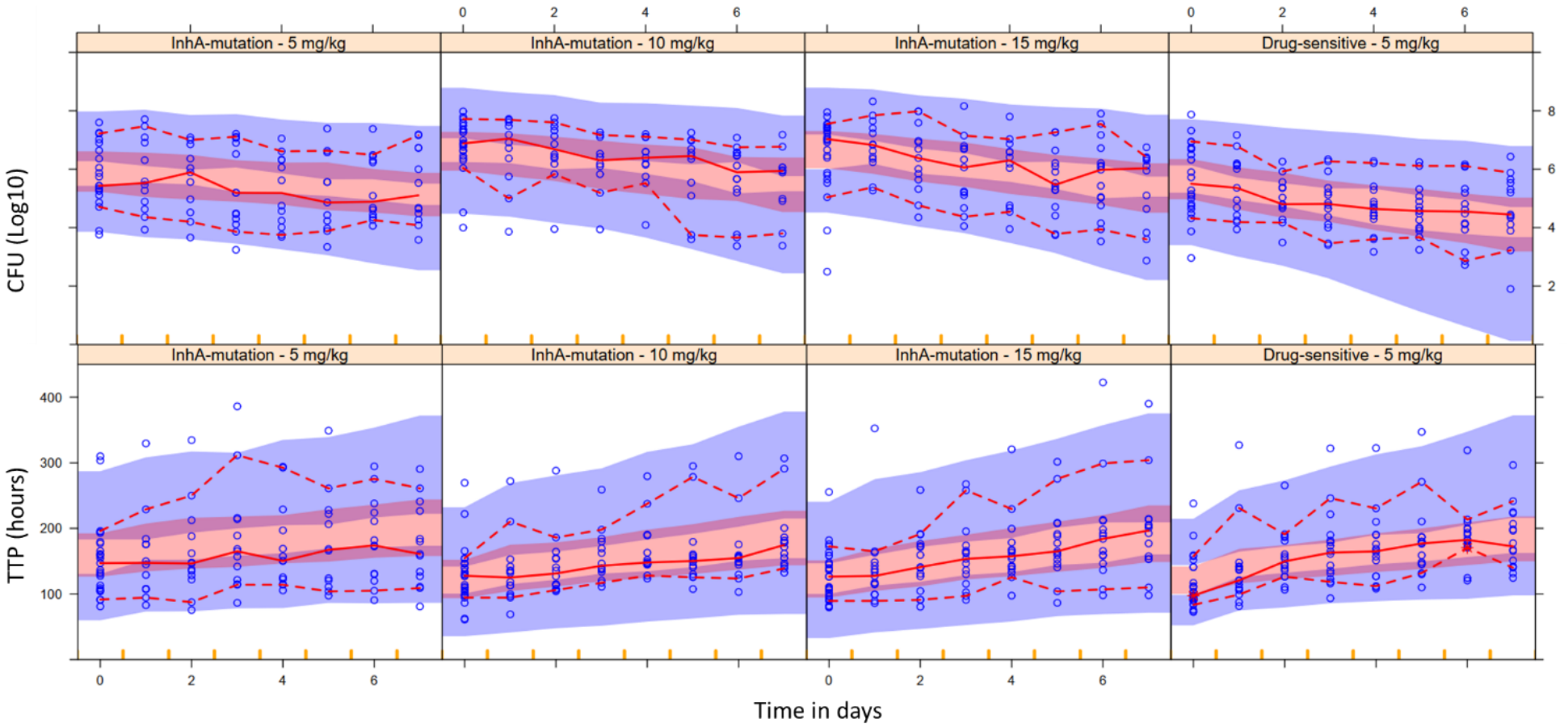

Figure 6.2: Visual predictive check of the PK/PD model of the CFU and TTP, stratified by arm. The solid and dashed lines are the 10th, 50th, and 90th percentiles of the observations, while the shaded areas represent the 95% model-predicted confidence intervals for the same percentiles. The two samples collected pre-treatment (baseline) have been collapsed together as day 0.

The bactericidal effect of isoniazid was best described by using an Emax function driven by "effective" concentration in a hypothetical effect compartment, as opposed to the concentration in plasma ($p \ll 0.001$). **Figure 6.3** depicts this relationship (Panel A) and shows the model-predicted profiles of "effective" concentration for a typical participant with intermediate *NAT2* acetylator status administered the three isoniazid doses levels (Panel B).

The inhA-mutated isolates had a significantly higher EC_{50} compared to the drug-sensitive isolates ($p \ll 0.001$) as shown in **Table 6.2**, reflecting the lower potency of isoniazid against this strain. For the drug-sensitive *M.tb* arm (5 mg/kg), the bactericidal activity was predicted at or near the maximal kill ($Kill_{max}$) throughout the treatment, thus the model estimated extremely low but unstable values of EC_{50}, which was then fixed to 0.01 mg/L. A sensitivity analysis showed that using this or lower values had no substantial effect on the model results. Testing for different maximal bactericidal effects of isoniazid ($Kill_{max}$) between inhA-mutated and drug-sensitive *M.tb* did not produce a significant difference (p=0.30), so the same $Kill_{max}$ value was used in both groups. Of note, while we observed a weak positive relationship between higher MIC values and an increase of EC_{50}, this effect did not reach statistical significance (p=0.035) and was not included in the final model. It should be noted that MIC was missing in 32 participants (54%).

The effect compartment introduced a "delay" with a half-life of around 17 hours before isoniazid concentration in plasma is active against *M.tb*. This delay also causes a certain degree of "accumulation" of the effective drug concentration over the first days of treatment, as illustrated in **Figure 6.3** panel B. While this has little to no effect on the kill of drug-sensitive *M.tb* (for which the effective isoniazid concentrations were above the EC_{80} throughout treatment), this delay matters for inhA-mutated *M.tb*: for participants in the 15- and 10-

mg/kg arms, the effective concentration profile only achieved stable values above the EC_{80} (and thus near maximal kill) after 24 and 48 hours, respectively. Of note, the typical effective concentration profile for the 5-mg/kg arm was below the EC_{80} threshold throughout the observed period. This reflects the poor bactericidal effect of the 5-mg/kg dose, as elucidated in the simulation below.

Table 6.2: Final model Population parameter estimates

Parameter	Typical value (95% CI[a])	Variability (95% CI[a])
Baseline CFU for drug-sensitive (log_{10}CFU)	5.75 (5.19 – 6.09)	0.892[b] (0.543 – 1.20)
Baseline CFU for inhA - 5 mg/kg (log_{10}CFU)	5.87 (5.18 – 6.36)	
Baseline CFU for inhA – 10-15 mg/kg (log_{10}CFU)	6.63 (6.27 – 7.01)	
Additive error in CFU (log_{10} CFU)	0.493 (0.428 – 0.565)	
Growth Rate in MGIT drug-sensitive – k_{growth} (1/day)	1.65 (1.45 – 1.97)	
Growth Rate in MGIT for inhA - k_{growth} (1/day)	1.19 (1.04 – 1.42)	
Delay of growth in MGIT after INH treatment (h)	5.85 (0.971 – 11.2)	14.2[d] (10.4 – 17.3)
MGIT detection threshold (log_{10} CFU)	9.31 (8.93 – 9.78)	
Proportional error in TTP (%)	13.3 (11.1 – 14.9)	
EC_{50} for drug-sensitive (mg/L)	0.01 Fixed	
EC_{50} for inhA (mg/L)	0.544 (0.125 – 3.22)	
Gamma – γ ()	2.88 (1.04 – 7.93)	
$Kill_{max}$ (1/day)	0.42 (0.355 – 0.907)	62.0[c] (52.0 – 66.0)
$T_{1/2_{E0}}$ – half-life of effect compartment delay (h)	17.0 (3.94 – 31.3)	
Correlation of the CFU-TTP errors (%)	-36.7 (-52.5 – -22.4)	

The ε-shrinkage for CFU = 8% and TTP = 17%.

[a] Estimated from non-parametric bootstrap of the final model (n=200, stratified on arm).

[b] is the between-subject variability of the parameter estimate expressed as standard deviation (in the log10 scale)

[c] is the between-subject variability of the parameter expressed as approximate coefficient of variation (CV%)

[d] is the between-occasion variability of the parameter expressed as approximate coefficient of variation (CV%)

Coefficient of variation was calculated by $\sqrt{(e^{\omega^2} - 1)}$, where ω^2 represent the variance.

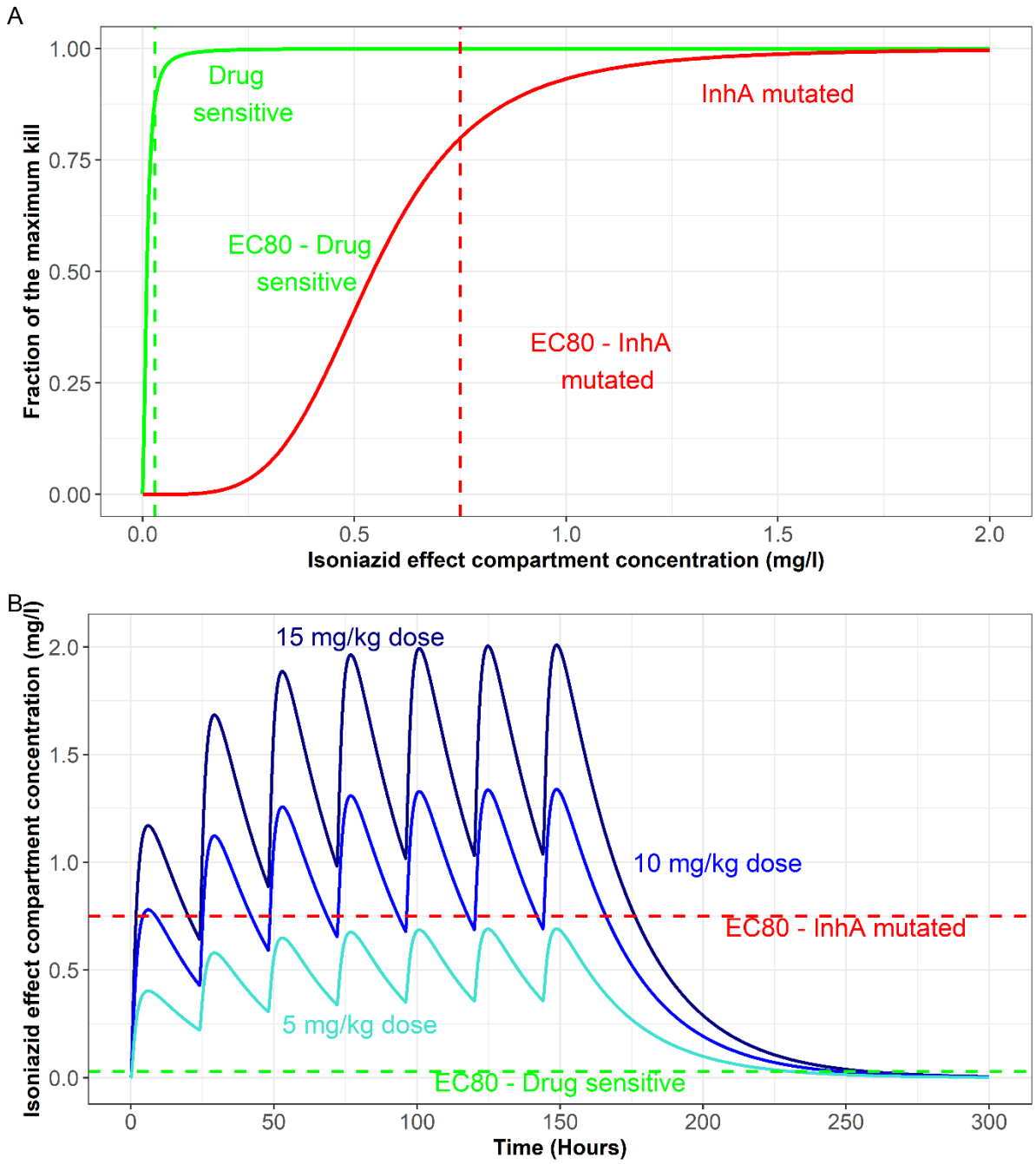

Figure 6.3: Panel A displays the PK/PD relationship of isoniazid against M.tb. The green and the red profiles represent the PK/PD relationship of the drug-sensitive and inhA-mutated M.tb, respectively. The red and green dotted lines represents the EC80 of the inhA-mutated and drug-sensitive M.tb, respectively. Panel B displays isoniazid concentration profiles in the effect compartment of a typical individual with intermediate NAT2 acetylators status dosed with 5, 10, and 15 mg/kg dose. The red and green lines represents the EC80 of the inhA-mutated M.tb and drug sensitive M.tb respectively.

6.4.3 Dosing simulation.

The simulated effect of dose escalation on the drop of log_{10}CFU from baseline for a typical individual (51-kg body weight and 44-kg fat-free-mass) is illustrated in **Figure 6.4**. For drug-sensitive *M.tb*, no apparent difference in CFU decline was detected among the three *NAT2* genotypes, and on day 7 a drop of 1.3 log_{10}CFU (0.186 log_{10}CFU drop daily) was predicted. For inhA-resistant *M.tb*, on the other hand, *NAT2* acetylator status made a difference in terms of bacterial kill: slow *NAT2* acetylators achieve CFU drops comparable with the drug-sensitive arm at 10 mg/kg, intermediate *NAT2* acetylators need 15 mg/kg, while fast *NAT2* acetylators do not achieve the CFU drop even with 15 mg/kg, the highest dose tested.

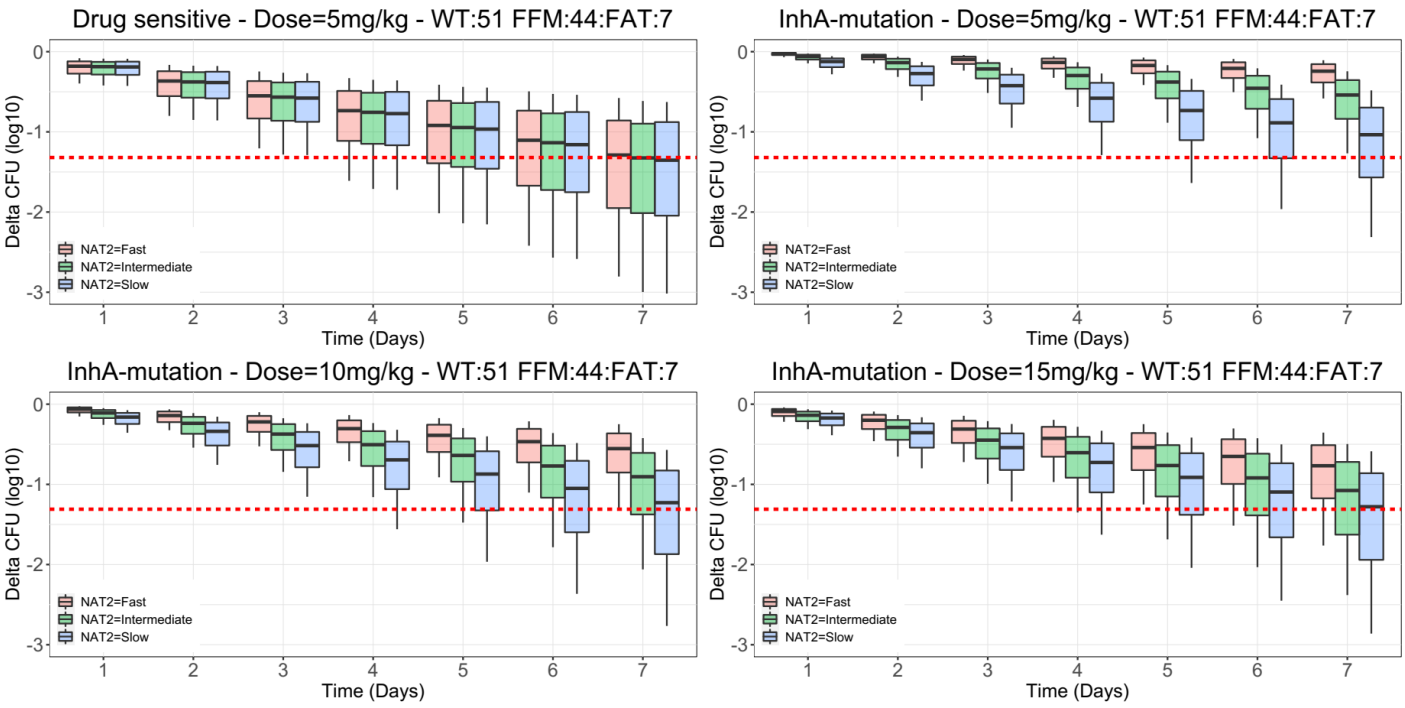

Figure 6.4: Boxplot of the simulated drop in log_{10} CFU, stratified by arm, across the 7 days the participants were on isoniazid monotherapy, for a typical individual weighing 51 kg and fat-free mass of 44 kg. Orange, green, and blue boxplots represent fast, intermediate, and slow NAT2 acetylation status. The dotted red line represents the median drop in log_{10} CFU for the drug sensitive (the reference group) after 7 days of isoniazid monotherapy.

6.5 Discussion

Our study adds to the accumulating evidence on the usefulness of high-dose isoniazid in MDR-TB treatment (Katiyar et al., 2008; Lempens et al., 2018; Piubello et al., 2014; Rieder & Van Deun, 2017), providing additional insight into its activity against inhA-mutated isolates with low-level isoniazid resistance (Karakousis et al., 2008). The model predicts that against inhA-mutated isolates, a dose of 10 mg/kg for slow, 15 mg/kg for intermediate, and >15 mg/kg for fast *NAT2* acetylators produce EBA comparable to that observed in the drug-sensitive group administered the standard dose of 5 mg/kg. The WHO recommends 10 mg/kg against MDR-TB (World Health Organization, 2016),which our results suggest might be suboptimal against inhA-mutated isolates for the rapid and intermediate acetylators.

We found that isoniazid's bactericidal action against inhA-mutated isolates was slightly delayed compared to plasma levels, which was accounted for using an effect compartment; this delay agrees with a previous descriptive analysis of these data (Dooley et al., 2020). Some mechanistic reasons can be provided for this delay; namely, the concentration of isoniazid must first accumulate to a particular threshold in the effect compartment before it is effective against the inhA-mutated isolates, leading to a delay in the killing of the *M.tb*. The effect compartment model accounts for any delay that might lead to a lag in observing the dose-response dynamic. Isoniazid has numerous potential sources of delay (Upton & Mould, 2014). First, since *M.tb* bacilli are mostly in the lung tissue and lesions, the drug must first distribute from plasma to this target site before a response is observed; this would lead to delay in drug-response across all isolates. Second, overexpression of isoniazid target by inhA promoter mutations may lengthen the time required for isoniazid-NAD adducts to saturate available inhA targets to a sufficient concentration for the effect to be observed. Even though the residence time of isoniazid in the lung tissue and lesions is short (Prideaux et al., 2015;

Strydom et al., 2019), the residence time of the activated INH-NAD adduct (isoniazid pro-drug) at the target site on inhA is relatively long (Abel zur Wiesch et al., 2017; Rawat et al., 2003). Third, inhA mutation causes loss in microbial fitness (O'Sullivan et al., 2010), which might lead to mutated isolates replicating more slowly; therefore, the killing effect of isoniazid, which is presumably growth rate-dependent (Unissa et al., 2016), may be slower in onset.

The model predicted an EC_{80} of 0.75 mg/L, which falls within the range of inhA-mutated MIC of 0.2-1 mg/L (Lempens et al., 2018). A trend was observed with increasing EC_{50} as MIC increased, but the effect did not reach statistical significance and was not included in the final model. The exclusion of MIC from the final model was also driven by the large variability associated with the determination of MIC (Xuesong Wen et al., 2016), the fact that observed MIC values depend on the dilution series and are actually interval censored data, and the lack of MIC data for approximately 54% of the participants. Lastly, MIC results can take days or longer to obtain, and very few laboratories have the capacity to perform this test, which ultimately limits the real-world utility of including MIC in a model offering clinical dosing strategies.

A delay in the onset of the bacterial growth in MGIT was observed after the bacteria were exposed to isoniazid. This is possibly due to the post-antibiotic effect (PAE) associated with isoniazid (Awaness & Mitchison, 1973; Dickinson & Mitchison, 1968), or to the fact that, to better survive drug exposure, bacteria may become metabolically dormant and take a longer time to start growing in MGIT (Caño-Muñiz et al., 2017). This is also in agreement with results by Bowness et al. (Bowness et al., 2015), which showed that two samples with the same CFU had shorter TTP when captured at an earlier vs. a later occasion during treatment. CFU counts are primarily dependent on the number of viable bacteria in a sample, whereas TTP measurements are dependent on both the number of viable bacteria and how fast they grow.

M.tb exposed to increasing sizes and/or numbers of isoniazid pulses in vitro show successively longer PAEs (and presumably greater disconnect between CFU and TTP). This might also relate to the slower apparent onset of isoniazid activity against inhA mutants (especially in MGIT) since they 'see' smaller pulses than DS-*M.tb* and require cumulative effects of multiple small pulses (e.g., more saturation of drug target), as suggested by Awaness et al. (Awaness & Mitchison, 1973), to exert the same killing and post-antibiotic effect.

The estimated growth rate in our model is in line with what is expected for *M.tb* in-vitro and what have been previously published (Svensson et al., 2018). A difference between drug-sensitive and inhA-mutated *M.tb* growth rate in MGIT was observed. This might have been brought about by the loss in microbial fitness (O'Sullivan et al., 2010), resulting in the inhA-mutated isolates growing at a slower rate compared to the drug-sensitive isolates. This finding has been extensively explored by le Roux et al. (le Roux et al., 2020).

During the model development process, several descriptors of effective concentration were tested, including AUC_{24}, however the model favoured instantaneous concentration in the effect compartment as the main driver. Apart from delay in the onset of drug action, this might be due to the fact that the majority of the active drug (INH-NAD adduct) remains in the mycobacterial cell and is not able to cross the cell envelope (Bardou et al., 1998). Therefore, the amount of bound target does not decline in parallel with the plasma concentration of isoniazid, the pro-drug. Thus, the time required for the pro-drug to reach the threshold required for bacterial kill can be reduced with a higher peak concentration (Abel zur Wiesch et al., 2017). Given this reliance on peak concentration, fluctuating isoniazid concentration in the effect compartment drives bacterial kill and may explain the model preference.

Individuals respond very differently to treatment depending on weight, age, genetic factors, administration conditions (fasting versus fed), and co-morbidities. Therefore, the one-size-

fits-all dosing strategy long-employed for programmatic ease can be harmful, especially in individual clinical scenarios where current doses of TB drugs are on the steep part of the dose-response curve. Examples include rifampicin (Nabisere et al., 2020), which is systematically underdosed, particularly in underweight people and people living with HIV (Guiastrennec et al., 2018), as well as bedaquiline, a potent new drug for which black populations experience 50% lower exposures (McLeay et al., 2014). These observations and our finding of different optimal doses against inhA-mutated isolates, dependent on *NAT2* acetylator, highlights the importance of tailoring treatment to ensure similar exposures and treatment outcomes in a diverse global population. Ideally *NAT2* genotyping would be available as a package similar to point-of-care PCR testing platforms for bacterial resistance genotyping. We can only hope that our results will be an incentive for industry to provide such technology in future.

6.5.1 Limitations

Our study has several limitations, many of which we believe have been alleviated by using a model-based approach for data analysis. CFU and TTP data are known to be very noisy (Rockwood et al., 2016); this was mitigated by jointly modelling the two biomarkers and characterising their correlation within each observation. Missing MIC information in 54% of the participants may have limited our power to detect an effect, but when testing the available MIC values, these were not found to provide useful information after the stratification in drug-sensitive vs. inhA which was obtained with genetic testing. Furthermore, our model was unable to characterise an exposure-response relationship in the drug-sensitive arm. This may be because all participants in this arm received the standard 5-mg/kg dose, which has been reported to achieve close to the maximum EBA (EBA90) in most patients irrespective of acetylator status (Donald et al., 2007).

Isoniazid bactericidal activity in drug-sensitive *M.tb* is known to be greatest during the first 2 days of treatment and then to decrease (Wang et al., 2012). To capture this, our model would have required additional components, such as a decline in kill rate with time or a tolerance model, but the available data were inadequate to support more complexity. Despite this, our model was able to describe the overall maximum kill achieved by the standard dose against drug-sensitive *M.tb*. The overall drop in CFU predicted by our model is comparable with previously reported isoniazid EBA (Donald & Diacon, 2008) of drug-sensitive *M.tb*, after 5 days of 300-mg isoniazid monotherapy and the EBA0-2 and the biphasic kill curve has not been as prominent in more recent studies (De Jager et al., 2017). One shortfall of EBA studies is their limited ability to generalise results to later treatment periods, as bactericidal activity might differ then. Similarly, our model may have limited ability to predict the role of isoniazid later in treatment, when fewer actively-metabolizing bacilli remain.

6.6 Conclusion

For isoniazid, unlike most other TB drug, we currently have the opportunity to use simple molecular tests to detect and characterize levels of drug resistance, which is the major factor to determine the necessary drug exposure. Since resistance can be detected earlier, dose adjustments can occur at the start of treatment based on presence of inhA mutation.

The study results show that a dose of 15 mg/kg against inhA-mutated *M.tb* has a high probability of achieving early bactericidal activity similar to that of standard dose against drug-sensitive *M.tb*. *NAT2* genotype information could help customize isoniazid dose selection against inhA-mutated *M.tb*, as slow acetylators could be dosed at 10 mg/kg (consistent with WHO recommendations), intermediate acetylators at 15 mg/kg, while fast acetylators are likely to require more than 15 mg/kg. Such tailored dosing will ensure similar exposures across *NAT2* genotypes, minimizing toxicity risks associated with higher exposures

and potential for reduced efficacy. Based on these data, the current dose for treatment for MDR-TB of 10 mg/kg as recommended by WHO may be suboptimal for fast and intermediate acetylators. However, the safety and tolerability of 15 mg/kg or higher doses must be investigated in long-term studies.

6.7 Supplemental Methods

6.7.1 Study procedures.

Sputum samples of 10 mL or more were taken overnight over 16 hours at pre-entry (Day -1), Day 0 (pre-treatment), and daily while on isoniazid monotherapy for 7 days. The captured samples were placed in refrigerated containers then transported to the laboratory (Task Applied Science, Cape Town, South Africa), where they were homogenized and cultured on solid media to capture colony forming units (CFU) and on liquid culture media to capture time to positivity (TTP) as specified in the earlier publication (Dooley et al., 2020). Minimal inhibitory concertation (MIC) was determined using the 1% agar proportion method.

PK sampling was carried out on day 6 after commencing isoniazid monotherapy, blood samples were drawn at pre-dose, 0.5, 1, 2, 4, 6, 8, 12, and 24 hours post-dosing. After spinning, aliquots of plasma were frozen at −70°C within one hour of collection. After thawing, drug plasma concentrations were determined by liquid chromatography-tandem mass spectrometry performed in the Division of Clinical Pharmacology, University of Cape Town. Isoniazid calibration range was 0.105 to 25.0 mg/L. The isoniazid assay's inter-day accuracy ranged from 92.2% to 104.5%, and the coefficient of variation (%CV) of the precision ranged from 6.5% to 10.8%.

NAT2 acetylator status was determined based on whole blood, which was immediately refrigerated between 2 and 8°C within one hour of collection. Samples of 1 mL aliquots were then frozen at −20°C. A 2530 base pair domain of the *NAT2* gene (http://www.ncbi.nlm.nih.gov/nuccore/219871) was amplified directly from EDTA-blood using the PhusionTM Blood Direct PCR kit (Thermo Fischer Scientific, USA). The amplified *NAT2* region (spanning nucleotides 93 to 2623) was visualized by gel electrophoresis and confirmed by restriction enzyme digestion, using HincII and HindII(13). The PCR product was analysed via bi-directional sequencing, using primers targeting overlapping sections of the *NAT2* protein-coding region; the sequencing reactions were performed in an ABI PRISM Genetic Analyser 3130x1, using the BIG DYE Terminator ready sequencing kit (Applied Biosystems), at the Central Analytical Facility, Stellenbosch University. All sequencing reaction products were compared against the reference *NAT2* gene sequence (BLUM et al., 1990), using the Sequencher® DNA sequence analysis software (Gene Codes Corp., USA [http://www.genecodes.com]). The *NAT2* gene positions 282, 341, 481, 590, 803, and 857 were used to predict *NAT2* acetylator phenotype. *NAT2* was assigned the following phenotype: fast, intermediate, and slow utilizing the Sabbagh et.al suggestion (Sabbagh et al., 2009).

6.7.2 Pharmacokinetic model development

To describe the PK of isoniazid, one- and two-compartment models were tested with first-order absorption (with or without lag time or a chain of transit compartments) and first-order elimination. Since isoniazid is mainly hepatically cleared, a well-stirred liver model, as described by Chirehwa et al., (Chirehwa et al., 2018a) was tested to capture the effect of first-pass metabolism. The liver hepatic blood flow Q_h (Yang et al., 2007) was assumed to be 90 L/h in a typical individual (44 kg fat-free mass) and adjusted for the effect of body size using

allometric scaling (Mehvar, 2018), while the free fraction (f_u) of isoniazid in plasma was fixed to 95% (Sturkenboom et al., 2015). The pre-hepatic bioavailability of a typical individual was fixed to a reference value of 1.

Random effects at occasion (corresponding to each dose), and/or subject level were included on the pharmacokinetic parameters if statistically significant using a log-normal distribution. Between-occasion variability (BOV) was tested on absorption parameters, while between-subject variability (BSV) was tested on disposition parameters. A combination of proportional and additive error was used to model unexplained residual variability. *NAT2* genotype effect was tested on the clearance, and allometric scaling was applied on all clearance and volume of distribution parameters (Anderson & Holford, 2008) to account for body-size effect.

6.7.3 Pharmacokinetics/pharmacodynamic (PK/PD) model development

The characterisation of the dose concentration-effect relationship was obtained in stages. First, we developed a PK model to describe drug concentration over time, then we used the model-predicted concentration-time profile as "data" in the PD model to describe the bactericidal effect. The PK model was based solely on the PK data, while the PD model was based on the PD data and the prediction from the PK model. This was done to uncouple the two models to minimise computation burden and model instability. Zhang et al. (L. Zhang et al., 2003) has reported that, in a situation with rich PK data such as ours, this sequential method performs as well as simultaneous modelling method, which is the gold standard, but more complex.

To describe the bacterial load in patients and the bactericidal action of isoniazid, we tested several approaches. First, we used empirical models with constant exponential decline rates

(mono- or bi-exponential). Alternatively, we tested a one-compartment model assuming first-order killing of bacteria. The bacterial load in each patient at the time of sputum collection was “directly” observed as CFU, while the TTP was “indirectly” obtained by modelling the growth of the *M.tb* isolate in the MGIT. The model for *M.tb* growth in MGIT assumed that the bacterial load in the sputum determined the initial number of bacteria in the inoculum, which would then grow in the MGIT until the TTP is achieved when their number reaches the detection threshold. For *M.tb* growth in MGIT, we evaluated exponential and logistic growth models, with or out without an initial delay. The CFU and TTP values in each individual at each time point are obtained from a single sputum sample. This might result in correlation between the two measurements since whatever circumstance influences one observation may affect the other. To quantify this phenomenon, we introduced a correlation between CFU and TTP residual errors using the L2 data item feature in NONMEM (Keizer, 2010).

To link the drug concentration to its bactericidal effect, we tested the effect of isoniazid exposure in each patient on the bacterial kill rate. We tried using overall AUC (constant kill), AUC/MIC, or the time-varying concentration of isoniazid, either in plasma or within a hypothetic effect compartment (Upton & Mould, 2014), on the instantaneous kill rate. An effect compartment is a hypothetical compartment that describes the drug exposure at the site of action (Wright et al., 2011), i.e., the active concentration which modulates the drug action. It accounts for the delay in the emerging of the drug effect relative to its plasma concentration. This delay is defined using a first-order rate constant ke_0 (Upton & Mould, 2014).

$$\frac{dC_{eff}}{dt} = k_{e0} \cdot \left(C_p - C_{eff}\right)$$

Where C_{eff} is the concentration in the effect compartment, and C_p the plasma concentration. **Figure E6.1** displays the difference between the concentration in plasma and the effect compartment. The concentration in the effect compartment is smoother and resides longer in the compartment compared to concentration in plasma. A sigmoid Emax model was used to characterize the relationship between the drug concentration in the effect compartment and the induced killing of the isolates:

$$Drug\ effect = Kill(C_{eff}) = Kill_{max} \cdot \frac{C_{eff}^{\gamma}}{EC_{50}^{\gamma} + C_{eff}^{\gamma}}$$

Where $Kill_{max}$ is the maximum induced kill achieved by isoniazid, EC_{50} the concentration at which 50% of $Kill_{max}$ is achieved, and γ is the Hill coefficient, which defines the shape of the concentration-effect relationship.

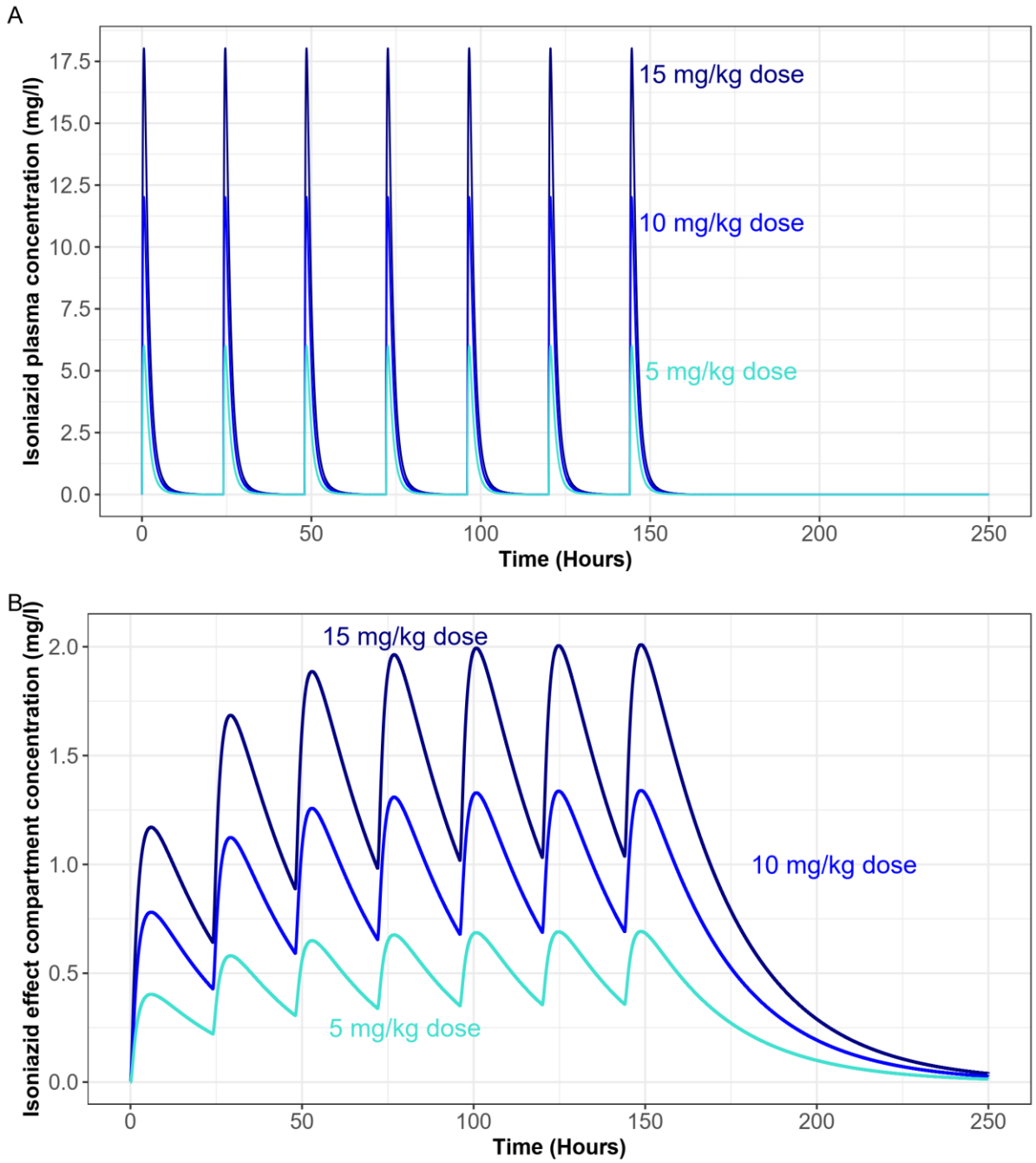

Figure E6.1: Plot of the profile of plasma concentration (panel A) and effect compartment concentration of the three dosing arms (5, 10, and 15 mg/kg dose).

We assumed that a MGIT turns positive at a threshold lower than *M.tb* population carrying capacity. Modelling the time-variant decline in the bacteria load induced by effective concentration required the definition of a precise sputum sampling time. Since the sputum was captured within a time period of 16 hours from 16:00 to 8:00, the mid-point of midnight was imputed as the sputum sampling time. A sensitivity analysis was carried out to assess if

the value of this imputation would greatly impact the estimated final model parameter. Inclusion of random effects for BOV and BSV were tested on the PK/PD model parameters. Stochastic simulation and estimations (SSEs) (n=200) were performed using perl speaks NONMEM to investigate estimation properties of the model and study design in terms of bias and precision (Keizer et al., 2013).

6.7.4 Handling of missing data

Concentrations below the limit of quantification (BLQ) were handled similarly to the M6 method suggested by Beal (Beal, 2001). BLQ values were imputed as half of their respective LLOQ and when the terminal phase of a pharmacokinetic profile contained a series of LLOQ values, only the first one was used for estimation in the model fit, while subsequent LLOQ values were ignored in the fit but retained for simulation-based diagnostics such as VPCs. Finally, the additive component of the error for all imputed value was inflated by LLOQ/2 to mitigate the effect of the imputation.

Participants with missing genotype were allocated to either of the three phenotypes using a mixture model (Keizer et al., 2012) with three subpopulations. The proportions of each subpopulation were fixed to those observed amongst the patients with available genotype information.

MIC information was missing in 54% of the participants. This was due to the fact that cultures used for MIC determination were obtained from samples originally grown before treatment started. The study took a very long time to recruit and was interrupted due to factors outside the control of the study team, such as the temporary non-availability of study isoniazid following the tsunami incident in Japan. It was intended to batch-test all MICs at the end of the study to keep method-inherent variation low, but it was found that many cultures did not

grow well enough for MIC testing following years of storage. The often-multiple mutations were probably an additional handicap for regrowth. When analysing the data, participants with missing MIC information were assigned the median value of the corresponding group, drug-sensitive or inhA-mutation. Additionally, whenever MIC was tested as a covariate in the model, we used a "centred" covariate model, where the effect is modulated by the difference of each individual MIC from the median value (also stratified by drug sensitive vs inhA-mutated). Since the median value is imputed for individuals with missing MIC, these subjects have no effect of MIC and they do not contribute to the test. On the other hand, they are kept in the analysis to inform all the other model parameters. This method of handling missing covariate values is known to be a robust way to minimise the impact of missing data, even though it may lead to the increase unexplained between-subject variability on the parameter on which the covariate is tested, since the potential explanatory value of the covariate (MIC) is not available in some patients (Johansson & Karlsson, 2013).

For the participant with no pharmacokinetic samples, we used the pharmacokinetic model to predict the expected isoniazid time concentration profile based on that participant's covariates (including NAT2), and the exposure was then used to modulate the killing of *M.tb*.

6.8 Supplemental Results

6.8.1 Pharmacokinetic model

The final model describing isoniazid's pharmacokinetics was a two-compartment PK model with first-order absorption, transit compartment absorption, and first-order elimination using a well-stirred liver model. The well-stirred liver model's use to capture the effect of first-pass metabolism significantly improved the model fit (ΔAIC = -6.13). Allometric scaling was applied to all the clearance and volume parameters (including the liver), to account for the effect of

body size, and it improved the fit explaining part of the between-subject variability. Fat-free mass was found to be a more suitable descriptor of body weight for allometric scaling of all disposition parameters. The clearance of isoniazid was significantly affected by *NAT2* genotype ($p \ll 0.001$), as CL_{int} varied greatly between rapid (46.3 L/h), intermediate (23.9 L/h), and slow acetylators (9.25 L/h). Parameter estimates of the PK of isoniazid are displayed in **Table E6.1**. Model evaluation through VPC (**Figure E6.2)** shows that the model described the data well since the percentiles of the raw data (summarised as solid and dashed lines) fell within or near their respective model-predicted confidence intervals for all time points.

Table E6.1: Final PK parameter estimates for isoniazid.

Parameter	**Typical value (95% CI[a])**	**Variability [b], %CV (95% CI[a])**
CL_{int}[c] (L/h) *NAT2* Rapid	46.3 (36.6 – 59.1)	35.9 (31.7 – 39.6)*
CL_{int}[c] (L/h) *NAT2* Intermediate	23.9 (20.4 – 28.1)	
CL_{int}[c] (L/h) *NAT2* Slow	9.25 (8.01 – 10.74)	
V_c [d] (L)	30.9 (28.0 – 34.2)	
Q/F [c] (L/h)	8.15 (7.35 – 8.82)	
V_p [d] (L)	15.3 (13.0 – 17.7)	
k_a (1/h)	3.28 (2.48 – 4.62)	72.2 (54.6 – 88.4)[#]
MTT (h)	0.112 (0.0648 – 0.170)	112 (82.6 - 149)[#]
NN ()	2.32 (1.64 – 3.27)	
Q_H[c] (L/h)	90 FIXED	
fu (%)	95 FIXED	
Prehepatic relative bioavailability	1 FIXED	23.1(18.6 – 29.9)[#]
Proportional error (%)	12.7 (11.2 – 14.8)	
Additive error (mg/L)	0.021[e] FIXED	

Abbreviations: CL_{int} clearance intrinsic; V_c apparent central volume of distribution for INH; V_P apparent peripheral volume of distribution for INH; Q/F apparent intercompartmental clearance for INH; k_a first-order rate constant of INH absorption; MTT absorption mean transit time; NN Number of absorption transit compartment; Q_H blood liver flow (Yang et al., 2007); fu unbound fraction of isoniazid in plasma (Alghamdi et al., 2018).

[a] 95% confidence intervals (CIs) were obtained with the SIR procedure

[b] Variability was modelled with log-normal distribution and is presented as an approximate percentage CV.

[c] Clearance parameters are allometrically scaled based on fat-free mass (typical value reported for 44 kg, which was the median fat-free mass weight of the study population).

[d] Volume pf distribution parameters are scaled based on weight (typical value reported for 51 kg, which was the median weight of the study population).

[e] Additive error was fixed to 20% of the LLOQ.

**** Between subject variability.***

[#] Between occasion variability

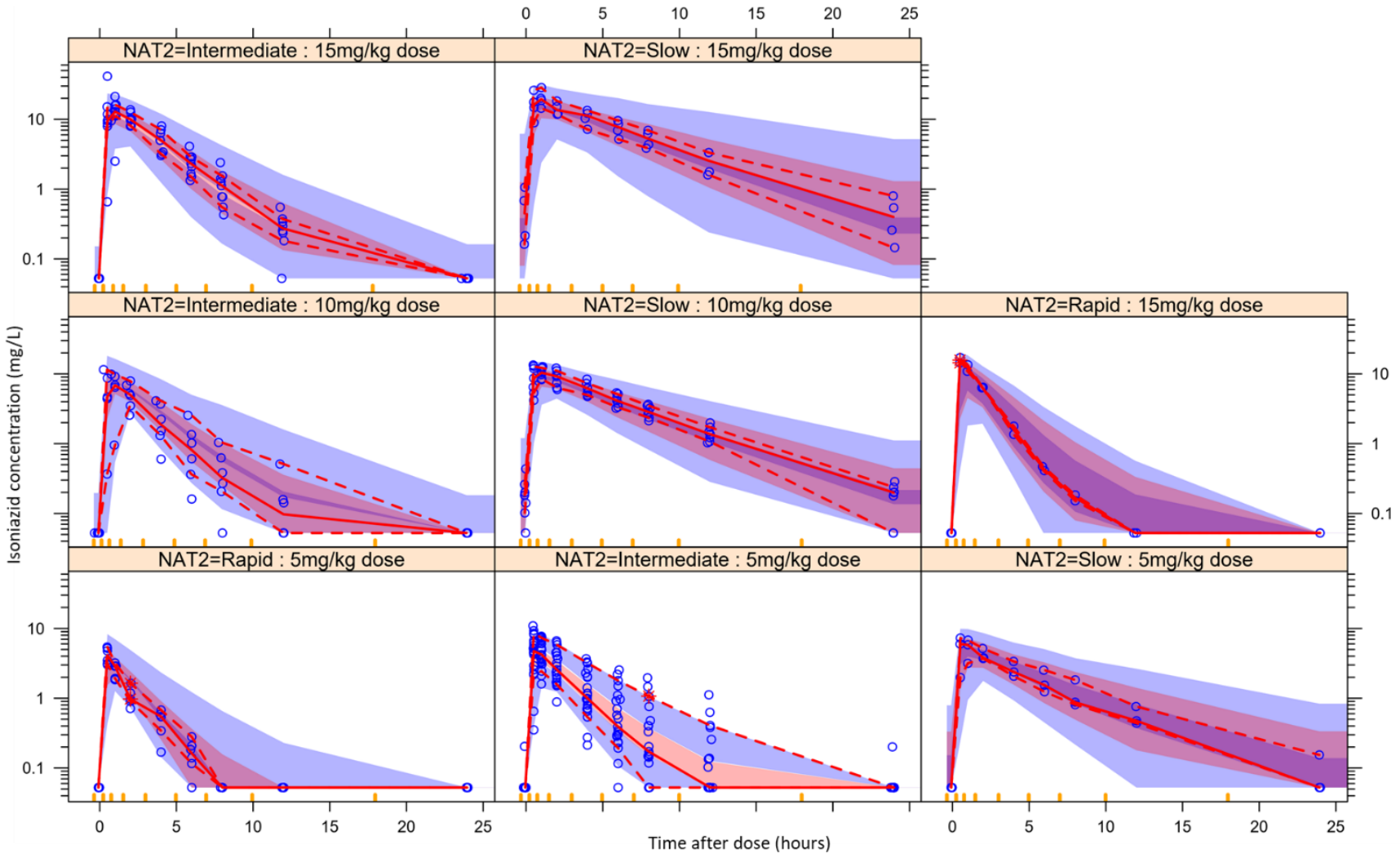

Figure E6.2: Visual predictive check of the isoniazid model, stratified by dose and NAT2 genotype. The solid and dashed lines are the 5th, 50th, and 95th percentiles of the observations, while the shaded areas represent the 95% model-predicted confidence intervals for the same percentiles

6.8.2 Pharmacokinetics/pharmacodynamic model

The empirical model with an exponential decline of bacterial load could roughly describe the decrease in *M.tb* in the sputum, but it did not explain the delay in the onset of killing for the inhA arms. The introduction of a delay in the onset of drug action or a bi-exponential decline provided a slight improvement of the model fit but made the parameter estimates unstable and unreliable. When assessing the effect of isoniazid PK on bacterial decline within this empirical model, which assumes time-invariant rates of decline, we could only test a "static" metric of drug exposure, so we used AUC_{24}. The inclusion of AUC significantly improved the fit and was a better explanatory variable than dose level (i.e., study arm). Interestingly, replacing AUC_{24} with AUC_{24}/MIC led to worsening of the model fit and an increase in the unexplained variability.

Switching to a compartmental model with time-varying kill rate provided much more flexibility in fitting the data compared to the empirical exponential model. The effect of isoniazid on the first-order killing of *M.tb* was best described by using an effect compartment, which could satisfactorily describe the delayed onset of killing action against inhA-mutated *M.tb*. We used an Emax function to characterize the relationship between effective concentration (in the effect compartment) and kill rate and we estimated significantly different values of EC_{50} for drug-sensitive and InhA-mutated *M.tb* ($p \ll 0.001$), reflecting that isoniazid is much more potent against sensitive strains. After including the categorization drug-sensitive vs. inhA-mutated, we found limited additional explanatory value of the individual values of MIC on EC_{50} ($p=0.035$). Testing the effect of MIC only within the inhA-mutated subpopulation also did not reach the stipulated statistical significance threshold ($p=0.0425$).

While the lack of explanatory value of MIC after the differentiation between drug-sensitive and inhA-mutated (which was based on the result of the molecular test) could be due to large proportion of missing values, we used a methodology known to minimise the impact of missingness. Even in the patients with available MIC values, these did not meaningfully explain variability in the model. This is in line with the large variability associated with the determination of MIC (Xuesong Wen et al., 2016); minor variations in the incubation period, the storage of samples, lab techniques, may all play a role in the observed value. Moreover, MIC values depend on the dilution series (generally by a factor of 2) and are actually interval-censored data, thus potentially carrying an uncertainty of up to 50%.

The stochastic simulations and estimations investigating the estimation property of the model revealed a relative bias <15% and relative standard error <30% for the typical values of all PD parameters. The sensitivity analysis confirmed that a change in the sputum sampling time within the 16-hours sampling window did not substantially impact the model parameters characterizing the drug effect.

Chapter 7: Conclusions

The optimal treatment of HIV and tuberculosis coinfection remains a challenge, specifically in neglected populations who are commonly excluded from clinical trials. Several studies have found a lower tuberculosis treatment success rate among co-infected patients (Engelbrecht et al., 2017). The optimising of tuberculosis and HIV treatment is imperative, as low drug exposure can lead to the development of resistance, which will make TB/HIV control worse in the future.

The research presented in this thesis contributes to filling this research gap of identifying optimal tuberculosis regimens in neglected populations, especially pregnant women and patients with co-morbidities or DR-TB. Firstly, we developed a population pharmacokinetic model of isoniazid (used for preventative treatment) and efavirenz in pregnant women using data from the largest study of its kind, incorporating genetic polymorphism and describing drug-drug interaction. Secondly, we utilised population pharmacokinetic model to explore the effect of pregnancy on bedaquiline concentration and described its exposure in breastmilk of mothers treated for rifampicin-resistant tuberculosis. Thirdly, in the case of DR-TB, we characterised the pharmacokinetics of standard to high dose isoniazid (5 – 15 mg/kg), administered either as monotherapy or part of the MDR-TB treatment regimen, hence exploring drug-drug interaction within the MDR-TB regimen. Finally, we developed a pharmacokinetics/pharmacodynamics model describing the association between isoniazid exposures (at high or standard dose) and its early bactericidal activity against drug-sensitive or inhA-mutated *M.tb* and identified the optimal dose in patients with inhA-mutated strain.

This chapter discusses the main findings and their implication, the strengths and limitations of our analyses, and recommendation for further research.

7.1 Pharmacokinetics and drug-drug interactions of isoniazid and efavirenz in pregnant women living with HIV in high TB incidence settings: importance of genotyping

Chapter 3 focussed on the effect of pregnancy, genetic polymorphisms, and co-administered drugs on the pharmacokinetics of isoniazid and efavirenz. HIV and pregnancy are both known to weaken the immune system, hence increasing susceptibility to infections and reactivation of tuberculosis. Therefore, the WHO recommends preventative therapy along with ART. In 2018 the recommended preventative treatment was 6-month of daily isoniazid (World Health Organization, 2018) and efavirenz was the commonest ART at the time.

The study's main findings were a modest reduction in isoniazid and efavirenz exposure due to pregnancy and a drug-drug interaction between isoniazid and efavirenz, which led to an increase in efavirenz exposures which was only pronounced in *CYP2B6* intermediate and slow metabolizers. We show that the metabolizers genotype greatly affects the exposure of both drugs. The reduction in exposure due to pregnancy is modest, but it may be clinically relevant for rapid *NAT2* or *CYP2B6* metabolizers who already experience lower exposures These findings, together with the observed five-fold difference in exposure between rapid and slow metabolizers, stress the importance of genetic testing and therapeutical monitoring, especially with the side effects associated with both drugs.

A limitation of the P1078 study was the use of the postpartum visit at 7-23 weeks as control when assessing the effect of pregnancy on the pharmacokinetics of isoniazid and efavirenz, as the elapsed weeks might not be sufficient for all the pregnant induced effects to resolve. Therefore, there is a need for a study with better control to confirm the findings. Furthermore, since efavirenz is highly protein-bound, we recommend using unbound concentration when assessing the pregnancy effect on its pharmacokinetics, which was not

captured in our study. In addition, the P1078 study was not powered to identify the effect of the different ARV on isoniazid exposure as most of the study participants (88%) were on efavirenz-based ARV, therefore further studies are required to confirm the effect of efavirenz on isoniazid. However, dolutegravir has recently replaced efavirenz as the first-line ARV (WHO, 2021a) because of its superior tolerability and low risk of resistance emergence (Phillips et al., 2020; Walmsley et al., 2015). Dolutegravir has a low potential to invoke DDIs since it neither induces nor inhibits the drug-metabolizing enzyme or transporters, hence it is preferred in comparison to efavirenz, which induces and inhibits several enzymes and transporters described in **section 1.5.1**. Therefore, there are no expected drug-drug interactions between isoniazid and dolutegravir.

The primary study by Gupta, et al., 2019 reported a significantly higher rate of adverse pregnancy outcomes in women who received IPT during pregnancy compared to those on placebo during pregnancy and who received IPT postpartum. This finding is important in the context of future use of IPT for TB prevention during pregnancy(Gupta, et al., 2019).

7.2 Bedaquiline exposure in pregnancy and breastfeeding in women with rifampicin-resistant tuberculosis.

Chapter 4 describes the pharmacokinetics of bedaquiline during pregnancy and its exposure in breast milk. The recommended treatment of rifampicin-resistance (RR) tuberculosis includes bedaquiline, even in pregnant women, although there is limited data on its pharmacokinetics during pregnancy. There is also scarce data on the excretion of bedaquiline into breast milk. Our findings show that bedaquiline exposure is lower in pregnant compared to non-pregnant historical data. We show that bedaquiline significantly accumulates in breast milk, and breastfed infants ingest mg/kg doses of bedaquiline comparable to maternal dose.

While this is potentially protecting the infants from tuberculosis, especially if the mother is still infectious, there is also the potential of toxic bedaquiline concentration in the infant, which is associated with QTc prolongation. The risk of toxicity is increased due to babies' immature CYP3A4, which are reported to mature approximately at one year of age (Phillips et al., 2020). In addition, we show that the foetus is exposed to the drug in utero. The presence of measurable bedaquiline concentration in infants 6 weeks after delivery could lead to the development of resistance should the infants develop RR-TB.

This analysis had a very small sample size for the postpartum visit due to loss of follow-up and a limited sampling schedule (PK samples were captured within 6 hours timeframe). For this reason, it is only thanks to the use of population PK modelling that we were able to interpret this data and compare it to the concentrations expected at that point in treatment if the pregnancy had no effect. This limits the robustness of our findings. Hence, there is a need for a similar study with a larger sample size, more intensive and longer sampling periods to confirm our findings. Similar to efavirenz, bedaquiline is highly protein-bound, hence unbound concentration would be more informative when assessing the pregnancy effect on its pharmacokinetics, however in our study, we only quantified total drug concentration. In addition, we showed that bedaquiline significantly accumulates in breastmilk, hence further studies on the safety of high bedaquiline concentration in breastmilk for the breastfeeding infant are needed, considering that the drug's pharmacokinetics might differ between infants and adults. There is a possibility that other drugs within the MDR-TB regimen might accumulate in breastmilk to the same extent as bedaquiline; this makes the understanding of the penetration of MDR-TB drugs into breastmilk a research priority.

7.3 Pharmacokinetics of standard vs high-dose isoniazid for treatment of multidrug resistant tuberculosis.

Chapter 5 discuss the pharmacokinetics of a standard to high dose of isoniazid as monotherapy or within the MDR-TB regimen. The WHO has recommended high dose isoniazid as part of MDR-TB regimen, however there is limited information on the PK of isoniazid at high dose and in the context of MDR-TB regimen. The high dose has the potential of saturating the metabolic pathways while the other drugs within the MDR-TB regimen might interact with isoniazid. The main findings of our analysis were lower exposure and dose-dependent bioavailability of isoniazid when administered within the MDR-TB regimen, most likely due to a drug-drug interaction with one of the drugs within the MDR-TB regimen. We suspect that the drug-drug interaction might be with cycloserine/terizidone, as similar results were observed in a paediatric and preclinical study (Winckler et al., 2021). This low isoniazid exposure, if confirmed, may warrant a dose adjustment as the current exposures may be subtherapeutic. We also report a modest increase in isoniazid due to ethionamide co-administration. Furthermore, we report saturable isoniazid metabolism, which starts becoming apparent at doses greater than 10 mg/kg. This leads to a modest increase in isoniazid concentrations beyond linearity, but the concentrations may become concerningly high in NAT2 slow acetylators who may experience toxicity. This highlights the importance of genotyping.

The main limitation of the study was that nearly all the participants administered isoniazid as part of the MDR-TB treatment regimen also received three other drugs (pyrazinamide, moxifloxacin, and cycloserine/terizidone), hence the model was unable to discriminate if any of the three was responsible for the low isoniazid exposure. Pyrazinamide is administered with isoniazid as part of the DS-regimen, and moxifloxacin has been previously dosed with

isoniazid, and there was no huge drop in isoniazid bioavailability observed (Naidoo et al., 2017), hence the two are unlikely to be the perpetrator. Therefore, further studies are necessary to confirm if cycloserine/terizidone is indeed the cause for the lower isoniazid bioavailability observed in the study. Since isoniazid exposure is heavily influenced by *NAT2* genotype, this information should be captured within the study to better quantify the drug-drug interaction if present. However, *NAT2* genetic information of the participants on the MDR-TB regimen (which had the low isoniazid bioavailability) was not available, which was one of the limitations of our study. Additionally, determining the mechanism of the drug-drug interaction between isoniazid and ethionamide would assist in better understanding the interaction and identifying ways of overcoming the interaction. In additional, the study aimed for the participants to be administered a mg/kg dose. However, isoniazid formulation was only available in a formulation of 100 mg, therefore in some patients the dose was above the calculated mg/kg dose. Lastly, a better characterization of INH toxicity would be important, which together with therapeutical drug monitoring and genotyping, could assist in dose individualisation.

7.4 A semi-mechanistic model of the bactericidal activity of high-dose isoniazid against multi-drug-resistant tuberculosis.

Chapter 6 describe the association between standard and high dose isoniazid and its early bactericidal activity against *M.tb* with the aim of identifying the optimal dose. The accumulating evidence of the effectiveness of high dose isoniazid against MDR-TB treatment led to WHO recommending high dose as part of MDR-TB regimen, however the optimal dose is unknown. Our results show that a dose of 15 mg/kg against inhA-mutated isolates has a high probability of achieving early bactericidal activity similar to the standard dose against

drug-sensitive isolates. We report that NAT2 genotype is essential in individualising the dose as slow NAT2 acetylators require only 10 mg/kg dose against the inhA-mutated *M.tb.* The study findings highlight the importance of *NAT2* genotype when dosing isoniazid in patients with inhA-mutated *M.tb*. The optimal dose for the three acetylator statuses differed, hence it is vital to include both genotype and resistance testing as part of the point of care tests before recommending tuberculosis treatment.

Another important finding was the lack of explanatory value of MIC since adding MIC to the PD model did not improve the model's predictability, which might be due to the uncertainties known to be linked to MIC. The use and value of MIC information in PK-PD studies in TB is a subject of much debate. The known limitations of MIC have fuelled the debate; this included MIC imprecision due to the fact that MIC values depend on dilution series and result in interval-censored data, minor variation in methods (e.g. inoculum preparation, media, incubation temperature and incubation period) can result in a large variation of the MIC, different combination of growth and kill rates can result in the same MIC, does not account for the post-antibiotic effect, and Mouton et al., 2018 discussed that the greater contribution to observed variation in MIC is assay variation, which has the capability of masking MICs variation due to difference in strains. Our study drug-sensitive MIC values indeed greatly overlap with the InhA-mutated MIC values, meaning the two groups were not well separated. When testing the effect of MIC on EC50 before splitting DS vs inhA, it was not significant, even after excluding participants with the missing MIC values. While this is possibly due to the limitations in the MIC testing outlined above, this is a reminder that MIC testing is not an entirely straightforward and universal procedure, even in a clinical trial setting with rigorous protocols. In a more general setting, different labs may produce different values of MIC when testing the same sample. Therefore, resistance status might be a more generalizable result

on which optimal dosing could be more reliably decided. The other advantage of resistance status over MIC is practicality since bacterial mutations can be identified within hours with currently available PCR methods, whereas MIC requires weeks to determine and is thus not practical for treatment guidance in the first 14-days.

The model used to describe the PK/PD of isoniazid limitation was its inability to characterise an exposure-response relationship in the drug-response arm, as all participants in this arm received the standard 5-mg/kg dose. Therefore, more data on participants with DS-*M.tb* with varying isoniazid doses is required to better describe its kill curve in the drug-sensitive population. On the other hand, it has been reported that the maximal killing power is reached by 5 mg/kg isoniazid dose (EBA90) in most patients irrespective of acetylator status, hence NAT2 does not seem to matter at this dose as much for DS (Donald et al., 2007).

We were unable to replicate the biphasic kill previous described for isoniazid using the current data, as intensive and longer treatment period pharmacodynamics data would be needed to develop a more complex model that captures the *M.tb* drug tolerability (hence capturing the biphasic kill) and has the capability to predict the kill curve of isoniazid later in treatment when the population of the *M.tb* is different, and there are less actively-metabolizing *M.tb*. For this PK/PD analysis, we used a simpler version of the pharmacokinetics model developed in Chapter 5. Due to the simple nature of the model, the run times were faster, however it's ability to predict the individual AUC to a good degree sufficient to modulate the kill of *M.tb* was not compromised. The study highlights the large variability and noisiness of the two tuberculosis biomarkers (CFU and TTP), calling attention to the need to develop better biomarkers that are good predictors of treatment outcome and capable of quantifying bacteria burden for both the actively growing and the slow or none growing *M.tb.*

7.5 Implication of findings on tuberculosis and HIV treatment and research

7.5.1 Neglected populations

Neglected populations account for approximately 20% of the global tuberculosis burden and have unique attributes which might lead to unreliable extrapolation from other populations (Gupta, et al., 2019). Therefore, it is critical that these populations are represented in clinical trials. These populations might benefit the most from a clinical trial setting where they are rigorously monitored as their disease, drug response, toxicity, and drug-drug interaction might be complex or different from the average population. Indeed, these populations require protection to ensure the safety of the unborn baby and infants for pregnant and breastfeeding women and to reduce the risk of DDIs and subtherapeutic concentration for the co-infected and individuals with a drug-resistant strain. However, these individuals do end up receiving these medications. Hence, it is critical that the neglected populations are protected through research and not by excluding them from the clinical trials. Therefore, when designing clinical trials, it is essential to include neglected populations or have open protocols that can cater for the development of opportunistic substudies for this population. The data captured in such substudies, even if scanty and opportunistically sampled, can be analysed using pharmacometrics models which are capable of handling both sparse and smaller sample sizes.

Clinical trials assessing the effect of pregnancy on the pharmacokinetics of a drug should capture the participant's albumin values, specifically for highly protein-bound drugs, whose pharmacokinetics might be influenced by changes in albumin levels due to pregnancy. In addition, creatine clearance should be captured for renally cleared drugs to better quantify the effect of pregnancy on kidney function. It is also important to identify a suitable control group to quantify the effect of pregnancy in a robust way. For this purpose, while the women

being their own control is great, there is a potential of lingering pregnancy changes that can influence the drug's pharmacokinetics and thus impair the comparison. For this reason, if pregnant women are recruited within a broader trial, this may provide an ideal control group of patients recruited in the same centres that underwent the same study procedures and received the same drug formulations.

In addition, clinical trials involving breastfeeding mothers should sample breastmilk to quantify the amount of drug the infant is ingesting, taking into account that the drug's pharmacokinetics might difference between infants and adults, and assessing the potential risk and benefits of the drug exposure in the infant. Physiological based Pharmacokinetics (PBPK) modelling is another area of interest utilised in describing drug exposures, especially when clinical pharmacokinetics data is lacking, which is currently the case for pregnant and breastfeeding women. PBPK modelling could be used to describe the potential impact of physiological and anatomy changes during pregnancy on the drug's pharmacokinetics and also the drug exposure in breastmilk (Metushi et al., 2016). Therefore, PBPK is a predictive tool that can be used to assess the benefit and risk to inform decision making for dose adjustment or prohibition of such medication in pregnant or breastfeeding women to ensure the safety of both the mother and the baby.

7.5.2 Pharmacogenetic testing and therapeutical drug monitoring

Interindividual variability to a standard dose of a regimen is a crucial problem in clinical practice, as it could lead to non-responsive or adverse drug reactions. A significant portion of the variability in drug response can be attributed to genetic factors which could potentially influence the drug pharmacokinetics and/or pharmacodynamics (Gervasini et al., 2010). If available, pharmacogenetic information can be used to identify individuals at risk of

subtherapeutic or toxic exposures, hence increasing the number of responders while reducing the occurrence of adverse events. The FDA encourage the capturing of genetic information to aid in optimising dose, which has led to the modification of some drug labs to include pharmacogenetic information (Drozda et al., 2018; Flockhart et al., 2009). The regulatory agencies play a big role in establishing clinically and commercially robust pharmacogenetic testing by developing guidelines specifying drugs for which predictive genotyping should be considered before initiating treatment therapy (Gervasini et al., 2010).

Therapeutical drug monitoring (TDM) is another useful tool to check the exposure in patients and individualise the therapy accordingly. While TDM can be used to identify the patient's phenotype (e.g., fast vs. slow metaboliser), the observed concentrations will also reflect nongenetic factors that influence (DDIs, adherence, organ function and disease) the exposure of a drug. The disadvantage of therapeutical drug monitoring over pharmacogenetic testing is that the drug quantifying procedure is time-consuming, expensive, and laborious. The usefulness of pharmacogenetic testing depends on the availability of well-established information about the influence of genetic factors on drug exposure, but once that is available, genetic testing is becoming less expensive and more widely available.

Drugs that are heavily influenced by polymorphic metabolic pathways like isoniazid and efavirenz would greatly benefit from pharmacogenetic testing. Two common isoniazid related adverse events are peripheral neuropathy and hepatitis (Werely et al., 2007). Peripheral neuropathy is associated with higher plasma isoniazid concentration and slow *NAT2* acetylators. However, the drug-induced peripheral neuropathy is preventable by supplementation of pyridoxine, which is currently recommended for all isoniazid therapy (LOTTE et al., 1964). The risk of isoniazid-induced hepatitis is higher in slow acetylators, who tend to have higher concentrations of isoniazid and its metabolite acetylhydrazine for longer

periods than rapid acetylators, as both parent and metabolite have been linked to liver injury (Metushi et al., 2016). Isoniazid efficacy is also linked to *NAT2* genotype since the exposures significantly differ between the three phenotypes. Hence fast and intermediate acetylators have lower bactericidal activity than slow acetylators administered similar isoniazid doses (Donald et al., 2007). Central nervous system (CNS) complication is the most common efavirenz adverse event. CNS toxicity is related to efavirenz plasma levels and has been linked to *CYP2B6* genotype (Rotger et al., 2005). Isoniazid pharmacogenetic marker *NAT2* already has a test kit, while for efavirenz, TDM assay has been utilised for drug efficacy and to avoid toxicity (Gervasini et al., 2010). Recently a prototype automated pharmacogenomics assay on the Genexpert platform, which is widely available globally but not yet applied to pharmacogenomics, has been developed to robustly identify NAT2 acetylator using a volume of 24 µL blood sample (Verma et al., 2021). The prototype is easy to implement, scalable hence could be used at point of care, and requires minimal hands-on time for sample preparation, facilitating its use in resource-constrained settings like South Africa.

7.5.3 Handling of sparse or noisy data

The thesis emphasizes how nonlinear mixed-effects modelling is a powerful tool for efficiently analysing clinical trial data especially sparse and noisy data. The bedaquiline pharmacokinetics data analysed in chapter 4 had a small sample size and was sparse; however, with the help of a pharmacokinetic model, we could extract the information presented in that chapter. Furthermore, PK/PD models can be used to predict and extrapolate through simulations of validated models and have better capabilities of handling both sparse and noisy data. The PK/PD model developed in chapter 6 can be used to optimise other

tuberculosis drugs. While the consideration like the use of joint models can be utilised when analysing noisy longitudinal data that have correlating biomarkers or several biomarkers that need to be considered at once, as the models have better capabilities of extracting signal from noise.

7.6 Overall summary and conclusion

This thesis reports the results of the population pharmacokinetic and pharmacodynamic modelling analyses of some tuberculosis and HIV drugs. The focus of the work was on neglected populations and drug-drug interactions. In this thesis, I show that the exposures of the two anti-tuberculosis drugs, isoniazid and bedaquiline and an antiretroviral efavirenz are reduced by pregnancy. However, the main determinants of isoniazid and efavirenz drug exposure were metabolizing genotypes, which resulted in a five-fold difference between rapid and slow metabolizers of both drugs. I also show that the difference in exposure of isoniazid due to genotype affected its early bactericidal activity against inhA-mutated *M.tb* strain, suggesting that 10 mg/kg, 15 mg/kg and higher than 15 mg/kg doses are required for slow, intermediate, and rapid acetylators, respectively to match the bactericidal rates achieved with a standard dose of isoniazid (5 mg/kg) against DS-*M.tb*. These findings highlight the potential benefit of utilising genetic testing or therapeutic-drug-monitoring to individualise dosing for drugs heavily influenced by metabolising genotypes like isoniazid and efavirenz. Recently there has been development in the developing of a genetic test for isoniazid, and our results were part of the motivation (Schluger, 2021; Verma et al., 2021). In this thesis, I also characterised and quantified saturable pharmacokinetics of isoniazid and a significant reduction in isoniazid exposure, possibly due to an interaction with one of the

MDR-TB drugs. We postulate that the perpetrator of the interaction is terizidone/cycloserine. Finally, I showed that there is a significant accumulation of bedaquiline in breastmilk, highlighting the need to evaluate the safety of such exposures in breastfed infants. The same may happen for other antitubercular drugs used in the MDR-TB treatment and should be investigated.

The thesis highlights some knowledge gaps and research strategies that need to be prioritised to further improve tuberculosis and HIV treatment and how pharmacometrics modelling will be an invaluable tool in that pursuit. This includes the opportunistic inclusion of neglected populations in existing clinical trials (like the one presented in chapter 4), then developing separate trials for these subpopulations, which might be laborious and costly. Pharmacometrics' contribution to such a study is its capability to analyse data from such trials even if the sample size is small and the data is sparse. The thesis also shows the strength in pooling data from several studies, as presented in chapter 5, to extract information that could not be achieved through analysing a single study independently, and pharmacometrics excels at analysing pooled data.

References

Aarons, L. (1991). Population pharmacokinetics: theory and practice. *British Journal of Clinical Pharmacology*, *32*(6), 669–670. http://www.ncbi.nlm.nih.gov/pubmed/1768557

Abel zur Wiesch, P., Clarelli, F., & Cohen, T. (2017). Using Chemical Reaction Kinetics to Predict Optimal Antibiotic Treatment Strategies. *PLOS Computational Biology*, *13*(1), e1005321. https://doi.org/10.1371/journal.pcbi.1005321

Ad Hoc Committee. (1995). Treatment of Tuberculosis and Tuberculosis Infection in Adults and Children. *Clinical Infectious Diseases*, *21*(1), 9–27. https://doi.org/10.1093/clinids/21.1.9

Al-Khatib, S. M., Stevenson, W. G., Ackerman, M. J., Bryant, W. J., Callans, D. J., Curtis, A. B., Deal, B. J., Dickfeld, T., Field, M. E., Fonarow, G. C., Gillis, A. M., Granger, C. B., Hammill, S. C., Hlatky, M. A., Joglar, J. A., Kay, G. N., Matlock, D. D., Myerburg, R. J., & Page, R. L. (2018). 2017 AHA/ACC/HRS guideline for management of patients with ventricular arrhythmias and the prevention of sudden cardiac death: Executive summary. *Heart Rhythm*, *15*(10), e190–e252. https://doi.org/10.1016/j.hrthm.2017.10.035

Alghamdi, W. A., Al-Shaer, M. H., & Peloquin, C. A. (2018). Protein Binding of First-Line Antituberculosis Drugs. *Antimicrobial Agents and Chemotherapy*, *62*(7). https://doi.org/10.1128/AAC.00641-18

Anderson, B. J., & Holford, N. H. G. (2008). Mechanism-Based Concepts of Size and Maturity in Pharmacokinetics. *Annual Review of Pharmacology and Toxicology*, *48*(1), 303–332. https://doi.org/10.1146/annurev.pharmtox.48.113006.094708

Andries, K., Verhasselt, P., Guillemont, J., Göhlmann, H. W. H., Neefs, J.-M., Winkler, H., Gestel, J. Van, Timmerman, P., Zhu, M., Lee, E., Williams, P., Chaffoy, D. de, Huitric, E., Hoffner, S., Cambau, E., Truffot-Pernot, C., Lounis, N., & Jarlier, V. (2005). A Diarylquinoline Drug Active on the ATP Synthase of Mycobacterium tuberculosis. *Science*, *307*(5707), 223–227. https://doi.org/10.1126/SCIENCE.1106753

Argyrou, A., Jin, L., Siconilfi-Baez, L., Angeletti, R. H., & Blanchard, J. S. (2006). Proteome-wide Profiling of Isoniazid Targets in Mycobacterium tuberculosis. *Biochemistry*, *45*(47), 13947–13953. https://doi.org/10.1021/bi061874m

Argyrou, A., Vetting, M. W., Aladegbami, B., & Blanchard, J. S. (2006). Mycobacterium tuberculosis dihydrofolate reductase is a target for isoniazid. *Nature Structural & Molecular Biology*, *13*(5), 408–413. https://doi.org/10.1038/nsmb1089

Awaness, A. M., & Mitchison, D. A. (1973). Cumulative effects of pulsed exposures of mycobacterium tuberculosis to isoniazid. *Tubercle*, *54*(2), 153–158. https://doi.org/10.1016/0041-3879(73)90035-4

Banerjee, A., Dubnau, E., Quemard, A., Balasubramanian, V., Um, K. S., Wilson, T., Collins, D., de Lisle, G., & Jacobs, W. R. (1994). inhA, a gene encoding a target for isoniazid and ethionamide in Mycobacterium tuberculosis. *Science (New York, N.Y.)*, *263*(5144), 227–230. https://doi.org/10.1126/science.8284673

Bardou, F., Raynaud, C., Ramos, C., Laneelle, M. A., Lanrelle, G., Lanéelle, M. A., & Lanéelle, G. (1998). Mechanism of isoniazid uptake in Mycobacterium tuberculosis. *Microbiology*, *144*(9), 2539–2544. https://doi.org/10.1099/00221287-144-9-2539

Barrett, J.S., Joshi, A. S., Chai, M., Ludden, T. M., Fiske, W. D., & Jr., H. J. P. (2002). Population pharmacokinetic meta-analysis with efavirenz. *Int. Journal of Clinical Pharmacology and Therapeutics*, *40*(11), 507–519. https://doi.org/10.5414/CPP40507

Barrett, Jeffrey S, Fossler, M. J., David Cadieu, K., & Gastonguay, M. R. (2008).

Pharmacometrics: A Multidisciplinary Field to Facilitate Critical Thinking in Drug Development and Translational Research Settings. *Journal of Clinical Pharmacology*, *48*, 632–649. https://doi.org/10.1177/0091270008315318

Barry, C. E., Boshoff, H. I., Dartois, V., Dick, T., Ehrt, S., Flynn, J., Schnappinger, D., Wilkinson, R. J., & Young, D. (2009). The spectrum of latent tuberculosis: rethinking the biology and intervention strategies. *Nature Reviews Microbiology 2009 7:12*, *7*(12), 845–855. https://doi.org/10.1038/nrmicro2236

Beal, S. L. (2001). Ways to fit a PK model with some data below the quantification limit. *Journal of Pharmacokinetics and Pharmacodynamics*, *28*(5), 481–504. https://doi.org/10.1023/A:1012299115260

BERNSTEIN, J., LOTT, W. A., STEINBERG, B. A., & YALE, H. L. (1952). Chemotherapy of experimental tuberculosis. V. Isonicotinic acid hydrazide (nydrazid) and related compounds. *American Review of Tuberculosis*, *65*(4), 357–364. https://doi.org/10.1164/ART.1952.65.4.357

Bertrand, J., Verstuyft, C., Chou, M., Borand, L., Chea, P., Nay, K. H., Blanc, F.-X. F. X., Mentre, F., Taburet, A. M. A.-M., Sok, T., Goldfeld, A. E., Blanc, F.-X. F. X., Laureillard, D., Marcy, O., Fernandez, M., Chan, S., Nerrienet, E., Vong, S., Madec, Y., … Taburet, A. M. A.-M. (2014). Dependence of Efavirenz- and Rifampicin-Isoniazid-Based Antituberculosis Treatment Drug-Drug Interaction on CYP2B6 and NAT2 Genetic Polymorphisms: ANRS 12154 Study in Cambodia. *Journal of Infectious Diseases*, *209*(3), 399–408. https://doi.org/10.1093/infdis/jit466

Beste, D. J. V., Espasa, M., Bonde, B., Kierzek, A. M., Stewart, G. R., & McFadden, J. (2009). The Genetic Requirements for Fast and Slow Growth in Mycobacteria. *PLoS ONE*, *4*(4), e5349. https://doi.org/10.1371/journal.pone.0005349

Bhatt, N. B., Barau, C., Amin, A., Baudin, E., Meggi, B., Silva, C., Furlan, V., Grinsztejn, B., Barrail-Tran, A., Bonnet, M., Taburet, A. M., ANRS 12146-CARINEMO Study Group, the A. 12146-C. S., & ANRS 12146-CARINEMO Study Group. (2014). Pharmacokinetics of Rifampin and Isoniazid in Tuberculosis-HIV-Coinfected Patients Receiving Nevirapine- or Efavirenz-Based Antiretroviral Treatment. *Antimicrobial Agents and Chemotherapy*, *58*(6), 3182–3190. https://doi.org/10.1128/AAC.02379-13

Black, M. (1974). Editorial: Isoniazid and the liver. *American Review of Respiratory Disease*, *110*(1), 1–3. https://doi.org/10.1164/ARRD.1974.110.1.1

BLUM, M., GRANT, D. M., McBRIDE, W., HEIM, M., & MEYER, U. A. (1990). Human Arylamine N -Acetyltransferase Genes: Isolation, Chromosomal Localization, and Functional Expression. *DNA and Cell Biology*, *9*(3), 193–203. https://doi.org/10.1089/dna.1990.9.193

Boeckmann, A. J., Beal, S. L., & Sheiner, L. B. (2011). NONMEM User's Guide, Part V. Introductory Guide. *NONMEM Project Group*, *April*, 48. https://doi.org/10.1017/CBO9781107415324.004

Boffito, M., Back, D. J., Blaschke, T. F., Rowland, M., Bertz, R. J., Gerber, J. G., Miller, V., Aweeka, F., & Back, J. (2003). Roundtable Report Protein Binding in Antiretroviral Therapies on behalf of the roundtable participants *. In *AIDS RESEARCH AND HUMAN RETROVIRUSES* (Vol. 19, Issue 9). www.liebertpub.com

Bonnett, S. A., Dennison, D., Files, M., Bajpai, A., & Parish, T. (2018). A class of hydrazones are active against non-replicating Mycobacterium tuberculosis. *PLOS ONE*, *13*(10), e0198059. https://doi.org/10.1371/journal.pone.0198059

Bose, P. D., Sarma, M. P., Medhi, S., Das, B. C., Husain, S. A., & Kar, P. (2011). Role of

polymorphic N-acetyl transferase2 and cytochrome P4502E1 gene in antituberculosis treatment-induced hepatitis. *Journal of Gastroenterology and Hepatology*, *26*(2), 312–318. https://doi.org/10.1111/j.1440-1746.2010.06355.x

Böttger, E. C. (2011). Chapter 14: Drug Resistance in *Mycobacterium tuberculosis*: Molecular Mechanisms and Laboratory Susceptibility Testing. In P.R Donald & P. . van Helden (Eds.), *Antituberculosis Chemotherapy* (Vol. 10, pp. 128–144). S. Karger AG. https://doi.org/10.1159/000324630

Boukouvala sotiria, Hein David, Grant Denis, Sim Edith, Minchin Rodney, Agundez Jose, & Rodrigus-Lima Fernado. (2016). *Database of arylamine N-acetyltransferases (NATs)*. Democritus University of Thrace. https://nat.mbg.duth.gr/

Bowness, R., Boeree, M. J., Aarnoutse, R., Dawson, R., Diacon, A., Mangu, C., Heinrich, N., Ntinginya, N. E., Kohlenberg, A., Mtafya, B., Phillips, P. P. J., Rachow, A., Plemper van Balen, G., & Gillespie, S. H. (2015). The relationship between Mycobacterium tuberculosis MGIT time to positivity and cfu in sputum samples demonstrates changing bacterial phenotypes potentially reflecting the impact of chemotherapy on critical sub-populations. *Journal of Antimicrobial Chemotherapy*, *70*(2), 448–455. https://doi.org/10.1093/jac/dku415

Brill, M. J. E. M., Svensson, E. M. E., Pandie, M., Maartens, G., & Karlsson, M. M. O. (2017). Confirming model-predicted pharmacokinetic interactions between bedaquiline and lopinavir/ritonavir or nevirapine in patients with HIV and drug-resistant tuberculosis. *International Journal of Antimicrobial Agents*, *49*(2), 212–217. https://doi.org/10.1016/J.IJANTIMICAG.2016.10.020

Bristol-Myers Squibb. (2015). *Sustiva® (efavirenz) prescribing information (US)*. www.fda.gov/medwatch.

Brussee, J. M., Yu, H., Krekels, E. H. J., de Roos, B., Brill, M. J. E., van den Anker, J. N., Rostami-Hodjegan, A., de Wildt, S. N., & Knibbe, C. A. J. (2018). First-Pass CYP3A-Mediated Metabolism of Midazolam in the Gut Wall and Liver in Preterm Neonates. *CPT: Pharmacometrics and Systems Pharmacology*, *7*(6), 374–383. https://doi.org/10.1002/psp4.12295

Cahill, J. B., Bailey, E. M., Chien, S., & Johnson, G. M. (2005). Levofloxacin Secretion in Breast Milk: A Case Report. *Pharmacotherapy*, *25*(1), 116–118. https://doi.org/10.1592/phco.25.1.116.55616

Caño-Muñiz, S., Anthony, R., Niemann, S., & Alffenaar, J.-W. C. (2017). New Approaches and Therapeutic Options for Mycobacterium tuberculosis in a Dormant State. *Clinical Microbiology Reviews*, *31*(1). https://doi.org/10.1128/CMR.00060-17

Chan Kwong, A. H.-X. P., Calvier, E. A. M. M., Fabre, D., Gattacceca, F., & Khier, S. (2020). Prior information for population pharmacokinetic and pharmacokinetic/pharmacodynamic analysis: overview and guidance with a focus on the NONMEM PRIOR subroutine. *Journal of Pharmacokinetics and Pharmacodynamics*, *47*(5), 431–446. https://doi.org/10.1007/s10928-020-09695-z

Chaves, R. G., & Lamounier, J. A. (2004). Uso de medicamentos durante a lactação. *Jornal de Pediatria*, *80*(5), s189–s198. https://doi.org/10.1590/S0021-75572004000700011

Chen, C., Ortega, F., Rullas, J., Alameda, L., Angulo-Barturen, I., Ferrer, S., & Simonsson, U. S. (2017). The multistate tuberculosis pharmacometric model: a semi-mechanistic pharmacokinetic-pharmacodynamic model for studying drug effects in an acute tuberculosis mouse model. *Journal of Pharmacokinetics and Pharmacodynamics*, *44*(2), 133–141. https://doi.org/10.1007/s10928-017-9508-2

Chesov, D., Ciobanu, N., Lange, C., Heyckendorf, J., & Crudu, V. (2017). High-dose isoniazid in the shorter-course multidrug-resistant tuberculosis regimen in the Republic of Moldova. *European Respiratory Journal*, *50*(4), 1701340. https://doi.org/10.1183/13993003.01340-2017

Chigutsa, E., Patel, K., Denti, P., Visser, M., Maartens, G., Kirkpatrick, C. M. J., McIlleron, H., & Karlsson, M. O. (2013). A time-to-event pharmacodynamic model describing treatment response in patients with pulmonary tuberculosis using days to positivity in automated liquid mycobacterial culture. *Antimicrobial Agents and Chemotherapy*, *57*(2), 789–795. https://doi.org/10.1128/AAC.01876-12

Chirehwa, M. T., Court, R., de Kock, M., Wiesner, L., de Vries, N., Harding, J., Gumbo, T., Maartens, G., Warren, R., Denti, P., & McIlleron, H. (2020). Population Pharmacokinetics of Cycloserine and Pharmacokinetic/Pharmacodynamic Target Attainment in Multidrug-Resistant Tuberculosis Patients Dosed with Terizidone. *Antimicrobial Agents and Chemotherapy*, *64*(11). https://doi.org/10.1128/AAC.01381-20

Chirehwa, M. T., Court, R., de Kock, M., Wiesner, L., de Vries, N., Harding, J., Gumbo, T., Maartens, G., Warren, R., Denti, P., & McIlleron, H. (2021). Effect of Isoniazid Intake on Ethionamide Pharmacokinetics and Target Attainment in Multidrug-Resistant Tuberculosis Patients. *Antimicrobial Agents and Chemotherapy*, *65*(10). https://doi.org/10.1128/AAC.00278-21

Chirehwa, M. T., McIlleron, H., Wiesner, L., Affolabi, D., Bah-Sow, O., Merle, C., Denti, P., N'Diaye, A., Mbaye, I. M., De Jong, B., Anagonou, S., Diatema, S., Gomina, I. K., Gossa, S., Tanimomo, B., Bekou, W., Galperine, T., Furco, A., Diallo, M., … Saint-Martin, C. (2018a). Effect of efavirenz-based antiretroviral therapy and high-dose rifampicin on the pharmacokinetics of isoniazid and acetyl-isoniazid. *Journal of Antimicrobial Chemotherapy*, *74*(1), 139–148. https://doi.org/10.1093/jac/dky378

Chirehwa, M. T., McIlleron, H., Wiesner, L., Affolabi, D., Bah-Sow, O., Merle, C., Denti, P., N'Diaye, A., Mbaye, I. M., De Jong, B., Anagonou, S., Diatema, S., Gomina, I. K., Gossa, S., Tanimomo, B., Bekou, W., Galperine, T., Furco, A., Diallo, M., … Saint-Martin, C. (2018b). Effect of efavirenz-based antiretroviral therapy and high-dose rifampicin on the pharmacokinetics of isoniazid and acetyl-isoniazid. *Journal of Antimicrobial Chemotherapy*, *7800*, 7719. https://doi.org/10.1093/jac/dky378

Chirehwa, M. T., Rustomjee, R., Mthiyane, T., Onyebujoh, P., Smith, P., McIlleron, H., & Denti, P. (2016). Model-Based Evaluation of Higher Doses of Rifampin Using a Semimechanistic Model Incorporating Autoinduction and Saturation of Hepatic Extraction. *Antimicrobial Agents and Chemotherapy*, *60*(1), 487–494. https://doi.org/10.1128/AAC.01830-15

Collart, L., Blaschke, T. F., Boucher, F., & Prober, C. G. (1992). Potential of population pharmacokinetics to reduce the frequency of blood sampling required for estimating kinetic parameters in neonates. *Developmental Pharmacology and Therapeutics*, *18*(1–2), 71–80. http://www.ncbi.nlm.nih.gov/pubmed/1483365

Cordes, H., Thiel, C., Aschmann, H. E., Baier, V., Blank, L. M., & Kuepfer, L. (2016). A Physiologically Based Pharmacokinetic Model of Isoniazid and Its Application in Individualizing Tuberculosis Chemotherapy. *Antimicrobial Agents and Chemotherapy*, *60*(10), 6134–6145. https://doi.org/10.1128/aac.00508-16

Court, R., Chirehwa, M. T., Wiesner, L., de Vries, N., Harding, J., Gumbo, T., Maartens, G., & McIlleron, H. (2019). Effect of tablet crushing on drug exposure in the treatment of multidrug-resistant tuberculosis. *The International Journal of Tuberculosis and Lung Disease*, *23*(10), 1068–1074. https://doi.org/10.5588/ijtld.18.0775

Culyba, M. J., Mo, C. Y., & Kohli, R. M. (2015). Targets for Combating the Evolution of Acquired Antibiotic Resistance. *Biochemistry*, *54*(23), 3573–3582. https://doi.org/10.1021/acs.biochem.5b00109

Dannenberg, A. M. (2009). Liquefaction and cavity formation in pulmonary TB: A simple method in rabbit skin to test inhibitors. *Tuberculosis*, *89*(4), 243–247. https://doi.org/10.1016/j.tube.2009.05.006

Dargan, P., Kalsi, Wood, D., & Waring. (2011). Does cytochrome P450 liver isoenzyme induction increase the risk of liver toxicity after paracetamol overdose? *Open Access Emergency Medicine*, *3*, 69. https://doi.org/10.2147/OAEM.S24962

Dartois, V. (2014). The path of anti-tuberculosis drugs: from blood to lesions to mycobacterial cells. *Nature Reviews Microbiology*, *12*(3), 159–167. https://doi.org/10.1038/nrmicro3200

Daskapan, A., Idrus, L. R., Postma, M. J., Wilffert, B., Kosterink, J. G. W., Stienstra, Y., Touw, D. J., Andersen, A. B., Bekker, A., Denti, P., Hemanth Kumar, A. K., Jeremiah, K., Kwara, A., McIlleron, H., Meintjes, G., van Oosterhout, J. J., Ramachandran, G., Rockwood, N., Wilkinson, R. J., … Alffenaar, J.-W. C. (2019). A Systematic Review on the Effect of HIV Infection on the Pharmacokinetics of First-Line Tuberculosis Drugs. *Clinical Pharmacokinetics*, *58*(6), 747–766. https://doi.org/10.1007/s40262-018-0716-8

De Jager, V., Van Der Merwe, L., Venter, A., Donald, P. R., & Diacon, A. H. (2017). Time Trends in Sputum Mycobacterial Load and Two-Day Bactericidal Activity of Isoniazid-Containing Antituberculosis Therapies. *Antimicrobial Agents and Chemotherapy*, *61*(4). https://doi.org/10.1128/AAC.02088-16

de Kock, M., Tarning, J., Barnes, K. I., & Denti, P. (2017). Response to "Lactation Status and Studies of Pyrimethamine Pharmacokinetics in Pregnancy." *CPT: Pharmacometrics & Systems Pharmacology*, *6*(11), 731–731. https://doi.org/10.1002/psp4.12256

Denti, P., Wasmann, R. E., Francis, J., McIlleron, H., Sugandhi, N., Cressey, T. R., Mirochnick, M., Capparelli, E. V., & Penazzato, M. (2022). One dose does not fit all: revising the WHO paediatric dosing tool to include the non-linear effect of body size and maturation. *The Lancet Child & Adolescent Health*, *6*(1), 9–10. https://doi.org/10.1016/S2352-4642(21)00302-3

Desta, Z., Gammal, R. S., Gong, L., Whirl-Carrillo, M., Gaur, A. H., Sukasem, C., Hockings, J., Myers, A., Swart, M., Tyndale, R. F., Masimirembwa, C., Iwuchukwu, O. F., Chirwa, S., Lennox, J., Gaedigk, A., Klein, T. E., & Haas, D. W. (2019). Clinical Pharmacogenetics Implementation Consortium (CPIC) Guideline for CYP2B6 and Efavirenz-Containing Antiretroviral Therapy. *Clinical Pharmacology and Therapeutics*, *106*(4), 726–733. https://doi.org/10.1002/cpt.1477

Desta, Z., Saussele, T., Ward, B., Blievernicht, J., Li, L., Klein, K., Flockhart, D. A., & Zanger, U. M. (2007). Impact of CYP2B6 polymorphism on hepatic efavirenz metabolism *in vitro*. *Pharmacogenomics*, *8*(6), 547–558. https://doi.org/10.2217/14622416.8.6.547

Desta, Z., Soukhova, N. V, & Flockhart, D. A. (2001). Inhibition of Cytochrome P450 (CYP450) Isoforms by Isoniazid: Potent Inhibition of CYP2C19 and CYP3A. *Antimicrobial Agents and Chemotherapy*, *45*(2), 382–392. https://doi.org/10.1128/AAC.45.2.382-392.2001

Diacon, A. H., Donald, P. R., Pym, A., Grobusch, M., Patientia, R. F., Mahanyele, R., Bantubani, N., Narasimooloo, R., De Marez, T., van Heeswijk, R., Lounis, N., Meyvisch, P., Andries, K., & McNeeley, D. F. (2012). Randomized Pilot Trial of Eight Weeks of Bedaquiline (TMC207) Treatment for Multidrug-Resistant Tuberculosis: Long-Term Outcome, Tolerability, and Effect on Emergence of Drug Resistance. *Antimicrobial Agents and*

Chemotherapy, *56*(6), 3271–3276. https://doi.org/10.1128/AAC.06126-11

Diacon, A. H., Maritz, J. S., Venter, A., van Helden, P. D., Dawson, R., & Donald, P. R. (2012). Time to liquid culture positivity can substitute for colony counting on agar plates in early bactericidal activity studies of antituberculosis agents. *Clinical Microbiology and Infection*, *18*(7), 711–717. https://doi.org/10.1111/j.1469-0691.2011.03626.x

Dickinson, J. ., & Mitchison, D. A. (1968). In vitro and in vivo studies to assess the suitability of antituberculous drugs for use in intermittent chemotherapy regimens. *Tubercle*, *49*, 66–70.

Dickinson, L., Amin, J., Else, L., Boffito, M., Egan, D., Owen, A., Khoo, S., Back, D., Orrell, C., Clarke, A., Losso, M., Phanuphak, P., Carey, D., Cooper, D. A., Emery, S., & Puls, R. (2015). Pharmacokinetic and Pharmacodynamic Comparison of Once-Daily Efavirenz (400 mg vs. 600 mg) in Treatment-Naive HIV-Infected Patients: Results of the ENCORE1 Study. *Clinical Pharmacology and Therapeutics*, *98*(4), 406–416. https://doi.org/10.1002/cpt.156

Dickmann, L. J., & Isoherranen, N. (2013). Quantitative Prediction of CYP2B6 Induction by Estradiol During Pregnancy: Potential Explanation for Increased Methadone Clearance During Pregnancy. *Drug Metabolism and Disposition*, *41*(2), 270–274. https://doi.org/10.1124/dmd.112.047118

Donald, P. R., Parkin, D. P., Seifart, H. I., Schaaf, H. S., van Helden, P. D., Werely, C. J., Sirgel, F. A., Venter, A., & Maritz, J. S. (2007). The influence of dose and N-acetyltransferase-2 (NAT2) genotype and phenotype on the pharmacokinetics and pharmacodynamics of isoniazid. *European Journal of Clinical Pharmacology*, *63*(7), 633–639. https://doi.org/10.1007/s00228-007-0305-5

Donald, P.R., & Diacon, A. H. (2008). The early bactericidal activity of anti-tuberculosis drugs: a literature review. *Tuberculosis*, *88*, S75–S83. https://doi.org/10.1016/S1472-9792(08)70038-6

Donald, Peter R, Sirgel, F. A., Botha, F. J., Seifart, H. I., Parkin, D. P., Vandenplas, M. L., Van De Wal, B. W., Maritz, J. S., & Mitchison, D. A. (1997). The Early Bactericidal Activity of Isoniazid Related to Its Dose Size in Pulmonary Tuberculosis. In *Am J Respir Crit Care Med* (Vol. 156).

Dooley, K. E., Denti, P., Martinson, N., Cohn, S., Mashabela, F., Hoffmann, J., Haas, D. W., Hull, J., Msandiwa, R., Castel, S., Wiesner, L., & Chaisson, R. E. (2015). Pharmacokinetics of Efavirenz and Treatment of HIV-1 Among Pregnant Women With and Without Tuberculosis Coinfection. *Journal of Infectious Diseases*, *211*(2), 197–205. https://doi.org/10.1093/infdis/jiu429

Dooley, K. E., Denti, P., Martinson, N., Cohn, S., Mashabela, F., Hoffmann, J., Haas, D. W., Hull, J., Msandiwa, R., Castel, S., Wiesner, L., Chaisson, R. E., & McIlleron, H. (2015). Pharmacokinetics of Efavirenz and Treatment of HIV-1 Among Pregnant Women With and Without Tuberculosis Coinfection. *Journal of Infectious Diseases*, *211*(2), 197–205. https://doi.org/10.1093/infdis/jiu429

Dooley, K. E., Miyahara, S., von Groote-Bidlingmaier, F., Sun, X., Hafner, R., Rosenkranz, S. L., Ignatius, E. H., Nuermberger, E. L., Moran, L., Donahue, K., Swindells, S., Vanker, N., Diacon, A. H., Issa, R., Lane, C., Lojacono, M., Mahachi, R., Murtaugh, W., Purdue, L., … Ssenyonga, R. (2020). Early Bactericidal Activity of Different Isoniazid Doses for Drug-Resistant Tuberculosis (INHindsight): A Randomized, Open-Label Clinical Trial. *American Journal of Respiratory and Critical Care Medicine*, *201*(11), 1416–1424. https://doi.org/10.1164/rccm.201910-1960OC

Drozda, K., Pacanowski, M. A., Grimstein, C., & Zineh, I. (2018). Pharmacogenetic Labeling of FDA-Approved Drugs: A Regulatory Retrospective. *JACC: Basic to Translational Science*, *3*(4), 545. https://doi.org/10.1016/J.JACBTS.2018.06.001

Dutta, N. K., & Karakousis, P. C. (2017). Mechanisms of Action and Resistance of the Antimycobacterial Agents. In *Antimicrobial Drug Resistance* (pp. 359–383). Springer International Publishing. https://doi.org/10.1007/978-3-319-46718-4_25

Dye, C., Scheele, S., >Dolin, P., Pathania, V., & Raviglione, M. C. (1999). Global Burden of Tuberculosis. *JAMA*, *282*(7), 677. https://doi.org/10.1001/jama.282.7.677

Eckhardt, B. J., & Gulick, R. M. (2017). Drugs for HIV Infection. *Infectious Diseases*, *2*, 1293-1308.e2. https://doi.org/10.1016/B978-0-7020-6285-8.00152-0

Egbelowo, O., Sarathy, J. P., Gausi, K., Zimmerman, M. D., Wang, H., Wijnant, G. J., Kay, F., Gengenbacher, M., Van, N., Degefu, Y., Nacy, C., Aldridge, B. B., Carter, C. L., Denti, P., & Dartois, V. (2021). Pharmacokinetics and target attainment of SQ109 in plasma and human-like tuberculosis lesions in rabbits. *Antimicrobial Agents and Chemotherapy*, *65*(9). https://doi.org/10.1128/AAC.00024-21/SUPPL_FILE/AAC.00024-21-S0001.PDF

Eke, A. C., Olagunju, A., Momper, J., Penazzato, M., Abrams, E. J., Best, B. M., Capparelli, E. V., Bekker, A., Belew, Y., Kiser, J. J., Struble, K., Taylor, G., Waitt, C., Mirochnick, M., Cressey, T. R., Colbers, A., Abrams, E., Aldrovandi, G., Bekker, A., … Little, M. (2021). Optimizing Pharmacology Studies in Pregnant and Lactating Women Using Lessons From HIV: A Consensus Statement. *Clinical Pharmacology and Therapeutics*, *110*(1), 36–48. https://doi.org/10.1002/cpt.2048

Engelbrecht, M. C., Kigozi, N. G., Chikobvu, P., Botha, S., & Rensburg, H. C. J. van. (2017). Unsuccessful TB treatment outcomes with a focus on HIV co-infected cases: a cross-sectional retrospective record review in a high-burdened province of South Africa. *BMC Health Services Research*, *17*(1). https://doi.org/10.1186/S12913-017-2406-X

Ette, E. I., & Williams, P. J. (2013). *Pharmacometrics: the science of quantitative pharmacology*. John Wiley & Sons.

European medicines agency. (2011). *Guideline on bioanalytical method validation*. www.ema.europa.eu/contact

European medicines agency. (2013). *CHMP assessment report: SIRTURO*. www.ema.europa.eu

FDA, & Center fr drug evaluation and research. (2018). *Bioanalytical Method Validation Guidance for Industry Biopharmaceutics Bioanalytical Method Validation Guidance for Industry Biopharmaceutics Contains Nonbinding Recommendations*. http://www.fda.gov/Drugs/GuidanceComplianceRegulatoryInformation/Guidances/default.htmand/orhttp://www.fda.gov/AnimalVeterinary/GuidanceComplianceEnforcement/GuidanceforIndustry/default.htm

FDA, U. (1999). *Office of Training and Communications Division of Communications Management Drug Information Branch* (Vol. 20857). Tel. http://www.fda.gov/cder/guidance/index.htmorhttp://www.fda.gov/cber/guidelines.htm

Feghali, M. N., & Mattison, D. R. (2011). Clinical Therapeutics in Pregnancy. *Journal of Biomedicine and Biotechnology*, *2011*, 1–13. https://doi.org/10.1155/2011/783528

Feghali, M., Venkataramanan, R., & Caritis, S. (2015). Pharmacokinetics of drugs in pregnancy. *Seminars in Perinatology*, *39*(7), 512–519. https://doi.org/10.1053/j.semperi.2015.08.003

Fellay, J., Marzolini, C., Decosterd, L., Golay, K. P., Baumann, P., Buclin, T., Telenti, A., & Eap,

C. B. (2005). Variations of CYP3A activity induced by antiretroviral treatment in HIV-1 infected patients. *European Journal of Clinical Pharmacology*, *60*(12), 865–873. https://doi.org/10.1007/s00228-004-0855-8

Feng, X., Zhu, W., Schurig-Briccio, L. A., Lindert, S., Shoen, C., Hitchings, R., Li, J., Wang, Y., Baig, N., Zhou, T., Kim, B. K., Crick, D. C., Cynamon, M., McCammon, J. A., Gennis, R. B., & Oldfield, E. (2015). Antiinfectives targeting enzymes and the proton motive force. *Proceedings of the National Academy of Sciences*, *112*(51), E7073–E7082. https://doi.org/10.1073/PNAS.1521988112

Flockhart, D. A. DA, Skaar, T., Berlin, D. S. D., Klein, T. E. TE, & Nguyen, A. T. (2009). *Clinically Available Pharmacogenomics Tests*. *86*(1). /pmc/articles/PMC2730436/

Gabrielsson, J., & Weiner, D. (2016). *Pharmacokinetic and Pharmacodynamic Data Analysis Concepts and Applications 5 th edition* (5th editio). Swedish Pharmaceutical Press.

García-Closas, M., Heind, D. W., Silvermana, D., Malatsk, N., Yeager, M., Jacobs, K., Doll, M. A., Figueroa, J. D., Baris, D., Schwenn, M., Kogevinas, M., Johnson, A., Chatterjee, N., Moore, L. E., Moeller, T., Real, F. X., Chanock, S., & Rothman, N. (2011). A single nucleotide polymorphism tags variation in the arylamine N-acetyltransferase 2 phenotype in populations of European background. *Pharmacogenetics and Genomics*, *21*(4), 231. https://doi.org/10.1097/FPC.0B013E32833E1B54

Gausi, K., Ignatius, E. H., Sun, X., Kim, S., Moran, L., Wiesner, L., von Groote-Bidlingmaier, F., Hafner, R., Donahue, K., Vanker, N., Rosenkranz, S. L., Swindells, S., Diacon, A. H., Nuermberger, E. L., Dooley, K. E., & Denti, P. (2021). A Semimechanistic Model of the Bactericidal Activity of High-Dose Isoniazid against Multidrug-Resistant Tuberculosis: Results from a Randomized Clinical Trial. *American Journal of Respiratory and Critical Care Medicine*, *204*(11), 1327–1335. https://doi.org/10.1164/rccm.202103-0534OC

Gausi, K., Wiesner, L., Norman, J., Wallis, C. L., Onyango-Makumbi, C., Chipato, T., Haas, D. W., Browning, R., Chakhtoura, N., Montepiedra, G., Aaron, L., McCarthy, K., Bradford, S., Vhembo, T., Stranix-Chibanda, L., Masheto, G. R., Violari, A., Mmbaga, B. T., Aurpibul, L., … Denti, P. (2020). Pharmacokinetics and Drug-Drug Interactions of Isoniazid and Efavirenz in Pregnant Women Living With HIV in High TB Incidence Settings: Importance of Genotyping. *Clinical Pharmacology & Therapeutics*, *109*(4), 1034–1044. https://doi.org/10.1002/cpt.2044

Gervasini, G., Benítez, J., Carrillo, J. A., Antonio, J., & Pharmacogenetic, C. (2010). Pharmacogenetic testing and therapeutic drug monitoring are complementary tools for optimal individualization of drug therapy. *European Journal of Clinical Pharmacology*, *8*, 755–774. https://doi.org/10.1007/s00228-010

Gilbert-Barness, E. (1995). Maternal-Fetal Toxicology: A Clinician's Guide. *Archives of Pediatrics & Adolescent Medicine*, *149*(9), 1045. https://doi.org/10.1001/archpedi.1995.02170220111027

Global Alliance for TB Drug Development. (2008). Handbook of Anti-Tuberculosis Agents. In *Tuberculosis* (Vol. 88, Issue 2). https://doi.org/10.1016/S1472-9792(08)70002-7

Gobburu, J. V. S., & Marroum, P. J. (2001). Utilisation of Pharmacokinetic- Pharmacodynamic Modelling and Simulation in Regulatory Decision-Making. *Clinical Pharmacokinetics*, *40*(12), 883–892. https://doi.org/10.2165/00003088-200140120-00001

Gordi, T., Xie, R., Huong, N. V., Huong, D. X., Karlsson, M. O., & Ashton, M. (2005). A semiphysiological pharmacokinetic model for artemisinin in healthy subjects incorporating autoinduction of metabolism and saturable first-pass hepatic extraction. *British Journal of Clinical Pharmacology*, *59*(2), 189–198.

https://doi.org/10.1111/j.1365-2125.2004.02321.x
Gordi, T., Xie, R., & Jusko, W. J. (2005). Semi-mechanistic pharmacokinetic/pharmacodynamic modelling of the antimalarial effect of artemisinin. *British Journal of Clinical Pharmacology*, *60*(6), 594–604. https://doi.org/10.1111/j.1365-2125.2005.02508.x
Grimsrud, K. N., Sherwin, C. M. T., Constance, J. E., Tak, C., Zuppa, A. F., Spigarelli, M. G., & Mihalopoulos, N. L. (2015). Special population considerations and regulatory affairs for clinical research. *Clinical Research and Regulatory Affairs*, *32*(2), 47. https://doi.org/10.3109/10601333.2015.1001900
Guiastrennec, B., Ramachandran, G., Karlsson, M. O., Kumar, A. K. H., Bhavani, P. K., Gangadevi, N. P., Swaminathan, S., Gupta, A., Dooley, K. E., & Savic, R. M. (2018). Suboptimal Antituberculosis Drug Concentrations and Outcomes in Small and HIV-Coinfected Children in India: Recommendations for Dose Modifications. *Clinical Pharmacology and Therapeutics*, *104*(4), 733–741. https://doi.org/10.1002/cpt.987
Gupta, A., Hughes, M. D., Garcia-Prats, A. J., McIntire, K., & Hesseling, A. C. (2019). Inclusion of key populations in clinical trials of new antituberculosis treatments: Current barriers and recommendations for pregnant and lactating women, children, and HIV-infected persons. *PLOS Medicine*, *16*(8), e1002882. https://doi.org/10.1371/journal.pmed.1002882
Gupta, A., Mathad, J. S., Abdel-Rahman, S. M., Albano, J. D., Botgros, R., Brown, V., Browning, R. S., Dawson, L., Dooley, K. E., Gnanashanmugam, D., Grinsztejn, B., Hernandez-DIaz, S., Jean-Philippe, P., Kim, P., Lyerly, A. D., Mirochnick, M., Mofenson, L. M., Montepiedra, G., Piper, J., … White, A. (2016). Toward Earlier Inclusion of Pregnant and Postpartum Women in Tuberculosis Drug Trials: Consensus Statements From an International Expert Panel. *Clinical Infectious Diseases*, *62*(6), 761–769. https://doi.org/10.1093/CID/CIV991
Gupta, A., Montepiedra, G., Aaron, L., Theron, G., McCarthy, K., Bradford, S., Chipato, T., Vhembo, T., Stranix-Chibanda, L., Onyango-Makumbi, C., Masheto, G. R., Violari, A., Mmbaga, B. T., Aurpibul, L., Bhosale, R., Mave, V., Rouzier, V., Hesseling, A., Shin, K., … Weinberg, A. (2019). Isoniazid Preventive Therapy in HIV-Infected Pregnant and Postpartum Women. *New England Journal of Medicine*, *381*(14), 1333–1346. https://doi.org/10.1056/NEJMOA1813060/SUPPL_FILE/NEJMOA1813060_DATA-SHARING.PDF
Gupta, A., Montepiedra, G., Aaron, L., Theron, G., McCarthy, K., Bradford, S., Chipato, T., Vhembo, T., Stranix-Chibanda, L Onyango-Makumbi, C Masheto, G. ., Violari, A., Mmbaga, B. ., Aurpibul, L., Bhosale, R., Mave, V., Rouzier, V., Hesseling, A Shin, K., Zimmer, B., Costello, D., Sterling, T. ., … Weinberg, A, I. P. T. A. S. T. (2019). Isoniazid Preventive Therapy in HIV-Infected Pregnant and Postpartum Women. *The New England Journal of Medicine*, *381*, 1333–1346. https://doi.org/10.1056/NEJMoa1813060
Haas, D. W., Gebretsadik, T., Mayo, G., Menon, U. N., Acosta, E. P., Shintani, A., Floyd, M., Stein, C. M., & Wilkinson, G. R. (2009). Associations between CYP2B6 Polymorphisms and Pharmacokinetics after a Single Dose of Nevirapine or Efavirenz in African Americans . *The Journal of Infectious Diseases*, *199*(6), 872–880. https://doi.org/10.1086/597125
Hein, D. W., & Doll, M. A. (2012). Accuracy of various human NAT2 SNP genotyping panels to infer rapid, intermediate and slow acetylator phenotypes. *Pharmacogenomics*, *13*(1), 31. https://doi.org/10.2217/PGS.11.122
Hellmold, H., Rylander, T., Magnusson, M., Reihnér, E., Warner, M., & Gustafsson, J.-A. (1998). Characterization of Cytochrome P450 Enzymes in Human Breast Tissue from Reduction Mammaplasties. *The Journal of Clinical Endocrinology & Metabolism*, *83*(3), 886–895.

https://doi.org/10.1210/JCEM.83.3.4647
Hillemann, D., Richter, E., & Rüsch-Gerdes, S. (2006). Use of the BACTEC Mycobacteria Growth Indicator Tube 960 Automated System for Recovery of Mycobacteria from 9,558 Extrapulmonary Specimens, Including Urine Samples. *Journal of Clinical Microbiology*, *44*(11), 4014–4017. https://doi.org/10.1128/JCM.00829-06
HINSHAW, C. (1946). TREATMENT OF TUBERCULOSIS WITH STREPTOMYCIN. *Journal of the American Medical Association*, *132*(13), 778. https://doi.org/10.1001/jama.1946.02870480024007
Holdiness, M. R. (1984). Clinical Pharmacokinetics of the Antituberculosis Drugs. *Clinical Pharmacokinetics*, *9*(6), 511–544. https://doi.org/10.2165/00003088-198409060-00003
Holford, N. H. G., & Anderson, B. J. (2017). Allometric size: The scientific theory and extension to normal fat mass. *European Journal of Pharmaceutical Sciences*, *109*, S59–S64. https://doi.org/10.1016/j.ejps.2017.05.056
Holzinger, E. R., Grady, B., Ritchie, M. D., Ribaudo, H. J., Acosta, E. P., Morse, G. D., Gulick, R. M., Robbins, G. K., Clifford, D. B., Daar, E. S., McLaren, P., & Haas, D. W. (2012). Genome-wide association study of plasma efavirenz pharmacokinetics in AIDS Clinical Trials Group protocols implicates several CYP2B6 variants. *Pharmacogenetics and Genomics*, *22*(12), 858–867. https://doi.org/10.1097/FPC.0b013e32835a450b
Hong, B.-L., D'Cunha, R., Li, P., Al-Shaer, M. H., Alghamdi, W. A., An, G., & Peloquin, C. (2020). A Systematic Review and Meta-analysis of Isoniazid Pharmacokinetics in Healthy Volunteers and Patients with Tuberculosis. *Clinical Therapeutics*, *42*(11), e220–e241. https://doi.org/10.1016/j.clinthera.2020.09.009
Hooker, A. C., Staatz, C. E., & Karlsson, M. O. (2007). Conditional weighted residuals (CWRES): A model diagnostic for the FOCE method. *Pharmaceutical Research*, *24*(12), 2187–2197. https://doi.org/10.1007/s11095-007-9361-x
Howard, C. R., & Lawrence, R. A. (1999). Drugs and Breastfeeding. *Clinics in Perinatology*, *26*(2), 447–478. https://doi.org/10.1016/S0095-5108(18)30061-7
Huang, Y. (2003). Cytochrome P450 2E1 genotype and the susceptibility to antituberculosis drug-induced hepatitis. *Hepatology*, *37*(4), 924–930. https://doi.org/10.1053/jhep.2003.50144
Huang, Z., Fasco, M. J., Figge, H. L., Keyomarsi, K., & Kaminsky, L. S. (1996). Expression of cytochromes P450 in human breast tissue and tumors. *Drug Metabolism and Disposition*, *24*(8).
Husain, A., Zhang, X., Doll, M. A., States, J. C., Barker, D. F., & Hein, D. W. (2007). Identification of N- Acetyltransferase 2 (NAT2) Transcription Start Sites and Quantitation of NAT2 - Specific mRNA in Human Tissues. *Drug Metabolism and Disposition*, *35*(5), 721–727. https://doi.org/10.1124/dmd.106.014621
Iscan, M., Klaavuniemi, T., Çoban, T., Kapucuo˘ Glu, N., Pelkonen, O., & Raunio, H. (2001). The expression of cytochrome P450 enzymes in human breast tumours and normal breast tissue. In *Breast Cancer Research and Treatment* (Vol. 70).
Iulio, J. di, Fayet, A., Arab-Alameddine, M., Rotger, M., Lubomirov, R., Cavassini, M., Furrer, H., Günthard, H. F., Colombo, S., Csajka, C., Eap, C. B., Decosterd, L. A., & Telenti, A. (2009). In vivo analysis of efavirenz metabolism in individuals with impaired CYP2A6 function. *Pharmacogenetics and Genomics*, *19*(4), 300–309. https://doi.org/10.1097/FPC.0b013e328328d577
Jannsen Products. (2015). *Sirturo (bedaquiline) Medication guide*. www.fda.gov/medwatch.
Jeong, H. (2010). Altered drug metabolism during pregnancy: hormonal regulation of drug-

metabolizing enzymes. *Expert Opinion on Drug Metabolism & Toxicology*, *6*(6), 689–699. https://doi.org/10.1517/17425251003677755

Jhun, B. W., & Koh, W.-J. (2020). Treatment of Isoniazid-Resistant Pulmonary Tuberculosis. *Tuberculosis and Respiratory Diseases*, *83*(1), 20. https://doi.org/10.4046/trd.2019.0065

Johansson, Å. M., & Karlsson, M. O. (2013). Comparison of Methods for Handling Missing Covariate Data. *The AAPS Journal*, *15*(4), 1232–1241. https://doi.org/10.1208/s12248-013-9526-y

Karakousis, P. C., Williams, E. P., & Bishai, W. R. (2008). Altered expression of isoniazid-regulated genes in drug-treated dormant Mycobacterium tuberculosis. *Journal of Antimicrobial Chemotherapy*, *61*(2), 323–331. https://doi.org/10.1093/jac/dkm485

Katiyar, S. K., Bihari, S., Prakash, S., Mamtani, M., & Kulkarni, H. (2008). A randomised controlled trial of high-dose isoniazid adjuvant therapy for multidrug-resistant tuberculosis. *The International Journal of Tuberculosis and Lung Disease : The Official Journal of the International Union against Tuberculosis and Lung Disease*, *12*(2), 139–145. http://www.randomization.com

Keizer, R. J. (2010). *Pharmacometrics in early clinical drug development*. Utrecht university.

Keizer, R. J., Zandvliet, A. S., Beijnen, J. H., Schellens, J. H. M., & Huitema, A. D. R. (2012). Performance of Methods for Handling Missing Categorical Covariate Data in Population Pharmacokinetic Analyses. *The AAPS Journal*, *14*(3), 601–611. https://doi.org/10.1208/s12248-012-9373-2

Keizer, R., Karlsson, M., & Hooker, A. (2013). Modeling and Simulation Workbench for NONMEM: Tutorial on Pirana, PsN, and Xpose. *CPT: Pharmacometrics & Systems Pharmacology*, *2*(6), 50. https://doi.org/10.1038/psp.2013.24

Khoo, S. H., Gibbons, S., Seden, K., & Back, D. J. (2014). *SYSTEMATIC REVIEW : Drug-drug Interactions between Antiretrovirals and medications used to treat TB , Malaria , Hepatitis B & C and opioid dependence*. *5656*. http://www.who.int/hiv/topics/treatment/drug_drug_interactions_review.pdf

Kjellsson, M. C., Via, L. E., Goh, A., Weiner, D., Low, K. M., Kern, S., Pillai, G., Barry, C. E., & Dartois, V. (2012). Pharmacokinetic evaluation of the penetration of antituberculosis agents in rabbit pulmonary lesions. *Antimicrobial Agents and Chemotherapy*, *56*(1), 446–457. https://doi.org/10.1128/AAC.05208-11

Klein, D. J., Boukouvala, S., McDonagh, E. M., Shuldiner, S. R., Laurieri, N., Thorn, C. F., Altman, R. B., & Klein, T. E. (2016a). PharmGKB Summary: Isoniazid Pathway, Pharmacokinetics (PK). *Pharmacogenetics and Genomics*, *26*(9), 436. https://doi.org/10.1097/FPC.0000000000000232

Klein, D. J., Boukouvala, S., McDonagh, E. M., Shuldiner, S. R., Laurieri, N., Thorn, C. F., Altman, R. B., & Klein, T. E. (2016b). PharmGKB summary. *Pharmacogenetics and Genomics*, *26*(9), 436–444. https://doi.org/10.1097/FPC.0000000000000232

Kodadhala, V., Gudeta, A., Zerihun, A., Lewis, O., Ahmed, S., Gajjala, J., & Thomas, A. (2016). Postpartum Tuberculosis: A Diagnostic and Therapeutic Challenge. *Case Reports in Pulmonology*, *2016*, 1–6. https://doi.org/10.1155/2016/3793941

le Roux, S. P., Upton, C., Vanker, N., Dooley, K. E., & Diacon, A. H. (2020). Resistance-conferring Mycobacterial Mutations and Quantification of Early Bactericidal Activity. *American Journal of Respiratory and Critical Care Medicine*, rccm.202007-2740LE. https://doi.org/10.1164/rccm.202007-2740LE

Lehloenya, R. J., Muloiwa, R., Dlamini, S., Gantsho, N., Todd, G., & Dheda, K. (2015). Lack of cross-toxicity between isoniazid and ethionamide in severe cutaneous adverse drug

reactions: a series of 25 consecutive confirmed cases. *Journal of Antimicrobial Chemotherapy*, *70*(9), 2648–2651. https://doi.org/10.1093/jac/dkv158

Lehmann, J. (1946). PARA-AMINOSALICYLIC ACID IN THE TREATMENT OF TUBERCULOSIS. *The Lancet*, *247*(6384), 15–16. https://doi.org/10.1016/S0140-6736(46)91185-3

Lempens, P., Meehan, C. J., Vandelannoote, K., Fissette, K., de Rijk, P., Van Deun, A., Rigouts, L., & de Jong, B. C. (2018). Isoniazid resistance levels of Mycobacterium tuberculosis can largely be predicted by high-confidence resistance-conferring mutations. *Scientific Reports*, *8*(1), 3246. https://doi.org/10.1038/s41598-018-21378-x

Li, H., Salinger, D. H., Everitt, D., Li, M., Del Parigi, A., Mendel, C., Nedelman, J. R., Parigi, A. Del, Mendel, C., & Nedelman, J. R. (2019). Long-Term Effects on QT Prolongation of Pretomanid Alone and in Combinations in Patients with Tuberculosis. *Antimicrobial Agents and Chemotherapy*, *63*(10). https://doi.org/10.1128/AAC

Lim, F. H., Lovering, A. M., Currie, A., & Jenkins, D. R. (2017). Linezolid and lactation: measurement of drug levels in breast milk and the nursing infant. *Journal of Antimicrobial Chemotherapy*, *72*(9), 2677–2678. http://academic.oup.com/jac/article/72/9/2677/3852242/Linezolid-and-lactation-measurement-of-drug-levels

Linguissi, L. S. G., Mayengue, P. I., Sidibé, A., Vouvoungui, J. C., Missontsa, M., Madzou-Laboum, I. K., Essassa, G. B., Oyakhirome, S., Frank, M., Penlap, V., & Ntoumi, F. (2014). Prevalence of national treatment algorithm defined smear positive pulmonary tuberculosis in HIV positive patients in Brazzaville, Republic of Congo. *BMC Research Notes*, *7*(1), 578. https://doi.org/10.1186/1756-0500-7-578

LOTTE, A., HATTON, F., PERDRIZET, S., & ROUILLON, A. (1964). A concurrent comparison of intermittent (twice-weekly) isoniazid plus streptomycin and daily isoniazid plus PAS in the domiciliary treatment of pulmonary tuberculosis. *Bulletin of the World Health Organization*, *31*(2), 247. /pmc/articles/PMC2555171/?report=abstract

Loveday, M., Hlangu, S., & Furin, J. (2020). Breastfeeding in women living with tuberculosis. *The International Journal of Tuberculosis and Lung Disease*, *24*(9), 880–891. https://doi.org/10.5588/ijtld.20.0122

Loveday, Marian, Hughes, J., Sunkari, B., Master, I., Hlangu, S., Reddy, T., Chotoo, S., Green, N., & Seddon, J. A. (2021). Maternal and Infant Outcomes among Pregnant Women Treated for Multidrug/Rifampicin-Resistant Tuberculosis in South Africa. *Clinical Infectious Diseases*, *72*(7), 1158–1168. https://doi.org/10.1093/cid/ciaa189

Ludden, T. M. (1991). Nonlinear Pharmacokinetics Clinical Implications. In *DRUG DISPOSITION Clin. Pharmacokinel* (Vol. 20, Issue 6). https://doi.org/10.2165/00003088-199120060-00001

Luetkemeyer, A. F., Rosenkranz, S. L., Lu, D., Grinsztejn, B., Sanchez, J., Ssemmanda, M., Sanne, I., Mcilleron, H., Havlir, D. V., & Haas, D. W. (2015). Combined effect of CYP2B6 and NAT2 genotype on plasma efavirenz exposure during rifampin-based antituberculosis therapy in the STRIDE study. *Clinical Infectious Diseases*, *60*(12), 1860–1863. https://doi.org/10.1093/cid/civ155

MacLean, E., Broger, T., Yerlikaya, S., Fernandez-Carballo, B. L., Pai, M., & Denkinger, C. M. (2019). A systematic review of biomarkers to detect active tuberculosis. *Nature Microbiology*, *4*(5), 748–758. https://doi.org/10.1038/s41564-019-0380-2

Maher, J. E., Goldenberg, R. L., Tamura, T., Cliver, S. P., Hoffman, H. J., Davis, R. O., & Boots, L. (1993). Albumin levels in pregnancy: a hypothesis—decreased levels of albumin are related to increased levels of alpha-fetoprotein. *Early Human Development*, *34*(3), 209–

215. https://doi.org/10.1016/0378-3782(93)90178-W

Mariappan, T. T., & Singh, S. (2003). Regional gastrointestinal permeability of rifampicin and isoniazid (alone and their combination) in the rat. *The International Journal of Tuberculosis and Lung Disease : The Official Journal of the International Union against Tuberculosis and Lung Disease*, *7*(8), 797–803. http://www.ncbi.nlm.nih.gov/pubmed/12921157

Marzolini, C., Telenti, A., Decosterd, L. A., Greub, G., Biollaz, J., & Buclin, T. (2001). Efavirenz plasma levels can predict treatment failure and central nervous system side effects in HIV-1-infected patients. *AIDS*, *15*(1), 71–75. https://doi.org/10.1097/00002030-200101050-00011

Mathad, J. S., Bhosale, R., Sangar, V., Mave, V., Gupte, N., Kanade, S., Nangude, A., Chopade, K., Suryavanshi, N., Deshpande, P., Kulkarni, V., Glesby, M. J., Fitzgerald, D., Bharadwaj, R., Sambarey, P., & Gupta, A. (2014). Pregnancy Differentially Impacts Performance of Latent Tuberculosis Diagnostics in a High-Burden Setting. *PLoS ONE*, *9*(3), e92308. https://doi.org/10.1371/journal.pone.0092308

McDonagh, E. M., Boukouvala, S., Aklillu, E., Hein, D. W., Altman, R. B., & Klein, T. E. (2014). PharmGKB summary. *Pharmacogenetics and Genomics*, *24*(8), 409–425. https://doi.org/10.1097/FPC.0000000000000062

McLeay, S. C., Vis, P., van Heeswijk, R. P. G. G., & Green, B. (2014). Population Pharmacokinetics of Bedaquiline (TMC207), a Novel Antituberculosis Drug. *Antimicrobial Agents and Chemotherapy*, *58*(9), 5315–5324. https://doi.org/10.1128/AAC.01418-13

Mehvar, R. (2018). Clearance concepts: Fundamentals and application to pharmacokinetic behavior of drugs. *Journal of Pharmacy and Pharmaceutical Sciences*, *21*(1S), 88s-102s. https://doi.org/10.18433/jpps29896

Metushi, I., Uetrecht, J., & Phillips, E. (2016). Mechanism of isoniazid-induced hepatotoxicity: then and now. *British Journal of Clinical Pharmacology*, *81*(6), 1030–1036. https://doi.org/10.1111/bcp.12885

Miller, J. (1980). Acute Isoniazid Poisoning in Childhood. *Archives of Pediatrics & Adolescent Medicine*, *134*(3), 290. https://doi.org/10.1001/archpedi.1980.02130150044011

Mirzayev, F., Viney, K., Linh, N. N., Gonzalez-Angulo, L., Gegia, M., Jaramillo, E., Zignol, M., & Kasaeva, T. (2021). World Health Organization recommendations on the treatment of drug-resistant tuberculosis, 2020 update. *European Respiratory Journal*, *57*(6), 2003300. https://doi.org/10.1183/13993003.03300-2020

Mitchison, D. A., & Selkon, J. B. (1956). The bactericidal activities of antituberculous drugs. *American Review of Tuberculosis*, *74*(2 Part 2), 109–116; discussion, 116–123. https://doi.org/10.1164/artpd.1956.74.2-2.109

Monedero-Recuero, I., Gegia, M., Wares, D. F., Chadha, S. S., & Mirzayev, F. (2021). Situational analysis of 10 countries with a high burden of drug-resistant tuberculosis 2 years post-UNHLM declaration: progress and setbacks in a changing landscape. *International Journal of Infectious Diseases*, *108*, 557–567. https://doi.org/10.1016/j.ijid.2021.06.022

Motsoaledi, A., & Matsotso, M. . (2019). *MULTI-DRUG RESISTANT TUBERCULOSIS: A POLICY FRAMEWORK ON DECENTRALISED AND DEINSTITUTIONALISED MANAGEMENT FOR SOUTH AFRICA*.

Mould, D., & Upton, R. (2012). Basic Concepts in Population Modeling, Simulation, and Model-Based Drug Development. *CPT: Pharmacometrics & Systems Pharmacology*, *1*(9), 6. https://doi.org/10.1038/psp.2012.4

Mould, D., & Upton, R. (2013). Basic Concepts in Population Modeling, Simulation, and Model-

Based Drug Development-Part 2: Introduction to Pharmacokinetic Modeling Methods. *CPT: Pharmacometrics & Systems Pharmacology*, *2*(4), 38. https://doi.org/10.1038/psp.2013.14

Mouton, J. W., Ambrose, P. G., Canton, R., Drusano, G. L., Harbarth, S., MacGowan, A., Theuretzbacher, U., & Turnidge, J. (2011). Conserving antibiotics for the future: New ways to use old and new drugs from a pharmacokinetic and pharmacodynamic perspective. *Drug Resistance Updates*, *14*(2), 107–117. https://doi.org/10.1016/j.drup.2011.02.005

Mouton, J. W., Muller, A. E., Canton, R., G. Giske, C., Kahlmeter, G., & Turnidge, J. (2018). MIC-based dose adjustment: facts and fables—authors' response. *Journal of Antimicrobial Chemotherapy*, *73*(9), 2585–2586. https://doi.org/10.1093/jac/dky195

Mrozikiewicz, P. M., Cascorbi, I., Brockmöller, J., & Roots, I. (1996). Determination and allelic allocation of seven nucleotide transitions within the arylamine N-acetyltransferase gene in the Polish population. *Clinical Pharmacology and Therapeutics*, *59*(4), 376–382. https://doi.org/10.1016/S0009-9236(96)90104-6

Muma, N., & Shi, H. (1968). *DEPARTMENT OF PHARMACOLOGY AND TOXICOLOGY Pharmacology and Toxicology Graduate Programs*. http://www.pharmtox.pharm.ku.edu/

Murray, J. F., Schraufnagel, D. E., & Hopewell, P. C. (2015). Treatment of tuberculosis: A historical perspective. *Annals of the American Thoracic Society*, *12*(12), 1749–1759. https://doi.org/10.1513/ANNALSATS.201509-632PS/SUPPL_FILE/DISCLOSURES.PDF

Nabisere, R., Musaazi, J., Denti, P., Aber, F., Lamorde, M., Dooley, K. E., Aarnoutse, R., Sloan, D. J., & Sekaggya-Wiltshire, C. (2020). Pharmacokinetics, SAfety/tolerability, and EFficacy of high-dose RIFampicin in tuberculosis-HIV co-infected patients on efavirenz- or dolutegravir-based antiretroviral therapy: Study protocol for an open-label, phase II clinical trial (SAEFRIF). *Trials*, *21*(1), 1–9. https://doi.org/10.1186/s13063-020-4132-7

Nachega, J. B., Uthman, O. A., Anderson, J., Peltzer, K., Wampold, S., Cotton, M. F., Mills, E. J., Ho, Y. S., Stringer, J. S. A., McIntyre, J. A., & Mofenson, L. M. (2012). Adherence to antiretroviral therapy during and after pregnancy in low-income, middle-income, and high-income countries: A systematic review and meta-analysis. *Aids*, *26*(16), 2039–2052. https://doi.org/10.1097/QAD.0b013e328359590f

Naidoo, A., Chirehwa, M., McIlleron, H., Naidoo, K., Essack, S., Yende-Zuma, N., Kimba-Phongi, E., Adamson, J., Govender, K., Padayatchi, N., & Denti, P. (2017). Effect of rifampicin and efavirenz on moxifloxacin concentrations when co-administered in patients with drug-susceptible TB. *Journal of Antimicrobial Chemotherapy*, *72*(5), 1441–1449. https://doi.org/10.1093/jac/dkx004

Nasiruddin, M., Neyaz, M. K., & Das, S. (2017). Nanotechnology-Based Approach in Tuberculosis Treatment. *Tuberculosis Research and Treatment*, *2017*, 1–12. https://doi.org/10.1155/2017/4920209

Nguyen, L. (2016). Antibiotic resistance mechanisms in M. tuberculosis: an update. *Archives of Toxicology*, *90*(7), 1585–1604. https://doi.org/10.1007/s00204-016-1727-6

Ngwalero, P., Brust, J. C., van Beek, S. W., Wasserman, S., Maartens, G., Meintjes, G., Joubert, A., Norman, J., Castel, S., Gandhi, N. R., Denti, P., McIlleron, H., Svensson, E. M., & Wiesner, L. (2021). Relationship between plasma and intracellular concentrations of bedaquiline and its M2 metabolite in South African patients with rifampin-resistant TB. *Antimicrobial Agents and Chemotherapy*. https://doi.org/10.1128/AAC.02399-20

Nielsen, E. I., & Friberg, L. E. (2013). Pharmacokinetic-Pharmacodynamic Modeling of

Antibacterial Drugs. *Pharmacological Reviews*, *65*(3), 1053–1090. https://doi.org/10.1124/pr.111.005769

O'Sullivan, D. M., McHugh, T. D., & Gillespie, S. H. (2010). Mapping the fitness of Mycobacterium tuberculosis strains: A complex picture. In *Journal of Medical Microbiology* (Vol. 59, Issue 12, pp. 1533–1535). Microbiology Society. https://doi.org/10.1099/jmm.0.019091-0

Ogasawara, K., Breder, C. D., Lin, D. H., & Alexander, G. C. (2018). Exposure– and Dose–response Analyses in Dose Selection and Labeling of FDA-approved Biologics. *Clinical Therapeutics*, *40*(1), 95-102.e2. https://doi.org/10.1016/j.clinthera.2017.11.012

Olagunju, A., Bolaji, O., Amara, A., Else, L., Okafor, O., Adejuyigbe, E., Oyigboja, J., Back, D., Khoo, S., & Owen, A. (2015). Pharmacogenetics of pregnancy-induced changes in efavirenz pharmacokinetics. *Clinical Pharmacology and Therapeutics*, *97*(3), 298–306. https://doi.org/10.1002/cpt.43

Olofsen, E., & Dahan, A. (2015). Using Akaike's information theoretic criterion in mixed-effects modeling of pharmacokinetic data: a simulation study. *F100Research*, *2*(71), 1–17. https://doi.org/10.12688/f1000research.2-71.v2

Orrell, C., Bienczak, A., Cohen, K., Bangsberg, D., Wood, R., Maartens, G., & Denti, P. (2016). Effect of mid-dose efavirenz concentrations and CYP2B6 genotype on viral suppression in patients on first-line antiretroviral therapy. *International Journal of Antimicrobial Agents*, *47*(6), 466–472. https://doi.org/10.1016/j.ijantimicag.2016.03.017

Ouyang, D. W., Shapiro, D. E., Lu, M., Brogly, S. B., French, A. L., Leighty, R. M., Thompson, B., Tuomala, R. E., & Hershow, R. C. (2009). Increased risk of hepatotoxicity in HIV-infected pregnant women receiving antiretroviral therapy independent of nevirapine exposure. *AIDS (London, England)*, *23*(18), 2425–2430. https://doi.org/10.1097/QAD.0b013e32832e34b1

Ozturk, Z., & Tatliparmak, A. (2017). Leprosy treatment during pregnancy and breastfeeding: A case report and brief review of literature. *Dermatologic Therapy*, *30*(1), e12414. https://doi.org/10.1111/DTH.12414

Parkin, D. P., Vandenplas, S., Botha, F. J. H., Vandenplas, M. L., Seifart, H. I., van Helden, P. D., Van Der Walt, B. J., Donald, P. R., & Van Jaarsveld, P. P. (1997). Trimodality of isoniazid elimination: Phenotype and genotype in patients with tuberculosis. *American Journal of Respiratory and Critical Care Medicine*, *155*(5), 1717–1722. https://doi.org/10.1164/ajrccm.155.5.9154882

Patin, E., Harmant, C., Kidd, K. K., Kidd, J., Froment, A., Mehdi, S. Q., Sica, L., Heyer, E., & Quintana-Murci, L. (2006). Sub-Saharan African coding sequence variation and haplotype diversity at the NAT2 gene. *Human Mutation*, *27*(7), 720. https://doi.org/10.1002/humu.9438

Peloquin, C. A., Jaresko, G. S., Yong, C. L., Keung, A. C. F., Bulpitt, A. E., & Jelliffe, R. W. (1997). Population pharmacokinetic modeling of isoniazid, rifampin, and pyrazinamide. *Antimicrobial Agents and Chemotherapy*, *41*(12), 2670–2679. https://doi.org/10.1128/AAC.41.12.2670

Pérez-Molina, J. A. (2002). Safety and Tolerance of Efavirenz in Different Antiretroviral Regimens: Results from a National Multicenter Prospective Study in 1,033 HIV-Infected Patients. *HIV Clinical Trials*, *3*(4), 279–286. https://doi.org/10.1310/3Q91-YT2D-BUT4-8HN6

Phillips, A. N., Bansi-Matharu, L., Venter, F., Havlir, D., Pozniak, A., Kuritzkes, D. R., Wensing, A., Lundgren, J. D., Pillay, D., Mellors, J., Cambiano, V., Jahn, A., Apollo, T., Mugurungi,

O., Ripin, D., Da Silva, J., Raizes, E., Ford, N., Siberry, G. K., … Bertagnolio, S. (2020). Updated assessment of risks and benefits of dolutegravir versus efavirenz in new antiretroviral treatment initiators in sub-Saharan Africa: modelling to inform treatment guidelines. *The Lancet HIV*, *7*(3), e193–e200. https://doi.org/10.1016/S2352-3018(19)30400-X

Phillips, I. R., & Shephard, E. A. (2017). Drug metabolism by flavin-containing monooxygenases of human and mouse. *Expert Opinion on Drug Metabolism & Toxicology*, *13*(2), 167–181. https://doi.org/10.1080/17425255.2017.1239718

Piacenti, F. J. (2006). An Update and Review of Antiretroviral Therapy. *Pharmacotherapy*, *26*(8), 1111–1133. https://doi.org/10.1592/phco.26.8.1111

Pinheiro, E. A., & Stika, C. S. (2020). Drugs in pregnancy: Pharmacologic and physiologic changes that affect clinical care. *Seminars in Perinatology*, *44*(3), 151221. https://doi.org/10.1016/j.semperi.2020.151221

Piubello, A., Harouna, S. H., Souleymane, M. B., Boukary, I., Morou, S., Daouda, M., Hanki, Y., & Van Deun, A. (2014). High cure rate with standardised short-course multidrugresistant tuberculosis treatment in Niger: No relapses. *International Journal of Tuberculosis and Lung Disease*, *18*(10), 1188–1194. https://doi.org/10.5588/ijtld.13.0075

Poole, N. F., & Meyer, A. E. (1960). Stability of Isoniazid in Aqueous Solutions and Plasma. *Experimental Biology and Medicine*, *104*(4), 560–562. https://doi.org/10.3181/00379727-104-25907

Price Evans, D. A., Manley, K. A., & McKusick, V. A. (1960). Genetic Control of Isoniazid Metabolism in Man. *British Medical Journal*, *2*(5197), 485. https://doi.org/10.1136/BMJ.2.5197.485

Prideaux, B., Via, L. E., Zimmerman, M. D., Eum, S., Sarathy, J., O'Brien, P., Chen, C., Kaya, F., Weiner, D. M., Chen, P. Y., Song, T., Lee, M., Shim, T. S., Cho, J. S., Kim, W., Cho, S. N., Olivier, K. N., Barry, C. E., & Dartois, V. (2015). The association between sterilizing activity and drug distribution into tuberculosis lesions. *Nature Medicine*, *21*(10), 1223–1227. https://doi.org/10.1038/nm.3937

Pym, A. S., Diacon, A. H., Tang, S.-J., Conradie, F., Danilovits, M., Chuchottaworn, C., Vasilyeva, I., Andries, K., Bakare, N., De Marez, T., Haxaire-Theeuwes, M., Lounis, N., Meyvisch, P., Van Baelen, B., van Heeswijk, R. P. G., & Dannemann, B. (2016). Bedaquiline in the treatment of multidrug- and extensively drug-resistant tuberculosis. *European Respiratory Journal*, *47*(2), 564–574. https://doi.org/10.1183/13993003.00724-2015

Qasqas, S. A., Mcpherson, C., Frishman, W. H., & Elkayam, U. (2004). Cardiovascular Pharmacotherapeutic Considerations During Pregnancy and Lactation CLINICAL PHARMACOLOGY. *Cardiology in Review*, *12*, 201–221. https://doi.org/10.1097/01.crd.0000102420.62200.e1

Ranjan, R., Srivastava, A., Bharti, R., Roy, T., Verma, S., Ray, L., & Misra, A. (2019). Preclinical development of inhalable D-cycloserine and ethionamide to overcome pharmacokinetic interaction and enhance efficacy against mycobacterium tuberculosis. *Antimicrobial Agents and Chemotherapy*, *63*(6). https://doi.org/10.1128/AAC.00099-19

Rao, K. V, Kailasam, S., Menon, N. K., & Radhakrishna, S. (1971). Inactivation of isoniazid by condensation in a syrup preparation. *Bulletin of the World Health Organization*, *45*(5), 625–632. /pmc/articles/PMC2427966/?report=abstract

Rawat, R., Whitty, A., & Tonge, P. J. (2003). The isoniazid-NAD adduct is a slow, tight-binding inhibitor of InhA, the Mycobacterium tuberculosis enoyl reductase: adduct affinity and drug resistance. *Proceedings of the National Academy of Sciences of the United States of*

America, *100*(24), 13881–13886. https://doi.org/10.1073/pnas.2235848100

Review on Antimicrobial Resistance. (2014). *Antimicrobial Resistance: Tackling a crisis for the health and wealth of nations*.

Rieder, H. L., & Van Deun, A. (2017). Rationale for high-dose isoniazid in the treatment of multidrug-resistant tuberculosis. *The International Journal of Tuberculosis and Lung Disease*, *21*(1), 123–124. https://doi.org/10.5588/ijtld.16.0619

Robson, J. M., & Sullivan, F. M. (1963). Antituberculosis drugs. *Pharmacological Reviews*, *15*, 169–223. http://www.ncbi.nlm.nih.gov/pubmed/13974496

Rockwood, N., Du Bruyn, E., Morris, T., & Wilkinson, R. J. (2016). Assessment of treatment response in tuberculosis. *Expert Review of Respiratory Medicine*, *10*(6), 643–654. https://doi.org/10.1586/17476348.2016.1166960

Rotger, M., Colombo, S., Furrer, H., Bleiber, G., Buclin, T., Lee, B. L., Keiser, O., Biollaz, J., Décosterd, L., Telenti, A., Battegay, M., Bernard, M. C., Bernasconi, E., Bucher, H., Burgisser, P., Egger, M., Erb, P., Fierz, W., Flepp, M., … Weber, R. (2005). Influence of CYP2B6 polymorphism on plasma and intracellular concentrations and toxicity of efavirenz and nevirapine in HIV-infected patients. *Pharmacogenetics and Genomics*, *15*(1), 1–5. https://doi.org/10.1097/01213011-200501000-00001

Rotger, M., Csajka, C., & Telenti, A. (2006). Genetic, ethnic, and gender differences in the pharmacokinetics of antiretroviral agents. *Current HIV/AIDS Reports*, *3*(3), 118–125. https://doi.org/10.1007/BF02696655

Royal pharmaceurical society. (2011). *Pharmaceutical Issues when Crushing, Opening or Splitting Oral Dosage Forms*. http://www.rpharms.com/best-practice/specials.asp

Rozwarski, D. A. (1998). Modification of the NADH of the Isoniazid Target (InhA) from Mycobacterium tuberculosis. *Science*, *279*(5347), 98–102. https://doi.org/10.1126/science.279.5347.98

Saag, M. S., Gandhi, R. T., Hoy, J. F., Landovitz, R. J., Thompson, M. A., Sax, P. E., Smith, D. M., Benson, C. A., Buchbinder, S. P., del Rio, C., Eron, J. J., Fätkenheuer, G., Günthard, H. F., Molina, J.-M., Jacobsen, D. M., & Volberding, P. A. (2020). Antiretroviral Drugs for Treatment and Prevention of HIV Infection in Adults. *JAMA*, *324*(16), 1651. https://doi.org/10.1001/jama.2020.17025

Sabbagh, A., Darlu, P., Crouau-Roy, B., & Poloni, E. S. (2011). Arylamine N-Acetyltransferase 2 (NAT2) Genetic Diversity and Traditional Subsistence: A Worldwide Population Survey. *PLoS ONE*, *6*(4), e18507. https://doi.org/10.1371/journal.pone.0018507

Sabbagh, A., Darlu, P., & Vidaud, M. (2009). Evaluating NAT2PRED for inferring the individual acetylation status from unphased genotype data. *BMC Medical Genetics*, *10*(1), 148. https://doi.org/10.1186/1471-2350-10-148

Sarathy, J. P., Gruber, G., & Dick, T. (2019). Re-Understanding the Mechanisms of Action of the Anti-Mycobacterial Drug Bedaquiline. *Antibiotics*, *8*(4). https://doi.org/10.3390/ANTIBIOTICS8040261

Savic, R. M., Jonker, D. M., Kerbusch, T., & Karlsson, M. O. (2007). Implementation of a transit compartment model for describing drug absorption in pharmacokinetic studies. *Journal of Pharmacokinetics and Pharmacodynamics*, *34*(5), 711–726. https://doi.org/10.1007/s10928-007-9066-0

Schalkwijk, S., Greupink, R., & Burger, D. (2017). Free dug concentrations in pregnancy: Bound to measure unbound? *British Journal of Clinical Pharmacology*, *83*(12), 2595–2598. https://onlinelibrary.wiley.com/doi/full/10.1111/bcp.13432

Schatz, A., Bugle, E., & Waksman, S. A. (1944). Streptomycin, a Substance Exhibiting Antibiotic

Activity Against Gram-Positive and Gram-Negative Bacteria.* . *Experimental Biology and Medicine*, *55*(1), 66–69. https://doi.org/10.3181/00379727-55-14461

Schluger, N. W. (2021). Using Isoniazid More Safely and More Effectively: The Time Is Now. *American Journal of Respiratory and Critical Care Medicine*, *204*(11), 1248–1250. https://doi.org/10.1164/rccm.202108-1938ED

Sekaggya-Wiltshire, C., Chirehwa, M., Musaazi, J., Von Braun, A., Buzidye, A., Fehr, J., Kambugu, A., Castelnuovo, B., Lamorde, M., & Denti, P. (2018). Low anti-tuberculosis drug concentrations in HIV-Tuberculosis co-infected adults with low body weight. *Internantional Workshop on Clinical Pharmacology of Tuberculosis Drugs*, 51–52. http://regist2.virology-education.com/abstractbook/2018/abstractbook_11tbpk.pdf

Sekaggya Wiltshire, C., Lamorde, M., Scherrer, A., Musaazi, J., Corti, N., Allan, B., Nakijoba, R., Nalwanga, D., Henning, L., Von Braun, A., Okware, S., Castelnuovo, B., Kambugu, A., & Fehr, J. (2014). Low isoniazid and rifampicin concentrations in TB/HIV co-infected patients in Uganda. *Journal of the International AIDS Society*, *17*, 19585. https://doi.org/10.7448/IAS.17.4.19585

Selwyn, P. A., Hartel, D., Lewis, V. A., Schoenbaum, E. E., Vermund, S. H., Klein, R. S., Walker, A. T., & Friedland, G. H. (1989). A Prospective Study of the Risk of Tuberculosis among Intravenous Drug Users with Human Immunodeficiency Virus Infection. *New England Journal of Medicine*, *320*(9), 545–550. https://doi.org/10.1056/NEJM198903023200901

Seng, K.-Y., Hee, K.-H., Soon, G.-H., Chew, N., Khoo, S. H., & Lee, L. S.-U. (2015). Population pharmacokinetic analysis of isoniazid, acetylisoniazid, and isonicotinic acid in healthy volunteers. *Antimicrobial Agents and Chemotherapy*, *59*(11), 6791–6799. https://doi.org/10.1128/AAC.01244-15

Sheiner, L. B., Stanski, D. R., Vozeh, S., Miller, R. D., & Ham, J. (1979). Simultaneous modeling of pharmacokinetics and pharmacodynamics: Application to *d* -tubocurarine. *Clinical Pharmacology & Therapeutics*, *25*(3), 358–371. https://doi.org/10.1002/cpt1979253358

Singh, N., & Perfect, J. R. (2007). Immune Reconstitution Syndrome and Exacerbation of Infections after Pregnancy. *Clinical Infectious Diseases*, *45*(9), 1192–1199. https://doi.org/10.1086/522182

Singh, R., Dwivedi, S. P., Gaharwar, U. S., Meena, R., Rajamani, P., & Prasad, T. (2020). Recent updates on drug resistance in Mycobacterium tuberculosis. *Journal of Applied Microbiology*, *128*(6), 1547–1567. https://doi.org/10.1111/jam.14478

Sloan, D. J., Mwandumba, H. C., Garton, N. J., Khoo, S. H., Butterworth, A. E., Allain, T. J., Heyderman, R. S., Corbett, E. L., Barer, M. R., & Davies, G. R. (2015). Pharmacodynamic Modeling of Bacillary Elimination Rates and Detection of Bacterial Lipid Bodies in Sputum to Predict and Understand Outcomes in Treatment of Pulmonary Tuberculosis. *Clinical Infectious Diseases: An Official Publication of the Infectious Diseases Society of America*, *61*(1), 1. https://doi.org/10.1093/CID/CIV195

Smith, T., Wolff, K. A., & Nguyen, L. (2012). Molecular Biology of Drug Resistance in Mycobacterium tuberculosis. In *Current topics in microbiology and immunology* (Vol. 374, pp. 53–80). NIH Public Access. https://doi.org/10.1007/82_2012_279

Snyder, B., Polasek, T. M., & Doogue, M. P. (2012). Drug interactions: principles and practice. *Australian Prescriber*, *35*(3), 85–88. https://doi.org/10.18773/austprescr.2012.037

Southwood, R. L., Fleming, V. H., & Huckaby, G. (2018). *Concepts in clinical pharmacokinetics* (R. Bloom, K. Eckles, J. Hershey, & D. Wade (eds.); Seventh Ed). American Society of Health-System Pharmacists.

Squibb, B.-M. (2010). *SUSTIVA ® (efavirenz) capsules and tablets. Full prescribing information.*

Statistics South Africa. (2021). *STATISTICAL RELEASE P0302: Mid-year population estimates 2021*. www.statssa.gov.za,info@statssa.gov.za,Tel+27123108911

Stewart, G. R., Robertson, B. D., & Young, D. B. (2003). Tuberculosis: a problem with persistence. *Nature Reviews Microbiology 2003 1:2*, *1*(2), 97–105. https://doi.org/10.1038/nrmicro749

Strydom, N., Gupta, S. V., Fox, W. S., Via, L. E., Bang, H., Lee, M., Eum, S., Shim, T., Barry, C. E., Zimmerman, M., Dartois, V., & Savic, R. M. (2019). Tuberculosis drugs' distribution and emergence of resistance in patient's lung lesions: A mechanistic model and tool for regimen and dose optimization. *PLOS Medicine*, *16*(4), e1002773. https://doi.org/10.1371/journal.pmed.1002773

Sturgill-Koszycki, S., Schlesinger, P., Chakraborty, P., Haddix, P., Collins, H., Fok, A., Allen, R., Gluck, S., Heuser, J., & Russell, D. (1994). Lack of acidification in Mycobacterium phagosomes produced by exclusion of the vesicular proton-ATPase. *Science*, *263*(5147), 678–681. https://doi.org/10.1126/science.8303277

Sturkenboom, M. G. G., van der Lijke, H., Jongedijk, E. M., Th. Kok, W., Greijdanus, B., Uges1, D. R. A., & Alffenaar, J.-W. C. (2015). Quantification of isoniazid, pyrazinamide and ethambutol in serum using liquid chromatography-tandem mass spectrometry. *JOURNAL OF APPLIED BIOANALYSIS*, *1*(3), 89–98. https://pdfs.semanticscholar.org/244e/c3af63976551588db5b4b72aba9576010599.pdf

Svensson, E. M., Aweeka, F., Park, J.-G., Marzan, F., Dooley, K. E., & Karlsson, M. O. (2013). Model-Based Estimates of the Effects of Efavirenz on Bedaquiline Pharmacokinetics and Suggested Dose Adjustments for Patients Coinfected with HIV and Tuberculosis. *Antimicrobial Agents and Chemotherapy*, *57*(6), 2780–2787. https://doi.org/10.1128/AAC.00191-13

Svensson, E. M., Murray, S., Karlsson, M. O., & Dooley, K. E. (2015). Rifampicin and rifapentine significantly reduce concentrations of bedaquiline, a new anti-TB drug. *Journal of Antimicrobial Chemotherapy*, *70*(4), 1106–1114. https://doi.org/10.1093/jac/dku504

Svensson, E., van der Walt, J.-S., Barnes, K. I., Cohen, K., Kredo, T., Huitema, A., Nachega, J. B., Karlsson, M. O., & Denti, P. (2012). Integration of data from multiple sources for simultaneous modelling analysis: experience from nevirapine population pharmacokinetics. *British Journal of Clinical Pharmacology*, *74*(3), 465–476. https://doi.org/10.1111/j.1365-2125.2012.04205.x

Svensson, R. J., Svensson, E. M., Aarnoutse, R. E., Diacon, A. H., Dawson, R., Gillespie, S. H., Moodley, M., Boeree, M. J., & Simonsson, U. S. H. (2018). Greater Early Bactericidal Activity at Higher Rifampicin Doses Revealed by Modeling and Clinical Trial Simulations. *The Journal of Infectious Diseases*, *218*(6), 991–999. https://doi.org/10.1093/infdis/jiy242

Timmins, G. S., & Deretic, V. (2006). Mechanisms of action of isoniazid. *Molecular Microbiology*, *62*(5), 1220–1227. https://doi.org/10.1111/j.1365-2958.2006.05467.x

Torfs, E., Piller, T., Cos, P., & Cappoen, D. (2019). Opportunities for overcoming mycobacterium tuberculosis drug resistance: Emerging mycobacterial targets and host-directed therapy. *International Journal of Molecular Sciences*, *20*(12), 2868. https://doi.org/10.3390/ijms20122868

Toutoungi, M., Carroll, R. A., Enrico, J.-F., & Perey, L. (1985). CHEESE, WINE, AND ISONIAZID. *The Lancet*, *326*(8456), 671. https://doi.org/10.1016/S0140-6736(85)90038-8

Tran, J. H., & Montakantikul, P. (1998). The Safety of Antituberculosis Medications During

Breastfeeding. *Journal of Human Lactation*, *14*(4), 337–340. https://doi.org/10.1177/089033449801400427

Tsutsumi, K., Kotegawa, T., Matsuki, S., Tanaka, Y., Ishii, Y., Kodama, Y., Kuranari, M., Miyakawa, I., & Nakano, S. (2001). The effect of pregnancy on cytochrome P4501A2, xanthine oxidase, and N-acetyltransferase activities in humans. *Clinical Pharmacology and Therapeutics*, *70*(2), 121–125. https://doi.org/10.1067/mcp.2001.116495

Twisk, J. W. R. (2013). *Applied Longitudinal Data Analysis for Epidemiology*. Cambridge University Press. https://doi.org/10.1017/CBO9781139342834

UNAIDS. (2020a). *Global AIDS Update - seizing the moment -Tackling entrenched inequalities to end epidemics*.

UNAIDS. (2020b). *Tuberculosis and HIV — Progress towards the 2020 target*.

UNAIDS. (2021). *UNAIDS fact sheet - global and reginal statistics on the status of the AIDS epidemic*.

Unissa, A. N., Subbian, S., Hanna, L. E., & Selvakumar, N. (2016). Overview on mechanisms of isoniazid action and resistance in Mycobacterium tuberculosis. *Infection, Genetics and Evolution*, *45*, 474–492. https://doi.org/10.1016/J.MEEGID.2016.09.004

Upton, R., & Mould, D. (2014). Basic Concepts in Population Modeling, Simulation, and Model-Based Drug Development: Part 3-Introduction to Pharmacodynamic Modeling Methods. *CPT: Pharmacometrics & Systems Pharmacology*, *3*(1), 88. https://doi.org/10.1038/psp.2013.71

Upton, R. N., & Mould, D. R. D. R. (2014). Basic concepts in population modeling, simulation, and Model-Based drug development: Part 3—Introduction to pharmacodynamic modeling methods. *CPT: Pharmacometrics & Systems Pharmacology*, *3*(1), 1–16. https://doi.org/10.1038/psp.2013.71

van Heeswijk, R. P. G., Dannemann, B., & Hoetelmans, R. M. W. (2014). Bedaquiline: a review of human pharmacokinetics and drug-drug interactions. *Journal of Antimicrobial Chemotherapy*, *69*(9), 2310–2318. https://doi.org/10.1093/jac/dku171

Verma, R., Patil, S., Zhang, N., Moreira, F. M. F., Vitorio, M. T., Santos, A. da S., Wallace, E., Gnanashanmugam, D., Persing, D. H., Savic, R. M., Croda, J., & Andrews, J. R. (2021). A Rapid Pharmacogenomic Assay to Detect *NAT2* Polymorphisms and Guide Isoniazid Dosing for Tuberculosis Treatment. *American Journal of Respiratory and Critical Care Medicine*, *204*(11), 1317–1326. https://doi.org/10.1164/rccm.202103-0564OC

Vilchèze, C., & Jacobs JR., W. R. (2014). Resistance to Isoniazid and Ethionamide in Mycobacterium tuberculosis : Genes, Mutations, and Causalities. *Microbiology Spectrum*, *2*(4). https://doi.org/10.1128/microbiolspec.MGM2-0014-2013

Vo, H., Jung, J., Kim, T., & Shin, S. (2017). Development of Statistical Pharmacokinetic Modeling and Analysis Methodologies. In *International Journal of Conceptions on Computing and Information Technology* (Vol. 5, Issue 1). http://wairco.org/IJCCIT/July2017Paper9.pdf

Vocat, A., Hartkoorn, R. C., Lechartier, B., Zhang, M., Dhar, N., Cole, S. T., & Sala, C. (2015). Bioluminescence for Assessing Drug Potency against Nonreplicating Mycobacterium tuberculosis. *Antimicrobial Agents and Chemotherapy*, *59*(7), 4012–4019. https://doi.org/10.1128/AAC.00528-15

von Wintersdorff, C. J. H., Penders, J., van Niekerk, J. M., Mills, N. D., Majumder, S., van Alphen, L. B., Savelkoul, P. H. M., & Wolffs, P. F. G. (2016). Dissemination of Antimicrobial Resistance in Microbial Ecosystems through Horizontal Gene Transfer. *Frontiers in Microbiology*, *7*(7), 1585–1604. https://doi.org/10.3389/fmicb.2016.00173

Walmsley, S., Baumgarten, A., Berenguer, J., Felizarta, F., Florence, E., Khuong-Josses, M.-A., Kilby, J. M., Lutz, T., Podzamczer, D., Portilla, J., Roth, N., Wong, D., Granier, C., Wynne, B., & Pappa, K. (2015). Brief Report. *JAIDS Journal of Acquired Immune Deficiency Syndromes*, *70*(5), 515–519. https://doi.org/10.1097/QAI.0000000000000790

Wang, J., Sönnerborg, A., Rane, A., Josephson, F., Lundgren, S., Ståhle, L., & Ingelman-Sundberg, M. (2006). Identification of a novel specific CYP2B6 allele in Africans causing impaired metabolism of the HIV drug efavirenz. *Pharmacogenetics and Genomics*, *16*(3), 191–198. https://doi.org/10.1097/01.fpc.0000189797.03845.90

Wang, P.-Y., Xie, S.-Y., Hao, Q., Zhang, C., & Jiang, B.-F. (2012). *NAT2* polymorphisms and susceptibility to anti-tuberculosis drug-induced liver injury: a meta-analysis [Review article]. *The International Journal of Tuberculosis and Lung Disease*, *16*(5), 589–595. https://doi.org/10.5588/ijtld.11.0377

Warren, R. M., Streicher, E. M., Gey van Pittius, N. C., Marais, B. J., van der Spuy, G. D., Victor, T. C., Sirgel, F., Donald, P. R., & van Helden, P. D. (2009). The clinical relevance of Mycobacterial pharmacogenetics. *Tuberculosis*, *89*(3), 199–202. https://doi.org/10.1016/j.tube.2009.03.001

Wen, Xia, Wang, J.-S., Neuvonen, P. J., & Backman, J. T. (2002). Isoniazid is a mechanism-based inhibitor of cytochrome P450 1A2, 2A6, 2C19 and 3A4 isoforms in human liver microsomes. *European Journal of Clinical Pharmacology*, *57*(11), 799–804. https://doi.org/10.1007/s00228-001-0396-3

Wen, Xuesong, Gehring, R., Stallbaumer, A., Riviere, J. E., & Volkova, V. V. (2016). Limitations of MIC as sole metric of pharmacodynamic response across the range of antimicrobial susceptibilities within a single bacterial species. *Scientific Reports*, *6*(1), 1–8. https://doi.org/10.1038/srep37907

Werely, C. J., Donald, P. R., & van Helden, P. D. (2007). NAT2 polymorphisms and their influence on the pharmacology and toxicity of isoniazid in TB patients. *Personalized Medicine*, *4*(2), 123–131. https://doi.org/10.2217/17410541.4.2.123

Westin, A. A., Reimers, A., & Spigset, O. (2018). Should pregnant women receive lower or higher medication doses? *Tidsskrift for Den Norske Laegeforening : Tidsskrift for Praktisk Medicin, Ny Raekke*, *138*(17). https://doi.org/10.4045/TIDSSKR.18.0065

WHO. (2017). *TUBERCULOSIS REPORT 2017 GLOBAL*. http://apps.who.int/bookorders.

WHO. (2019). *WHO consolidated guidelines on drug-resistant tuberculosis treatment*.

WHO. (2020a). *GLOBAL TUBERCULOSIS REPORT 2020*. http://apps.who.int/bookorders.

WHO. (2020b). *Meeting report of the WHO expert consultation on the definition of extensively drug-resistant tuberculosis, Meeting report of the WHO expert consultation on the definition of extensively drug-resistant tuberculosis*. http://apps.who.int/bookorders.

WHO. (2020c). *WHO consolidated guidelines on tuberculosis. Module 4, Treatment : drug-resistant tuberculosis treatment.* https://www.who.int/publications/i/item/9789240007048

WHO. (2021a). *CONSOLIDATED GUIDELINES ON HIV PREVENTION, TESTING, TREATMENT, SERVICE DELIVERY AND MONITORING: RECOMMENDATIONS FOR A PUBLIC HEALTH APPROACH*. http://apps.who.int/bookorders.

WHO. (2021b). *Global progress report on HIV, viral hepatitis and sexually transmitted infections, 2021*.

Wilkins, J. J., Langdon, G., McIlleron, H., Pillai, G., Smith, P. J., & Simonsson, U. S. H. (2011). Variability in the population pharmacokinetics of isoniazid in South African tuberculosis patients. *British Journal of Clinical Pharmacology*, *72*(1), 51–62.

https://doi.org/10.1111/j.1365-2125.2011.03940.x
Wilson, J. T. (1983). Determinants and Consequences of Drug Excretion in Breast Milk. *Drug Metabolism Reviews*, *14*(4), 619–652. https://doi.org/10.3109/03602538308991402
Winckler, J. L., Schaaf, H. S., Draper, H. R., McIlleron, H., Norman, J., van der Laan, L. E., Wiesner, L., Donald, P. R., Hesseling, A. C., & Garcia-Prats, A. J. (2021). Pharmacokinetics of high-dose isoniazid in children affected by multidrug-resistant TB. *The International Journal of Tuberculosis and Lung Disease*, *25*(11), 896–902. https://doi.org/10.5588/ijtld.20.0870
Winder, F. (1982). *Mode of action of the antimycobacterial agents and associated aspects of the molecular biology of mycobacteria: The Biology of Mycobacteria.* (C. Ratledge & J. Stanford (eds.)). Academic Press.
Wood, A. J. J., & Iseman, M. D. (1993). Treatment of Multidrug-Resistant Tuberculosis. *New England Journal of Medicine*, *329*(11), 784–791. https://doi.org/10.1056/NEJM199309093291108
World Health Organization. (2016). *Frequently asked questions about the implementation of the new WHO recommendation on the use of the shorter MDR-TB regimen under programmatic conditions*. https://www.who.int/tb/areas-of-work/drug-resistant-tb/treatment/FAQshorter_MDR_regimen.pdf
World Health Organization. (2018). *Latent tuberculosis infection Updated and consolidated guidelines for programmatic management*. https://www.who.int/tb/publications/2018/latent-tuberculosis-infection/en/
Wright, D. F. B., Winter, H. R., & Duffull, S. B. (2011). Understanding the time course of pharmacological effect: A PKPD approach. *British Journal of Clinical Pharmacology*, *71*(6), 815–823. https://doi.org/10.1111/j.1365-2125.2011.03925.x
Wright, J. M., Stokes, E. F., & Sweeney, V. P. (1982). Isoniazid-Induced Carbamazepine Toxicity and Vice Versa. *New England Journal of Medicine*, *307*(21), 1325–1327. https://doi.org/10.1056/NEJM198211183072107
Yang, J., Jamei, M., Yeo, K. R., Rostami-Hodjegan, A., & Tucker, G. T. (2007). Misuse of the well-stirred model of hepatic drug clearance. In *Drug Metabolism and Disposition* (Vol. 35, Issue 3, pp. 501–502). https://doi.org/10.1124/dmd.106.013359
Zabost, A., Brzezińska, S., Kozińska, M., Błachnio, M., Jagodziński, J., Zwolska, Z., & Augustynowicz-Kopeć, E. (2013). Correlation of N-acetyltransferase 2 genotype with isoniazid acetylation in polish tuberculosis patients. *BioMed Research International*, *2013*. https://doi.org/10.1155/2013/853602
Zanger, U. M., & Klein, K. (2013). Pharmacogenetics of cytochrome P450 2B6 (CYP2B6): Advances on polymorphisms, mechanisms, and clinical relevance. In *Frontiers in Genetics* (Vol. 4, Issue MAR). https://doi.org/10.3389/fgene.2013.00024
Zhang, L., Beal, S. L., & Sheiner, L. B. (2003). Simultaneous vs. Sequential Analysis for Population PK/PD Data I: Best-Case Performance. *Journal of Pharmacokinetics and Pharmacodynamics*, *30*(6), 387–404. https://doi.org/10.1023/B:JOPA.0000012998.04442.1f
Zhang, Y., Yew, W. W., & Barer, M. R. (2012). Targeting persisters for tuberculosis control. *Antimicrobial Agents and Chemotherapy*, *56*(5), 2223–2230. https://doi.org/10.1128/AAC.06288-11
Zhang, Y., & Young, D. (1994). Molecular genetics of drug resistance in Mycobacterium tuberculosis. *Journal of Antimicrobial Chemotherapy*, *34*(3), 313–319. https://doi.org/10.1093/jac/34.3.313

Zhou, Y., Ingelman-Sundberg, M., & Lauschke, V. M. (2017). Worldwide Distribution of Cytochrome P450 Alleles: A Meta-analysis of Population-scale Sequencing Projects. *Clinical Pharmacology and Therapeutics*, *102*(4), 688–700. https://doi.org/10.1002/cpt.690

Appendix 1: NONMEM scripts

Final NONMEM scripts for results presented in chapter 3 - Isoniazid

```
$SIZES      MAXFCN=100000000

$PROBLEM    INH-IMPAACT

$INPUT ID STUDY=DROP VISIT_ID=DROP DV EFVCONC=DROP DRUG_NAME=DROP FIXED_IN_R=DROP
VISIT DATETIME=DROP MDV EVID WHAT=DROP OCC SS=DROP II=DROP OCCEFV=DROP
EFVPROBLEM=DROP INHPROBLEM INHDOSE=AMT EFVDOSE=DROP DAT2=DROP TIME NWEIGHT
HEMO WBC ANC PLAT AGE RACE SITE GAGE CREATINE HEIGHT ARM EFVTIME=DROP INHTIME=DROP
POSTWEEK VPCEFV=DROP VPCINH BLQEFV=DROP BLQ CYP2 NAT CYP2A REGIMEN=DROP DAYSEFV
RCOPIES EFV INH DOSMISS DOSMISS_EFV=DROP PILLPERC ADHEREPERC CMT FLAG NWT NREGIME
WEIGHT

$DATA      PEFV1.csv IGNORE=# IGNORE=(INHPROBLEM.EQ.1)

;$ABBREVIATED COMRES=2

$SUBROUTINE ADVAN6 TOL=9 ;TOL is the precision to solve differential equations

ATOL=9 ; absolute tolerance,10^ATOL of your dose unit. A lower value makes the model run faster

$MODEL      NCOMPARTMENTS=3 COMP=(ABS DEFDOSE) COMP=(CENTRAL) COMP=(PERI)

$PK

A_0(1)=0.000001

A_0(2)=0.000001 ; An average steady state value

A_0(3)=0.000001

IF (AMT.GT.0.OR.EVID.GE.3) THEN

        TDOSE=TIME

        TAD=0

ENDIF

TAD=TIME-TDOSE
```

```
; ---------- BOV
BOVCL = ETA(7)
IF(VISIT.EQ.2) BOVCL = ETA(8)
BOVV = ETA (9)
IF(VISIT.EQ.2) BOVV = ETA(10)
BOVKA=ETA(11)
IF(OCC.EQ.2)  BOVKA=ETA(12)
IF(OCC.EQ.3)  BOVKA=ETA(13)
IF(OCC.EQ.4)  BOVKA=ETA(14)
BOVBIO=ETA(15)
IF(OCC.EQ.2)  BOVBIO=ETA(16)
IF(OCC.EQ.3)  BOVBIO=ETA(17)
IF(OCC.EQ.4)  BOVBIO=ETA(18)
BOVMTT = ETA(19)
IF(OCC.EQ.2)  BOVMTT=ETA(20)
IF(OCC.EQ.3)  BOVMTT=ETA(21)
IF(OCC.EQ.4)  BOVMTT=ETA(22)
; ------- BSV
BSVCL   = ETA(1)
BSVV   = ETA(2)
BSVKA   = ETA(3)
BSVBIO = ETA(4)
BSVV3 = ETA(5)
BSVQ = ETA(6)
; ---------- Calculation of Fat-free Mass
; These formulas require WT in KG and HT in m !!!
```

```
;--------- IMPUTING MISSING WEIGHT
IF (WEIGHT.NE.999) THEN
        WT = WEIGHT
 ELSE
        WT = 67
 ENDIF
 IF (HEIGHT.NE.-99) THEN
        HT = HEIGHT
 ELSE
        HT = 158
 ENDIF
; Conversion from cm to m
HTM = HT/100
;IF (SEX.EQ.0) THEN  ; female
        WHSMAX=37.99
 WHS50=35.98
;ELSE       ;males
        ;WHSMAX=42.92
        ;WHS50=30.93
;ENDIF
HTM2 = HTM**2
FFM = (WHSMAX*HTM2*WT)/(WHS50*HTM2+WT)
FAT = WT-FFM
; ------- Typical values of covariates
TVWT = 67
TVFAT = 28
```

```
TVFFM = 39

;--------- Allometric scaling and covariates

ALLMCL_WT = (WT/TVWT)**0.75

ALLMV_WT = (WT/TVWT)

ALLMCL_FAT = (FAT/TVFAT)**0.75

ALLMV_FAT = (FAT/TVFAT)

ALLMCL_FFM = (FFM/TVFFM)**0.75

ALLMV_FFM = (FFM/TVFFM)

;           Allometry for liver

ALLMCL_WT_HEP = (WT/70)**0.75

ALLMV_WT_HEP = (WT/70)

ALLMCL_FFM_HEP = (WT/56.1)**0.75

ALLMV_FFM_HEP = (WT/56.1)

; --------------Clearance adjusted to NAT2

P_NAT = NAT

IF (NAT.EQ.9999.AND.MIXNUM.EQ.1) P_NAT = 0

IF (NAT.EQ.9999.AND.MIXNUM.EQ.2)  P_NAT = 1

IF (NAT.EQ.9999.AND.MIXNUM.EQ.3)  P_NAT = 2

;-----------------------------------------------------------------------------------------------------------------------------

TVCL_NAT =  THETA(1) ; intermediate or uknown

IF(P_NAT.EQ.0) TVCL_NAT =  THETA(11) ;FAST

IF(P_NAT.EQ.2) TVCL_NAT =  THETA(12) ;SLOW

;           Pregnancy effect

PREGNANCY=1

IF (VISIT .EQ. 1) PREGNANCY=1+THETA(19) ; If pregnant

;------introducing new variables for VPC----------
```

```
EFV_GENO = EFV*10 + GENO

NAT_EFV = NAT*10 + EFV

NAT_VISIT = NAT*10 + VISIT

PNAT_EFV = P_NAT*10 + EFV

PNAT_VISIT = P_NAT*10 + VISIT

NAT_CYP2A = NAT*10 + CYP2A

CYP2A_EFV = CYP2A*10 +EFV

;--- The dataset needs to include ID_OCC, which has a unique value for each occasion for plotting

OCC_ID = ID*10 + OCC

;---------Typical values----------------------------------------------------------------------------------------------

TVCL = TVCL_NAT*PREGNANCY*ALLMCL_FFM

TVV = THETA(2)*ALLMV_WT

TVKA = THETA(3)

TVBIO = THETA(4)

TVV3 = THETA(7)*ALLMV_WT

TVQ = THETA(8)*ALLMCL_WT

TVMTT   = THETA(9)

NN      = THETA(10)

;---------------------------HEPATIC CL---------------------------------------;

TVQH=THETA(14)*ALLMCL_FFM_HEP   ; PLASMA FLOW RATE

TVFU=THETA(15)          ; UNBOUND PLASMA FRACTION OF INH

;-----------Define parameters-------------------------------------------------------------------------------

CL  = TVCL*EXP(BSVCL+BOVCL) ; CLEARANCE

V   = TVV*EXP(BSVV) ; CENTRAL VOL.

KA  = TVKA*EXP(BSVKA+BOVKA) ; ABS. RATE CONSTANT

BIO = TVBIO*EXP(BSVBIO+BOVBIO) ; BIOAVAILABILITY
```

```
V3 = TVV3*EXP(BSVV3) ; PERIPH VOL

Q = TVQ*EXP(BSVQ) ; INTER COMPT CL

MTT = TVMTT*EXP(BOVMTT)

QH=TVQH

FU=TVFU

CLINT=CL

;--------  Transfer constants for liver model ---------

; define hepatic extraction

EH  = (CLINT*FU)/((CLINT*FU)+QH) ; fraction undergoing first pass extraction

FH  = 1 - EH ; fraction available after 1st pass to go to systemic circulation

; COMPUTE RATE CONSTANTS

K32  = Q/V3   ; from peripheral to central

K23 = Q/V     ; from central to peripheral

K20 = QH*EH /V

;---------------- CODE for TRANSIT COMPARTMENT ----------------------------------------------------------------

F1=0 ; I need to set bioavailability in compartment 1 to 0

KTR = (NN+1)/MTT

IF (NEWIND.NE.2.OR.EVID.GE.3) THEN ; new individual, or reset event

; The values read here will be stored in TDOS and PD in this very PK call.

        TNXD=TIME ; Time of the dose

        PNXD=AMT ; Amount. If it's zero, the DE is deactivated.

ENDIF


TDOS=TNXD ; This will either save here the temporary values if it's a new individual...

PD=PNXD ; ...or the values which were read one record ahead during the execution of the previous

record.
```

```
IF(AMT.GT.0) THEN ; This reads one record ahead and stores the data to be used when running the
following record
; IF(AMT.GT.0.AND.ALAG1.EQ.0) THEN ; Use this instead if there is ALAG, as it will also checks if the
ALAG is not 0
        TNXD=TIME
        PNXD=AMT
ENDIF
; Uncomment this if you have ALAG or if you use ADDL
; IF (DOSTIM.GT.0) THEN ; This will account for the ADDL or lagged doses. It will overwrite the time, if
it a non-event record
;       TNXD=DOSTIM
;       PNXD=AMT
; ENDIF
; To speed up the computation, I calculate here all the non-time-varying quantities used in $DES
PIZZA = LOG(BIO*PD*KTR + 0.00001) - GAMLN(NN+1); without +0.00001, it won't work with ETAs in
bioavailability
; IF(NEWIND.LE.1.OR.EVID.GE.3) THEN ; assign negative Cmax Tmax for the new subject
    ; COM(1)=-1 ; holder of Cmax
    ; COM(2)=-1 ; holder of Tmax
; ENDIF
$DES

TEMPO=T-TDOS ; this is time after dose, it should always be >= 0
KTT=0
TRANSIT_ABS = 0
IF(PD.GT.0.AND.TEMPO.GT.0) THEN ; This happens only id PD>0, so only if a dose has been detected
```

```
        KTT=KTR*(TEMPO)
        TRANSIT_ABS = EXP(PIZZA+NN*LOG(KTT)-KTT)
ENDIF
DADT(1)= TRANSIT_ABS -KA*A(1)
DADT(2)=KA*A(1)*FH -K23*A(2) +K32*A(3) -K20*A(2)
DADT(3)=K23*A(2)-K32*A(3)
; ;------CMAX AND TMAX
; CT=A(2)/V ; (or other expression for concentration)
; IF(CT.GT.COM(1)) THEN
        ; COM(1)=CT
        ; COM(2)=T
; ENDIF
$ERROR
IPRED = A(2)/V
IRES = DV-IPRED
PROP = IPRED*THETA(5)
ADD = THETA(6)
LLOQ=0.105 ; INH LLOQ in ug/ml
   IMPUTED_BLQ=LLOQ/2
 ; BLQ==2 are consecutive BLQ samples in a series, which I want to disergard
   IF (ICALL/=4.AND.BLQ==2) THEN
            PROP=0
            ADD=IMPUTED_BLQ*1000000 ; Using this large error has the same effect as ignoring,
expect the record is still there, so I can use it in VPCs.
   ENDIF
W = SQRT(ADD**2+PROP**2)
```

```
IF (W.LE.0.0001) W=0.0001
IWRES = IRES/W
Y = IPRED + W*ERR(1)
; To prevent simulation (ICALL==4) of negative values. It set a positive lower bound for Y, so that VPCs in the log-scale can be plotted
;IF (ICALL==4.AND.Y<=0.000001) Y=0.000001
; For simulation, like in case of VPC
   IF (ICALL==4.AND.Y<=LLOQ) THEN
         Y=IMPUTED_BLQ ; All BLQ values in simulation get imputed to LLOQ/2. This also prevents negative values
   ENDIF
; To calculate time after dose.
IF(AMT.GT.0) THEN
      TIMEDOSE = TIME
      AMOUNTDOSE = AMT
ENDIF
TAD = TIME-TIMEDOSE
VARCL = BSVCL + BOVCL
VARBIO = BSVBIO + BOVBIO
VARAUC = BSVBIO + BOVBIO - BSVCL - BOVCL
;----------RETRIEVE AMOUNT IN EACH COMPARTMENT----------
AA1=A(1)
AA2=A(2)
AA3=A(3)

;----------Mixture modelling proportion of genotype----------
```

```
MIX_POP=MIXEST

MIX_PROB=MIXP

$MIX

 NSPOP=3          ; 3 SUB-POPULATIONS (FAST INTERMIDEATE SLOW PHENOTYPE)

P(1)=THETA(16)       ; PROBABILITY OF FAST PHENOTYPE

P(2)=THETA(17)        ; PROBABILITY OF INTERMIDEATE

P(3)=THETA(18)        ; PROBABILITY OF SLOW

;-----------------------------------------------------------------------------------------------------------------------

$THETA  (0,38.569,600) ; 1 CL INTER [L/h]

 (0,37.4844,400) ; 2 V [L]

 (0,2.68921,20) ; 3 KA [1/h]

 1 FIX ; 4 BIO

 (0,0.132342,1) ; 5 PROP []

 (0,0.0377911,1) ; 6 ADD [mg/L]

 (0,13.3098,300) ; 7 V3 [L]

 (0,3.32,90) ; 8 Q [L/h]

 (0,0.343919,20) ; 9_MTT

 (0,49.0805,500) ; 10_NN

 (0,71.7811,700) ; 11_CL FAST

 (0,14.4723,500) ; 12_CL SLOW

 1 FIX ; 13 DUMMY

 50 FIX ; 14 QH

 0.95 FIX ; 15 FU

 0.155 FIX ; 16 PROB FAST

 0.43 FIX ; 17 PROB INTERMEDIATE

 0.42 FIX ; 18 PROB SLOW
```

```
 (-0.99,0.259234,5) ; 19 CL pregnancy

$OMEGA  BLOCK(1)

 0.477952  ;   1 BSV CL

$OMEGA  BLOCK(1) FIX

 0  ;    2 BSV V

$OMEGA  BLOCK(1) FIX

 0  ;   3 BSV KA

$OMEGA  BLOCK(1) FIX

 0  ;  4 BSV BIO

$OMEGA  BLOCK(1) FIX

 0  ;    5 BSVV3

$OMEGA  BLOCK(1) FIX

 0  ;     6 BSVQ

;-----------------------------------------------------------------------------------------------------------------------

$OMEGA  BLOCK(1) FIX

 0  ;    7 BOVCL

$OMEGA  BLOCK(1) SAME

;-----------------------------------------------------------------------------------------------------------------------

$OMEGA  BLOCK(1) FIX

 0  ;     9 BOVV

$OMEGA  BLOCK(1) SAME

;-----------------------------------------------------------------------------------------------------------------------

$OMEGA  BLOCK(1)

 2.12775  ;   11 BOVKA

$OMEGA  BLOCK(1) SAME

$OMEGA  BLOCK(1) SAME
```

```
$OMEGA  BLOCK(1) SAME
;----------------------------------------------------------------------------------------------------------------------------
$OMEGA  BLOCK(1)
 0.0152131  ;  15 BOVBIO
$OMEGA  BLOCK(1) SAME
$OMEGA  BLOCK(1) SAME
$OMEGA  BLOCK(1) SAME
;----------------------------------------------------------------------------------------------------------------------------
$OMEGA  BLOCK(1)
 1.34719  ;     19 MTT
$OMEGA  BLOCK(1) SAME
$OMEGA  BLOCK(1) SAME
$OMEGA  BLOCK(1) SAME
$SIGMA  1  FIX
;----------------------------------------------------------------------------------------------------------------------------
$ESTIMATION  MSFO=run0185.msf  MAXEVAL=9999  PRINT=1  SIGDIG=2  SIGL=6  METH=1  INTER
NOABORT REPEAT
$COVARIANCE PRINT=E MATRIX=S
$TABLE      FILE=sdtab0185.csv FORMAT=, ID OCC VISIT TIME DV BLQ VPCINH TAD IPRED PRED IWRES
WRES CWRES OBJI WRESCHOL NOPRINT NOAPPEND ONEHEADER
$TABLE      FILE=patab0185.csv FORMAT=, ID OCC VISIT CL V KA Q V3 FU QH BIO MTT BSVCL BOVCL
BSVV BOVBIO BOVKA BOVMTT NOPRINT NOAPPEND ONEHEADER
$TABLE       FILE=cotab0185.csv FORMAT=, ID OCC VISIT WT HT HEMO WBC ANC PLAT AGE GAGE
CREATINE DAYSEFV RCOPIES DOSMISS NOPRINT NOAPPEND ONEHEADER
```

$TABLE FILE=catab0185.csv FORMAT=, ID OCC VISIT RACE SITE ARM CYP2 NAT P_NAT INH EFV PILLPERC ADHEREPERC NAT_EFV NAT_VISIT PNAT_EFV PNAT_VISIT NAT_CYP2A CYP2A_EFV NOPRINT NOAPPEND ONEHEADER

$TABLE FILE=mytab0185.csv FORMAT=, ID OCC VISIT Y DV AA1 AA2 AA3 TIME VPCINH TAD IPRED PRED IWRES WRES CWRES OBJI CL V KA Q V3 BIO MTT FU VARCL VARBIO VARAUC OCC_ID QH BSVCL BOVBIO BOVKA BOVMTT WT HEMO WBC ANC PLAT AGE RACE SITE GAGECR EATINE HT VPCINH BLQ DAYSEFV DOSMISS RCOPIES ARM CYP2 NAT P_NAT INH EFV PILLPERC ADHEREPERC FLAG NWEIGHT NREGIME NAT_EFV NAT_VISIT PNAT_EFV PNAT_VISIT NAT_CYP2A CYP2A_EFV EH FH NOPRINT NOAPPEND ONEHEADER ;GENOME MIX_POP MIX_PROB GENO MIX_POP CH

Final NONMEM scripts for results presented in chapter 3 – Efavirenz

$SIZES PD=-1000 LVR=-150 LTH=-200 MAXFCN=10000000 LNP4=-150000

$PROBLEM EFV_IMPAACT

$INPUT ID STUDY=DROP VISIT_ID=DROP INHCONC=DROP DV DRUG_NAME=DROP FIXED_IN_R=DROP VISIT DATETIME=DROP MDV EVID WHAT=DROP OCCINH=DROP SS=DROP II=DROP OCC EFVPROBLEM INHPROBLEM=DROP INHDOSE=DROP EFVDOSE=AMT DAT2=DROP TIME WEIGHT HEMO WBC ANC PLAT AGE RACE SITE GAGE CREATINE HEIGHT ARM EFVTIME=DROP INHTIME=DROP POSTWEEK VPCEFV VPCINH BLQ BLQINH=DROP CYP2 NAT CYP2A REGIMEN=DROP DAYSEFV RCOPIES EFV INH DOSMISS_INH=DROP DOSMISS PILLPERC ADHEREPERC DOSE CMT

$DATA cimpaact_clean24e.2018.11.23.csv

IGNORE=# IGNORE=(EFVPROBLEM.EQ.1)

;IGNORE=(ID=7550) ; IGNORE=(ID=3116) visit two.

;$ABBREVIATED COMRES=2

$SUBROUTINE ADVAN13 TRANS1 TOL=9 ; TOL is the precision to solve differential equations

ATOL=9 ; absolute tolerance,10^ATOL of your dose unit. A lower value makes the model run faster

$ABBREVIATED COMRES=2

```
; Options SSTOL and SSATOL are only going to work in 7.4.1 or later
$MODEL      NCOMPARTMENTS=4 COMP=(ABS DEFDOSE)
                 COMP=(CENTRAL DEFOBSERVATION) COMP=(PERI1)
                 COMP=(AUC INITIALOFF)
; COMP=(PERI2)


;--- ----------------------------------------------------------------------------------------------------------------------------------
$PK
; ------- BSV
BSVCL   = ETA(1)
BSVV   = ETA(2)
BSVKA   = ETA(3)
BSVBIO = ETA(4)
; ---------- BOV
BOVCL = ETA(5)
IF(VISIT.EQ.2) BOVCL = ETA(6)
BOVKA=ETA(7)
IF(OCC.EQ.2)  BOVKA=ETA(8)
IF(OCC.EQ.3)  BOVKA=ETA(9)
IF(OCC.EQ.4)  BOVKA=ETA(10)
BOVBIO=ETA(11)
IF(OCC.EQ.2)  BOVBIO=ETA(12)
IF(OCC.EQ.3)  BOVBIO=ETA(13)
IF(OCC.EQ.4)  BOVBIO=ETA(14)
BOVMTT =  ETA(15)
 IF(OCC.EQ.2)  BOVMTT=ETA(16)
```

```
IF(OCC.EQ.3)  BOVMTT=ETA(17)

IF(OCC.EQ.4)  BOVMTT=ETA(18)

BSVV3 = ETA(19)

BSVQ = ETA(20)

; ---------- Calculation of Fat-free Mass

; These formulas require WT in KG and HT in m !!!

;--------- IMPUTING MISSING WEIGHT

IF (WEIGHT.NE.999) THEN

        WT = WEIGHT

 ELSE

        WT = 67

 ENDIF

 IF (HEIGHT.GT.0) THEN

        HT = HEIGHT

 ELSE

        HT = 158

 ENDIF

; Conversion from cm to m

HTM = HT/100

;IF (SEX.EQ.0) THEN  ; female

        WHSMAX=37.99

        WHS50=35.98

;ELSE      ;males

        ;WHSMAX=42.92

        ;WHS50=30.93

;ENDIF
```

```
HTM2 = HTM**2

FFM = (WHSMAX*HTM2*WT)/(WHS50*HTM2+WT)

FAT = WT-FFM

; ------- Typical values of covariates

TVWT = 67

TVFAT = 28

TVFFM = 39

;--------- Allometric scaling and covariates

ALLMCL_WT = (WT/TVWT)**0.75

ALLMV_WT = (WT/TVWT)

ALLMCL_FAT = (FAT/TVFAT)**0.75

ALLMV_FAT = (FAT/TVFAT)

ALLMCL_FFM = (FFM/TVFFM)**0.75

ALLMV_FFM = (FFM/TVFFM)

; Allometry for liver

ALLMCL_WT_HEP = (WT/70)**0.75

ALLMV_WT_HEP = (WT/70)

ALLMCL_FFM_HEP = (WT/56.1)**0.75

ALLMV_FFM_HEP = (WT/56.1)

;--- ----------------------------------------------------------------------------------------------------------------

;categorising cyp2 phenotype to fast=0 intermediate=1 slow=2 extra_slow=3

GENOME = -99

IF (CYP2.LE.2) GENOME = 0

IF (CYP2.GE.3.AND.CYP2.LE.7) GENOME=1

IF (CYP2.GE.8.AND.CYP2.LT.11) GENOME=2

IF (CYP2.GE.11.AND.CYP2.LE.12) GENOME=3
```

```
P_GENOME = GENOME

IF (GENOME .LT. 0 .AND. MIXNUM .EQ. 1) P_GENOME = 0

IF (GENOME .LT. 0 .AND. MIXNUM .EQ. 2)  P_GENOME = 1

IF (GENOME .LT. 0 .AND. MIXNUM .EQ. 3)  P_GENOME = 2

IF (GENOME .LT. 0 .AND. MIXNUM .EQ. 4)  P_GENOME = 3

TVCL_CYP2=  THETA(1) ; intermediate

IF(P_GENOME.EQ.0) TVCL_CYP2 =  THETA(9) ;FAST

IF(P_GENOME.EQ.2) TVCL_CYP2 =  THETA(10) ;SLOW

;IF(P_GENOME.EQ.3) TVCL_CYP2 = THETA(11) ; EXTRA SLOW

;-----------------------------------------------------------------------------------------------------------------

;------introducing new variables for VPC----------

INH_NAT = INH*10 + NAT

GENOME_INH = GENOME*10 + INH

GENOME_VISIT = GENOME*10 + VISIT

PGENOME_INH = P_GENOME*10 + INH

PGENOME_VISIT = P_GENOME*10 + VISIT

GENOME_CYP2A = GENOME*10 + CYP2A

CYP2A_INH = CYP2A*10 +INH

PGENOME_CYP2A = P_GENOME*10 + CYP2A

;short names--------

NINH = INH_NAT

IGENOME = GENOME_INH

VGENOME = GENOME_VISIT

IPGENOME = PGENOME_INH

VPGENOME = PGENOME_VISIT

CGENOME = GENOME_CYP2A
```

```
ICYP2A = CYP2A_INH

PGCYP2A = PGENOME_CYP2A

;---------pregnancy effect-----------------------------------------------------------------------------------------

PREGNANCY=1

IF (VISIT .EQ. 1) PREGNANCY=1+THETA(19) ; If on pregant

;---------INH effect-------------------------------------------------------------------------------------------------

TV_INH = 1 ; not on INH

IF (P_GENOME.EQ.0 .AND. INH .EQ. 1) TV_INH=1+THETA(20) ; fast on INH

IF (P_GENOME.EQ.1 .AND. INH .EQ. 1) TV_INH=1+THETA(21) ; Inter on INH

IF (P_GENOME.EQ.2 .AND. INH .EQ. 1) TV_INH=1+THETA(21) ; slow on INH

;---------Typical values---------------------------------------------------------------------------------------

TVCL = TVCL_CYP2*PREGNANCY*TV_INH*ALLMCL_FFM

TVV = THETA(2)*ALLMV_WT

TVKA = THETA(3)

TVBIO = THETA(4)

TVMTT = THETA(7)

TVNN = EXP(THETA(8))

TVV3 = THETA(11)*ALLMV_WT

TVQ = THETA(12)*ALLMCL_WT

;--------------------------HEPATIC CL---------------------------------------;

TVQH=THETA(17)*ALLMCL_FFM_HEP   ; PLASMA FLOW RATE

TVFU=THETA(18)          ; UNBOUND PLASMA FRACTION OF INH

;----------Define parameters-----------------------------------------------------------------------------------------

CL  = TVCL*EXP(BSVCL+BOVCL) ; CLEARANCE

V   = TVV*EXP(BSVV) ; CENTRAL VOL.

KA  = TVKA*EXP(BSVKA+BOVKA) ; ABS. RATE CONSTANT
```

```
BIO = TVBIO*EXP(BSVBIO+BOVBIO) ; BIOAVAILABILITY

MTT =TVMTT*EXP(BOVMTT) ; MTT TIME

NN = TVNN ; Number of transit compartments

V3 = TVV3*EXP(BSVV3) ; PERIPH VOL

Q = TVQ*EXP(BSVQ) ; INTER COMPT CL

QH=TVQH

FU=TVFU

CLINT=CL

;--------  Transfer constants for liver model ---------

; define hepatic extraction

EH  = (CLINT*FU)/((CLINT*FU)+QH) ; fraction undergoing first pass extraction

FH  = 1 - EH ; fraction available after 1st pass to go to systemic circulation

; COMPUTE RATE CONSTANTS

K32  = Q/V3   ; from peripheral to central

K23 = Q/V     ; from central to peripheral

K20 = QH*EH /V

;---------------- CODE for TRANSIT COMPARTMENT ----------------------------------

F1=0 ; I need to set bioavailability in compartment 1 to 0 for this implementation of the transit compartment absorption

KTR = (NN+1)/MTT

IF (NEWIND/=2.OR.EVID>=3) THEN ; new individual, or reset event

   ; The values read here will be stored in TDOS and PD in this very PK call.

        TNXD=TIME ; Time of the dose

        PNXD=AMT ; Amount. If it's zero, the DE is deactivated.

ENDIF

TDOS=TNXD ; This will either save here the temporary values if it's a new individual...
```

```
PD=PNXD ; ...or the values which were read one record ahead during the execution of the previous record.
IF(AMT>0) THEN ; This reads one record ahead and stores the data to be used when running the following record
; IF(AMT.GT.0.AND.ALAG1.EQ.0) THEN ; Use this INSTEAD if there is ALAG, as it will also checks if the ALAG is not 0. Note that you normally do not want to include both ALAG and transit, this is a very exceptional case
        TNXD=TIME
        PNXD=AMT
ENDIF
; Uncomment this if you have ALAG or if you use ADDL
; IF (DOSTIM>0) THEN ; This will account for the ADDL or lagged doses. It will overwrite the time, if it a non-event record
;       TNXD=DOSTIM
;       PNXD=AMT
; ENDIF
; To speed up the computation, I calculate here all the non-time-varying quantities used in $DES
PIZZA = LOG(BIO*PD*KTR + 0.00001) - GAMLN(NN+1)  ; without +0.00001, it won't work with ETAs in bioavailability
; RESET code for CMAX
IF (NEWIND.NE.2.OR.EVID.GE.3) THEN ; Each time I have a new subject, or a reset
        COM(1)=0
        COM(2)=0
        TDOS = 0
ENDIF
; IF(NEWIND.LE.1.OR.EVID.GE.3) THEN ; assign negative Cmax Tmax for the new subject
```

```
    ; COM(1)=-1 ; holder of Cmax
    ; COM(2)=-1 ; holder of Tmax
; ENDIF
;----- CODE for SS approximate initialisation - Liver 2 + 2-compartments -------
; Liver-adjusted clearance and bioavaialability
CL_HEP = QH*EH
BIO_HEP = BIO * FH
; CALCULATE ALPHA AND BETA
TMP0 = K20*K32  ; ALPHA * BETA
TMP1 = K20+K23+K32 ; ALPHA + BETA
TMPDELTA = SQRT(TMP1*TMP1 - 4* TMP0) ; SQ ROOT FROM EQUATION
SOL1 = (TMP1 + TMPDELTA) / 2 ; ALPHA
SOL2 = (TMP1 - TMPDELTA) / 2 ; BETA
ALFA  = SOL1
BBETA = SOL2
VBETA = CL_HEP / SOL2 ; VBETA=CL/BETA
; work out equivalent absorption time lumping KA and MTT together
TAU_EQ = MTT+1/KA
KA_EQ = 1/TAU_EQ
; treat both compartments as one single compartment at steady state (C2 = aprox. C3 = Cmin)
; SUBSTITUTE V BY VBETA AND K BY SOL2
CMIN = ( (BIO_HEP*DOSE * KA_EQ) /(VBETA*(KA_EQ - SOL2)))*( (1 / (1- EXP(-SOL2 * 24)))-(1 / (1- EXP(-
KA_EQ*24))) )
A_0(1)= 0.0001
A_0(2)= V * CMIN
A_0(3)= V3 * CMIN
```

```
;-----------------------------------------------------------------------------------------------------------------------

$DES
TEMPO=T-TDOS ; this is time after dose, it should always be >= 0
KTT=0
DADT(1)=-KA*A(1)
IF(PD.GT.0.AND.TEMPO.GT.0) THEN ; This happens only id PD>0, so only if a dose has been detected
   KTT=KTR*(TEMPO)
   DADT(1)=EXP(PIZZA+NN*LOG(KTT)-KTT)-KA*A(1)
ENDIF
DADT(2) = KA*A(1)*FH -K23*A(2) +K32*A(3) -K20*A(2)
DADT(3) = K23*A(2) -K32*A(3)
; ;------CMAX AND TMAX
; CT=A(2)/V ; (or other expression for concentration)
; IF(CT.GT.COM(1)) THEN
            ; COM(1)=CT
            ; COM(2)=T
; ENDIF
;------ ----------------------------------------------------------------------------------------------------------
; For Cmax Tmax
 CP = A(2)/V              ; plasma concentration
 IF (CP.GE.COM(1)) THEN
            COM(1) = CP             ; CMAX
            COM(2) = TEMPO          ; TIME OF CMAX
ENDIF
DADT(4) = CP
```

```
$ERROR

IPRED = A(2)/V

IRES = DV-IPRED

PROP = IPRED*THETA(5)

ADD = THETA(6)

LLOQ=0.0195 ; EFV LLOQ in ug/ml

IMPUTED_BLQ=LLOQ/2

 ; BLQ==2 are consecutive BLQ samples in a series, which I want to disergard

IF (ICALL/=4.AND.BLQ==2) THEN

        PROP=0

        ADD=IMPUTED_BLQ*1000000 ; Using this large error has the same effect as ignoring, expect the record is still there, so I can use it in VPCs.

ENDIF

W = SQRT(ADD**2+PROP**2)

IF (W.LE.0.0001) W=0.0001

IWRES = IRES/W

Y = IPRED + W*ERR(1)

; To prevent simulation (ICALL==4) of negative values. It set a positive lower bound for Y, so that VPCs in the log-scale can be plotted

;IF (ICALL==4.AND.Y<=0.000001) Y=0.000001

; For simulation, like in case of VPC

IF (ICALL==4.AND.Y<=LLOQ) THEN

        Y=IMPUTED_BLQ ; All BLQ values in simulation get imputed to LLOQ/2. This also prevents negative values

ENDIF

W = SQRT(ADD**2+PROP**2)
```

```
; To calculate time after dose.
IF(AMT>0) THEN
        TIMEDOSE = TIME
        AMOUNTDOSE = AMT
ENDIF
TAD = TIME-TIMEDOSE
VARCL = BSVCL + BOVCL
VARBIO = BSVBIO + BOVBIO
VARAUC = BSVBIO + BOVBIO - BSVCL - BOVCL
;--- ----------RETRIEVE AMOUNT IN EACH COMPARTMENT----------
AA1 = A(1)
AA2 = A(2)
AA3 = A(3)
CMAX = COM(1) ; CMAX
TMAX = COM(2) ; TIME OF CMAX
IF(AMT.GT.0) THEN
        TDOS = TIME
        PD   = AMT
; Reset CMAX code when a new dose is given (e.g. every day)
        COM(1)=0
        COM(2)=0
ENDIF
AUC = A(4) ; AUC as obtained integrating the concentration in $DES
AUC_INF = DOSE * BIO / (CL*0.005); this works for any linear model, it is the theoretical AUC from a
"clean" single dose or SS. Use the final individual parameters for this
```

```
;---------- ----------Mixture modelling proportion of genotype----------------------------------------------

MIX_POP=MIXEST

MIX_PROB=MIXP

$MIX

NSPOP=4           ; 3 SUB-POPULATIONS (FAST INTERMIDEATE SLOW PHENOTYPE)

P(1)=THETA(13)        ; PROBABILITY OF FAST PHENOTYPE

P(2)=THETA(14)         ; PROBABILITY OF INTERMIDEATE

P(3)=THETA(15)         ; PROBABILITY OF SLOW

P(4)=THETA(16)         ; PROBABILITY OF ultra- slow

;------ ----------------------------------------------------------------------------------------------------------

$THETA  (0,1950,3000) ; 1 CL [L/h]

 (0,136,800) ; 2 V [L]

 (0,1.75,5) FIX ; 3 KA [1/h]

 1 FIX ; 4 BIO

 (0,0.0692,0.5) ; 5 PROP []

 (0,0.351,1) ; 6 ADD [mg/L]

 (0,1.8,3) ; 7 MTT

 (0,3.02,20) ; 8 NN [LOG]

 (0,2700,5000) ; 9_CL FAST

 (0,546,2000) ; 10_CL SLOW

 (0,511,800) ; 11 V3 [L]

 (0,26.5,90) ; 12 Q [L/h]

 0.28 FIX ; 13 PROB FAST

 0.51 FIX ; 14 PROB INTERMEDIATE

 0.2 FIX ; 15 PROB SLOW

 0.001 FIX ; 16 PROB ULTRA-SLOW
```

```
 (0,50,90) FIX ; 17 QH

 (0,0.005,1) FIX ; 18 FU

 (-0.99,0.155,5) ; 19 CL PREGNANCY

 (-0.99,-0.0693,5) ; 20 CL fast on INH

 (-0.99,-0.139,5) ; 21 CL inter on INH

$OMEGA  BLOCK(1)

 0.289  ;   1 BSV CL

$OMEGA  BLOCK(1) FIX

 0  ;    2 BSV V

$OMEGA  BLOCK(1) FIX

 0  ;   3 BSV KA

$OMEGA  BLOCK(1) FIX

 0  ;  4 BSV BIO

;--------- ----------------------------------------------------------------------------------------

$OMEGA  BLOCK(1) FIX

 0  ;    5 BOVCL

$OMEGA  BLOCK(1) SAME

;-------------------------- ----------------------------------------------------------------------------------

$OMEGA  BLOCK(1)

 3.24  ;    7 BOVKA

$OMEGA  BLOCK(1) SAME

$OMEGA  BLOCK(1) SAME

$OMEGA  BLOCK(1) SAME

;-------------------------------------------------------------------------------------------------------------------------------

$OMEGA  BLOCK(1)

 0.0556  ;  11 BOVBIO
```

```
$OMEGA  BLOCK(1) SAME

$OMEGA  BLOCK(1) SAME

$OMEGA  BLOCK(1) SAME

;-------- ----------------------------------------------------------------------------------------------------

$OMEGA  BLOCK(1)

 1.68  ;     15 MTT

$OMEGA  BLOCK(1) SAME

$OMEGA  BLOCK(1) SAME

$OMEGA  BLOCK(1) SAME

;-------- ----------------------------------------------------------------------------------------------------------------

$OMEGA  BLOCK(1) FIX

 0  ;   19 BSVV3

$OMEGA  BLOCK(1) FIX

 0  ;    20 BSVQ

$SIGMA  1  FIX

;------------------- ----------------------------------------------------------------------------------------------------

$ESTIMATION  MSFO=run075e.msf  MAXEVAL=9999  PRINT=1  METHOD=1  INTER  NOABORT  NSIG=3

SIGL=9 ; RULES for precision SIGL=<TOL AND NSIG=<SIGL/3 NONINFETA=1 ETASTYPE=1 ; REPEAT ;

$COVARIANCE PRINT=E MATRIX=S PRECOND=1

$TABLE   WRESCHOL FILE=sdtab075e.csv ID OCC VISIT VPCEFV TAD AA1 AA2 AA3 Y DV PRED RES WRES

IPRED IRES IWRES CWRESI CWRES OBJI NOPRINT NOAPPEND ONEHEADER FORMAT=,

$TABLE    FILE=patab075e.csv ID OCC VISIT CL V KA Q V3 BIO BSVCL BOVCL BOVKA BOVBIO BOVMTT

MTT NN NOPRINT NOAPPEND ONEHEADER FORMAT=,

$TABLE    FILE=cotab075e.csv ID OCC VISIT TAD WT HT FFM FAT HT HEMO WBC ANC PLAT AGE GAGE

CREATINE VPCEFV BLQ DAYSEFV RCOPIES NOPRINT NOAPPEND ONEHEADER FORMAT=,
```

$TABLE FILE=catab075e.csv ID OCC VISIT RACE SITE BLQ ARM CYP2 NAT DOSMISS GENOME P_GENOME INH EFV CYP2A NINH IGENOME VGENOME IPGENOME VPGENOME CGENOME ICYP2A PGCYP2A NOPRINT NOAPPEND ONEHEADER FORMAT=,

$TABLE FILE=mytab075e.csv ID OCC VISIT VPCEFV TAD TIME Y DV AA1 AA2 AA3 PRED RES WRES IPRED IRES IWRES CWRESI CWRES OBJI CL V KA Q V3 BIO BSVCL BSVV BSVKA BSVBIO BOVCL BOVKA BOVBIO BOVMTT VARCL VARBIO VARAUC HT FFM FAT WT HEMO WBC ANC PLAT AGE RACE SITE GAGE CREATINE HT BLQ DAYSEFV RCOPIES ARM CYP2 NAT DOSMISS CYP2A GENOME INH EFV MIX_POP INH_NAT GENOME_INH GENOME_VISIT PGENOME_INH PGENOME_VISIT GENOME_CYP2A NOPRINT NOAPPEND ONEHEADER FORMAT=,

Final NONMEM scripts for results presented in chapter 4

```
$SIZES     PD=-1000 LVR=-150 LTH=-200 MAXFCN=10000000 LNP4=-150000
$PROBLEM    NAME_OF_THE_PROJECT
$INPUT    ID VISIT TIME DAT2=DROP PID=DROP NOMINAL_TIME=DROP WHAT=DROP ST_VISIT=DROP DV M2DV MDV OCC DVID OCC1 EVID AMT VPCTIME HT WT DAY=DROP FIXED_IN_R=DROP PARTICIPANT_ID=DROP VOMITED INFANTS_WEIGHT INFANTS_LENGTH BREASTFED EXCLUSIVE1 PROBLEM L2 LDV CMT MOLDV NDV GESTATION GESTWEEKS AGE CD4 PREVTB RESISTANCE EMITRICITABINVE EFAVIRENZ NEVIRAPINE LAMIVUDINE DOLUTEGRAVIR ABACAVIR LOPINAVIR RITONAVIR ZIDOVUDINE STAVUDINE EFV_DAYS PK_EFV_DAYS GEST_AGE GEST_AGE1 ALB CONC1
$DATA     BDQ_PK_NONMEM4.2021-08-30.csv IGNORE=# IGNORE=(PROBLEM.GT.0)
$ABBREVIATED DERIV2=NO ; Prevents  the computation of second derivatives,which are needed only for the Laplacian method.

$SUBROUTINE ADVAN13 TRANS1 TOL=9 ; TOL is the precision to solve differential equations
ATOL=6 ; absolute tolerance,10^ATOL of your dose unit. A lower value makes the model run faster
; Remember that ATOL is only going to work in $SUBROUTINE from 7.4.1, otherwise include ATOL in $ESTIMATION
; SSTOL=3 SSATOL=3 ; This is the tolerance used when calculating steady-state. Put a low value to avoid the model running forever.
$MODEL     NCOMPARTMENTS=8 COMP=(DEPOT DEFDOSE) COMP=(BDQC)
               COMP=(BDQPERI1) COMP=(BDQPERI2) COMP=(M2) COMP=(TRANSI1)
               COMP=(TRANSI2) COMP=(ALBUMIN)
;-------------- ----------------------------------------------------------------------------------------------------
$PK
;for VPC plots
DVID_VISIT= DVID*10 + VISIT
```

```
DVID_VISIT_RTV= DVID*100 + VISIT*10 + RITONAVIR
;----------------------------------------------------
IF (OCC==0) THEN
BOVCL = 0
BOVBIO = 0
BOVKA = 0
BOVMTT = 0
ENDIF
BOVCL = ETA(9)
IF (OCC==2)BOVCL = ETA(10)
IF (OCC==3)BOVCL = ETA(11)
IF (OCC==4)BOVCL = ETA(12)
BOVBIO = ETA(13)
IF (OCC==2)BOVBIO = ETA(14)
IF (OCC==3)BOVBIO = ETA(15)
IF (OCC==4)BOVBIO = ETA(16)
BOVKA = ETA(17)
IF (OCC==2)BOVKA = ETA(18)
IF (OCC==3)BOVKA = ETA(19)
IF (OCC==4)BOVKA = ETA(20)
BOVMTT = ETA(21)
IF (OCC==2)BOVMTT = ETA(22)
IF (OCC==3)BOVMTT = ETA(23)
IF (OCC==4)BOVMTT = ETA(24)
; ------- BSV
BSVCL   = ETA(1)
BSVCLM  = ETA(2)
BSVV   = ETA(25)
BSVKA   = ETA(3)
BSVBIO = ETA(4)
BSVV3 = ETA(5)
BSVQ = ETA(6)
BSVV4 = ETA(7)
BSVQ2 = ETA(8)

BSVVM = ETA(26)
BSVX0 = ETA(27)
BSVXSS = ETA(28)
BSVREP = ETA(29)
BSVWT0 = ETA(30)
BSVWT120 = ETA(31)
; ---------- Calculation of Fat-free Mass
; These formulas require WT in KG and HT in m !!!
; Conversion from cm to m
HTM = HT/100
SEX = 0
IF (SEX.EQ.0) THEN  ; female
```

```
        WHSMAX=37.99
        WHS50=35.98
ELSE      ;males
        WHSMAX=42.92
        WHS50=30.93
ENDIF
HTM2 = HTM**2
FFM = (WHSMAX*HTM2*WT)/(WHS50*HTM2+WT)
FAT = WT-FFM

; ------- Typical values of covariates
TVWT = 70
TVFAT =24
TVFFM = 40

;--------- Allometric scaling and covariates
ALLMCL_WT = (WT/TVWT)**0.75
ALLMV_WT = (WT/TVWT)
ALLMCL_FAT = (FAT/TVFAT)**0.75
ALLMV_FAT = (FAT/TVFAT)
ALLMCL_FFM = (FFM/TVFFM)**0.75
ALLMV_FFM = (FFM/TVFFM)
;---------Typical values----------------------------------------------------------------------------
;--- Model for Albumin
TVX0 = THETA(1)
TVXSS = THETA(2)
TVREP = THETA(3)
; BSVX0 = ETA(1)
; BSVXSS = ETA(2)
; BSVREP = ETA(3)
; SHPX0 = THETA(4)
; PHIX0 = EXP(BSVX0)
; PHI2X0 =(PHIX0**SHPX0-1)/SHPX0 ; Box-cox transformation
; SHPXSS = THETA(5)
; PHIXSS = EXP(BSVXSS)
; PHI2XSS =(PHIXSS**SHPXSS-1)/SHPXSS ; Box-cox transformation
X0 = TVX0*EXP(BSVX0)
XSS = TVXSS*EXP(BSVXSS)
REP = TVREP*EXP(BSVREP)
HL = LOG(2)/REP
A_0(8) = 3.5
;--- Model for weight
TVWT0 = THETA(6)
TVWT120 = THETA(7)
; BSVWT0 = ETA(4)
; BSVWT120 = ETA(5)
; SHPWT120 = THETA(8)
```

```
; PHIWT120 = EXP(BSVWT120)
; PHI2WT120 = (PHIWT120**SHPWT120-1)/SHPWT120 ; Box-cox transformation
WT0 = TVWT0*EXP(BSVWT0)
WT120 = TVWT120*EXP(BSVWT120)
SLOPE = (WT120 - WT0)/(120*7*24) ; TIME in hours, 120 weeks
;--- BDQ and M2 PK
;covariate
RTVCL=1
IF(LOPINAVIR.EQ.1 )RTVCL=(1+THETA(25))
RTVCLM=1
IF(LOPINAVIR.EQ.1 )RTVCLM=(1+THETA(26))
;--- Typical values fixed effects
TVMAT = THETA(9)
TVFR = THETA(10)
TVCL= THETA(11)*RTVCL
TVV= THETA(12)
TVQ1 = THETA(13)
TVVP1 = THETA(14)
TVQ2 = THETA(15)
TVVP2 = THETA(16)
TVCLM2 = THETA(17)*RTVCLM
TVVM2 = THETA(18)
;--- Covaraiate model
;--- Mechanistic
; Allomertic scaling and albumin effects coded in $DES and $ERROR since they are time changing
;--- Empiric; Effect of Black race on CL
; BLACK = 0
; IF(RACE.EQ.2) BLACK=1
BLACK=1
BLACKCL = 1 + BLACK*THETA(23)
; AGE on CL
AGECL = 1 + (32-AGE)*(THETA(24))
;--- Parameters
PHI = LOG(TVMAT/(1-TVMAT))+BOVMTT
MAT = 6*EXP(PHI)/(EXP(PHI)+1)
; Mean absorption time, overall time for both delay and 90% complete absorption, logit transformed
; to retain constraines even with BOV in MAT
FR = TVFR ; Fraction of MAT that is delay
MTT = MAT*FR
KAHL= MAT*(1-FR)/3.3
KA = LOG(2)/KAHL
KTR= 2/MTT
F1= 1
; AMT in mg in input file, MW TMC207 555.5 g/mol, DV as nmol/mL = µmol/L -->
;(AMT/1000)/(555.5)*1000000 = AMT*1.8002 µmol
```

```
CLB = TVCL*BLACKCL*AGECL*EXP(BSVCL)
VB = TVV*EXP(BSVV)
Q1B= TVQ1*EXP(BSVQ)
VP1B = TVVP1
Q2B = TVQ2
VP2B= TVVP2
CLM2B = TVCLM2*BLACKCL*AGECL*EXP(BSVCLM)
VM2B= TVVM2*EXP(BSVVM)
$DES
; --- Albumin
;DADT(8) = LOG(2)/(HL*7*24)*A(8)*(1- A(8)/XSS) ; Time in hours, unit of half life: weeks
; --- Body weight
WTTIME = WT0 + T*SLOPE ; Predicted individual WT at time T
; --- Time varying covariates
ALBRELI = A(8)/XSS
; Time varying individual albumin relative individual value albumin at SS
COVALBI = (ALBRELI)**THETA(22) ; Albumin effect on hepatic function --> CL
FM = (ALBRELI)**(-THETA(22)) ; Albumin effect on hepatic function --> fmALLCL = (WTTIME/70)**THETA(19) ; Allometric scaling CL/Q
ALLV= (WTTIME/70)**THETA(20) ; Allometric scaling V/VP
ALLCL = (WTTIME/70)**THETA(19)                    ; Allometric scaling CL/Q
; --- BDQ and M2 PK
CL = CLB*COVALBI*ALLCL
V = VB*ALLV
Q1 = Q1B*ALLCL
VP1 = VP1B*ALLV
Q2 = Q2B*ALLCL
VP2 = VP2B*ALLV
CLM2 = CLM2B/FM*COVALBI*ALLCL
VM2 = VM2B/FM*ALLV
DADT(1)= -KTR*A(1)
DADT(2) = A(7)*KA - A(2)*CL/V - A(2)*Q1/V + A(3)*Q1/VP1 - A(2)*Q2/V + A(4)*Q2/VP2 ; BDQ
DADT(3) = A(2)*Q1/V - A(3)*Q1/VP1
DADT(4) = A(2)*Q2/V - A(4)*Q2/VP2
DADT(5) = A(2)*CL/V - A(5)*CLM2/VM2 ; M2
DADT(6) = A(1)*KTR - A(6)*KTR ; transit1
DADT(7) = A(6)*KTR - A(7)*KA ; transit2
$ERROR
SCALE_MOLES=541.47/555.50 ;555.50 g/mol for bedaquiline and 541.47 g/mol for M2
; --- Body weight
WTTIMEE = WT0 + TIME*SLOPE
; --- Time varying covariates
FURELIP = THETA(2)/A(8)
; Time varying individual fraction unbound relative typical population value at SS (inversely
;proportional to albumin)
COVFUIP = (FURELIP)**THETA(21) ; Fu effect on V
ALBRELIE = A(8)/XSS
```

```
; Time varying individual albumin relative individual value albumin at SS
FME = (ALBRELIE)**(-THETA(22)) ; Albumin effect on hepatic function --> fm
ALLCLE = (WTTIMEE/70)**THETA(19) ; Allometric scaling CL/Q
ALLVE = (WTTIMEE/70)**THETA(20) ; Allometric scaling V/VP
; --- BDQ and M2 PK
VE = VB*ALLVE*COVFUIP
VM2E = VM2B/FME*ALLVE*COVFUIP
; FLAG 1 = BDQ PK, 2= M2 PK, 3= Albumin, 4= Body weight
DEL= 1E-12
IPRED=(A(2)/VE)
IF(DVID.EQ.2) IPRED=(A(5)/VM2E)* SCALE_MOLES
IF(DVID.EQ.3) IPRED = A(8)
IF(DVID.EQ.4) IPRED = WTTIMEE
; Error additive on log scale for PK, proportional for albumin and weight
BSVRUV1= ETA(32)
BSVRUV2= ETA(33)
W = 1*EXP(BSVRUV1)
IF(DVID.EQ.2) W = 1*EXP(BSVRUV2)
IF(DVID.EQ.3) W = IPRED
IF(DVID.EQ.4) W = IPRED
IF(W.EQ.0) W=1
IRES=DV-IPRED
IWRES=IRES/W
Y = IPRED * EXP(W*EPS(3))
IF(DVID.EQ.2) Y = IPRED * EXP( W*EPS(4))
IF(DVID.EQ.3) Y = IPRED * EXP(W*EPS(1))
IF(DVID.EQ.4) Y = IPRED * EXP(W*EPS(2))
LLOQ = 0.02
IF(DVID.EQ.2)LLOQ  =  0.01;LMOLDV
; IF(DVID.EQ.3)LLOQ  =  1;g/dl
; IF(DVID.EQ.4)LLOQ  =  20;kg
IF (ICALL==4.AND.Y<=LLOQ .AND. DVID<=2) Y = LLOQ/2
;-----------------------------------------------------------------------------------------
; ;calculating concentration in mg/L
; CONC = Y
; IF(DVID.EQ.1) CONC = EXP(Y)/(1000/555.5)
; IF(DVID.EQ.2) CONC = EXP(Y)/(1000/541.47)
; To calculate time after dose.
IF(AMT>0) THEN
        TIMEDOSE = TIME
        AMOUNTDOSE = AMT
ENDIF
TAD = TIME-TIMEDOSE
VARCL = BSVCL + BOVCL
VARBIO = BSVBIO + BOVBIO
VARAUC = BSVBIO + BOVBIO - BSVCL - BOVCL
VARABS = BOVKA + BSVKA - BOVMTT
```

```
;------- --RETRIEVE AMOUNT IN EACH COMPARTMENT-----------------------------------------------
AA1 = A(1)
AA2 = A(2)
AA3 = A(3)
AA4 = A(4)
AA5 = A(5)
AA6 = A(6)
AA7 = A(7)
AA8 = A(8)
;---------------------------------------- ----------------------------------------------------------------------------
$THETA  (0,3.64865) ; 1 X0 g/dl
 (0,4.04068) ; 2 Xss g/dl
 (0,0.0339911) ; 3 Rate constant return to normal 1/week
 -2.43936 FIX ; 4 shape factor BSVX0 boxcox
 -5.37749 FIX ; 5 shape factor BSVXSS boxcox
 (0,56.6371) ; 6 WT0 kg
 (0,62.6425) ; 7 WT120 kg
 -0.416034 FIX ; 8 Boxcox BSV WT120
 (1E-06,0.662045,1) ; 9 MAT
 (1E-06,0.466443,1) ; 10 FR
 (1E-06,2.61592) ; 11 CL
 (1E-06,198.34) ; 12 V
 (1E-06,3.658) ; 13 Q1
 (1E-06,8549.06) ; 14 VP1
 (1E-06,7.33504) ; 15 Q2
 (1E-06,2690.91) ; 16 VP2
 (1E-06,10.0496) ; 17 CLM2
 (1E-06,2203.71) ; 18 VM2; --- Covariates
 (1E-06,0.180912) ; 19 Allometric scaling baseline CL
 (1E-06,1) FIX ; 20 Allometric scaling V
 (1E-06,1) FIX ; 21 Time varying FU on BDQ+M2 disp
 (-10,1.64021,10) ; 22 Individual time varying effect of ALB BDQ+M2 CL
 (0,0.838743) ; 23 Effect of black race on CL/CM2
 (0,0.00880756,10) ; 24 AGE effect on CL/CLM2
 (-0.99,-0.65,10) ; 25 RTV CL
 (-0.99,-0.42,10) ; 25 RTV CLM2
; --- Albumin
; --- Body weight
; --- BDQ and M2 PK
; --- Albumin and body weight
;-----------------------------------------------------------------------------------------------------
$OMEGA  BLOCK(2)
 0.152776  ;  11 BSV CL
 0.13486 0.212124  ; 12 BSV CLM2
$OMEGA  BLOCK(1) FIX
 0  ;   3 BSV KA
```

```
$OMEGA  BLOCK(1)
 0.0803271  ;  4 BSV BIO
$OMEGA  BLOCK(1) FIX
 0  ;    5 BSVV3
$OMEGA  BLOCK(1)
 0.181182  ;     6 BSVQ
$OMEGA  BLOCK(1) FIX
 0  ;    7 BSVV4
$OMEGA  BLOCK(1) FIX
 0  ;    8 BSVQ2
;----------------------------------------------------------------------------------------------
$OMEGA  BLOCK(1) FIX
 0  ;    9 BOVCL
$OMEGA  BLOCK(1) SAME
$OMEGA  BLOCK(1) SAME
$OMEGA  BLOCK(1) SAME
;--------------------------------------------- ------------------------------------------------
$OMEGA  BLOCK(1)
 0.0382322  ;  13 BOVBIO
$OMEGA  BLOCK(1) SAME
$OMEGA  BLOCK(1) SAME
$OMEGA  BLOCK(1) SAME
;------------------------------------------------------------- ----------------------------------------------
$OMEGA  BLOCK(1) FIX
 0  ;   17 BOVKA
$OMEGA  BLOCK(1) SAME
$OMEGA  BLOCK(1) SAME
$OMEGA  BLOCK(1) SAME
;------------------------------------------------------------- ----------------------------------------------
$OMEGA  BLOCK(1)
 1.16205  ;  21 BOVMTT
$OMEGA  BLOCK(1) SAME
$OMEGA  BLOCK(1) SAME
$OMEGA  BLOCK(1) SAME
;------------------------------------------------------------- ----------------------------------
$OMEGA  BLOCK(1)
 0.171909  ;   25 BSV V
$OMEGA  BLOCK(1)
 0.150223  ;   26 BSVVM
; --- Albumin and body weight
$OMEGA  BLOCK(5)
 0.0253964  ;   27 BSVX0
 0.00787165 0.00965573  ;  28 BSVXSS
 -0.0831085 0.00887115 0.979314  ;  29 BSVREP
 0.0117627 0.00499615 -0.0379866 0.0421083  ;  30 BSVWT0
 0.00559706 0.00649501 -0.00226264 0.0369625 0.0494914  ; 31 BSVRWT120
;--------------------------------------------------------------------
```

```
$OMEGA  BLOCK(2)
 0.05392  ; 32 BSV RUVBDQ
 0.0295137 0.0522882  ; 33 BSV RUVM2
;---------------------------------------------------------------------- ----------------------------------
$SIGMA  0.00500974  ; 1 Prop error ALB
 0.00114573  ; 2 Prop error WT
$SIGMA  BLOCK(2)
 0.0518161  ; 3 Prop error TMC
 0.0189319 0.0366836  ; 4 Prop error M2$ESTIMATION METHOD=1 MAXEVAL=9999 PRINT=1
SIGL=9 NSIG=3 NOABORT INTERACTION
;---------------------------------------------------------------------- ----------------------------------
$ESTIMATION MSFO=run712.msf MAXEVAL=0 PRINT=1 METHOD=1 INTER NOABORT
        NSIG=3 NONINFETA=1 ETASTYPE=1 ; REPEAT

;As the model becomes more complex, you can use MATRIX=S and then remove the
$COVARIANCE step completely when the model is too complex to obtain precisions

;$COVARIANCE PRINT=E MATRIX=S UNCONDITIONAL

;---------------------------------------------------------------- ----------------------------------------
$TABLE     WRESCHOL ID OCC TIME TAD AA1 AA2 ; AA3 AA4
        Y DV PRED RES WRES IPRED IRES IWRES CWRES CWRESI OBJI
        NOPRINT NOAPPEND ONEHEADER FORMAT=, FILE=sdtab712.csv
;---------------------------------------------------------------------- ----------------------------------
$TABLE     ID KA MAT FR MTT CL V Q1 VP1 Q2 VP2 CLM2 VM2 X0 XSS REP
        WT0 WT120 BOVBIO BOVMTT BSVBIO BSVCL BSVV BSVQ BSVCLM
        BSVVM BSVRUV1 BSVRUV2 BSVX0 BSVXSS BSVREP BSVWT0 VARCL
        VARBIO VARAUC NOPRINT NOAPPEND ONEHEADER FORMAT=,
        FILE=patab712.csv
;-----------------------------------------------------------------------------------------------------------
$TABLE     ID OCC WT HT FFM FAT VPCTIME DOSE GESTATION GESTWEEKS
        EFV_DAYS PK_EFV_DAYS NOPRINT NOAPPEND ONEHEADER FORMAT=,
        FILE=cotab712.csv
;---------------------------------------------------------------------------- ------------------------------
$TABLE     ID OCC SEX VISIT DVID VOMITED DVID_VISIT PREVTB RESISTANCE
        EMITRICITABINVE EFAVIRENZ NEVIRAPINE LAMIVUDINE
        DOLUTEGRAVIR ABACAVIR LOPINAVIR RITONAVIR ZIDOVUDINE
        STAVUDINE NOPRINT NOAPPEND ONEHEADER FORMAT=,
        FILE=catab712.csv
;-------------------------------------------------------------------------------------------------------------------
$TABLE     ID OCC TIME VISIT DVID VPCTIME TAD AA1 AA2 MDV EVID AA3
        AA4 AA5 AA6 AA7 AA8 NDV CONC1  Y DV PRED RES WRES
        IPRED IRES IWRES CWRES CWRESI OBJI ID KA MAT FR MTT CL V
        Q1 VP1 Q2 VP2 CLM2 VM2 X0 XSS REP WT0 WT120 BOVBIO BOVMTT
        BSVBIO BSVCL BSVV BSVQ BSVCLM BSVVM BSVRUV1 BSVRUV2 BSVX0
        BSVXSS BSVREP BSVWT0 VARCL VARBIO VARAUC WT HT FFM FAT SEX
        VOMITED DOSE PROBLEM L2 DVID_VISIT GESTATION GESTWEEKS AGE
```

```
        CD4 PREVTB RESISTANCE EMITRICITABINVE EFAVIRENZ NEVIRAPINE
        LAMIVUDINE DOLUTEGRAVIR ABACAVIR LOPINAVIR RITONAVIR
        ZIDOVUDINE STAVUDINE EFV_DAYS DVID_VISIT_RTV PK_EFV_DAYS
        NOPRINT NOAPPEND ONEHEADER FORMAT=, FILE=mytab712.csv
;------------------------------------------------------------------------------- ----------------------------
```

Final NONMEM scripts for results presented in chapter 4 supplemental Milk data

```
;; 1. Based on: 763
;; 2. Description: -BSVACC & ERR vs EPS
;; x1. Author: user
; Settings for the memory of NONMEM
$SIZES      PD=-1000 LVR=-150 LTH=-200 MAXFCN=10000000 LNP4=-150000
$PROBLEM    NAME_OF_THE_PROJECT
$INPUT      ID OCC VISIT TIME DAT2=DROP PID=DROP NOMINAL_TIME=DROP
        WHAT=DROP ST_VISIT=DROP DV M2DV MDV DVID OCC1 EVID AMT
        VPCTIME HT WT DAY=DROP FIXED_IN_R=DROP PARTICIPANT_ID=DROP
        VOMITED INFANTS_WEIGHT INFANTS_LENGTH BREASTFED EXCLUSIVE1
        DOSE PROBLEM LL2 LDV CMT MOLDV LMOLDV GESTATION GESTWEEKS
        AGE CD4 PREVTB RESISTANCE EMITRICITABINVE EFAVIRENZ
        NEVIRAPINE LAMIVUDINE DOLUTEGRAVIR ABACAVIR LOPINAVIR
        RITONAVIR ZIDOVUDINE STAVUDINE EFV_DAYS PK_EFV_DAYS
        GEST_AGE GEST_AGE1 ALB CONC1 IKA IMAT IMTT ICL IV IQ1 IVP1
        IQ2 IVP2 ICLM2 IVM2 IX0 IXSS IIREP IWT0 IWT120 IFR
; IGNORE=@ will skip any line starting with any non-numerical character
$DATA       Milk_PK_data_2022.csv IGNORE=#
        IGNORE(DVID==1,DVID==2,DVID==3,DVID==4)


$ABBREVIATED DERIV2=NO ; Prevents  the computation of second derivatives,which are
needed only for the Laplacian method.


$SUBROUTINE ADVAN13 TRANS1 TOL=9 ; TOL is the precision to solve differential equations
        ATOL=6 ; absolute tolerance,10^ATOL of your dose unit. A lower value makes the
model run faster

$MODEL      NCOMPARTMENTS=10 COMP=(DEPOT DEFDOSE) COMP=(BDQC)
        COMP=(BDQPERI1) COMP=(BDQPERI2) COMP=(M2) COMP=(TRANSI1)
        COMP=(TRANSI2) COMP=(ALBUMIN) COMP=(BDQ_MILK)
        COMP=(M2_MILK)
;-------------------------------------------------------------------------------------------------------------------
---------------------
$PK

 IF (OCC==0) THEN
BOVACC = 0
M2_BOVACC = 0
```

```
 ENDIF


BOVACC=ETA(1)
IF(OCC.EQ.1)  BOVACC=ETA(2)
IF(OCC.EQ.3)  BOVACC=ETA(3)
IF(OCC.EQ.4)  BOVACC=ETA(4)


M2_BOVACC=ETA(5)
IF(OCC.EQ.1)  M2_BOVACC=ETA(6)
IF(OCC.EQ.3)  M2_BOVACC=ETA(7)
IF(OCC.EQ.4)  M2_BOVACC=ETA(8)

BSVKE0 = ETA(9)
BSVACC = ETA(10)
M2_BSVKE0 = ETA(11)
M2_BSVACC = ETA(12)
; ---------- Calculation of Fat-free Mass
; These formulas require WT in KG and HT in m !!!

; Conversion from cm to m
HTM = HT/100
SEX = 0
IF (SEX.EQ.0) THEN  ; female
          WHSMAX=37.99
          WHS50=35.98
ELSE       ;males
          WHSMAX=42.92
          WHS50=30.93
ENDIF
HTM2 = HTM**2
FFM = (WHSMAX*HTM2*WT)/(WHS50*HTM2+WT)
FAT = WT-FFM

; ------- Typical values of covariates
TVWT = 70
TVFAT =24
TVFFM = 40

;--------- Allometric scaling and covariates
ALLMCL_WT = (WT/TVWT)**0.75
ALLMV_WT = (WT/TVWT)

ALLMCL_FAT = (FAT/TVFAT)**0.75
ALLMV_FAT = (FAT/TVFAT)
```

```
ALLMCL_FFM = (FFM/TVFFM)**0.75
ALLMV_FFM = (FFM/TVFFM)
;-----------------------------


;---------Typical  values----------------------------------------------------------------------------------------------
-----------------------------------------------------------
;--- Model for Albumin
TVX0 = IX0
TVXSS = IXSS
TVREP = IIREP
X0 = TVX0;*EXP(BSVX0)
XSS = TVXSS;*EXP(BSVXSS)
REP = TVREP;*EXP(BSVREP)
HL = LOG(2)/REP
A_0(8) = 3.5

;--- Model for weight
TVWT0 = IWT0
TVWT120 = IWT120


WT0 = TVWT0;*EXP(BSVWT0)
WT120 = TVWT120;*EXP(BSVWT120)
SLOPE = (WT120 - WT0)/(120*7*24) ; TIME in hours, 120 weeks
;--- BDQ and M2 PK

FR = IFR ; Fraction of MAT that is delay
MTT = IMTT
KAHL= IMAT*(1-FR)/3.3
KA = IKA
KTR= 2/MTT
F1= 1;*EXP(BOVBIO+BSVBIO)
; AMT in mg in input file, MW TMC207 555.5 g/mol, DV as nmol/mL = µmol/L -->
;(AMT/1000)/(555.5)*1000000 = AMT*1.8002 µmol

CL = ICL ; CLB*COVALBI*ALLCL
V =  IV
Q1 = IQ1
VP1 = IVP1
Q2 = IQ2
VP2 = IVP2
CLM2 = ICLM2
VM2 = IVM2
```

```
BDQ_KE0 = THETA(1)*EXP(BSVKE0)
BDQ_ACCUM_FACTOR = THETA(2)*EXP(BOVACC+BSVACC)

M2_KE0 = THETA(1)*EXP(M2_BSVKE0)
M2_ACCUM_FACTOR = THETA(4)*EXP(M2_BSVACC+M2_BOVACC)


$DES

DADT(1)= -KTR*A(1)
DADT(2) = A(7)*KA - A(2)*CL/V - A(2)*Q1/V + A(3)*Q1/VP1 - A(2)*Q2/V + A(4)*Q2/VP2 ; BDQ
DADT(3) = A(2)*Q1/V - A(3)*Q1/VP1
DADT(4) = A(2)*Q2/V - A(4)*Q2/VP2
DADT(5) = A(2)*CL/V - A(5)*CLM2/VM2 ; M2
DADT(6) = A(1)*KTR - A(6)*KTR ; transit1
DADT(7) = A(6)*KTR - A(7)*KA ; transit2

  C2     =  A(2)/V                    ;Turn amounts into concentrations
  C5     =  A(5)/VM2

;-------------------------------------------------------------------------------------------------------------------
--
;BDQ concentration in MILK
 C9 = A(9)
 DADT(9) =  BDQ_KE0*BDQ_ACCUM_FACTOR*C2-BDQ_KE0*A(9)                    ;Differential
equation for effect compartment
 ;-------------------------------------------------------------------------------------------------------------------
---
;M2 concentration in MILK
 C10 = A(10)
 DADT(10) =  M2_KE0*M2_ACCUM_FACTOR*C5-M2_KE0*A(10)                    ;Differential
equation for effect compartment

;SCALE_MOLES=541.47/555.50 ;555.50 g/mol for bedaquiline and 541.47 g/mol for M2


$ERROR
SCALE_MOLES=541.47/555.50 ;555.50 g/mol for bedaquiline and 541.47 g/mol for M2


; ; --- Body weight
 WTTIMEE = WT0 + TIME*SLOPE

DEL= 1E-12
CONC_BDQ=A(2)/V
CONC_M2=(A(5)/VM2)*SCALE_MOLES
CONC_ALB= A(8)
```

```
CONC_WT= WTTIMEE
BDQ_MK=A(9)
M2_MK=A(10) * SCALE_MOLES
;No BLQ values were recorded for BDQ

BLQ=0
;-----------------------------------------------------------------------
; parent
IPRED_P=BDQ_MK

LLOQ_P = 0.078 ; DEFINE YOUR OWN LLOQ HERE
PROP_P = IPRED_P*THETA(7)
ADD_P = THETA(5)+(LLOQ_P*0.2)

;-------------------------------------------------------------------------------------
CENS=BLQ
;CENS_THR = LLOQ
IF (ICALL/=4.AND.CENS==1) THEN
        ADD_P = ADD_P +(LLOQ_P*0.5)
ENDIF

;---------------------------------------------------------------
NO_FIT = 0

IF (ICALL/=4.AND.CENS==2) THEN
        PROP_P = 0
        ADD_P = 10000000000
        NO_FIT = 1
ENDIF

W_P = SQRT((ADD_P)**2 + (PROP_P)**2)   ; PK(Parent)

;-----------------------------------------------------------------------
;metabolite
IPRED_M = M2_MK
LLOQ_M  = 0.0312;mg/L
PROP_M  = IPRED_M * THETA(8)
ADD_M   = 0.2*LLOQ_M + THETA(6)

;-------------------------------------------------------------------------------------
CENS=BLQ
;CENS_THR = LLOQ_M
IF (ICALL/=4.AND.CENS==1) THEN
        ADD_M = ADD_M +(LLOQ_M*0.5)
ENDIF

;---------------------------------------------------------------
```

```
NO_FIT = 0

IF (ICALL/=4.AND.CENS==2) THEN
        PROP_M = 0
        ADD_M = 10000000000
        NO_FIT = 1
ENDIF

W_M = SQRT((ADD_M)**2 + (PROP_M)**2)   ; PK(Metabolite)

;Error & Correlation----------------------------------------------------

;CENS_THR =0.3*LLOQ          ; check the readme section
;Redefine IPRED & weighting-----------------------------------------------------------------------
IPRED = IPRED_P
W = W_P
LLOQ=LLOQ_P
PROP = PROP_P
ADD = ADD_P

IF (DVID==6) THEN
IPRED = IPRED_M
W = W_M
LLOQ= LLOQ_M
PROP = PROP_M
ADD = ADD_M
ENDIF
; Protective code
IF (W.LE.0.000001) W=0.000001
IRES=DV-IPRED
IWRES=IRES/W
Y = IPRED + W*EPS(1)
; To prevent simulation (ICALL==4) of negative values. It set a positive lower bound for Y, so
that VPCs in the log-scale can be plotted
IF (ICALL==4.AND.Y<=LLOQ) Y = LLOQ/2
;-------------------------------------------------------------------------------------------------

; To calculate time after dose.
IF(AMT>0) THEN
        TIMEDOSE = TIME
        AMOUNTDOSE = AMT
ENDIF

TAD = TIME-TIMEDOSE

;----------------------------------------RETRIEVE AMOUNT IN EACH COMPARTMENT----------------
AA1 = A(1)
```

```
AA2 = A(2)
AA3 = A(3)
AA4 = A(4)
AA5 = A(5)
AA6 = A(6)
AA7 = A(7)
AA8 = A(8)
AA9 = A(9)
AA10 = A(10)
;-----------------------------------------------------------------------------------------------------------------------
$THETA  (0,0.113268,0.444921) ; 1 KE0_BDQ
 (0,12.3115) ; 2 ACCUM_FACTOR_BDQ
 (0,0) FIX ; 3 KE0_M2
 (0,3.9043) ; 4 ACCUM_FACTOR_M2
 (0,0) FIX ; 5 ADD_ERROR_BDQ
 (0,0) FIX ; 6 ADD_ERROR_M2
 (0,0.162209) ; 7 Prop_error_BDQ
 (0,0.175277) ; 8 Prop_error_M2
;-----------------------------------------------------
$OMEGA  BLOCK(1) FIX
 0  ;   1 BOVACC
$OMEGA  BLOCK(1) SAME
$OMEGA  BLOCK(1) SAME
$OMEGA  BLOCK(1) SAME
;-------------------------------------------------------------------------------------------
$OMEGA  BLOCK(1) FIX
 0  ; 5 M2_BOVACC
$OMEGA  BLOCK(1) SAME
$OMEGA  BLOCK(1) SAME
$OMEGA  BLOCK(1) SAME
;-------------------------------------------------------------------------------------------
$OMEGA  BLOCK(1) FIX
 0  ;   9 BSVKE0
$OMEGA  BLOCK(1)FIX
0 ;  10 BSVACC
$OMEGA  BLOCK(1) FIX
 0  ; 11 M2_BSVKE0
$OMEGA  BLOCK(1) FIX
 0  ; 12 M2_BSVACC
$SIGMA  1  FIX
;-----------------------------------------------------------------------------------------------------------------------
$ESTIMATION MSFO=run765.msf MAXEVAL=9999 PRINT=1 METHOD=1 INTER
        NOABORT NSIG=3 NONINFETA=1 ETASTYPE=1 ; REPEAT

;As the model becomes more complex, you can use MATRIX=S and then remove the
$COVARIANCE step completely when the model is too complex to obtain precisions
$COVARIANCE PRINT=E MATRIX=S UNCONDITIONAL
```

```
;-----------------------------------------------------------------------------------------------------------------------
$TABLE      WRESCHOL ID OCC TIME TAD AA1 AA2 ; AA3 AA4
            Y DV PRED RES WRES IPRED IRES IWRES CWRES CWRESI OBJI
            NOPRINT NOAPPEND ONEHEADER FORMAT=, FILE=sdtab765.csv
;-----------------------------------------------------------------------------------------------------------------------
$TABLE      ID BDQ_KE0 BDQ_ACCUM_FACTOR M2_ACCUM_FACTOR M2_KE0 BOVACC
            BSVKE0 BSVACC M2_BOVACC M2_BSVKE0 M2_BSVACC KA FR MTT CL V
            Q1 VP1 Q2 VP2 CLM2 VM2 X0 XSS REP WT0 WT120 NOPRINT
            NOAPPEND ONEHEADER FORMAT=, FILE=patab765.csv
;-----------------------------------------------------------------------------------------------------------------------
$TABLE      ID OCC WT HT FFM FAT VPCTIME DOSE GESTATION GESTWEEKS
            EFV_DAYS PK_EFV_DAYS NOPRINT NOAPPEND ONEHEADER FORMAT=,
            FILE=cotab765.csv
;-----------------------------------------------------------------------------------------------------------------------
$TABLE      ID OCC SEX VISIT DVID VOMITED DVID_VISIT PREVTB RESISTANCE
            EMITRICITABINVE EFAVIRENZ NEVIRAPINE LAMIVUDINE
            DOLUTEGRAVIR ABACAVIR LOPINAVIR RITONAVIR ZIDOVUDINE
            STAVUDINE NOPRINT NOAPPEND ONEHEADER FORMAT=,
            FILE=catab765.csv
;-----------------------------------------------------------------------------------------------------------------------
$TABLE      ID OCC TIME VISIT DVID VPCTIME TAD AA1 AA2 MDV EVID AA3
            AA4 AA5 AA6 AA7 AA8 AA9 AA10 CONC_BDQ CONC_M2 CONC_ALB
            CONC_WT Y DV PRED RES WRES IPRED IRES IWRES CWRES CWRESI
            OBJI ID ADD PROP BDQ_KE0 BDQ_ACCUM_FACTOR M2_ACCUM_FACTOR
            M2_KE0 BOVACC BSVKE0 BSVACC M2_BOVACC M2_BSVKE0 M2_BSVACC
            KA FR MTT CL V Q1 VP1 Q2 VP2 CLM2 VM2 X0 XSS REP WT0 WT120
            WT HT FFM FAT SEX VOMITED DOSE PROBLEM LL2 DVID_VISIT
            GESTATION GESTWEEKS AGE CD4 PREVTB RESISTANCE
            EMITRICITABINVE EFAVIRENZ NEVIRAPINE LAMIVUDINE
            DOLUTEGRAVIR ABACAVIR LOPINAVIR RITONAVIR ZIDOVUDINE
            STAVUDINE EFV_DAYS DVID_VISIT_RTV PK_EFV_DAYS NOPRINT
            NOAPPEND ONEHEADER FORMAT=, FILE=mytab765.csv
;-----------------------------------------------------------------------------------------------------------------------
------------------------------
```

Final NONMEM scripts for results presented in chapter 5

```
$SIZES      PD=-1000 LVR=-150 LTH=-200 MAXFCN=10000000 LNP4=-150000
$PROBLEM    A5312_INH
$INPUT      ID VISNO PATID DAT2=DROP TIME OCC SCHDHR WHAT=DROP MDV
            EVID DV AMT SSS=DROP III=DROP DRUG=DROP PKWEIGHT
            PATIENT_VIS=DROP NMDRUGCODE PKSAMPLENO VOMITED PKDAYTYPE
            TYPE VPCTIME EMBAD ETHAD INHAD KANAD MOXAD PZAAD TERAD
            SEX2_FEMALE WEIGHT HEIGHT AGE HIV1_POS IVDRUG HIVCD4COUNT
            ASTHMACOPD DIABETES SMOKING ALCOHOLUSE RESPIRATORYRATE
            PULSE XRAYZONES1 XRAYZONES2 XRAYZONES3 XRAYZONES6
            PREVIOUSTB COMPLETEDTREATMENT_1 CREATINEFIN POTASSIUMFIN
            EGFRFIN ALTFIN TSHFIN T4FIN TIMEON_RX TIMEON_ART LIDOC_SUB
```

```
        CRUSHED_SUB KANAAMT EMBAMT ETHAMT INHAMT PZAAMT CYCAMT
        LNINH INH_PROB MOXI_PROB EFVDOSE EFVDAYS EFAVIRENZ DOSE
        INHDOSE INH_DOSE BLQ CAVITIES FASTING1 ARM BMI RACETH
        RACE1 AGECAT BMI_GRP NAT NNAT2 PR PI PS STUDY EFVDOSE1
        EFVDIFF EFV ETHAMT1 ETHDIFF ETHDIFF1 ETHI PROBLEM T_EMB
        T_ETHIO T_INH T_KANA T_MOXY T_PZA T_TERIZ EMB_AUC MOX_AUC
        PZA_AUC ETH_AUC CYC_AUC KANA_AUC CMT
; IGNORE=@ will skip any line starting with any non-numerical character
$DATA     A5312PODtb_PKNONMEM.2020-09-04.csv IGNORE=#
        IGNORE(PROBLEM.EQ.1)
$ABBREVIATED PROTECT
;IGNORE=(BLQ.GT.0)
$ABBREVIATED COMRES=2
$SUBROUTINE ADVAN13 TOL=9 ;TOL is the precision to solve differential equations
        ATOL=9 ; absolute tolerance,10^ATOL of your dose unit. A lower value makes the
model run faster

$MODEL     NCOMPARTMENTS=5 COMP=(ABS,DEFDOSE) COMP=(CENTRAL)
        COMP=(PERI) COMP=(LIVER) COMP=(AUC INITIALOFF)
;------------ ----------------------------------------------------------------------------------------------------
$PK
;initialise compartments
A_0(1)=0.00000001
A_0(2)=0.00000001 ; An average steady state value
A_0(3)=0.00000001
A_0(4)=0.00000001
; ---------- BOV
BOVCL = ETA(7)
IF(OCC.EQ.2) BOVCL = ETA(8)
IF(OCC.EQ.3) BOVCL = ETA(9)
IF(OCC.EQ.4) BOVCL = ETA(10)
BOVV = ETA (11)
IF(OCC.EQ.2) BOVV = ETA(12)
IF(OCC.EQ.3) BOVV = ETA(13)
IF(OCC.EQ.4) BOVV = ETA(14)
BOVKA=ETA(15)
IF(OCC.EQ.2)  BOVKA=ETA(16)
IF(OCC.EQ.3)  BOVKA=ETA(17)
IF(OCC.EQ.4)  BOVKA=ETA(18)

BOVMTT = ETA(19)
IF(OCC.EQ.2)  BOVMTT=ETA(20)
IF(OCC.EQ.3)  BOVMTT=ETA(21)
IF(OCC.EQ.4)  BOVMTT=ETA(22)
TV_BOVBIO=ETA(23)
IF(OCC.EQ.2)  TV_BOVBIO=ETA(24)
IF(OCC.EQ.3)  TV_BOVBIO=ETA(25)
```

```
IF(OCC.EQ.4)  TV_BOVBIO=ETA(26)
BVVCL = ETA(27)
IF(VISNO == 2) BVVCL=ETA(28)
BVVV = ETA(29)
IF(VISNO == 2) BVVV=ETA(30)
; ------- BSV
BSVCL   = ETA(1)
BSVV   = ETA(2)
BSVKA   = ETA(3)
BSVBIO = ETA(4)
BSVV3 = ETA(5)
BSVQ = ETA(6)
; ---------- Calculation of Fat-free Mass
; These formulas require WT in KG and HT in m !!!
WT      = PKWEIGHT
IF(PKWEIGHT==-99) WT = WEIGHT
HT      = HEIGHT
IF(HEIGHT==-99) HT = 166.5
; Conversion from cm to m
HTM = HT/100
IF (SEX2_FEMALE.EQ.2) THEN  ; female
          WHSMAX=37.99
          WHS50=35.98
ELSE       ;males
          WHSMAX=42.92
          WHS50=30.93
ENDIF
HTM2 = HTM**2
FFM = (WHSMAX*HTM2*WT)/(WHS50*HTM2+WT)
FAT = WT-FFM
; ------- Typical values of covariates
TVWT = 51
TVFAT = 7
TVFFM = 44
;--------- Allometric scaling and covariates
ALLMCL_WT = (WT/TVWT)**0.75
ALLMV_WT = (WT/TVWT)
ALLMCL_FAT = (FAT/TVFAT)**0.75
ALLMV_FAT = (FAT/TVFAT)
ALLMCL_FFM = (FFM/TVFFM)**0.75
ALLMV_FFM = (FFM/TVFFM)
; Allometry for liver
ALLMCL_WT_HEP = (WT/70)**0.75
ALLMV_WT_HEP = (WT/70)
ALLMCL_FFM_HEP = (FFM/56.1)**0.75
ALLMV_FFM_HEP = (FFM/56.1)
;------------------identifying mutation----------------------------
```

```
MUTATION=1  ; INHA mutation
IF(ARM.EQ.4) MUTATION  =  2 ;No mutation
;----------------------------------------------------------------------
;---------Effect of NAT2 on CL--
VNAT = NNAT2
IF(NNAT2.LT.0 .AND. MIXNUM.EQ.1) VNAT = 0
IF(NNAT2.LT.0 .AND. MIXNUM.EQ.2) VNAT = 1
IF(NNAT2.LT.0 .AND. MIXNUM.EQ.3) VNAT = 2
ETH=0
IF(ETHI.GE.1) ETH=1
;-------VPC variables
NAT_CRU_DOS=STUDY*10000+ VNAT*1000+ABS(CRUSHED_SUB)*10+INHDOSE
CRU_DOS=STUDY*10000+ ABS(CRUSHED_SUB)*10+INHDOSE
DNAT = STUDY*100+ INHDOSE*10 + VNAT
NATD = STUDY*100+ VNAT*10 + INHDOSE
SINHDOSE =  STUDY*10000 + INHDOSE
SVNAT =  STUDY*10000 + VNAT
NATD_ETH = STUDY*10000+ETH*100+ VNAT*10 + INHDOSE
STUDYD = STUDY*10+ INHDOSE
FFMDOSE = DOSE/FFM
;----------------------------------------------------------------------
;INH dosing time
BINH_EMB=-99
IF(T_EMB.GT.0.AND.STUDY.EQ.2) BINH_EMB=0
IF(T_EMB.LE.0.AND.STUDY.EQ.2) BINH_EMB=1
BINH_ETHIO=-99
IF(T_ETHIO.GT.0.AND.STUDY.EQ.2) BINH_ETHIO=0
IF(T_ETHIO.LE.0.AND.STUDY.EQ.2) BINH_ETHIO=1
BINH_KANA=-99
IF(T_KANA.GT.0.AND.STUDY.EQ.2) BINH_KANA=0
IF(T_KANA.LE.0.AND.STUDY.EQ.2) BINH_KANA=1
BINH_MOXY=-99
IF(T_MOXY.GT.0.AND.STUDY.EQ.2) BINH_MOXY=0
IF(T_MOXY.LE.0.AND.STUDY.EQ.2) BINH_MOXY=1
BINH_PZA=-99
IF(T_PZA.GT.0.AND.STUDY.EQ.2) BINH_PZA=0
IF(T_PZA.LE.0.AND.STUDY.EQ.2) BINH_PZA=1
BINH_TEZ=-99
IF(T_TERIZ.GT.0.AND.STUDY.EQ.2) BINH_TEZ=0
IF(T_TERIZ.LE.0.AND.STUDY.EQ.2) BINH_TEZ=1
;---------Effect of NAT2 on CL--
TVCL_NAT =  THETA(1) ; intermediate
IF(VNAT.EQ.0) TVCL_NAT =  THETA(7) ;FAST
IF(VNAT.EQ.2) TVCL_NAT =  THETA(8) ;Slow
;----------Efect of study on bio----
TVBIO_STUDY =1
IF(STUDY.EQ.2 ) TVBIO_STUDY =  THETA(4)* (1+THETA(24)*(INH_DOSE - 10)) ;PODtd study
```

```
; ;----------Efect of CRUSHED on MTT----
; TVMTT_CRU =  THETA(11)
; IF(CRUSHED_SUB.EQ.1) TVMTT_CRU =  THETA(21) ;CRUSHED
;----------Efect of study on bio----
TVCL_ETHI =1
IF(ETHI.GE.1) TVCL_ETHI = (1+THETA(22)) ;On ethionamide
;----------Efect of study on BOVBIO----
BOVBIO = TV_BOVBIO
IF(STUDY.EQ.2) BOVBIO = TV_BOVBIO*THETA(20) ;PODtd study
;---------Typical values--------------------------------------------------------------------
TVCL = TVCL_NAT*TVCL_ETHI*ALLMCL_FFM
TVV = THETA(2)*ALLMV_FFM
TVKA = THETA(3)
TVBIO = TVBIO_STUDY
; TVLAG = THETA(7)
 TVV3 = THETA(9)*ALLMV_FFM
 TVQ = THETA(10)*ALLMCL_FFM
TVMTT   = THETA(11)
NN      = THETA(12)
;------------------- ----------------------------------------------------------------------------
TVQH=THETA(13)*ALLMCL_FFM_HEP   ; PLASMA FLOW RATE
TVFU=THETA(14)         ; UNBOUND PLASMA FRACTION OF INH
TVVH=THETA(15)*ALLMV_FFM_HEP
;-----------Define parameters----------------------------------------------------------------------
CL  = TVCL*EXP(BSVCL+BOVCL+BVVCL) ; CLEARANCE
V   = TVV*EXP(BSVV+BVVV+BOVV) ; CENTRAL VOL.
KA  = TVKA*EXP(BSVKA+BOVKA) ; ABS. RATE CONSTANT
BIO = TVBIO*EXP(BSVBIO+BOVBIO) ; BIOAVAILABILITY
; LAG =TVLAG*EXP(BOVLAG) ; LAG TIME
 V3 = TVV3*EXP(BSVV3) ; PERIPH VOL
 Q = TVQ*EXP(BSVQ) ; INTER COMPT CL
MTT = TVMTT*EXP(BOVMTT)
QH=TVQH
VH=TVVH
FU=TVFU
CLINT=CL
;-------------------------SATURABLE----------------------------------------;
      LOGKM = THETA(16) ; LOG KM - claculated from data set - median of max conc in the liver
      VMAX  = CLINT*EXP(LOGKM) ; max enzimatic rate from eq. CLint = Vmax/KM

;---------------- CODE for TRANSIT COMPARTMENT -----------------------------------
F1=0 ; I need to set bioavailability in compartment 1 to 0 for this implementation of the transit
compartment absorption
IF(CRUSHED_SUB.EQ.1)F1=BIO

KTR = (NN+1)/MTT
IF (NEWIND/=2.OR.EVID>=3) THEN ; new individual, or reset event
```

```
   ; The values read here will be stored in TDOS and PD in this very PK call.
        TNXD=TIME ; Time of the dose
        PNXD=AMT ; Amount. If it's zero, the DE is deactivated.
ENDIF
TDOS=TNXD ; This will either save here the temporary values if it's a new individual...
PD=PNXD ; ...or the values which were read one record ahead during the execution of the previous record.
IF(AMT>0.AND.CRUSHED_SUB.LE.0) THEN ; This reads one record ahead and stores the data to be used when running the following record
; IF(AMT.GT.0.AND.ALAG1.EQ.0) THEN ; Use this INSTEAD if there is ALAG, as it will also checks if the ALAG is not 0. Note that you normally do not want to include both ALAG and transit, this is a very exceptional case
        TNXD=TIME
        PNXD=AMT
ENDIF
; Uncomment this if you have ALAG or if you use ADDL
; IF (DOSTIM>0) THEN ; This will account for the ADDL or lagged doses. It will overwrite the time, if it a non-event record
;       TNXD=DOSTIM
;       PNXD=AMT
; ENDIF
; To speed up the computation, I calculate here all the non-time-varying quantities used in $DES
PIZZA = LOG(BIO*PD*KTR + 0.00001) - GAMLN(NN+1)  ; without +0.00001, it won't work with ETAs in bioavailability
; IF(NEWIND.LE.1.OR.EVID.GE.3) THEN ; assign negative Cmax Tmax for the new subject
    ; COM(1)=-1 ; holder of Cmax
    ; COM(2)=-1 ; holder of Tmax
; ENDIF
IF (NEWIND.NE.2.OR.EVID.GE.3) THEN ; Each time I have a new subject, or a reset
        COM(1)=0
        COM(2)=0
        TDOS = 0
ENDIF
;------ ---------------------------------------------------------------------------------------
S2=V
;---------------------------------- ---------------------------------------------------------------------
$DES
;--------  Transfer constants for liver model ---------
; define hepatic extraction
 CH = A(4) / VH ; drug conc in liver
    ; set saturable elimindation to zero for pts with negative concentrations in liver
    ; product of a logarith cannot be negative - this would not work
    ; normal Michalis-Mentel equation gives you a rate =k*A = CL*C
    ; but we want to get CL, so you divide the rate by concentration - and get saturable clearance
    ; equation is placed in $DES because saturable clearance changes over time
```

```
      SAT_CL=0
      IF (CH>0) SAT_CL=VMAX/(1+EXP(-(LOG(CH)-LOGKM))) / (CH)
     ;transformation based on better Emax model, wider search in log parametrisation

     EH  = (SAT_CL*FU)/((SAT_CL*FU)+QH) ; fraction undergoing first pass extraction
     FH  = 1 - EH ;fraction available after 1st pass to go to systemic circulation
; COMPUTE RATE CONSTANTS
K32  = Q/V3   ; from peripheral to central
K23 = Q/V     ; from central to peripheral
K24 = (QH/V)   ; from central to Liver
K42 = (QH*FH/VH) ; from liver to central

K40 = (QH*EH/VH) ; elimination rate in liver
TEMPO=T-TDOS ; this is time after dose, it should always be >= 0
KTT=0
DADT(1)=-KA*A(1)
IF(PD.GT.0.AND.TEMPO.GT.0.AND.CRUSHED_SUB.LE.0) THEN ; This happens only id PD>0, so
only if a dose has been detected
   KTT=KTR*(TEMPO)
   DADT(1)=EXP(PIZZA+NN*LOG(KTT)-KTT)-KA*A(1)
ENDIF

DADT(2) = K42*A(4)-K24*A(2)-K23*A(2)+K32*A(3)
DADT(3) = K23*A(2) -K32*A(3)
DADT(4) = KA*A(1)-K42*A(4)+K24*A(2)-K40*A(4)

 CP = A(2)/V              ; plasma concentration
 IF (CP.GE.COM(1)) THEN
          COM(1) = CP             ; CMAX
          COM(2) = TEMPO          ; TIME OF CMAX
ENDIF
DADT(5) = CP
;---------------------------------------------------------------
$ERROR
IPRED = A(2)/V
IRES = DV-IPRED
LLOQ=0.105 ; INH LLOQ in ug/ml
    IMPUTED_BLQ=LLOQ/2
PROP = IPRED*THETA(5)
ADD =  0.2*LLOQ + THETA(6)
IF(STUDY.EQ.2)ADD =  0.2*LLOQ + THETA(23)
; For ADD, in this case we are coding THETA(.) as the additive error on top of 20% of the LLOQ.
; So the lower bound of THETA(.) can be zero. If it goes to zero, we can fix it, and the additive
error
; will then be constrained to 20% of LLOQ + the value in THETA(.).
; REMEMBER about this when you report the value of ADD and its uncertainty! NONMEM
gives uncertainty on THETA, not ADD
```

```
; An alternative approach is to set the lower bound of the THETA for the additive error to 20% of the LLOQ.
; In that case, one does not have to worry about adjusting the precision. On the other hand, this cannot be done if you have different LLOQs within your analysis (e.g. different labs)
; For BLQ==1 (i.e. first BLQ value in a series), we add extra additive error on the concentrations, since the value in DV has been imputed
IF(ICALL.NE.4.AND.BLQ==1) ADD = ADD + (LLOQ/2)
; For BLQ==2 (i.e. the trailing BLQ values in a series), we don't want these to influence the fit,
; we only want them for simulation-based diagnostics such as the VPC.
; So we define a separate error structure for these points. It has no proportional component
; (PROP = 0, as we would not want these points to affect our estimate of proportional error)
; and a FIXED and HUGE additive component (ADD = 1000000000, large with respect to the readings of concentration),
; so that the values do not affect the fit.
; It's also a good idea to repeat the diagnostic plots without the BLQ=2 points
IF(ICALL.NE.4.AND.BLQ==2) THEN
        PROP = 0
        ADD = 100000000
ENDIF
W = SQRT(ADD**2+PROP**2)
IF (W.LE.0.0001) W=0.0001
IWRES = IRES/W
Y = IPRED + W*ERR(1)
; To prevent simulation (ICALL==4) of negative values. It set a positive lower bound for Y, so that VPCs in the log-scale can be plotted
;IF (ICALL==4.AND.Y<=0.000001) Y=0.000001
; For simulation, like in case of VPC
   IF (ICALL==4.AND.Y<=LLOQ) THEN
          Y=IMPUTED_BLQ ; All BLQ values in simulation get imputed to LLOQ/2. This also prevents negative values
   ENDIF
; To calculate time after dose.
IF(AMT.GT.0) THEN
        TIMEDOSE = TIME
        AMOUNTDOSE = AMT
ENDIF
TAD = TIME-TIMEDOSE
VARCL = BSVCL + BOVCL
VARBIO = BSVBIO + BOVBIO
VARAUC = BSVBIO + BOVBIO - BSVCL - BOVCL
;----- -----RETRIEVE AMOUNT IN EACH COMPARTMENT
AA1 = A(1)
AA2 = A(2)
 AA3 = A(3)
 AA4 = A(4)
CMAX = COM(1) ; CMAX
TMAX = COM(2) ; TIME OF CMAX
```

```
IF(AMT.GT.0) THEN
        TDOS = TIME
        PD   = AMT
; Reset CMAX code when a new dose is given (e.g. every day)
        COM(1)=0
        COM(2)=0
ENDIF

AUC = A(5) ; AUC as obtained integrating the concentration in $DES
AUC_INF = DOSE * BIO / (CL*0.95); this works for any linear model, it is the theoretical AUC
from a "clean" single dose or SS. Use the final individual parameters for this


; ;------- -----Mixture modelling proportion of genotype----------
MIX_POP=MIXEST
MIX_PROB=MIXP
$MIX
NSPOP=3          ; 3 SUB-POPULATIONS (FAST INTERMIDEATE SLOW PHENOTYPE)

P(1) = THETA(17)        ; PROBABILITY OF FAST PHENOTYPE
P(2) = THETA(18)        ; PROBABILITY OF INTERMIDEATE
P(3) = THETA(19)        ; PROBABILITY OF SLOW


;-------------------------------- ----------------------------------------------------------------------------
$THETA  (0,29.6,200) ; 1 CL inter [L/h]
$THETA  (0,41.2,800) ; 2 V [L]
$THETA  (0,5.5,50) ; 3 KA [1/h]
$THETA  (0,0.345,5) ; 4 BIO_PODRTB
$THETA  (0,0.123,0.5) ; 5 PROP []
$THETA  (0,0,1) FIX ; 6 ADD [mg/L]
$THETA  (0,51.7,200) ; 7 CL_Fast [L/h]
$THETA  (0,12.5,200) ; 8 CL_SLOW [L/h]
; $THETA  (0,1,3) ; 7 LAG
$THETA  (0,9.97,2800) ; 9 V3 [L]
$THETA  (0,2.26,90) ; 10 Q [L/h]
$THETA  (0,0.154,5) ; 11 MTT
$THETA  (0,2.55,6) ; 12 NN
 (0,90,100) FIX ; 13 QH
 (0,0.95,1) FIX ; 14 FU
 (0,1,10) FIX ; 15 VH
 (0,2.97,100) ; 16 KM [LOG]
$THETA  (0.001,0.193,60) FIX ; 17 fast
$THETA  (0.001,0.4912,60) FIX ; 18 inter
$THETA  (0.001,0.3158,60) FIX ; 19 slow
$THETA  (0,2.96,800) ; 20 BOVBIO_scale_PODRTB
```

```
$THETA  (0,0,5) FIX ; 21 MTT_CRUSHED
$THETA  (-0.99,-0.295,5) ; 22 CL_ETHI
$THETA  (0,0,1) FIX ; 23 ADD_PODRTB [mg/L]
$THETA  (-0.11,0.0816,5) ; 24 BIO_PODRTB dose effect
;--------- -----------------------------------------------------------------------------
$OMEGA  BLOCK(1)
 0.103  ;   1 BSV CL
$OMEGA  BLOCK(1) FIX
 0  ;    2 BSV V
$OMEGA  BLOCK(1) FIX
 0  ;   3 BSV KA
$OMEGA  BLOCK(1) FIX
 0  ;  4 BSV BIO
$OMEGA  BLOCK(1) FIX
 0  ;    5 BSVV3
$OMEGA  BLOCK(1) FIX
 0  ;     6 BSVQ
;---------------------------- -----------------------------------------------------------------------------
$OMEGA  BLOCK(1) FIX
 0  ;    7 BOVCL
$OMEGA  BLOCK(1) SAME
$OMEGA  BLOCK(1) SAME
$OMEGA  BLOCK(1) SAME
;-----------------------------------------------------------------------------------------------------------------------
-------------------------------------------
$OMEGA  BLOCK(1) FIX
 0  ;    11 BOVV
$OMEGA  BLOCK(1) SAME
$OMEGA  BLOCK(1) SAME
$OMEGA  BLOCK(1) SAME
;------------------------------------------- -------------------------------------------------------------
$OMEGA  BLOCK(1)
 2.41  ;   15 BOVKA
$OMEGA  BLOCK(1) SAME
$OMEGA  BLOCK(1) SAME
$OMEGA  BLOCK(1) SAME
;------------------------------------------------ ------------------------------------------------
$OMEGA  BLOCK(1)
 1.12  ;  19 BOVMTT
$OMEGA  BLOCK(1) SAME
$OMEGA  BLOCK(1) SAME
$OMEGA  BLOCK(1) SAME
;---------------------------------------------- ------------------------------------------------
$OMEGA  BLOCK(1)
 0.0457  ;  23 BOVBIO
$OMEGA  BLOCK(1) SAME
$OMEGA  BLOCK(1) SAME
```

```
$OMEGA  BLOCK(1) SAME
;---------------------------------------------- ----------------------------------------------
$OMEGA  BLOCK(1) FIX
 0  ;   27 BVVCL
$OMEGA  BLOCK(1) SAME
;---------------------------------------- ----------------------------------------------
$OMEGA  BLOCK(1) FIX
 0  ;    29 BVVV
$OMEGA  BLOCK(1) SAME
;------------------------------------------------- ---------------------------------
$SIGMA  1  FIX
;------------------------------------------------- ---------------------------------
$ETAS      FILE=run485.phm TBLN=2
$ESTIMATION METHOD=1 INTERACTION MAXEVAL=0 MCETA=1000 RANMETHOD=4P PRINT=1 NOABORT SIGDIG=3 SIGL=9 NONINFETA=1 ETASTYPE=1
$ESTIMATION MSFO=run500.msf MAXEVAL=9999 MCETA=5 RANMETHOD=4P PRINT=1 METHOD=1 INTER NOABORT SIGDIG=3 SIGL=9 NONINFETA=1ETASTYPE=1
;As the model becomes more complex, you can use MATRIX=S and then remove the $COVARIANCE step completely when the model is too complex to obtain precisions
$COVARIANCE PRINT=E MATRIX=S UNCONDITIONAL
$TABLE      WRESCHOL ID OCC STUDY TIME DV BLQ VPCTIME TAD IPRED PRED IWRES WRES CWRES CWRESI OBJI AA1 AA2 AA3 AA4 NOPRINT NOAPPEND ONEHEADER FILE=sdtab500.csv FORMAT=,
$TABLE     ID OCC STUDY CL V KA V3 Q BIO NN MTT QH VH FU EH FH CH LOGKM VMAX BSVCL BSVV BSVKA BSVBIO BSVV3 BSVQ BOVCL BOVKABOVBIO BOVMTT VARCL VARBIO VARAUC NOPRINT NOAPPENDONEHEADER FILE=patab500.csv FORMAT=,
$TABLE        ID OCC WT HT AGE FAT BMI DOSE SCHDHR WEIGHT HEIGHT HIVCD4COUNT RESPIRATORYRATE PULSE CREATINEFIN POTASSIUMFIN EGFRFIN ALTFIN TSHFIN T4FIN TIMEON_RX TIMEON_ART KANAAMT EMBAMT ETHAMT EFVDOSE EFVDAYS INHAMT PZAAMT CYCAMT LNINH INH_DOSE FFMDOSE PR PI PS EFVDIFF T_EMB T_ETHIO T_INH T_KANA T_MOXY T_PZA T_TERIZ EMB_AUC MOX_AUC PZA_AUC ETH_AUC CYC_AUC KANA_AUC EFVDOSE1 ETHAMT1 ETHDIFF ETHDIFF1 NOPRINT NOAPPEND ONEHEADER FILE=cotab500.csv FORMAT=,
$TABLE        ID OCC STUDY BLQ NMDRUGCODE PKSAMPLENO VOMITED PKDAYTYPETYPE EMBAD ETHAD INHAD KANAD INHDOSE ARM NAT DNAT VNAT MOXAD PZAAD TERAD SEX2_FEMALE HIV1_POS IVDRUG ASTHMACOPD SMOKING ALCOHOLUSE XRAYZONES1 XRAYZONES2XRAYZONES3 XRAYZONES6 PREVIOUSTB COMPLETEDTREATMENT_1 LIDOC_SUB CRUSHED_SUB INH_PROB MOXI_PROB EFAVIRENZ FASTING1 NATD RACETH RACE1 AGECAT CAVITIES BMI_GRP MUTATION NNAT2 EFV ETHI PROBLEM STUDYD BINH_EMB BINH_ETHIO BINH_KANA BINH_MOXY BINH_PZA BINH_TEZ NOPRINT NOAPPEND ONEHEADER FILE=catab500.csv FORMAT=,
$TABLE     ID OCC TIME PATID VISNO TAD VPCTIME Y AMT MDV EVID DV DOSE AA2 AA3 AA4 PRED RES WRES IPRED IRES IWRES CWRES OBJI CMAX TMAX AUC AUC_INF CL V KA V3 Q BIO NN MTT QH VH FU EH FH CH LOGKM VMAX BSVCL BSVV BSVKA BSVBIO BSVV3 BSVQ BOVCL BOVKA BOVBIO BOVMTT VARCL VARBIO VARAUC WT HT FFM FAT SCHDHR NMDRUGCODE PKSAMPLENO VOMITED PKDAYTYPE TYPE EMBAD ETHAD INHAD KANAD MOXAD PZAAD TERAD SEX2_FEMALE  HEIGHT AGE HIV1_POS IVDRUG HIVCD4COUNT ASTHMACOPD
```

DIABETES SMOKING ALCOHOLUSE RESPIRATORYRATE PULSE XRAYZONES1 XRAYZONES2 XRAYZONES3 XRAYZONES6 PREVIOUSTB COMPLETEDTREATMENT_1 CREATINEFIN POTASSIUMFIN EGFRFIN ALTFIN FFMDOSE TSHFIN T4FIN TIMEON_RX TIMEON_ART LIDOC_SUB CRUSHED_SUB KANAAMT EMBAMT ETHAMT INHAMT PZAAMT CYCAMT LNINH INH_PROB MOXI_PROB EFVDOSE EFVDAYS EFAVIRENZ INHDOSE INH_DOSE BLQ CAVITIES FASTING1 ARM BMI RACETH RACE1 AGECAT BMI_GRP NAT NNAT2 PR PI PS STUDY EFVDOSE1 EFVDIFF EFV ETHAMT1 ETHDIFF ETHDIFF1 ETHI PROBLEM VNAT DNAT NATD MIX_POP MIX_PROB NAT_CRU_DOS SVNAT NATD_ETH SINHDOSE STUDYD CRU_DOS T_EMB T_ETHIO T_INH T_KANA T_MOXY T_PZA T_TERIZ EMB_AUC MOX_AUC PZA_AUC ETH_AUC CYC_AUC KANA_AUC BINH_EMB BINH_ETHIO BINH_KANA BINH_MOXY BINH_PZA BINH_TEZ NOPRINT NOAPPEND ONEHEADER FILE=mytab500.csv FORMAT=,

Final NONMEM scripts for results presented in section 6.4.2

```
$PROBLEM    INH PKPD MODEL IN PATIENTS WITH INHA-MUTATED ISOLATES
$SIZES      PD=-1000 LVR=-150 LTH=-200 MAXFCN=10000000 LNP4=-150000 MMX=100
;DVID = 0 for dose, 3 for PK, 1 for CFU, 2 for TTP
$INPUT      ID PATID DAY DVID MDV WHAT=DROP DV INHDOSE ARM EVID AMT EVENT TDAY
KARNSCR HEIGHT WEIGHT BMI AGE IVDRUG RACE PETHNC RACE1 SEX AGECAT HIV CAVITIES
BMI_GRP OCC DOSE AUC HALF KE LTMAX CMAX TMAX CMIN NCACL LOGAUC L2 CW OB
CLINIC MIC DAT2=DROP TIME VPCTIME INSTN NAT BLQ ICL IV IKA IV3 IQ IBIO IMTT INN
MIC_MISSING MIC_IMPUTE CMT
$DATA      PKCFUTTP1_boot.csv  IGNORE=#  IGNORE=(DVID.EQ.3)
$SUBROUTINE ADVAN13 TRANS1 TOL=9 ATOL=9 SSTOL=6 SSATOL=6
$MODEL      NCOMPARTMENTS=5 COMP=(GUT,DEFDOSE) COMP=(CENTRAL)
          COMP=(PERIPH) COMP=( EFFECT,INITIALOFF)  COMP=(BACTERIA LOAD)
$PK
;PK parameter
CL      =  ICL ; CLEARANCE
V       =  IV ; CENTRAL VOL.
KA      =  IKA ; ABS. RATE CONSTANT
BIO     =  IBIO ; RELATIVE BIOAVAILABILITY
V3      = IV3 ; PERIPH VOL
Q       = IQ ; INTER COMPT CL
MTT  = IMTT
NN = INN
QH     = IQH
FU     = IFU
CLINT=CL
;--------  Transfer constants for liver model ---------
; define hepatic extraction
EH  = (CLINT*FU)/((CLINT*FU)+QH) ; fraction undergoing first pass extraction
FH  = 1 - EH ; fraction available after 1st pass to go to systemic circulation

; COMPUTE RATE CONSTANTS
K32  = Q/V3   ; from peripheral to central
K23 = Q/V     ; from central to peripheral
K20 = QH*EH /V
```

```
;---------------- CODE for TRANSIT COMPARTMENT
F1 =     0 ; I need to set bioavailability in compartment 1 to 0 for transit absorption
KTR = (NN+1)/MTT
IF (NEWIND/=2.OR.EVID>=3) THEN ; new individual, or reset event
   ; The values read here will be stored in TDOS and PD in this very PK call.
        TNXD=TIME     ; Time of the dose
        PNXD=AMT      ; Amount. If it's zero, the DE is deactivated.
        COM(1)=0      ; COMRESS 1
        COM(2)=0      ; COMRESS 2
        TIMEDOSE = TIME
        AMOUNTDOSE = AMT
ENDIF
TDOS=TNXD ; This will either save here the temporary values if it's a new individual...
PD=PNXD ; ...or the values which were read one record ahead during the execution of the previous record.

IF(AMT.GT.0) THEN ; This reads one record ahead and stores the data to be used when running the following record
; IF(AMT.GT.0.AND.ALAG1.EQ.0) THEN ; Use this instead if there is ALAG, as it will also checks if the ALAG is not 0
        TNXD=TIME
        PNXD=AMT
ENDIF
PIZZA = LOG(BIO*PD*KTR + 0.00001) - GAMLN(NN+1)
; INITIALIZING COMPARTMENTS TO SPEED UP COMPUTATION
A_0(1) = 1E-6
A_0(2) = 1E-6
A_0(3) = 1E-6
A_0(4) = 1E-6
;----------- PD parameters ------------;
BSVBASE = ETA(1)
BSVKILL = ETA(2)
BOVDEL=ETA(3)
IF(OCC.EQ.2)  BOVDEL=ETA(4)
IF(OCC.EQ.3)  BOVDEL=ETA(5)
IF(OCC.EQ.4)  BOVDEL=ETA(6)
IF(OCC.EQ.5)  BOVDEL=ETA(7
IF(OCC.EQ.6)  BOVDEL=ETA(8)
IF(OCC.EQ.7)  BOVDEL=ETA(9)
IF(OCC.EQ.8)  BOVDEL=ETA(10)
;--------------Defining  thetas for the baseline value
BASELINE =  THETA(1) ; Baseline for arm 2 and 3 (mutated bugs on 10 and 15mg/kg dose)
IF(ARM.EQ.1) BASELINE  =  THETA(2)  ; Baseline for arm 1 (mutated bugs on 5mg/kg dose)
IF(ARM.EQ.4) BASELINE  =  THETA(3)  ; Baseline for arm 4 (drug sensitive bugs on 5mg/kg dose)
LOGBASE = BASELINE +BSVBASE   ;Baseline CFU in log10
BASE =(10**LOGBASE)  ;Baseline CFU normal space
```

```
;------------------------Emax model
EMAX = THETA(4)
TV_EC50 = THETA(5) ;EC50 of mutated bugs
IF(MUTATION.EQ.0) TV_EC50  = THETA(6)  ;EC50 for drug sensitive bugs
EC50 = TV_EC50
GAMMA = THETA(7)
KE0 = THETA(17)         ; first-order rate constant delay in onset of action
;--------TTP growth model
TTP_GROWTH_MUT=THETA(10); Growth rate constant for drug sensitive bugs
IF(MUTATION.EQ.1) TTP_GROWTH_MUT  = THETA(11) ; Growth rate constant for mutated bugs
NUMBER_BUGS_TTP = THETA(12)
BUGS_TTP = (10**NUMBER_BUGS_TTP; Bacteria population in MGIT at TTP (threshold for MGIT to turn positive)
TTP_GROWTH = TTP_GROWTH_MUT ;Growth rate constant.
DEL = THETA(13)*EXP(BOVDEL) ;Delay in growth due to hibernation of the bugs
DELAY  = DEL
IF(DAY .LE. 0) DELAY  = 0
A_0(5)  = BASE ;
$DES
TEMPO = T-TDOS ; this is time after dose for the transit, it should always be >= 0
KTT = 0
DADT(1) = -KA*A(1)
IF(PD.GT.0.AND.TEMPO.GT.0) THEN ; This happens only if PD>0, so only if a dose has been ; detected
          KTT = KTR*(TEMPO)
          DADT(1) = EXP(PIZZA+NN*LOG(KTT)-KTT) -KA*A(1)
ENDIF
DADT(2) = KA*A(1)*FH -K23*A(2) +K32*A(3) -K20*A(2)
DADT(3) = K23*A(2) -K32*A(3)
C2     =  A(2)/V2
C4     = A(4)
DADT(4) =  KE0*(C2-C4)   ;Differential equation for effect compartment
  INDUCTION_INPUT = 0     ; to protect against negatice C2
  IF (C4>1E-6)INDUCTION_INPUT =EMAX*((C4**GAMMA)/(EC50**GAMMA+C4**GAMMA)) ; Effect of concentration on KILL
;Bacteria load compartment
 KILL   =  INDUCTION_INPUT ;- EBASE
 DADT(5) = -KILL*A(5)
$ERROR
CE=A(4)  ;EFFECT compartment amount
CP=A(2)/V2     ;Plasma concentration needs to be calculated again outside of $DES
CFU=A(5) ;Bactria load compartment

;Bacteria growth model
 BUGS_0 = CFU*EXP(BSVCFU)  ;Bacteria Population at baseline
 LL = (BUGS_TTP/BUGS_0)
```

```
 TTP = (LOG(LL)/TTP_GROWTH)+ DELAY ;TTP + delay time caused by hibernation bugs due to treatment

; $ERR for CFU
IPRED_CFU = LOG10(CFU)
ADD_CFU = THETA(14)
PROP_CFU = 0 ; IPRED_CFU * THETA(x)
W_CFU =  SQRT((ADD_CFU)**2);+ (PROP_CFU)**2)
; $ERR for TTP
IPRED_TTP = TTP
ADD_TTP = 0
PROP_TTP = IPRED_TTP * THETA(15)
W_TTP =  SQRT((PROP_TTP)**2); +(ADD_TTP)**2 )

; Correlation
RHO = THETA(16)
; Cholesky decomposition
ERROR_CFU = W_CFU * EPS(1)
ERROR_TTP = W_TTP * (RHO*EPS(1) + SQRT(1-RHO**2)*EPS(2))

; CFU or dose (DVID==0 or 1)
IPRED = IPRED_CFU
W = W_CFU
ERROR_TERM = ERROR_CFU
; DVID==2 is TTP
IF (DVID==2) THEN
        IPRED = IPRED_TTP
        W = W_TTP
        ERROR_TERM = ERROR_TTP
ENDIF
IRES = DV-IPRED
IWRES = IRES/W

Y = IPRED + ERROR_TERM
;----------------------------
$THETA  (0.001,6.64,50) ; 1 BASE_MUT
 (0.001,5.88,50) ; 2  BASE_MUT 5mg/kg
 (0.001,5.52,20) ; 3 BASE
 (0.01,0.0182,5) ; 4 Emax
 (0.0001,0.621,40) ; 5 EC50_MUT
 (0,0.01,40) FIX ; 6 EC50
 (0.0000001,1.88349,30)  ; 7 GAMMA
 (0,0.613,5) FIX ; 8 DUMMY
 (0,0.44,5) FIX ; 9 KILL_LAG
 (0,0.0698,10) ; 10 TTP_GROWTH
 (0,0.0505,10) ; 11 MUT_TTP_GROWTH
 (0.0001,9.36,30) ; 12 BUGS_TTP
```

```
 (0,5.29,60) ; 13 DELAY
 (0.001,0.493,5) ; 14 ADD ERROR
 (0.001,0.133,5) ; 15 PROP ERROR
 (-0.99,-0.383,0.99) ; 16 RHO
 (0,0.0695,5) ; 17 KE0
;(0,38.4,40) ; 18 KIN_SENS
$OMEGA  BLOCK(1)
 0.891  ;  1 BSVBASE
$OMEGA  BLOCK(1) FIX
 0  ;  2 BSVKILL
$OMEGA  BLOCK(1) FIX
 0  ;   3 BSVLAG
$OMEGA  BLOCK(1) FIX
 0  ;   4 BSVCFU
$OMEGA  BLOCK(1) FIX
 0  ;   5 BSVTTP
$OMEGA  BLOCK(1)
 0.0196  ; 6 BSVGROWTH
$OMEGA  BLOCK(1) FIX
 0  ;   7 BSVDEL
;----------------------------
$OMEGA  BLOCK(1)
 1.14  ;   8 BOVDEL
$OMEGA  BLOCK(1) SAME
$OMEGA  BLOCK(1) SAME
$OMEGA  BLOCK(1) SAME
$OMEGA  BLOCK(1) SAME
$OMEGA  BLOCK(1) SAME
$OMEGA  BLOCK(1) SAME
$OMEGA  BLOCK(1) SAME
;-------------------------
$OMEGA  BLOCK(1) FIX
 0  ; 16 BSVEC50
$OMEGA  BLOCK(1) FIX
 0  ; 17 BSVEBASE
$OMEGA  BLOCK(1) FIX
 0  ;  18 BSVKIN
$OMEGA  BLOCK(1) FIX
 0  ; 19 BSVKOUT
$OMEGA  BLOCK(1) FIX
 0  ; 20 BSVGAMMA
$OMEGA  BLOCK(1)
 0.38  ; 21 BSVEMAX
;-----------------------
$OMEGA  BLOCK(1) FIX
 0  ; 22 BOVEC50
$OMEGA  BLOCK(1) SAME
```

```
$OMEGA  BLOCK(1) SAME
$OMEGA  BLOCK(1) SAME
$OMEGA  BLOCK(1) SAME
$OMEGA  BLOCK(1) SAME
$OMEGA  BLOCK(1) SAME
$OMEGA  BLOCK(1) SAME
;----------------------
$OMEGA  BLOCK(1) FIX
 0  ;  30 BOVKIN
$OMEGA  BLOCK(1) SAME
$OMEGA  BLOCK(1) SAME
$OMEGA  BLOCK(1) SAME
$OMEGA  BLOCK(1) SAME
$OMEGA  BLOCK(1) SAME
$OMEGA  BLOCK(1) SAME
$OMEGA  BLOCK(1) SAME
$OMEGA  BLOCK(1) SAME
;--------------------
$OMEGA  BLOCK(1) FIX
 0  ;  38 BSVKE0
;----------------------
$SIGMA  BLOCK(1) FIX
 1
$SIGMA  BLOCK(1) FIX
$ESTIMATION MSFO=run406.msf MAXEVAL=99999 PRINT=1 SIGDIG=3 SIGL=9 METH=1 INTER
NOABORT
$COVARIANCE PRINT=E MATRIX=S UNCONDITIONAL
$TABLE      WRESCHOL FILE=sdtab406.csv ID OCC DAY TIME DV Y MDV IPRED
        PRED IWRES WRES CWRES OBJI WRESCHOL NOPRINT NOAPPEND
        ONEHEADER FORMAT=,
$TABLE      FILE=patab406.csv FORMAT=, ID TIME TAD CP CE CL V2 KA V3 Q
        BIO BASELINE LOGBASE CFU EMAX EC50 GAMMA INDUCTION_INPUT
        KILL BSVBASE BSVEC50 BSVEBASE BSVKILL BSVLAG BSVKILL
        BSVLAG BSVKIN BSVKOUT BSVGAMMA BSVEMAX BOVEC50 BOVKIN
        BSVKE0 BUGS_0 BUGS_TTP TTP_GROWTH BSVCFU BSVTTP BSVGROWTH
        BSVDEL BOVDEL NOPRINT NOAPPEND ONEHEADER
$TABLE      FILE=cotab406.csv FORMAT=, ID DAY HEIGHT WEIGHT BMI AGE
        MIC AUC KE DOSE HALF LTMAX CMAX TMAX CMIN NCACL LOGAUC ICL
        PKAUC IV IKA IV3 IQ IBIO MIC_IMPUTE NOPRINT NOAPPEND
        ONEHEADER
$TABLE      FILE=catab406.csv FORMAT=, ID DOSE ARM MUTATION KARNSCR
        NAT MUT_MIC IVDRUG RACE PETHNC RACE1 SEX AGECAT HIV
        CAVITIES BMI_GRP MGIT MGIT_MUT MGIT_DOSE MGIT_ARM MUT_AUC
        MGIT_MUT_SEX MGIT_MUT_HIV MGIT_MUT_AGECAT MGIT_MUT_AUC
        NOPRINT NOAPPEND ONEHEADER
$TABLE      FILE=mytab406.csv FORMAT=, ID PATID OCC DAY TDAY TAD TIME
        IPRED PRED AA1 AA2 AA3 AA4 AA5 IWRES WRES CWRES DVID OBJI
        Y DV EVID MDV DOSE CL V2 KA V3 Q BIO CP CE CFU ARM AUC
```

EMAX EC50 GAMMA INDUCTION_INPUT KILL MUTATION BASELINE
LOGBASE BSVBASE BSVKILL BSVEBASE BSVLAG BSVKILL BSVLAG
BSVKIN BSVKOUT BSVGAMMA BSVEMAX BOVEC50 BOVKIN BSVKE0
BUGS_0 BUGS_TTP TTP_GROWTH BSVDEL BOVDEL BSVEC50 BSVCFU
BSVTTP BSVGROWTH KARNSCR ICL IV IKA IV3 IQ IBIO PKAUC KE
HALF LTMAX CMAX TMAX CMIN NCACL LOGAUC NAT HEIGHT WEIGHT
BMI AGE MIC MUT_MIC IVDRUG RACE PETHNC RACE1 SEX AGECAT
HIV CAVITIES BMI_GRP MGIT MGIT_MUT MGIT_DOSE MGIT_ARM
MGIT_MUT_SEX MGIT_MUT_HIV MGIT_MUT_AGECAT MGIT_MUT_AUC CW
OB MIC_IMPUTE MUT_AUC NOPRINT NOAPPEND ONEHEADER

Final NONMEM scripts for results presented in section 6.8.1

```
$SIZES     PD=-1000 LVR=-150 LTH=-200 MAXFCN=10000000 LNP4=-150000
$PROBLEM    A5312_INH
$INPUT          ID PATID=DROP DAT2=DROP TIME INHDOSE RELATIME=DROPWHAT=DROP
SCHDHR TIMEHR DV FBLQ=DROP SITE HEIGHTOB=DROP HT =DROP WT DRUG1DS1
DRUG1DS2=DROP DRUG1DS3=DROP FASTING1=DROP FASTING2=DROP FASTING3=DROP
CRFDT=DROP SYSTEMDT=DROP ARM FIXED_IN_R=DROP DATETIME=DROP MDV EVID OCC SS
II VPCTIME AMT BLQ KARNSCR BMI AGE IVDRUG RACETH PETHNC RACE1 SEX AGECAT HIV
CAVITIES BMI_GRP SAMPCOM=DROP NAT P_NAT P_NAT_liver       NNAT2 PR PI PS
$DATA      PKNONMEM.2020.05.12.csv IGNORE=#
;$ABBREVIATED COMRES=2
$SUBROUTINE ADVAN13 TOL=9 ;TOL is the precision to solve differential equations
ATOL=9 ; absolute tolerance,10^ATOL of your dose unit. A lower value makes the model run
faster
$MODEL      NCOMPARTMENTS=3 COMP=(ABS DEFDOSE) COMP=(CENTRAL)
         COMP=(PERI)
$PK
;initialise compartments
A_0(1)=0.0001
A_0(2)=0.0001 ; An average steady state value
A_0(3)=0.0001
; ---------- BOV
BOVCL = ETA(7)
IF(OCC.EQ.2) BOVCL = ETA(8)
BOVV = ETA (9)
IF(OCC.EQ.2) BOVV = ETA(10)
BOVKA=ETA(11)
IF(OCC.EQ.2)  BOVKA=ETA(12)
BOVBIO=ETA(13)
IF(OCC.EQ.2)  BOVBIO=ETA(14)
BOVMTT = ETA(15)
IF(OCC.EQ.2)  BOVMTT=ETA(16)
; ------- BSV
BSVCL   = ETA(1)
BSVV   = ETA(2)
BSVKA   = ETA(3)
```

```
BSVBIO = ETA(4)
BSVV3 = ETA(5)
BSVQ = ETA(6)
; ---------- Calculation of Fat-free Mass
; These formulas require WT in KG and HT in m !!!
; Conversion from cm to m
HTM = HT/100
IF (SEX.EQ.2) THEN  ; female
        WHSMAX=37.99
        WHS50=35.98
ELSE      ;males
        WHSMAX=42.92
        WHS50=30.93
ENDIF
HTM2 = HTM**2
FFM = (WHSMAX*HTM2*WT)/(WHS50*HTM2+WT)
FAT = WT-FFM
; ------- Typical values of covariates
TVWT = 51
TVFAT = 7
TVFFM = 44
;--------- Allometric scaling and covariates
ALLMCL_WT = (WT/TVWT)**0.75
ALLMV_WT = (WT/TVWT)
ALLMCL_FAT = (FAT/TVFAT)**0.75
ALLMV_FAT = (FAT/TVFAT)
ALLMCL_FFM = (FFM/TVFFM)**0.75
ALLMV_FFM = (FFM/TVFFM)
; Allometry for liver
ALLMCL_WT_HEP = (WT/70)**0.75
ALLMV_WT_HEP = (WT/70)
ALLMCL_FFM_HEP = (FFM/56.1)**0.75
ALLMV_FFM_HEP = (FFM/56.1)
;------------------identifying mutation----------------------------
MUTATION=1  ; INHA mutation
IF(ARM.EQ.4) MUTATION  =  2 ;No mutation
;---------------------------------------------
VNAT = NNAT2
IF(NNAT2.LT.0) VNAT =  1
DNAT = INHDOSE*10 + VNAT
NATD = VNAT*10 + INHDOSE
;---------Effect of NAT2 on CL--
TVCL_NAT =  THETA(1) ; intermediate
IF(NNAT2.EQ.0) TVCL_NAT =  THETA(7) ;FAST
IF(NNAT2.EQ.2) TVCL_NAT =  THETA(8) ;Slow
;---------Typical values-------------------------------
TVCL = TVCL_NAT*ALLMCL_FFM
```

```
TVV = THETA(2)*ALLMV_FFM
TVKA = THETA(3)
TVBIO = THETA(4)
; TVLAG = THETA(7)
 TVV3 = THETA(9)*ALLMV_FFM
 TVQ = THETA(10)*ALLMCL_FFM
TVMTT   = THETA(11)
NN      = EXP(THETA(12))
;-----------------------------------------------------
TVQH=THETA(13)*ALLMCL_FFM_HEP   ; PLASMA FLOW RATE
TVFU=THETA(14)         ; UNBOUND PLASMA FRACTION OF INH
;-----------Define parameters-------------------------------
CL  = TVCL*EXP(BSVCL+BOVCL) ; CLEARANCE
V   = TVV*EXP(BSVV) ; CENTRAL VOL.
KA  = TVKA*EXP(BSVKA+BOVKA) ; ABS. RATE CONSTANT
BIO = TVBIO*EXP(BSVBIO+BOVBIO) ; BIOAVAILABILITY
; LAG =TVLAG*EXP(BOVLAG) ; LAG TIME
 V3 = TVV3*EXP(BSVV3) ; PERIPH VOL
 Q = TVQ*EXP(BSVQ) ; INTER COMPT CL
MTT = TVMTT*EXP(BOVMTT)
QH=TVQH
FU=TVFU
CLINT=CL
;--------  Transfer constants for liver model ---------
; define hepatic extraction
EH  = (CLINT*FU)/((CLINT*FU)+QH) ; fraction undergoing first pass extraction
FH  = 1 - EH ; fraction available after 1st pass to go to systemic circulation
; COMPUTE RATE CONSTANTS
K32  = Q/V3   ; from peripheral to central
K23 = Q/V     ; from central to peripheral
K20 = QH*EH /V
;---------------- CODE for TRANSIT COMPARTMENT -----------------
F1=0 ; I need to set bioavailability in compartment 1 to 0 for this implementation of the transit
compartment absorption
KTR = (NN+1)/MTT
IF (NEWIND/=2.OR.EVID>=3) THEN ; new individual, or reset event
   ; The values read here will be stored in TDOS and PD in this very PK call.
         TNXD=TIME ; Time of the dose
         PNXD=AMT ; Amount. If it's zero, the DE is deactivated.
ENDIF
TDOS=TNXD ; This will either save here the temporary values if it's a new individual...
PD=PNXD ; ...or the values which were read one record ahead during the execution of the
previous record.
IF(AMT>0) THEN ; This reads one record ahead and stores the data to be used when running
the following record
```

```
; IF(AMT.GT.0.AND.ALAG1.EQ.0) THEN ; Use this INSTEAD if there is ALAG, as it will also checks if the ALAG is not 0. Note that you normally do not want to include both ALAG and transit, this is a very exceptional case
          TNXD=TIME
          PNXD=AMT
ENDIF
; Uncomment this if you have ALAG or if you use ADDL
; IF (DOSTIM>0) THEN ; This will account for the ADDL or lagged doses. It will overwrite the time, if it a non-event record
;          TNXD=DOSTIM
;          PNXD=AMT
; ENDIF
; To speed up the computation, I calculate here all the non-time-varying quantities used in $DES
PIZZA = LOG(BIO*PD*KTR + 0.00001) - GAMLN(NN+1)  ; without +0.00001, it won't work with ETAs in bioavailability
; IF(NEWIND.LE.1.OR.EVID.GE.3) THEN ; assign negative Cmax Tmax for the new subject
    ; COM(1)=-1 ; holder of Cmax
    ; COM(2)=-1 ; holder of Tmax
; ENDIF
;-----------------------------------------------------------------
$DES
TEMPO=T-TDOS ; this is time after dose, it should always be >= 0
KTT=0
DADT(1)=-KA*A(1)
IF(PD.GT.0.AND.TEMPO.GT.0) THEN ; This happens only id PD>0, so only if a dose has been detected
  KTT=KTR*(TEMPO)
  DADT(1)=EXP(PIZZA+NN*LOG(KTT)-KTT)-KA*A(1)
ENDIF
DADT(2) = KA*A(1)*FH -K23*A(2) +K32*A(3) -K20*A(2)
DADT(3) = K23*A(2) -K32*A(3)
; ;------CMAX AND TMAX
; CT=A(2)/V ; (or other expression for concentration)
; IF(CT.GT.COM(1)) THEN
          ; COM(1)=CT
          ; COM(2)=T
; ENDIF
;---------------------------------------
$ERROR
IPRED = A(2)/V
IRES = DV-IPRED
LLOQ=0.105 ; INH LLOQ in ug/ml
   IMPUTED_BLQ=LLOQ/2
PROP = IPRED*THETA(5)
ADD =  0.2*LLOQ + THETA(6)
```

```
IF(ICALL.NE.4.AND.BLQ==1) ADD = ADD + (LLOQ/2)
IF(ICALL.NE.4.AND.BLQ==2) THEN
        PROP = 0
        ADD = 100000000
ENDIF

W = SQRT(ADD**2+PROP**2)
IF (W.LE.0.0001) W=0.0001
IWRES = IRES/W
Y = IPRED + W*ERR(1)
; For simulation, like in case of VPC
   IF (ICALL==4.AND.Y<=LLOQ) THEN
          Y=IMPUTED_BLQ ; All BLQ values in simulation get imputed to LLOQ/2. This also
prevents negative values
   ENDIF
; To calculate time after dose.
IF(AMT.GT.0) THEN
        TIMEDOSE = TIME
        AMOUNTDOSE = AMT
ENDIF

TAD = TIME-TIMEDOSE
VARCL = BSVCL + BOVCL
VARBIO = BSVBIO + BOVBIO
VARAUC = BSVBIO + BOVBIO - BSVCL - BOVCL
;-------------RETRIEVE AMOUNT IN EACH COMPARTMENT-------------------------
AA1 = A(1)
AA2 = A(2)
;-------------------------------------------------------------------------
$THETA  (0,23.8928,200) ; 1 CL inter [L/h]
$THETA  (0,30.9084,800) ; 2 V [L]
$THETA  (0,3.38634,50) ; 3 KA [1/h]
$THETA  1 FIX ; 4 BIO
$THETA  (0,0.127322,0.5) ; 5 PROP []
$THETA  (0,1.87573E-006,1) ; 6 ADD [mg/L]
$THETA  (0,46.3074,200) ; 7 CL_Fast [L/h]
$THETA  (0,9.24943,200) ; 8 CL_SLOW [L/h]
$THETA  (0,9.56441,2800) ; 9 V3 [L]
$THETA  (0,8.17796,90) ; 10 Q [L/h]
$THETA  (0,0.112065,5) ; 11 MTT
$THETA  (0,0.839863,6) ; 12 NN [LOG]
 (0,90,100) FIX ; 13 QH
 (0,0.95,1) FIX ; 14 FU
;-------------------------------
$OMEGA  BLOCK(1)
 0.0391373  ;   1 BSV CL
$OMEGA  BLOCK(1) FIX
```

```
 0  ;    2 BSV V
$OMEGA  BLOCK(1) FIX
 0  ;   3 BSV KA
$OMEGA  BLOCK(1) FIX
 0  ;  4 BSV BIO
$OMEGA  BLOCK(1) FIX
 0  ;    5 BSVV3
$OMEGA  BLOCK(1) FIX
 0  ;     6 BSVQ
;----------------------------------------------------------------------
$OMEGA  BLOCK(1) FIX
 0  ;    7 BOVCL
$OMEGA  BLOCK(1) SAME
;-------------------------------------------------------
$OMEGA  BLOCK(1) FIX
 0  ;     9 BOVV
$OMEGA  BLOCK(1) SAME
;-------------------------------------
$OMEGA  BLOCK(1)
 0.510084  ;   11 BOVKA
$OMEGA  BLOCK(1) SAME
;---------------------------------------------
$OMEGA  BLOCK(1)
 0.057305  ;  13 BOVBIO
$OMEGA  BLOCK(1) SAME
;-----------------------------------------------------
$OMEGA  BLOCK(1)
 1.26029  ;  15 BOVMTT
$OMEGA  BLOCK(1) SAME
;---------------------------------------------------------------------
$SIGMA  1  FIX
;---------------------------------------------------------------------
$ESTIMATION MSFO=run070g.msf MAXEVAL=9999 PRINT=1 METHOD=1 INTER
        NOABORT SIGDIG=3 SIGL=9 NONINFETA=1 ETASTYPE=1 REPEAT
$COVARIANCE PRINT=E MATRIX=S UNCONDITIONAL
$TABLE      WRESCHOL FILE=sdtab070g.csv ID OCC TIME DV BLQ VPCTIME TAD
        IPRED PRED IWRES WRES CWRES CWRESI OBJI AA1 AA2 NOPRINT
        NOAPPEND ONEHEADER FORMAT=,
$TABLE      FILE=patab070g.csv ID OCC CL V KA V3 Q BIO NN MTT BSVCL
        BSVV BSVKA BSVBIO BSVV3 BSVQ BOVCL BOVKA BOVBIO BOVMTT
        VARCL VARBIO VARAUC NOPRINT NOAPPEND ONEHEADER FORMAT=,
$TABLE      FILE=cotab070g.csv ID OCC WT HT AGE FFM FAT BMI DRUG1DS1
        NOPRINT NOAPPEND ONEHEADER FORMAT=,
$TABLE      FILE=catab070g.csv ID OCC BLQ SITE INHDOSE ARM NAT DNAT
        NATD KARNSCR IVDRUG RACETH PETHNC RACE1 SEX AGECAT HIV
        CAVITIES BMI_GRP MUTATION NNAT2 NOPRINT NOAPPEND ONEHEADER
        FORMAT=,
```

```
$TABLE      FILE=mytab070g.csv ID OCC TIME TAD Y AMT MDV EVID SS II DV
            AA1 AA2 ; AA3 AA4
            PRED RES WRES IPRED IRES IWRES CWRES CWRESI OBJI CL V KA
            V3 Q BIO NN MTT BSVCL BSVV BSVKA BSVBIO BSVV3 BSVQ BOVCL
            BOVKA BOVBIO VARCL VARBIO VARAUC SEX WT HT FFM FAT VPCTIME
            BLQ SITE INHDOSE ARM MUTATION KARNSCR BMI AGE IVDRUG
            RACETH PETHNC DRUG1DS1 RACE1 AGECAT HIV CAVITIES BMI_GRP
            NAT DNAT NATD NNAT2 NOPRINT NOAPPEND
            ONEHEADER FORMAT=,
```